



TECHNICAL UNIVERSITY OF BRAUNSCHWEIG
Faculty for Physics and Geological Sciences

Eco-balance of a Solar Electricity Transmission from North Africa to Europe

Diploma Thesis

of

Nadine May

First Referee: Prof. Dr. Wolfgang Durner

Second Referee: Prof. Dr. Otto Richter

Braunschweig, 17th August 2005

Preface

In the following I would like to thank several persons very much for their assistance without the making of this thesis would never been possible.

I would like to thank Prof. Dr. Wolfgang Durner and Prof. Dr. Otto Richter for giving an expert's opinion on my thesis.

Special thanks are dedicated to Dr. Franz Trieb at the German Aerospace Centre (DLR) in Stuttgart who looked after my thesis and first made me sensitive for this special theme of renewable energies and always offer me a new way of thinking.

Besides, I would like to thank Dr. Peter Viebahn who was always a great help in answering questions referring the preparing of the eco-balance.

At this place I would like to mention the colleagues of the section systems analysis and technology assessment at the institute of technical thermodynamics at the DLR in Stuttgart. It was a pleasure to work with them and in their environment I was able to acquire a lot of new knowledge.

Further on I would like to send many thanks to Mr Klaus Treichel und Mr Bo Normark from ABB who were a decisive help in compiling technical data.

Summary

The present energy supply is mainly based on fossil energy sources. Because of decreasing resources, a worldwide increasing energy demand and the resulting growth of environmental pollution, it's necessary to tap other sources in the long term. In this context it is pointed to the large potential of solar energy in North Africa, which theoretically meets the world's energy demand many times. On-site solar electricity can be produced by solar thermal power plants and then be transmitted via high voltage direct current transmission (HVDC) over long distances to Europe. In this thesis the environmental impacts are described which result from the installation of the infrastructure. Furthermore a GIS-Analysis is carried out to set power lines under ecological aspects. Within the scope of an eco-balance the resulting lines together with solar thermal power plants are investigated regarding possible impacts on the environment and material and energetic expenditures respectively. It can be shown that the power lines slightly contribute to all impacts compared with the plants. If the results of the impact assessment are normalized to one kilowatt-hour and set against a reference contemporary electricity mix, the impacts are distinctly lower than in the reference in all areas. Only a larger quantity of material expenditures is necessary to build up the infrastructure.

Table of contents

1	Introduction	1
2	Electricity supply in Europe and North Africa	3
2.1	Present electricity supply	3
2.2	Utilization of renewable energy sources	6
2.2.1	Solar thermal power plants	7
2.2.2	Irradiation potential in the Mediterranean region	8
2.2.3	Total yield of the solar thermal potential	11
2.3	Energy supply networks	13
2.4	Closing of the Mediterranean ring	16
3	Basics of the transmission of electricity	19
3.1	Energy-technological comparison of overhead line & cable	19
3.2	Alternating Current	22
3.3	Direct current	28
3.3.1	Technology	28
3.3.2	History of HVDC	30
3.3.3	Principle of HVDC	30
3.3.4	Possible and existing applications of HVDC	31
3.3.5	Overhead line transmission losses	32
3.3.6	Cable transmission losses	35
4	Comparison of costs	36
5	Environmental impacts of overhead lines	38
5.1	Space requirement	40
5.2	Landscape-image	41
5.3	Electric and magnetic fields	43
5.4	Risk potential for fauna and flora	49
5.5	Risk potential for soil and groundwater	52
6	Environmental impacts of underground cables	54
7	Environmental impacts of submarine cables	57
8	Ecologically-optimized line laying (GIS-analysis)	62
8.1	Generation of an exclusion mask	63
8.1.1	Exclusion criterion: protected area	64
8.1.2	Exclusion criterion: industrial location	65
8.1.3	Exclusion criterion: populated places	66
8.1.4	Exclusion criterion: sea depth	67
8.1.5	Exclusion criterion: hydrological feature	67
8.1.6	Exclusion criterion: geomorphologic feature	68
8.2	Generation of an isotropic friction image	70
8.2.1	Land cover	70
8.2.2	Cultural and religious sites	72
8.2.3	Infrastructure	73
8.2.4	Natural hazards	74
8.3	Generation of an anisotropic friction image	82
8.4	Calculation of the cost-distance image and line laying	84

9	Analysis of the results	86
9.1	Line 1: Algeria-Aachen	86
9.2	Line 2: Libya-Milano	87
9.3	Line 3: Egypt-Vienna	88
9.4	Evaluation.....	89
10	Product Eco-balance - Life Cycle Assessment.....	94
10.1	ISO Standardization	95
10.2	Material flow networks	98
11	Life Cycle Assessment of a solar electricity production and transmission scheme	102
11.1	Goal and scope definition	102
11.1.1	Specification of system boundaries	102
11.1.2	Subject of modelling	103
11.1.3	Databases and processes	103
11.1.4	Used Modules	104
11.1.5	Services.....	105
11.1.6	Limitations and geographic consistency	105
11.1.7	Selection of Impact Categories.....	106
11.2	Inventory Analysis	107
11.2.1	Modelling of the solar thermal power plant.....	107
11.2.2	Modelling of the HVDC line	110
11.3	Impact Assessment and Interpretation	114
11.3.1	Solar thermal power plant.....	115
11.3.2	HVDC transmission line.....	117
11.3.3	Comparison of the balances of all three lines.....	119
11.3.4	Energetic amortization time	122
11.3.5	Additional load with changed modules (reference year 2010)...	123
11.3.6	Normalization with respect to a reference electricity mix in 2010/2030 124	
12	Results and conclusions	127
13	Bibliography.....	129
14	Used datasets	137
Annex.....		140

List of illustrations

Fig. 1: Course of the day of the power demand in Germany every third Wednesday of the month in the year 2000	4
Fig. 2: Utilization of power plants to meet the base load, medium load and top load	5
Fig. 3: Electricity mix 2004 within the UCTE.....	5
Fig. 4: 'SEE' Ideal scenario of a sustainable, global energy supply until 2050	6
Fig. 5: Principle of a combined current and heat production by solar thermal power plants	7
Fig. 6: Different kinds of solar thermal power plants.	8
Fig. 7: Annual sum 2002 of the Direct Normal Solar Irradiation [kWh/m ²] in the Mediterranean countries and on the Arabic peninsula	9
Fig. 8: Monthly energy yield of a solar thermal power plant at sites with a different irradiation potential.....	10
Fig. 9: Plant simulation at the site El Kharga in Egypt.....	10
Fig. 10: Plant simulation at the site Madrid in Spain.....	10
Fig. 11: Plant simulation at the site Freiburg in Germany.....	11
Fig. 12: Theoretical space requirement to meet the electricity demand of the world, Europe (EU-25) and Germany	12
Fig. 13: Synergies between Europe and North Africa	13
Fig. 14: European and North African energy supply system	15
Fig. 15: Interconnected networks in the Mediterranean region.	16
Fig. 16: Imports (+) and exports (-) in GWh between Mediterranean countries in the year 2000	17
Fig. 17: Planned closing of the ring	18
Fig. 18: 400kV conductor (left) and scheme of a compound wire (right)	20
Fig. 19: Mast images for high and extra-high voltage overhead lines:	20
Fig. 20: Scheme of a submarine cable	22
Fig. 21: Three-phase alternating current	22
Fig. 22: 4-bundle conductor of a high voltage line.....	25
Fig. 23: Comparison of transmission capacities of AC- and DC-cables	27
Fig. 24: Schematic diagram of a monopolar (above) and bipolar system (below) ..	29
Fig. 25: Schematic diagram of a HVDC transmission.	31
Fig. 26: HVDC losses in dependence on transmission voltage and distance.....	34
Fig. 27 : Comparison of AC and DC investment costs	36
Fig. 28: Required number of parallel standing pylons to transfer 10 GW	41
Fig. 29: Typical pylon constructions of a HVAC and HVDC overhead line	41
Fig. 30: Left: Electric field under a HVAC overhead line in a height of 1 m over the ground; Right: Electric field under a 450kV HVDC overhead line	44
Fig. 31: Left: Natural, static field; Right: 'Lightning Arrester Effect'.....	45
Fig. 32: Magnetic field below a HVAC overhead line in height of 1 m over the ground.....	47
Fig. 33: Management of the safety strip of the line.....	51
Fig. 34: Costs for the maintenance of the line	52
Fig. 35: Left: Magnetic field over a AC underground cable; Right: Specific heat resistance of a sandy soil with a different humidity	55
Fig. 36: Direct current submarine cables in the North and Baltic Sea	57
Fig. 37: Profile through the 'Street of Otranto'	57

Fig. 38: Environmental impacts of a submarine cable in dependency on the depth under the seabed (here as GOK) during the operating and laying phase.....	61
Fig. 39: Map of the Direct Normal Solar Irradiation [kWh/m ² /y] with excluded areas	62
Fig. 40: Joint intersection of DCW und GLCC.....	67
Fig. 41: Exclusion mask for the Mediterranean region.....	69
Fig. 42: Land cover in the Mediterranean region	70
Fig. 43: Population density in the Mediterranean region.....	72
Fig. 44: Distance image of the electricity network in the Mediterranean region in kilometres.....	74
Fig. 45: Danger of earthquakes	75
Fig. 46: Danger of volcano eruptions	76
Fig. 47: Danger of winter storms.....	76
Fig. 48: Danger of tornados	77
Fig. 49: Danger of hail	77
Fig. 50: Danger of lightning.....	78
Fig. 51: Danger of tsunami.....	78
Fig. 52: Isotropic total friction image.....	82
Fig. 53: Directional Bias Function.....	84
Fig. 54: Cost-distance image for line 1 (left) and line 2 (right).....	85
Fig. 55: Resulting course of HVDC lines for a solar electricity import.....	86
Fig. 56: Ground profile [height above sea level] of line 1 from Aachen to Algeria and the associated hypsographic elevation model.....	87
Fig. 57: Ground profile [height above sea level] of line 2 from Milano to Tunisia and the associated hypsographic elevation model.....	88
Fig. 58: Ground profile [height above sea level] of line 3 from Vienna to Egypt and the associated hypsographic elevation model.....	89
Fig. 59: Degree of land use and visibility of the lines.....	91
Fig. 60: Line distances to the reference network.....	92
Fig. 61: Product chain 'from cradle to grave'.....	94
Fig. 62: Petri-Grid with the essential grid elements.....	99
104	
Fig. 63: Electricity mix 2010 und 2030	104
Fig. 64: Material flow network of a parabolic trough.....	109
Fig. 65: Sub network for the production of the solar field.....	109
Fig. 66: Material flow network of a HVDC transmission line.....	111
Fig. 67: Sub network for the cable manufacture.....	112
Fig. 68: Sub network for the overhead line manufacture.....	112
Fig. 69: Subdivision of the lines in two sections for the modelling of the transport.....	113
Fig. 70: Proportional shares of the plant and the line in environmental impacts (line 1, reference year 2030).....	114
Fig. 71: Impacts and resource consumptions of the solar field components and life cycle phases of the solar field (line 1, reference year 2030).....	116
Fig. 72: Impacts and resource consumptions of single plant components and life cycle phases of the plant respectively (line 1, reference year 2030).....	116
Fig. 73: Impacts and resource consumptions in the phases of life of the HVDC transmission line (line 1, reference year 2030).....	118
Fig. 74: Impacts and resource consumptions of the overhead line components and the transport (line 1, reference year 2030).....	118

Fig. 75: Impacts and resource consumptions of the submarine cable components and the transport (line 1, reference year 2030).	119
Fig. 76: Line comparison for cumulated energy expenditure and global warming potential.	120
Fig. 77: Line comparison for summer smog and particle load.	120
Fig. 78: Line comparison for acidification and eutrophication potential.	121
Fig. 79: Line comparison for CO ₂ and iron.	121
Fig. 80: Line comparison for bauxite and copper.	121
Fig. 81: Proportional additional load of the respective line from the year 2030 if a changed electricity mix and changed production chains with the reference year 2010 are taken as a base.	123
Fig. 82: Normalization of the LCA results for line 1 (plant+HVDC line in 2030) on 1 kWh, solar electricity, reference: electricity mix in 2030 and 2010 respectively has been set on 100%.	124
Fig. 83: Normalization of all lines with the reference year 2030 on 1 kWh _{el} and comparison with the reference electricity mix in 2030 and 2010 respectively	126
Fig. 84: GLOBE-Dataset	141
Fig. 85: ETOPO2-Dataset	141
Fig. 86: Line laying model.	142
Fig. 87: Exclusion mask for the line.	143
Fig. 88: Land cover in the Mediterranean region.	144
Fig. 89: Digital elevation model	145
Fig. 90: Exclusion mask for the solar thermal power plant.	146
Fig. 91: Proportional shares of the plant and the line in environmental impacts (line 2, reference year 2030).	160
Fig. 92: Proportional shares of the plant and the line in environmental impacts (line 3, reference year 2030).	160
Fig. 93: Impacts in the life cycle phases of the HVDC line 2 (2030).	161
Fig. 94: Impacts of the overhead line section of line 2 (2030).	162
Fig. 95: Impacts of the submarine cable section of line 2 (2030).	162
Fig. 96: Impacts in the life cycle phases of the HVDC line 3 (2030).	163
Fig. 97: Impacts of the overhead line section of line 3 (2030).	163
Fig. 98: Impacts of the submarine cable section of line 3 (2030).	164
Fig. 99: Life cycle phases of the solar thermal power plant 2 (2030).	167
Fig. 100: Components and life cycle phases of the solar field of plant 2 (2030).	168
Fig. 101: Life cycle phases of the solar thermal power plant 3 (2030).	168
Fig. 102: Components and life cycle phases of the solar field of plant 3 (2030).	169

List of tables

Tab. 1: Voltage levels inside Germany	14
Tab. 2: Planned interconnections between Mediterranean neighbouring states	18
Tab. 3: Existing HVDC installations	32
Tab. 4: Losses in dependence on transmission voltage (double-bipol)	34
Tab. 5: Literature information about HVDC losses.	35
Tab. 6: Present costs from the literature.	37
Tab. 7: Measurements of a HVAC and HVDC overhead line	40

Tab. 8: Examples of magnetic flux densities.....	47
Tab. 9: Basic threshold for electric and magnetic fields.....	49
Tab. 10: Reference values for the permanent stay in electric and magnetic fields (population).....	49
Tab. 11: Comparison of the field strength nearby the sea-electrode with the minimum field strength for the release of a reaction in case of the herring....	59
Tab. 12: Start and target points of the lines.....	63
Tab. 13: Risk classes of single natural hazards.....	79
Tab. 14: Insurance rates and base factors.....	80
Tab. 15: Total insurance rates.....	80
Tab. 16: Ratio of raised costs to base costs (= 1.0).....	81
Tab. 17: Line shares of the concerned countries in kilometres.....	90
Tab. 18: Statistical parameters of the line distance to the reference network in km.	92
Tab. 19: Line distances to selective cities in km.....	92
Tab. 20: Fields of examination of the Federal Environmental Agency.....	97
Tab. 21: Extended eco-account-frame with yields/reference flows (green) and expenditures (red).....	99
Tab. 22: Used impact categories and expenditures.....	106
Tab. 23: Technical assumption for a 10 GW base load production of a solar thermal power plant in 2030.....	108
Tab. 24: Parameters for the long-distance transport of 10 GW of electric load...	110
Tab. 25: Transported energy amounts in 30 years operating time.....	111
Tab. 26: Energetic amortization time for all lines.....	122
Tab. 27: Comparative values of 1 kWh _{el} solar electricity with the German high voltage electricity mix in 2010 und 2030.....	124
Tab. 28: Decrease of the alongside meridian distance to the poles.....	140
Tab. 29: Features for the visibility analysis.....	140
Tab. 30: Flächenanteile in the land cover of line 1.....	147
Tab. 31: Flächenanteile an der Landbedeckung von Trasse 2.....	147
Tab. 32: Flächenanteile an der Landbedeckung von Trasse 3.....	147
Tab. 33: Parameter determination for the modelling of the HVDC line 1.....	148
Tab. 34: Parameter determination for the modelling of the HVDC line 2.....	148
Tab. 35: Parameter determination for the modelling of the HVDC line 3.....	149
Tab. 36: Parameter determination for the modelling of the solar thermal power plant (line 1).....	150
Tab. 37: Parameter determination for the modelling of the solar thermal power plant (line 2).....	150
Tab. 38: Parameter determination for the modelling of the solar thermal power plant (line 3).....	151
Tab. 39: Inventory data of the HVDC line 1 (2030).....	152
Tab. 40: Inventory data of the HVDC line 2 (2030).....	152
Tab. 41: Inventory data of the HVDC line 3 (2030).....	153
Tab. 42: Inventory data of the solar thermal power plant of line 1 (2030).....	153
Tab. 43: Inventory data of the solar thermal power plant of line 2 (2030).....	155
Tab. 44: Inventory data of the solar thermal power plant of line 3 (2030).....	157
Tab. 45: Results of the impact assessment of the HVDC line 1 (2030) normalized to 1 kWh.....	160
Tab. 46: Results of the impact assessment of the HVDC line 2 (2030) normalized to 1 kWh.....	161

Tab. 47: Results of the impact assessment of the HVDC line 3 (2030) normalized to 1 kWh.....	161
Tab. 48: Results of the impact assessment for the HVDC line 1 (2010) normalized to 1 kWh.....	164
Tab. 49: Results of the impact assessment for the HVDC line 2 (2010) normalized to 1 kWh.....	164
Tab. 50: Results of the impact assessment for the HVDC line 3 (2010) normalized to 1 kWh.....	165
Tab. 51: Results of the impact assessment for the plant (line 1, 2030) normalized to 1 kWh.....	165
Tab. 52: Results of the impact assessment for the plant (line 2, 2030) normalized to 1 kWh.....	166
Tab. 53: Results of the impact assessment for the plant (line 3, 2030) normalized to 1 kWh.....	166
Tab. 54: Results of the impact assessment for the plant (line 1, 2010) normalized to 1 kWh.....	169
Tab. 55: Results of the impact assessment for the plant (line 1, 2010) normalized to 1 kWh.....	170
Tab. 56: Results of the impact assessment for the plant (line 3, 2010) normalized to 1 kWh.....	170
Tab. 57: Additional load of line 1 (reference year 2010).....	171
Tab. 58: Additional load of line 2 (reference year 2010).....	171
Tab. 59: Additional load of line 3 (reference year 2010).....	171
Tab. 60: End result of line 1 normalized to 1 kWh.....	172
Tab. 61: End result of line 2 normalized to 1 kWh.....	172
Tab. 62: End result of line 3 normalized to 1 kWh.....	172

List of Acronyms

ABB	Asea Brown Boveri
AC	Alternating Current
Al/St	Aluminium/Steel
AVHRR	Advanced Very High Resolution Radiometer
BGR	Bundesanstalt für Geowissenschaften und Rohstoffe (Federal Institute for Geoscience and Natural Resources)
BImSchV	Bundesimmissionsschutzverordnung (Federal Immission Control Act)
BNatSchG	Bundesnaturschutzgesetz (Federal Nature Conservation Act)
CAD	Computer Aided Design
CENTREL	Interconnected network of Poland, Hungary, Czech Republic and Slovakia
COMELEC	Maghreb Electricity Committee
DC	Direct Current
DCW	Digital Chart of the World
DEM	Digital Elevation Model
DIN	Deutsche Industrienorm (German Industry Norm)
DLR	Deutsches Zentrum für Luft- und Raumfahrt (German Aerospace Centre)
DMA	Defense Mapping Agency
DNI	Direct normal irradiation
DSMW	Digital Soil Map of the World
DTED	Digital Terrain Elevation Data
EAT	Energetische Amortisationszeit (Energy Amortisation Period)
EEA	European Environment Agency
ELTAM-Projekt	Egypt, Libya, Tunisia, Algeria, Morocco
ERS-1	First European Remote Sensing Satellite

ESA	European Space Agency
ESRI	Environmental Systems Research Institute
ETOPO2	2 Minute Earth Topography
EU-25	the 25 member states of the European Union
EWG	Europäische Wirtschaftsgemeinschaft (European Economic Community)
Eq.	Equivalent
FAO	Food and Agriculture Organization of the United Nations
FCKW	Fluor-Chlor-Kohlenwasserstoffe (Chlorofluorocarbons)
FFH	Flora-Fauna-Habitat
GIS	Geographic information system
GLCC	Global Land Cover Characterization
GLOBE	Global Land One-kilometre Base Elevation
GOK	Geländeoberkante (top ground surface)
GTOPO30	30 Second Global Elevation data
GuD	Gas- und Dampfkraftwerk (gas and steam power plant)
HVAC	High Voltage Alternating Current
HVDC	High Voltage Direct Current
ICNIRP	International Commission Non-Ionizing Radiation Protection
IEC	International Electrotechnical Commission
IFEU	Institut für Energie- und Umweltforschung (Institute for Energy and Environmental Research)
IFU	Institut für Umweltinformatik (Institute for Environmental Informatics)
IPCC	Intergovernmental Panel on Climate Change
IPS/UPS	Integrated Power System/Unified Power System
ISO	International Organization for Standardization
IUCN-WCPA	Union for the Conservation of Nature and Natural Resources – World Commission on Protected Areas
JRC	Joint Research Center
KEA	Kumulierter Energieaufwand (cumulated energetic expenditure)
LCA	Life Cycle Assessment
LEJLS	Interconnected network of Libya, Egypt, Jordan, Lebanon und Syria
MAGHREB	Morocco, Algeria, Tunisia
MED-CSP	Concentrating Solar Power for the Mediterranean Region
NGA	National Geospatial-Intelligence Agency
NDVI	Normalized Difference Vegetation Index
NGDC	National Geophysical Data Center
NIMA	National Imagery and Mapping Agency, früher DMA
NMS	Northern Mediterranean Countries
NOAA	National Oceanic and Atmospheric Administration
NORDEL	Interconnected network of Norway, Sweden, Denmark, Finland
OD	Original Data
OME	Observatoire Méditerranéen de l'Énergie
PM10	Particle < 10 µm
PPLP	Polypropylen-Laminated Paper
PSI	Pilkington Solar International
PVC	Polyvinylchlorid
RWE	Rheinisch-Westfälisches Elektrizitätswerk
SACOI	Sardinia-Corsica-Italy
SBP	Schlaich, Bergermann & Partner
SEE	Solar Energy Economy
SEGS	Solar Electricity Generating System
SEMC	Southern and Eastern Mediterranean Countries
SNL	Sandia National Laboratory
SOKRATES	Solarthermische Kraftwerkstechnologie für den Schutz des Erdklimas
STEPS	Site Elevation for Concentrating Solar Power Systems
STP	Solar Thermal Power Plant
TESIS	Trans-European Synchronously Interconnected System
UBA	Umweltbundesamt (Federal Environmental Agency)
UCTPE	Union for the Co-ordination of Production and Transmission of Electricity
UCTE	Union for the Co-ordination of Transmission of Electricity
UHVDC	Ultra High Voltage Direct Current

UNEP-WCMC	United Nations Environment Programme - World Conservation Monitoring Centre
UNESCO	United Nations Educational, Scientific and Cultural Organization
USGS	U.S. Geological Survey
UVP	Umweltverträglichkeitsprüfung (Environmental Impact Assessment)
UVPG	Gesetz zur Umweltverträglichkeitsprüfung (Law to the Environmental Impact Assessment)
VBA	Visual Basic for Applications
VDE	Verband der Elektrotechniker
VDEW	Verband der Elektrizitätswirtschaft
VPE	Vernetztes Polyethylen
WDPA	World Database on Protected Areas
WGS84	World Geodetic System 1984
WHO	World Heritage Organization
WI	Wuppertaler Institut

Units

W, kW, MW	Watt, Kilo watt, Mega watt
kWh, GWh, TWh	Kilo watt hour, Giga watt hour, Tera watt hour
kWh _{el}	Kilo watt hour, electric
MJ	Mega joule
ppb, ppm	Parts per billion, parts per million
V, kV, μ V	Volt, Kilo volt, Mikro volt
A, mA, MVA	Ampere, Milli ampere, Mega volt ampere
μ T	Mikro tesla
Ω	Ohm
Hz, kHz, GHz	Hertz, Kilo hertz, Giga hertz
dB	Decibel
$^{\circ}$ C	Degree Celsius
K	Kelvin

1 Introduction

The long-term expansion of a sustainable energy supply should meet all criterions of the Agenda 21 (Rio Agenda 21, 1992). This is not achievable without including renewable energies as the conventional fossil and nuclear power economy shows serious deficits regarding these criterions. A sustainable energy supply is characterized by a low consumption of resources, the compatibility with the climate, a riskless energy production and a fair energy distribution between industrialized and developing countries and between generations respectively. These principles stand in contrast to the present energy supply, which, moreover, is approaching a continuous increase in costs in the near future because of decreasing resources, among other things. If external costs for environmental damages were included, an additional increase in costs would be the consequence.

The environmental impacts, which are caused by using fossil sources, are mainly emissions during the plant operation. These emissions endanger human health, push the acidification and eutrophication processes in ecosystems and support global warming. Here limits are often reached concerning the ability of regeneration of some ecosystems.

Besides, there is still a certain difficulty registering, valuating and quantifying environmental impacts exactly. The assumption of that is a causal correlation between the impact and the resultant damage (BMU, 2004a). However, global warming due to the release of CO₂, N₂O and CH₄ is mainly considered as real. That is why many countries, among them Germany¹, set themselves concrete goals to reduce the industrial production of CO₂.

The impacts through the use of renewable energy sources are exclusively caused by material and energetic expenditures regarding the production of construction materials and the construction of power plant installations. Lower external costs result because of this. These costs and the investment costs, which also decrease with time, could reach together the cost level of fossil energies till 2030 at the

¹ The share of renewables of primary energy should be doubled until 2010, from that time the share should be increased by 10 % per decade so that in 2050 a share of 50 % can be reached. For the generation of current even a share of 68 % is aspired. With it and additional increases of efficiency and savings Germany wants to achieve a reduction of the CO₂-Output by 80 % compared with 1990 (Kyoto-Goal minus 21 % until 2010) (BMU, 2004b).

latest (BMU, 2004a). Nevertheless, immediate action is needed to establish renewable energies on the market if the lifetime of plants and the time for developing new technologies are considered.

The potential of renewable energy resources is unlimited, but there can be differences in spatial distribution and temporal deviations. The area around the tropic in North Africa belongs to the regions with the highest solar radiation intensity of the world and is therefore populated sparsely. A fast expansion of renewable energies should take account of foreign resources as well as state-owned resources. Especially the North African potential of solar radiation is far beyond the on-site demand so that a transcontinental export of solar electricity could be a source of revenue in the long term for these regions. On the other hand the import of solar electricity could benefit the European countries to fulfil their commitment for the reduction of carbon emissions.

The recent situation of energy supply in Europe together with the existing infrastructure should be considered in the second section of this thesis. Compared with this the potential of the solar thermal power technology is described to use the solar energy resources in North Africa.

The third section looks into different technologies to transmit electric energy. At the same time these technologies are compared with each other. Environmental impacts are explained in the fifth and seventh section.

Afterwards three lines connecting the regions of supply in North Africa with the regions of demand in Europe shall be modelled by means of collected findings. The course of the transmission lines is selected under ecological aspects and with help of a Geographical Information System.

Then a balance-sheet of impacts, which are correlated with the entire project, is prepared in the tenth section. At the end of this comprehensive consideration the question has to be answered, whether and to which extent the import of solar current is conducive to establish a sustainable energy supply. For that purpose the results from the eco-balance are compared, among other things, with a reference energy mix, which is mainly composed of fossil energy sources.

2 Electricity supply in Europe and North Africa

2.1 Present electricity supply

All natural energy sources that are not transformed or refined by technological processes are described as primary energy carrier like mineral oil, natural gas, coal and uranium. Renewable energies like solar radiation, wind power, geothermal energy and biomass also belongs to it. These forms of energy are transformed into secondary energy, which is directly usable or transportable. Nevertheless, the transformation in electric energy, petrol or hydrogen involves losses in the form of heat. The actual energy supplied to the consumer is called final energy. This energy is transformed into useful energy again, which appears as light of a bulb or heat of a heating system. Here additional losses occur, depending on the degree of efficiency of the respective end user (Beck, 2000).

Electricity plays an important role in the technical and information age as it can be derived from all primary energies and transformed very easily into other forms of energy. In addition to this, it can be transported with low costs. Electric energy is linked to charge carrier and appears as electric current or charge in a storage battery or capacitor. If charge carrier in an electric field move from a higher potential to a lower one, a flow of electric current occurs. The transport of charge carrier is linked to the electric field, whereas the wire only determines the direction of the flow.

The demand of electricity underlies daily and seasonal variations. Figure 1 shows the typical course of the day of the electric load curves, which is representative of Germany, for several months of the year 2000. In winter the maximum power of nearly 75,000 MW is retrieved during lunchtime and in the evening. Altogether the load curves move on a high level and only decrease perceptibly after midnight. The demand is generally lower in summer, displaying only at lunchtime a distinct peak.

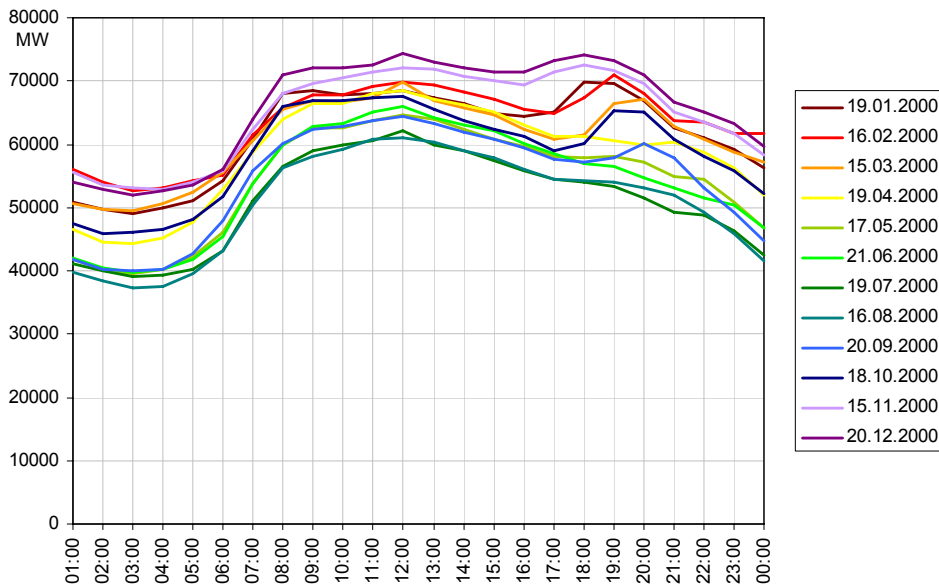


Fig. 1: Course of the day of the power demand in Germany every third Wednesday of the month in the year 2000 (Source: ESA, 2004).

A disadvantage of electric energy is that it can only be stored in small units. It means that the equivalent quantity of power generated has to be transported and used up at the same time in order to meet the need. This balance of power is an expression of the law of supply and demand (Beck, 2000).

The regulation happens by connecting and disconnecting power plants, among other things. Here the base demand is met from not adjustable run-of-river power plants and nuclear power plants (base load). Moreover, lignite power plants are used for that. Slight rises of the demand can be compensated by connecting hard coal power plants (medium load). Additional required energy (peak load) is provided by gas turbine power plants and pumped hydro power plants as figure 2 shows (Leuschner, 2005).

Altogether the electric energy supplied is a mix of different sources of energy, which must be tapped and mined respectively with different technologies. The electricity mix of the European interconnected network called UCTE of the year 2004 is illustrated in figure 3. The present situation, which is based on the use of numerous large power plants that supply electricity downhill to many decentralized consumers, is termed a central power supply. Up to now the potentials of decentralized resources of energy like renewables have been exploited just to a small degree. Hydropower is an exception of that with a share of 12.9 % of the total generation. The rest is provided by conventional power plants with a share of 52

%, by nuclear power plants with a share of 32 % and by the remaining renewables with a share of 2.6 %. Overall share of renewable energies comes to approximately 16 % in 2004. Given these facts, the aim to achieve a share of 22 % in Europe in 2010 is not so far away (UCTE, 2005a).

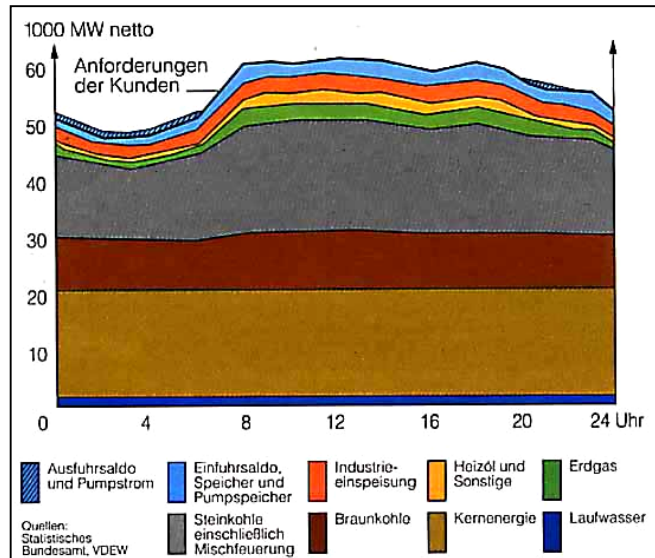


Fig. 2: Utilization of power plants to meet the base load, medium load and top load (Source: Statistisches Bundesamt/VDEW, in: Leuschner, 2005).

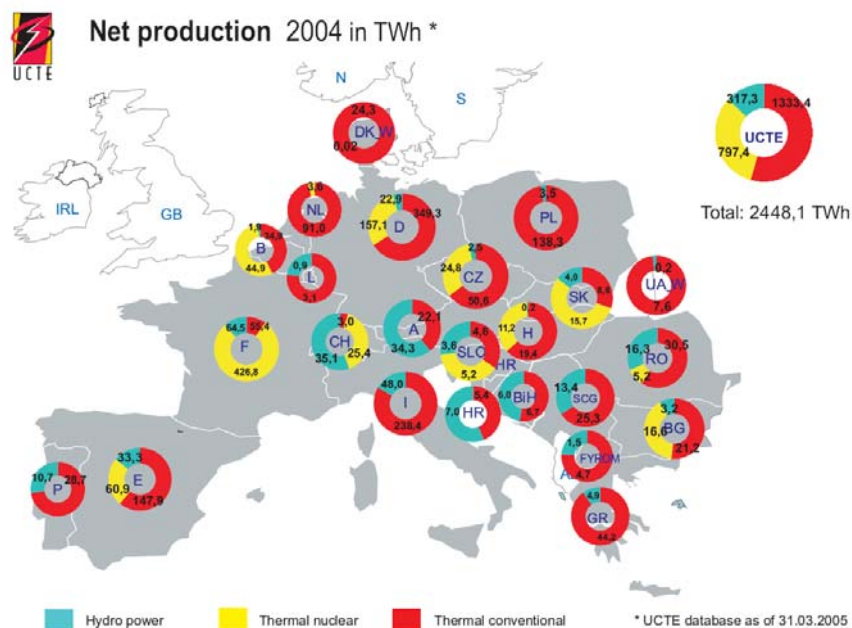


Fig. 3: Electricity mix 2004 within the UCTE (Source: UCTE, 2005b).

2.2 Utilization of renewable energy sources

In the long term the present energy system is not able to guarantee a reliable energy supply for all nations of the world. The constant growth of population and the technological development cause a worldwide increase in the energy demand, until 2050 about 33 % compared to 2000 (Nitsch, 2003), while fossil reserves run short. Even today there are obvious bottlenecks in providing electric energy and fuels in particular, whereby the prices are rising continuously. The statistical reach of mineral oil and gas is just 43 years and 64 years respectively with reference to 2001 and on the assumption of a steady consumption. Uranium has a reach of 40 years without considering the processing of nuclear fuel. The reach of coal is with 200 years the longest (BGR, 2003 in: BMU, 2004b).

Alternatives must be found which guarantee a sure energy supply and preserve the climate and the environment. Besides, this energy must be provided free of risks and with low costs in order to avoid military conflicts on energy resources and an additional, environmental pollution. Renewable energies meet all these requirements of a sustainable energy supply today and in the future (BMU, 2004b).

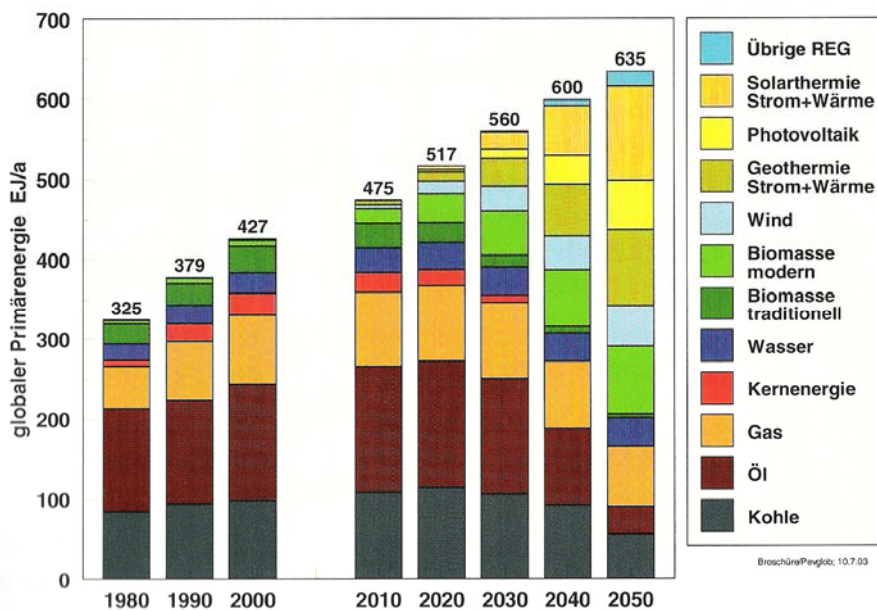


Fig. 4: 'SEE' Ideal scenario of a sustainable, global energy supply until 2050 (Source: Nitsch, 2003).

The scenario 'SEE' shows one possible way to a sustainable, global energy supply until 2050, when renewables meet 73 % of the primary energy demand. All renewable energy sources are substantially involved in it. Nuclear energy is totally given up by 2040 and, above all, the share of mineral oil is reduced about 75 % in 2050 in comparison with 2000. From 2030 this scenario also contains a noticeable share of contribution of solar energy composed of one third photovoltaic and two thirds solar thermal energy. The latter contains solar collectors for the heat supply and solar thermal power plants, whose technology is explained in more detail in the next section.

2.2.1 Solar thermal power plants

Solar thermal power plants are systems concentrating the sunlight. The light is reflected by the surface of a mirror and, in case of a Parabolic Trough or Linear Fresnel system, directed to a central absorber tube, where synthetic heat-transfer oil is heated up to 400 °C or steam is directly produced by evaporating water. In case of oil cooling, the oil is led to a heat exchanger, where the energy can be transferred to evaporate water. The resulting steam drives a steam turbine, which in the end generates electric current.

Solar Tower Systems make use of air or salt as heat carrier. In this way, temperatures over 800 °C can be achieved making it possible to run a gas turbine and afterwards a steam turbine (GuD). Top solar-electric efficiencies lie between 18 - 23 %.

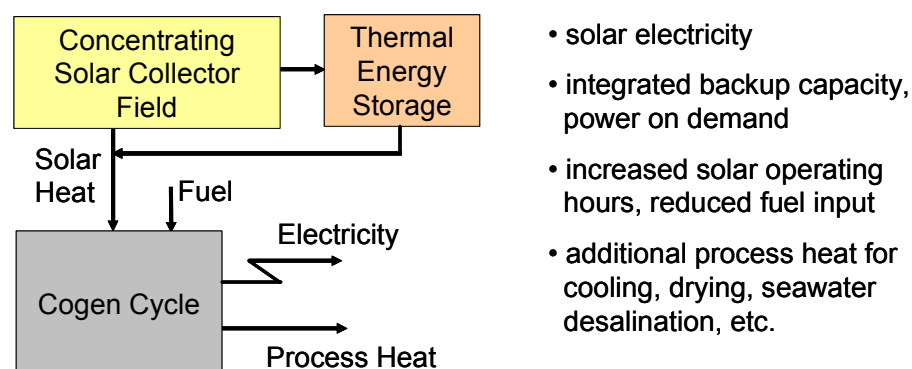


Fig. 5: Principle of a combined current and heat production by solar thermal power plants (Source: DLR, 2005).

Currently, a solar thermal power capacity of 354 MW² is installed worldwide. Within a ten years period a power capacity of 7000 MW could be established (Trieb et al., 1998). A profitable use of such systems depends on the irradiation potential and therefore the levelized electricity costs as well. The latter are the costs which must be expended for the generation of one kilowatt hour of electric energy. Storage of heat guarantees the plant operation during the daytime when there is no radiation available. Till now the broad launch to the market of this technology has not been successful yet, but with the increase in fossil energy costs this kind of utilization of renewable energies becomes visibly competitive.



Fig. 6: Different kinds of solar thermal power plants from the upper left corner clockwise: Linear Fresnel project (Solarmundo), Parabolic Trough ‘SEGS’ (California, PSI), Paraboloid Dish Sterling (SBP), Tower System project ‘Solar Two’ (California, SNL) (Source: DLR, 2005; Trieb & Milow, 2000).

2.2.2 Irradiation potential in the Mediterranean region

The efficient use of a solar thermal power plant requires a high, direct solar irradiation at the location. This requirement is not met in Central Europe. At the German Aerospace Centre (DLR) a tool was developed to derive the Direct Normal Irradiation (DNI) from remote sensing data in a high temporal (1h) and spatial (1km) resolution. The DNI is the amount of energy which hits the mirror

² Altogether nine parabolic trough systems ‘SEGS’ with an overall power of 354 MW have been run in hybrid mode since the middle of the eighties in California (75 % solar, 25 % fossil).

perpendicular. An exact description of the tool can be found in Schillings et al. (2003).

Figure 7 shows the annual sum of Direct Normal Solar Irradiation for the year 2002 in the Mediterranean region. The best locations with up to 3000 kWh/m² lie in the latitude of the North African tropic (approximately 23° northern latitude) and mostly in uninhabited areas of the desert. European states, which are adjacent to the Mediterranean Sea, have values around 2000 kWh/m² and less. In Central Europe the average values amount to 700 kWh/m². In these latitudes there are also strong daily and seasonal variations of the irradiation through which a continuous plant operation is not assured.

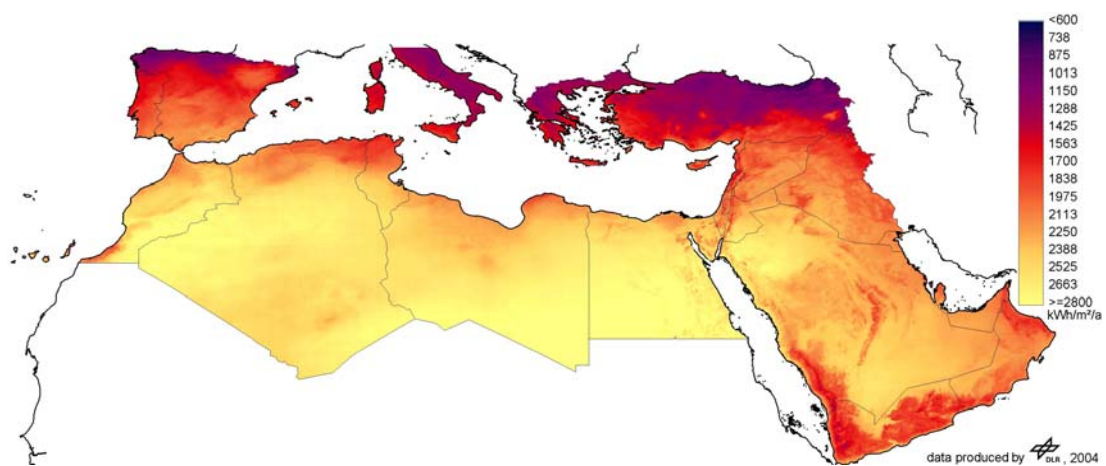


Fig. 7: Annual sum 2002 of the Direct Normal Solar Irradiation [kWh/m²] in the Mediterranean countries and on the Arabic peninsula (Source: DLR, 2005).

In figure 8 the monthly energy yield of a solar thermal power plant is shown at locations with different irradiation. The site *El Kharga* in Egypt represents the best case of all. Throughout the whole year the energy yield stays at almost 100 %, just in wintertime it can decline to approximately 80 %. The more the site is located to the North, the more distinct this decline of the yield looks. In *Madrid* and *Freiburg* values less than 20 % are achieved in wintertime. Only in summertime there is a similar high level of yield like in Egypt reached in *Madrid*.

The figures 9-11 represent the hourly monthly mean of the DNI for the three sites and the hourly monthly mean of the energy yield of a 50 MW 'SEGS' power plant with storage technology. This simulation demonstrates once more the different plant utilization at various sites and identifies *El Kharga* as the best location for a base load operation (*Meteonorm, 2005).

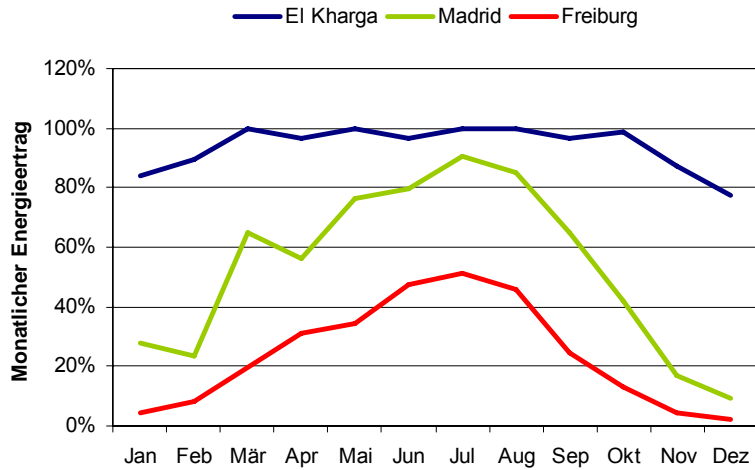


Fig. 8: Monthly energy yield of a solar thermal power plant at sites with a different irradiation potential (Source: *Meteonorm, 2005).

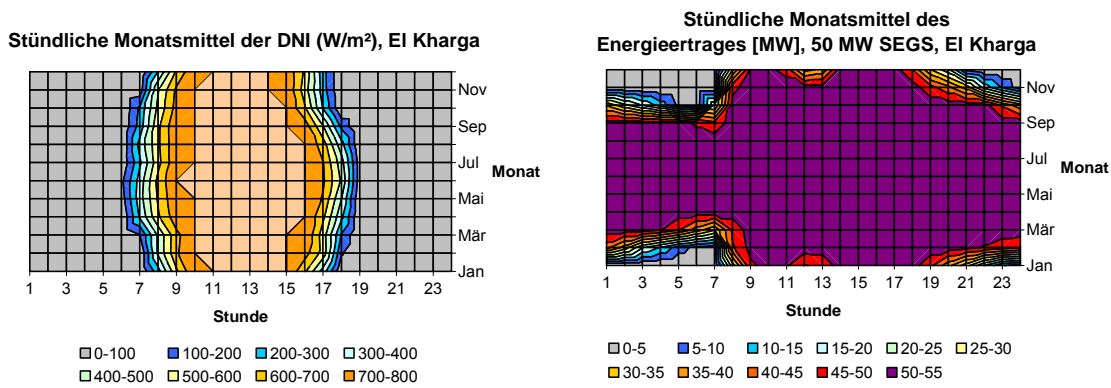


Fig. 9: Plant simulation at the site El Kharga in Egypt.

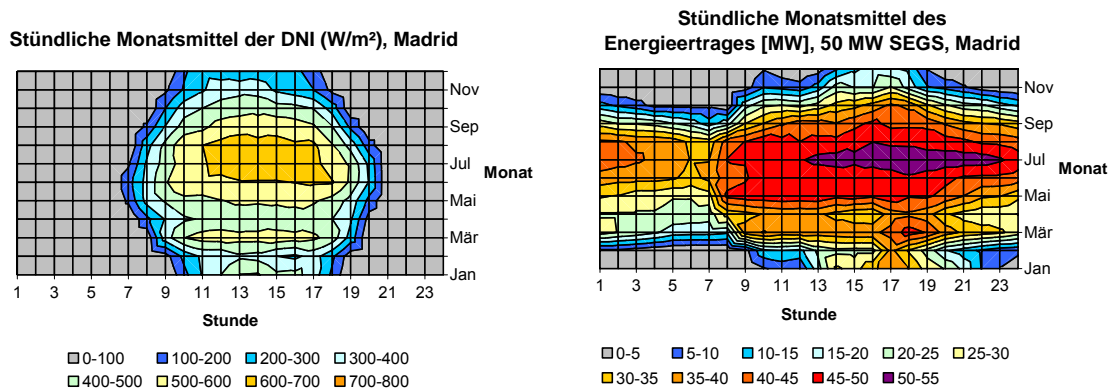


Fig. 10: Plant simulation at the site Madrid in Spain.

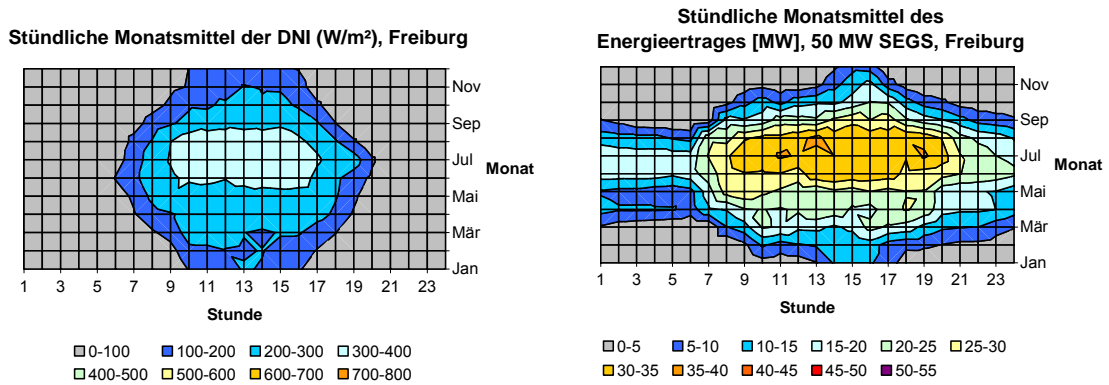


Fig. 11: Plant simulation at the site Freiburg in Germany.

The large solar thermal potentials are attached to remote areas in North Africa and can be tapped for use in Europe only via a power supply line³ connecting both regions. The following section will show to which extent these resources could make a contribution to meet the European electricity need.

2.2.3 Total yield of the solar thermal potential

An area of 3.49 million km² is available for potential locations of solar thermal power plants in the North African countries Morocco, Algeria, Tunisia, Libya and Egypt (DLR, 2005). If a solar electricity yield of 250 GWh_{el}/km² is taken as base for this area, a yield of 872,500 TWh_{el}/y would result. The actual world's energy demand of 16,076 TWh/y could theoretically be met many times better (BMU, 2004b; Statistisches Bundesamt, 2004).

In other words, an area of 254 km x 254 km would be enough to meet the total electricity demand of the world. The amount of electricity needed by the EU-25 states could be produced on an area of 110 km x 110 km. For Germany with a demand of 500 TWh/y an area of 45 km x 45 km is required, which concerns 0.03 % of all suited areas in North Africa (BMU, 2004b).

These considerations only serve to point at the large potential of this energy resource and technology respectively. It should not give the impression to be the only option for the expansion of renewable energies. Rather the point is to use all

³ The shipment of electrolytic hydrogen is not ready to be competitively brought on the market yet and that is why it is not taken into account here (Wirtz & Schuchardt, 2003).

renewable energies, which can be found in a respective country, and combine them all together to a well-balanced mix. Only if the demand increases beyond the national economic supply potentials, the supply of renewable energy by import solar electricity from solar thermal power plants is reasonable.

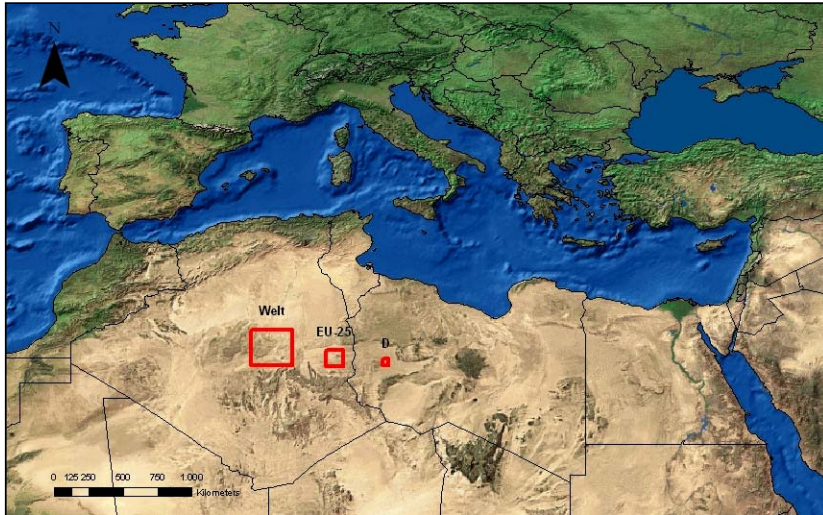


Fig. 12: Theoretical space requirement to meet the electricity demand of the world, Europe (EU-25) and Germany (Data from DLR, 2005).

Community for climate protection

Since the incipient industrialization the concentration of carbon dioxide has increased about a quarter to 360 ppm in the earth's atmosphere. This causes a rise in the air temperature near the ground of 0.6 ± 0.2 °C. A concentration of 450 ppm should not be exceeded until the end of the 21st century to keep the rise in temperature in the lower range. Otherwise an average increase in temperature of 1.4 - 5.8 °C could occur according to IPCC (BMU, 2004b). The emissions of carbon dioxide must be halved till the year 2100 to avert a climate change and all resulting, negative impacts on the biosphere. This aim can only be reached with a global community for climate protection.

Figure 13 indicates the synergies resulting from an international team work for the transmission of solar current from North Africa to Europe.

Climate changes concern the whole biosphere, but particularly areas of dense population, coastal zones and sensitive ecosystems are in serious danger. The energy supply must develop more into the direction of renewables to counteract

this. As already mentioned, the potential of solar energy and the available space are de facto unlimited in North Africa. The European countries could provide 'Know How' and enough capital for the project.

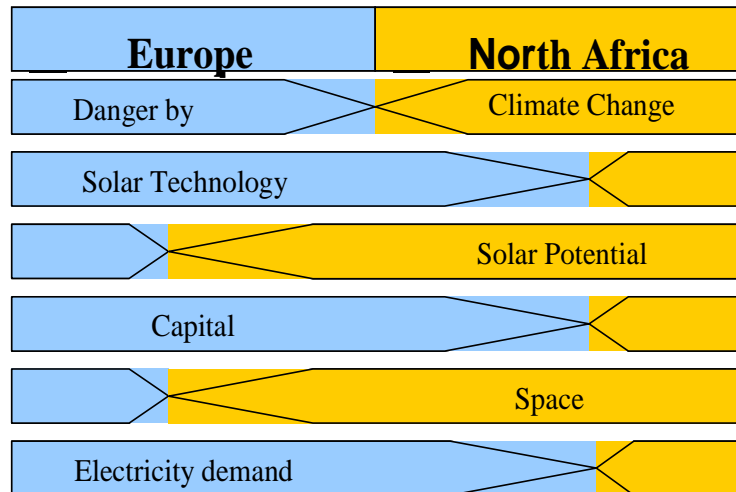


Fig. 13: Synergies between Europe and North Africa (Source: Knies & Bennouna, 1999).

The actual incentive for such a venture is, of course, the high electricity demand of the industrialized countries. Besides, it must not be forgotten that high domestic requirements of electricity and water are also foreseen in the near future on the African continent due to a high increase in population and the continuous economic development of the several countries. Here the desalination of seawater with solar thermal power plants could also be an interesting possibility. Apart from it, labour could be created and the political stability could be secured.

2.3 Energy supply networks

In this section and the following the 'Status Quo' of the European and North African energy transmission networks is described. First of all the basic features of these networks are explained in more detail and then their suitability for the transmission of solar electricity, which is produced in a decentralised way, is shown.

An energy supply network consists of different elements. At the beginning a turbine in a power plant is driven by exploiting a certain energy source. This turbine drives a generator. There, the mechanical energy is transformed into electric energy by the process of electro-magnetic induction. The alternating

current produced this way is also called inductive current. Voltages up to 30 kV can usually be produced by the plant itself. After that the voltage of alternating current can be increased by transformers for the purpose of transmitting electric energy over long distances. The voltage level is fixed in dependence on the power and the transport distance in order to transmit the current efficiently and with the lowest losses. A thumb rule to choose a suitable rated voltage is: transmission length in kilometre is equivalent to transmission voltage in kilovolt.

The European electricity supply network is very complex and operates on different voltage levels. Table 1 contains exemplarily all existing voltage levels in Germany and their function.

In wide parts of the UCTE 380 kV is the highest voltage level, whereas transmission voltages of 500 kV, 750 kV and even 1200 kV are used in other countries outside the UCTE, for instance Russia, in order to bridge very long distances. At a voltage over 800 kV it is also spoken of ultra high voltage (Kießling et al., 2001).

Tab. 1: Voltage levels inside Germany.

Rated voltage	Level	Space	Function
380 kV	extra-high voltage	overland	transport and distribution
220 kV	extra-high voltage	overland	distribution, supply of extended areas
110 kV	high voltage	national	supply of congested areas, railway, major industry
10/20 kV	medium voltage	regional	supply of industry, office building
0,23/0,4 kV	low voltage	local	supply of business, home

With the foundation of the *Union for the Co-ordination of Production and Transmission of Electricity* (UCPTE) in the year 1951 the network operators of 11 Central European states have decided on operating their networks synchronously with a frequency of 50 Hertz. The original intention of today's largest synchronous network was to transmit electricity by a stable and reliable system. Currently, the union counts 23 member states, 33 transmission providers and 230,000 km in the high voltage network. In 2004 430 million inhabitants were supplied with almost 2500 TWh at an installed plant power of 560 GW. Since 1999 the union has gone under the name UCTE (UCTE, 2005a).

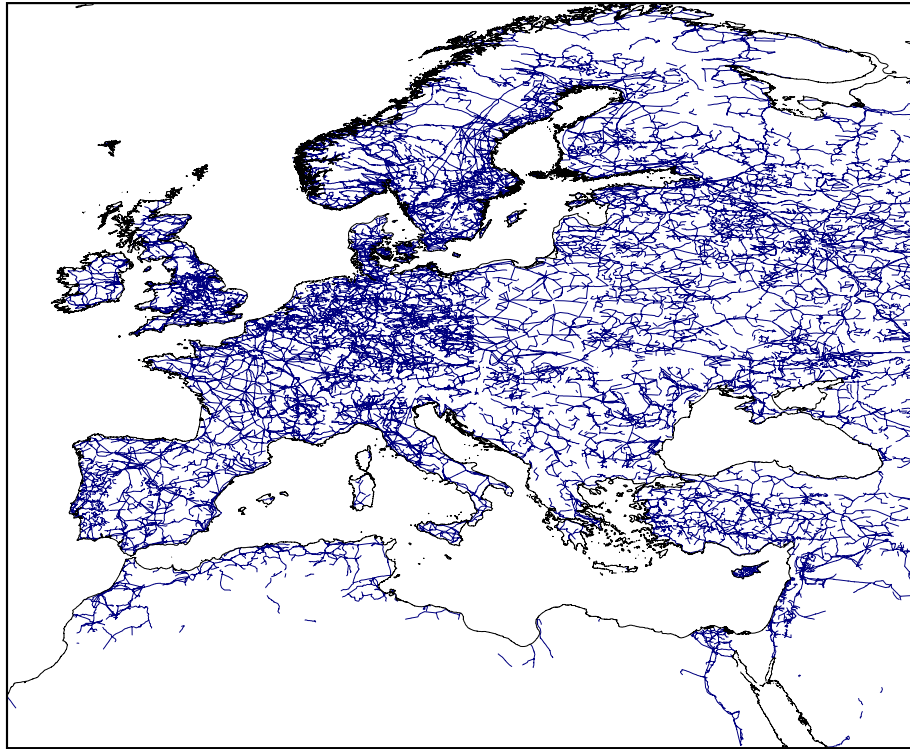


Fig. 14: European and North African energy supply system (Source: *Ph.D., 1998).

The benefits of such a consolidation are: to gain additional reserve capacity and to easily compensate local power and plant outages respectively. The so-called 'n-1 criteria' guarantees a secure supply by substituting one broken plant for another intact. Beside a higher load of the power plants, the electricity exchange over national borders is made easier. In the year 2004 electricity exchanges inside the UCTE interconnection network amounted to approximately 270 TWh for import and 281 TWh for export (UCTE, 2005a).

Both the British island network and the network of NORDEL are linked to the UCTE network by submarine cables. Since 1994 some European states have been able to make use of the major water power potentials of Scandinavia. The CENTREL states⁴ have been connected to the interconnection network since 1995 and have been full members only for short time. Since 1997 the interconnection with the MAGHREB⁵ states has been realized by a submarine cable, through which approximately 1.5 TWh/y have been exchanged. Rumania and Bulgaria have been the latest members since 2003. UCTE 2 as a former part of the

⁴ Czech Republic, Slovakia, Hungary, Poland

⁵ Morocco, Algeria, Tunisia

synchronous network was separated by the war in former Yugoslavia in the year 1991 and has been integrated again recently (UCTE, 2005a).

Figure 15 shows the entire region where the networks are operated synchronously (TESIS, red mark). Its expansion will be pushed in many places. In the near future electricity transmissions are planned between the UCTE block and the Turkish block and the interconnected network LEJLS⁶ (UCTE, 2005a). Nevertheless, even the well-developed network of the UCTE must be reinforced in many places by new lines in order to provide a secure supply.

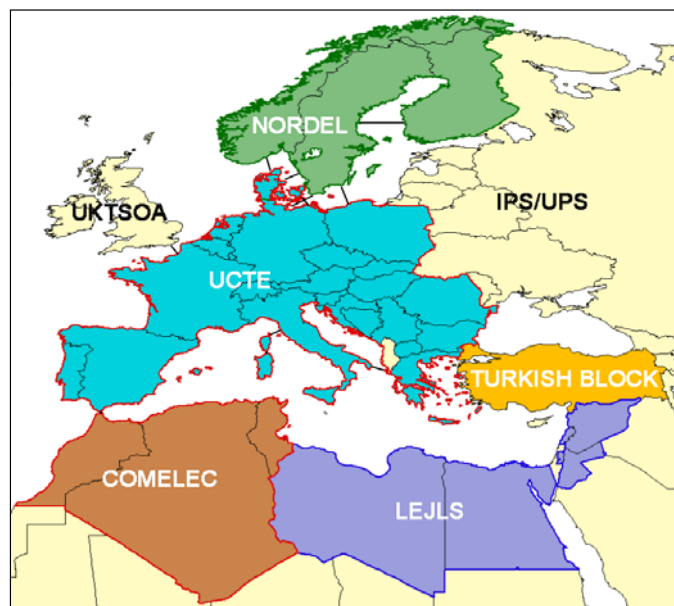


Fig. 15: Interconnected networks in the Mediterranean region.

2.4 Closing of the Mediterranean ring

As mentioned above, the expansion of the UCTE network on the North African states, the Balkan and the Arabic peninsula is planned. The so-called 'MED-Ring-Project' of the SEMC⁷ and the NMC⁸ is aimed at closing the networks around the Mediterranean Sea. But even today electricity imports and exports take place between these countries. Figure 16 shows the international electricity transmission in the year 2000. Typical countries which import electricity are Italy, Morocco, Albania and Lebanon. France proves to be the biggest electricity exporter with 24.6 TWh, mainly based on nuclear energy. In 2000 the exchange came to a total

⁶ Libya, Egypt, Jordan, Lebanon, Syria

⁷ SEMC: Algeria, Tunisia, Egypt, Jordan, Syria, Turkey, Lebanon, Morocco, Libya

⁸ NMC: Spain, Portugal, France, Italy, Greece, Slovenia, Croatia, Yugoslavia, Macedonia, Albania

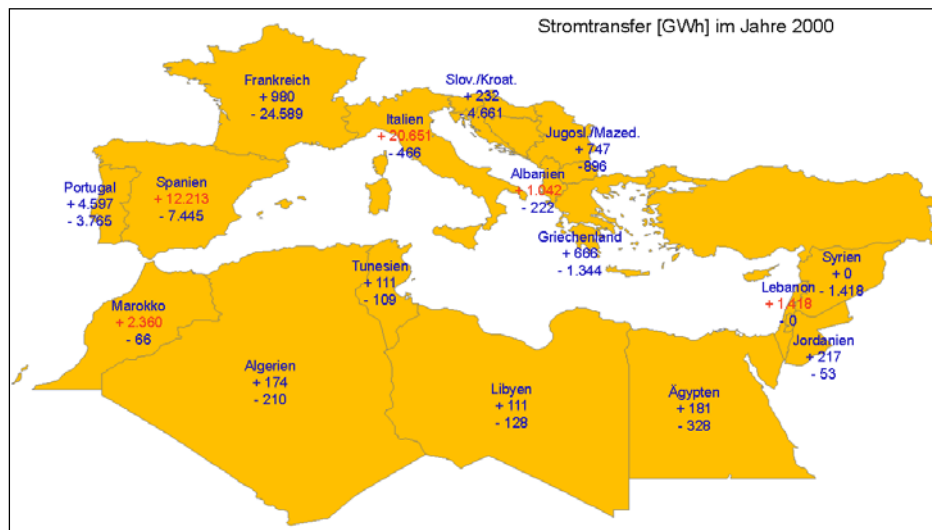


Fig. 16: Imports (+) and exports (-) in GWh between Mediterranean countries in the year 2000 (Source: nach OME, 2003).

of 45 TWh/y, but only 5 TWh/y were exchanged between the SEMC. In 2010 the whole Mediterranean electricity trade is expected to be 75 TWh/y (OME, 2003).

The major part of the existing network is based on the 220 kV voltage level. Only between Egypt, Jordan and Syria and between the several Mediterranean neighbouring states of the EU exist 380 kV lines. Since 2003 there has been a single 630 kV interconnection between Libya and Tunisia. Altogether the network reaches its limit of capacity of 350 MW. It must be reinforced at weak spots with further extra-high voltage lines of the 380 kV level and above so that future loads can be carried. Figure 17 and Table 2 contain different projects concerning additional interconnections between several countries or a general reinforcement of the existing network like the ELTAM project. Some of these projects refer to high voltage direct current (HVDC), which is described in detail in section 3.

The development of the MED ring makes progress. Recently, the interconnection between Tunisia and Libya has been checked. Final closing of the ring by coupling the Turkish block and the UCTE block will result from the connection between Syria and Turkey probably in 2006 (Eurelectric, 2003). There are too many bottlenecks yet in order to transmit large power ratings to congested areas of Europe and especially between both continents. Moreover, the integration of electric current from renewables is seen as problematically by the transmission providers, since possible fluctuations of load cause a higher need of regulation. These difficulties could be avoided if a base load of the solar thermal power plant

is assumed, which can be realized by a proper location and a thermal storage. Ultimately a direct link between regions of supply and regions of demand is needed for the transmission of solar current. Currently available technologies for this project are described in more detail in the next section.

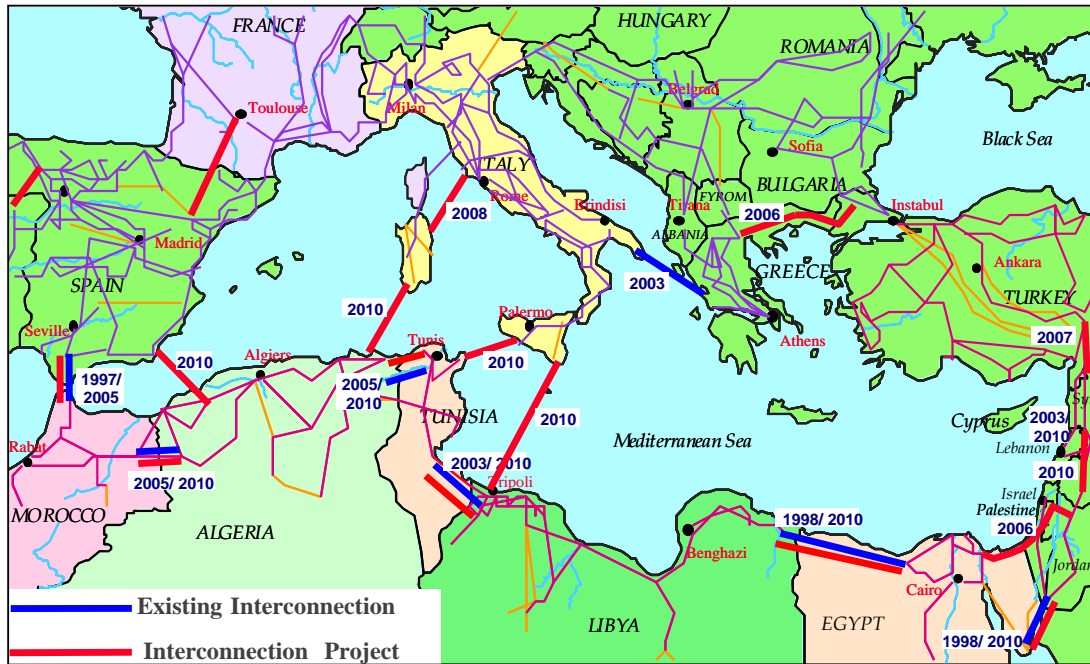


Fig. 17: Planned closing of the ring (Source: Hafner, 2005).

Tab. 2: Planned interconnections between Mediterranean neighbouring states (OME, 2003).

Project	Thermal limit [A]	Length [km]	Voltage [kV]	Design	Year of operation
Spain-Morocco (2.)	960	28,5	400 AC	Submarine cable	2005
Spain-Algeria	2000		500 DC	Submarine cable	2005/2010
Italy-Algeria			400/500 DC	Submarine cable	2010
Italy	Tunisia	500	500 DC	Submarine cable	2010
Algeria-Morocco (3.)	2 x 1720	250	220 (400) AC	Submarine cable	2003 (2005)
Algeria-Tunisia (5.)	1720	120	220 (400) AC	Submarine cable	2004 (2010)
Tunisia-Libya (3.)		210	400 AC	Submarine cable	2010
Libya-Egypt (2.)			400/500 AC	Overhead Line	2010
Reinforcement (ELTAM)			400 AC	Overhead Line	2010
Egypt-Jordan (2.)	880	20	500/400 DC	Submarine cable	2008
Egypt-Palästina	1440		220	Overhead Line	2005
Palästina (WB-Gaza)	1440		220/240	Overhead Line	2006
Palästina-Jordan	1450		400	Overhead Line	2006
Jordan-Syria (2.)		210	400 AC	Overhead Line	2010
Lebanon-Syria	1660	22	400 AC	Overhead Line	2003 (2010)
Syria-Turkey	1440	124	400 AC	Overhead Line	2007
Turkey-Greece	2165/2887	250	400 AC	Overhead Line	2010

3 Basics of the transmission of electricity

3.1 *Energy-technological comparison of overhead line & cable*

Altogether the share of cables at the public mains supply has almost trebled in Germany since 1960 (25 %). Since then the share of overhead lines has decreased continuously from 75 % in 1960 to 29 % in 1995 despite the fact that the circuit length has doubled simultaneously to 1.245.000 km. This means on one hand that most of the new installations were cables and on the other hand that more and more overhead lines were replaced by cables. The low and medium voltage networks were primarily affected by these changes. In 1995 the share of cables amounted to just 4 % in the high voltage field ≥ 110 kV. This situation is transferable on other industrial nations as well (Peschke & v. Olshausen, 1998). Interest in cables rises with the electricity demand of congested areas, quite simply because of lack of space. But also by reasons of environmental protection and fading acceptance in the population, cables have become the preferred alternative to overhead lines.

Purely technically, overhead lines differ from cables by the way of laying and the used dielectric fluid. Air is the natural isolator of an overhead line. Depending on the operating voltage definite distances in the air must be observed, whereas cables can lay closer to each other as their electric field is shielded by specific isolation materials. But there is a reduced heat removal of cables buried in the ground, which in the end reduces their efficiency.

An overhead line is exposed to different effects of the weather, thus it has a higher risk of being damaged than a ground cable. Lightning strikes, wind and ice loads are such influences. Finally, the design of the pylon framework is determined by these influences and the number of circuits carried by the pylon. Because of lack of space up to six circuits on one pylon can often be found in Germany.

Compound conductor wires with different diameters are used in the high voltage and extra-high voltage area respectively. The wires consist of aluminium for the conduction and steel for the tensile strength. They are suspended by long-rod ceramic isolators from the mast. The actual pylon is almost exclusively a lattice steel construction with a concrete fundament. In Germany the Danube type mast

is often used if two circuits have to be carried. Apart from that, there are various, country-specific designs of pylons, but they possibly require wider corridors.

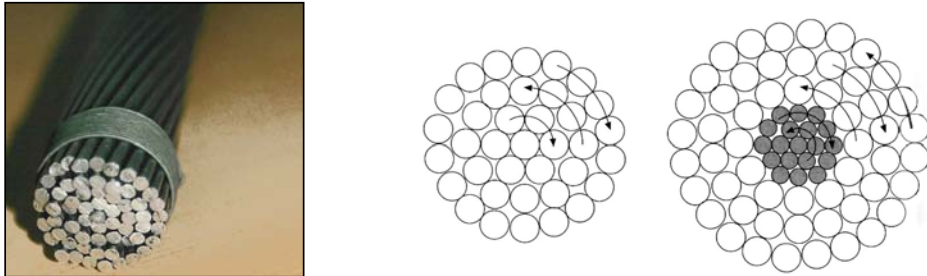


Fig. 18: 400kV conductor (left) and scheme of a compound wire (right)
 (Source: Poweron, 2005; Schlabbach, 2003).

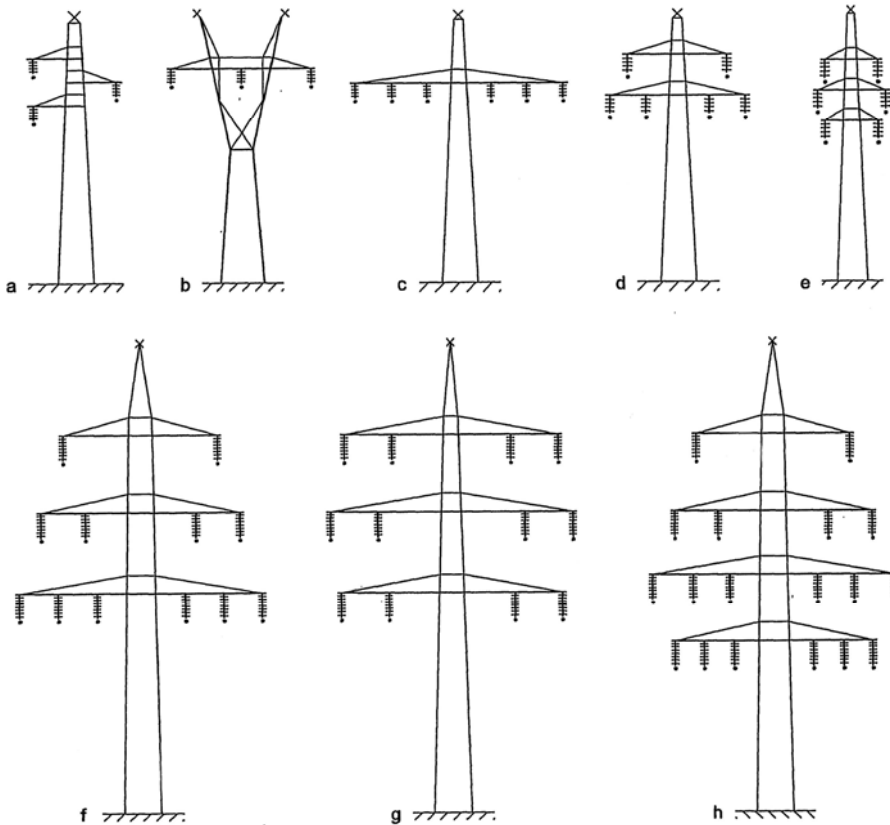


Fig. 19: Mast images for high and extra-high voltage overhead lines:
 a) asymmetric mast, b) 1-level mast with 2 earth wires, c) 1-level mast with 2 circuits and 1 earth wire, d) Danube mast, e) ton mast, f) Danube mast with 4 circuits, g) ton mast with 4 circuits, h) fir-tree mast with 6 circuits (Source: Kießling et al., 2001).

Underground or submarine cables are used as mono conductor in the high voltage area and are constructed as a long-stretched, concentric cylinder with several layers around it. The central, multiple-filament conductor made of copper is surrounded with a paper isolation jacket⁹ impregnated with a high-viscous substance¹⁰. Such a cable is also termed mass-impregnated cable. In case of a LPOF (low pressure oil filled) cable the paper isolation is filled with a low viscosity fluid¹¹ under pressure of some bars. But in the meantime homogenous, synthetic isolations (VPE) are often used for voltages up to 550 kV (VDEW, 2001; Peschke & v. Olshausen, 1998).

Each inner and outer field-smoothing layer (conductive paper and synthetic jacket respectively) prevents from partial discharges in hollow spaces of the isolation by eliminating gaps between isolation and conductor or isolation and screen. A metal sheath made of lead or aluminium protects the cable from outside humidity outside and, at the same time, shields the electric fields arising inside from the environment. The latter function can also be taken over from a screen of copper filaments by conducting leakage currents. Steel armours are used for mechanical protection. Finally, an outer jacket formed by a synthetic sheath of polyethylene or polypropylene protects from corrosion.

In case of synthetic cable a filament screen of copper, which serves the leakage of currents, is used instead of metal sheaths or armours. Additionally, an aluminium or copper foil compounded with the exterior, synthetic sheath protects from water as diffusion barrier.

Due to a higher, technical expenditure concerning the cable manufacture and therefore higher costs, cost and benefit of a cable and overhead line project are often set against one another within a planning approval procedure in Germany. In the end it has to be considered that the maximum load of an overhead line cannot be transmitted with an equivalent quantity of cables. The decision often turns out for the benefit of the overhead line under financial aspects.

⁹ Paper is produced of high-quality spruce or fir wood of Nordic forests, which has a high disruptive strength and little resin because of slow growth.

¹⁰ Nowadays it is used synthetic polybutene (PB) and polyisobutylene (PIB) respectively, formerly a specific mixture of oil and resin.

¹¹ The used isolation oil is a refined product of mineral oil, which is enriched with at least 20 % of synthetic dodecylbenzol (DDB) today.

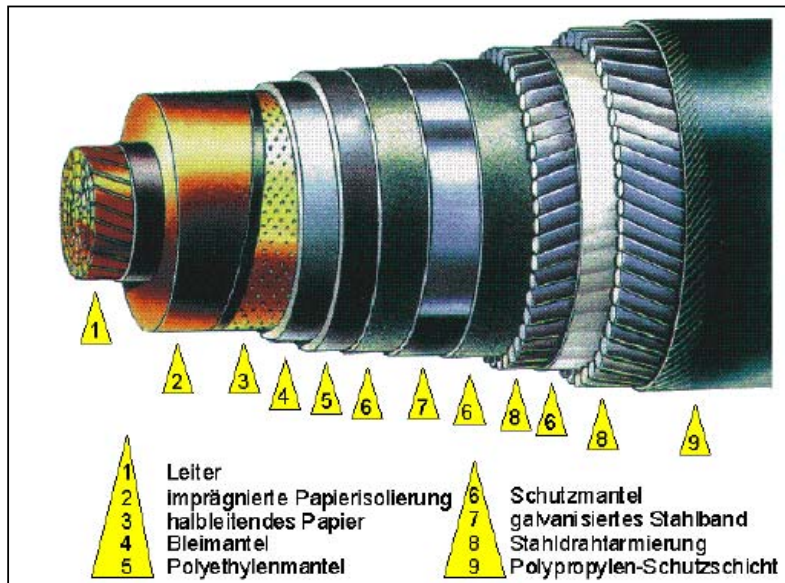


Fig. 20: Scheme of a submarine cable (Source: Kullnick & Marhold, 2000).

3.2 Alternating Current

In the European high voltage area electric energy is mainly transmitted in the form of three-phase alternating current, whose direction and amount changes with a sinusoidal periodicity. The frequency of the European electricity supply network amounts to 50 oscillations per second, which means, that the current flows 50 times per second in the same direction. Here, the current is also called three-phase alternating current because of three time-shifted phases. Single-phase alternating current is mainly applied in public railway traffic.

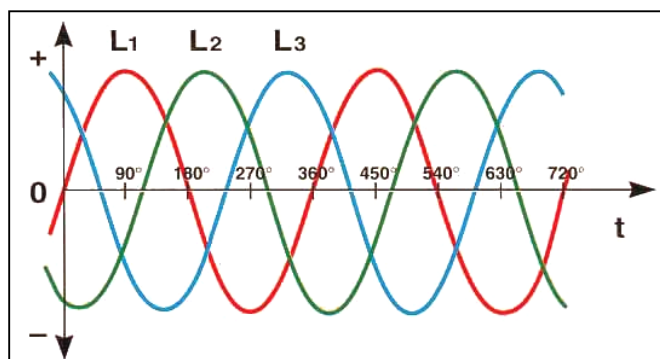


Fig. 21: Three-phase alternating current (Source: Leuschner, 2005).

Alternating current is produced in a power plant by a generator, whose electrical magnet is driven mechanically and passes three 120°-shifted coils during one rotation. Accordingly, the induced alternating currents are also 120°-phase-shifted. Each current is forwarded by the respective conductor. Because with symmetrical load the sum of the three currents amounts to zero at every moment, there is no need to have a return wire like single-phase alternating current.

The decisive advantage of three-phase alternating current is the simple regulation of voltage and frequency. The voltage can be stepped up and stepped down with few losses by a transformer and everywhere it is possible to branch off electrical power with the same. In addition, engines driven by alternating current can be produced small, compact and cheap (Leuschner, 2005).

One disadvantage is that the synchronicity of producer and consumer voltage is absolutely necessary. Otherwise, unwanted swings could lead to serious problems with the network stability. The failure of one conductor means the total failure of the circuit.

Losses of alternating current

The current-carrying conductor produces a magnetic field around itself. If it concerns alternating current, this magnetic field changes periodically and induces a voltage again. Thus the power line behaves like a coil and puts up resistance to the alternating current through self-induction, what in turn causes a decrease in current. In this connection it is spoken of the inductive reactance L when the voltage runs in front of the current at a maximum phase angle of 90°.

In the opposite case alternating current is intensified let through because of the capacitive reactance C so that the voltage runs after the current. The problem of charge storage especially occurs with cables, which behave like a condenser due to their multi-layered structure.

These resistances cause no heat losses in contrast to the ohmic resistance R , but there is a not utilizable reactive power which swings permanently between generator and power source and reduces this way the effective power. Equation 1 represents the correlation between the several resistances once more.

$$Z = R + i\omega L + \frac{1}{i\omega C} \quad [\text{Eq. 1}]$$

Z	impedance
R	effective resistance
L	inductive reactance
C	capacitive reactance
$L+C$	reactance
ω	angular frequency of alternating current ($= 2\pi f$)

The maximum transferable load and transmission length are more limited by the fall of voltage along the line than by the thermal power rating of the conductor. That is why installations for the compensation are used every 600 kilometres in practice (Rudervall et al., 2000).

Losses of an overhead line

In addition to current-dependent losses there are also voltage-dependent losses in the form of gas discharges in areas of heavy curved surface and high field strength. These requirements are fulfilled by the conductors. If then the electric field strength at the conductor surface also called fringe field strength exceeds the disruptive strength of air, the ionization of air molecules is possible. Electron-impact ionization can happen if previously released electrons hit neutral molecules again. The energy needed for that is taken from the electric field.

Such corona discharges can be perceived as a luminous appearance and crackling sounds. Therefore bundle conductors restricting the field strength at the fringe are utilized from 110 kV in Germany. At the same time the transferable load increases because the cross-section of the conductor is apparently enlarged by overlapping of the single fields (see figure 22).

In the annual mean the corona losses amount to approximately 2-3 kW/km for a 400 kV-system (Laures, 2003). Knoepfel (1995) states 1-10 kW/km for a 380 kV system and 2-60 kW/km for a 750 kV system that strongly depends on the respective atmospheric conditions and can be neglected in this order of magnitude.



Fig. 22: 4-bundle conductor of a high voltage line.

Altogether losses in high voltage AC-systems come to 15 %/1000 km (380 kV) and 8 %/1000 km (750 kV) respectively. In addition to this, each transformer station can lose 0.25 % of the energy (Knoepfel, 1995).

Losses of a cable

In case of cables it is also distinguished between current-dependent losses, which only appear while electricity flows, and voltage-dependent losses, which appear under the effect of an electric field in the isolation and therefore are described as dielectric losses.

Current heat losses in the conductor and additional losses in the metallic sheath, screen and armour belong to current-dependent losses. According to equation 1 current heat losses increase quadratically to the current. For that reason it is generally aimed at keeping the current as small as possible by raising the voltage.

Nevertheless, there are ohmic heat losses caused by the conductor material¹², which increase proportionally to the transmission length and furthermore depend on the conductor cross-section and the operational temperature. These current heat losses increase more if the frequency rises due to self-induced turbulent currents in the magnetic field of the conductor. As they are directed to the opposite of the operational current, this current is displaced at the edge of the conductor ('Skin-Effect'). Thus it cannot use the whole cross-section of the conductor and, in addition to this, the risk of exceeding the maximum allowable temperature of the conductor increases because of the high marginal current density.

¹² The specific electric resistance of copper is 0.017 and of aluminium 0.028 $\Omega \cdot \text{mm}^2 \cdot \text{m}^{-1}$ at 20°C.

Moreover, turbulent currents can be generated by magnetic field emissions of adjacent cables, which become more intense with an increasing distance of cables ('Proximity-Effect'). Here a triangle arrangement of phases has a better effect than side by side laying of cables.

Additional losses can occur in the residual metallic components of the cable. Induced current losses (longitudinal-voltage induction) and turbulent current losses in the jacket and the same losses together with magnetisation losses in the steel armour belong to it.

Applicability of an alternating current cable is limited by two aspects (Peschke & v. Olshausen, 1998):

- Maximum transmission length

The capacitive charging current increases proportional to the cable length and overlays the actual effective load at the same time. This is especially the case of cables with a multi-layered isolation. The capacity of a cable rises with the increasing relative permittivity and rated voltage. The maximum transmission length of a 380 kV-cable with 1000 mm² copper conductor and paper isolation amounts to just 35 km due to the capacitive charging current. A VPE-cable has a reach of 50 km instead. If dielectric losses are included, this length is more reduced. The resulting reduction of the voltage endangering stability along the line must be counteracted by compensational measures.

- Maximum transmission capacity

The transmission capacity only increases up to a certain voltage level, which depends on the dielectric properties, and after that decreases again. The higher the dielectric loss digit and the smaller the heat removal, the sooner the economic cut-off voltage is reached. Accordingly, the cut-off voltage of a 1600 mm² copper conductor with paper isolation comes to approximately 500 kV and with a VPE-isolation to more than 1200 kV. The transmission capacity of an underground cable is particularly limited by the removable heat lost. On optimum conditions a maximum heat removal rating of 90 W/m can be realized. Hence there is a thermal breakeven performance of approximately 1000 MVA for an oil-paper cable with 2500 mm² copper conductor and approximately

1450 MVA for a VPE-cable at a transmission voltage of 500 kV. Altogether an AC-cable system can only reach 50 % of the capacity of an overhead system in spite of lower heat losses. For the same transmission capacity it calls for a double cable system, an artificial cooling or a completely different transmission technology.

In figure 23 it is shown, how the transmission capacity of an AC-cable is rapidly reduced with an increasing distance. Moreover, it becomes clear that with an AC-cable at a lower voltage it is possible to bridge long distances, but less energy. Therefore compensational measures would be required, which are not realizable with submarine cables in practice. As long as several decades, direct current technology has been used for submarine cables. There are also advantages on shore. Since there are fewer problems with a bad heat removal, the isolation layer must be less thick, which in turn results in a lower cable price. Besides, a better utilization of the cable is achieved by the transmission of higher loads. In the next section it is gone into the particular technology of direct current.

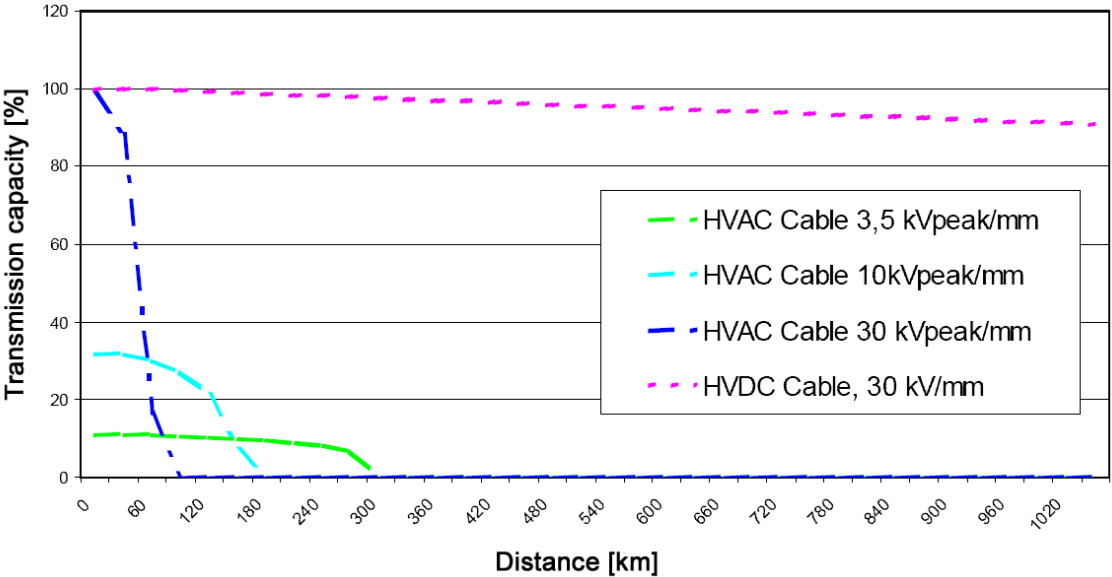


Fig. 23: Comparison of transmission capacities of AC- and DC-cables (Source: Asplund, o. J.).

3.3 Direct current

3.3.1 Technology

Electric direct current flows continuously in one direction with a constant amperage and can be generated by electrochemical processes or by rectification of alternating current. In case of technically generated direct current the amount of amperage can change periodically because of a rest of ripple.

Capacity and losses

The utilization of direct current has got diverse advantages compared with alternating current. First of all the transmission length is only limited by an ohmic resistance. The cheaper the power input is, the less important the heat losses are. Besides, there are no capacitive, inductive or dielectric losses which would be shown as a fall of voltage along the line. Current displacements at the edge of the conductor, which are typical for alternating current, do not matter as well so that the whole cross-section of the conductor can be used, theoretically, until the thermal breakeven performance.

The circumstance that no reactive power is transmitted with direct current causes a further increase in power by transmitting sheer effective power. Reactive power must only be provided for the inverse transformation by the rectifier.

In comparison with a three-phase AC-system of three conductors a high voltage direct current transmission requires two conductors (bipolar case) or just one conductor (monopolar case) while the current flows back via earth (see figure 24). This leads to lower costs for the lines, especially at long distances. The requirements on the line also turn out lower regarding pylon height and width.

If one conductor of a bipolar HVDC fails, a short-term back current is possible for approximately 10 minutes via earth while the transmission capacity is halved. This way much more time is available to bridge areas concerned than in case of a conventional system where failures occur within split seconds (Peschke & v. Olshausen, 1998; Schymroch, 1985).

Stability and controllability

HVDC can contribute to security of the network stability, for instance by connecting power plants with a high energy rating. Because no short-circuit currents can be transmitted, the short-circuit current is equal the nominal current in fact.

A direct current system has no problems with stability in principle and is quickly adjustable via rectifiers. However, rectifiers can only be less overloaded. The controllability of the power flow in amount and direction is also of a particular importance in decentralized markets. Since the source voltage and the voltage at the load are allowed to be asynchronous, HVDC as back-to-back station is predestined to couple networks with different frequencies (400 kV FG, 1966; Schymroch, 1985).

Disadvantages

Direct current has the disadvantage of not being directly transformable to another voltage, by which the erection of networks with different voltage levels becomes difficult as it corresponds to the recent situation of the energy economy. Besides, it is not so easy to switch off the current with conventional switches at a high network voltage. A subsequent branching of power is also difficult in an existing direct current system and is only possible via an additional rectifier, which shows higher investment costs and a higher space requirement than usual power substations (Beck, 2000).

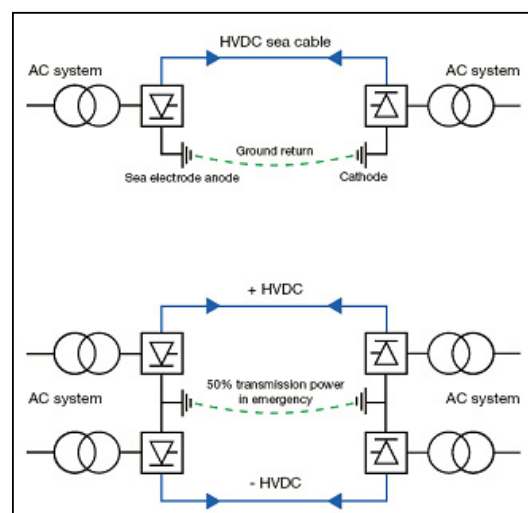


Fig. 24: Schematic diagram of a monopolar (above) and bipolar system (below) (Source: Söderberg & Abrahamsson, 2001).

3.3.2 History of HVDC

The first long-distance transmission of electric energy, where the transmission voltage was higher than the voltage at the load, was a HVDC transmission between Miesbach and Munich in 1882. It was erected by the two engineers Oskar von Miller and Marcel Deprez. This major project with a transmission length of 57 km and a transmission voltage of 2 kV was the proof that electric energy could be economically transmitted over long distances if the voltage is just high enough. The Bavarian hydropower could be tapped via this high voltage line.

The former direct current generators had power and voltage limits, especially at a high number of revolutions of the driving turbine. With the invention of the transformer it became possible to step up alternating current on a higher voltage level than it could be achieved with a generator. After many years of arguments alternating current could succeed, though there was no alternating current engine in the beginning. Direct current was only utilized in suburban traffic, electrolysis and other special applications of the industry. This competitive disadvantage could only be erased with the invention of the mercury vapour rectifier (Lebrecht, 1966).

The first commercial HVDC transmission between *Elbe – Berlin* been ready for action was dismantled after the end of war and put into operation again between *Kashira – Moskow* in the year 1950. It had a length of 100 km, a voltage of 200 kV and a power of 30 MW. Six years later the first submarine cable with a length of 95 km was laid from the Swedish mainland to Gotland. Altogether a power of 20 MW was transmitted at a voltage of 100 kV. In Germany the research into HVDC was resumed in 1959 by the *400kV-Forschungsgemeinschaft e.V.*, which was an association of companies of the electrical industry, on behalf of the *Deutsche Forschungsgemeinschaft*. In the dense interconnection network of Europe there were no areas of application of HVDC, especially as overhead line. HVDC was only used as submarine cable connecting islands with the mainland and tapping the large hydropower potentials in North Europe. In the course of the expansion of the West European interconnection network HVDC became more important as back-to-back station.

3.3.3 Principle of HVDC

The principle of the transmission of electric energy as HVDC transmission is shown in figure 25. First, alternating current, which is produced by the power plant,

is stepped-up on transmission voltage by a transformer. Afterwards alternating current is transformed into direct current by a connected rectifier. The high voltage direct current is then transmitted to demand centres via overhead line or cable. Finally, the direct current must be retransformed into alternating current so that it can be stepped-down on consumer voltage by a transformer.

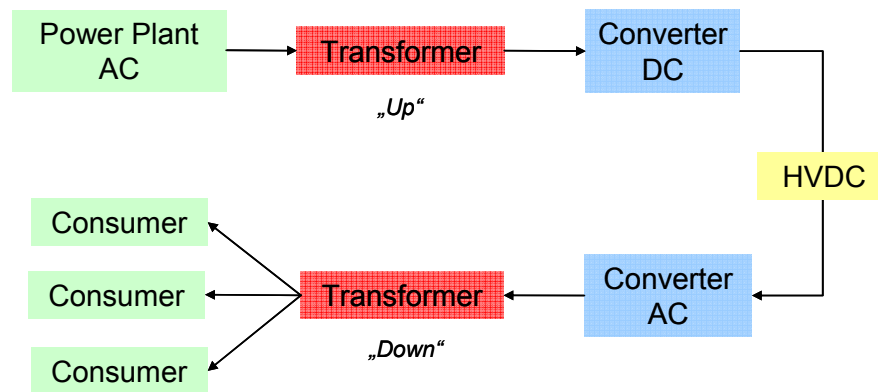


Fig. 25: Schematic diagram of a HVDC transmission.

3.3.4 Possible and existing applications of HVDC

Nowadays a power of about 75,000 MW is transmitted by HVDC lines in more than 92 projects all over the world. Nevertheless, the potential of this transmission technology is not fully utilized. For the long-distance transmission of electricity with overhead lines the voltage level will increase at 800 kV in the near future. This means that one pole will have a capacity of 2500 MW. In this context it is also spoken of 'Ultra High Voltage Direct Current' (UHVDC).

The development to higher transmission voltages is also foreseeable in the cable manufacture. Thus a bipolar ± 600 kV mass-impregnated cable would be able to transfer 2000 MW. Oil-pressure cables would be able to transfer 2400 MW at the same voltage level. Indeed, they can only be used for middle distances. Lately, HVDC-light cables are built in the range of ± 150 kV which are also able to transfer 700 MW (bipolar case) over long distances (ABB, 2005). Hence results the following applications for HVDC:

- 2-point transmission over long distances
- Utilization as submarine cable
- Utilization as underground cable in congested areas

- Connection of asynchronous networks via back-to-back station
- Connection of power plants
- Multi-terminal system (> 2 stations)

Tab. 3: Existing HVDC installations (Source: ABB, 2005).

HVDC/country	Design ^{*)}	Start of operation	Power [MW]	Voltage ±[kV]	Length [km]	System
SACOI/Sardinia-Corsica-Italy	SC, O	1967	300	200	423	Bipole, Multi-terminal
Cahora Bassa/Mozambique-South Africa	O	1977-79	1930	533	1420	Bipole, 2 lines
Inga-Shaba/Congo	O	1982	560	500	1700	2x Monopole
Itaipu/Brasilia	O	1984-87	6300	600	800	Double-Bipole
Québec-New England/Canada-USA	O	1990-92	2000	450	1480	Bipole, Multi-terminal
BalticCable/Swe-Ger	SC	1994	600	450	250	Monopole
SwedPol/Sweden-Poland	SC	2000	600	450	260	Monopole, Metallic return
Italy-Greece	UC, SC, O	2001	500	400	310	Monopole
Murraylink/Australia	UC	2002	220	150	177	Bipole, HVDC Light
NorNed/Nor-NL	SC	2007	700	450	580	2x Monopole

*O – overhead line, SC – submarine cable, UK – underground cable

3.3.5 Overhead line transmission losses

Current-dependent losses

There is only an ohmic resistance R [Ω] in DC circuits, which results from the relation of the voltage U [V] and the amperage I [A] according to the *Ohmic Law*:

$$R = \frac{U}{I} \quad [\text{Eq. 2}]$$

R is also called effective resistance and appears in the form of heat losses. This resistance increases proportional with the length of the conductor and, moreover, depends on the cross-section area. The lower the area is, the closer the passage for the electrons.

The specific, electric resistance ρ represents the material-dependent value of R at a temperature of 20 °C for a conductor cross-section area of 1 mm² and a conductor length of 1 m. The resistance load per length R' [Ω/km] for a certain operating temperature ϑ is calculated with the following equation:

$$R' = 1000 * \frac{\rho}{A * m} [1 + \alpha_{20}(\vartheta - 20^\circ\text{C})] \quad [\text{Eq. 3}]$$

- ρ specific, electric resistance at 20 °C [$\Omega \cdot \text{mm}^2/\text{m}$]
- A cross-section area [mm^2]
- m quantity of partial conductors
- α_{20} temperature coefficient [K^{-1}]
- ϑ operating temperature

The load P [W] in a certain moment results from the multiplication of the voltage and the amperage:

$$P = I * U \quad [\text{Eq. 4}]$$

The energy losses P_v appearing during the transmission of electricity because of the ohmic resistance can be determined by the combination of equation 3 and 4. Basically it is valid that the higher the voltage and the lower the amperage is, the lower the energy losses, which are proportional to the square of the amperage:

$$P_v = n * R' * d * I^2 \quad [\text{Eq. 5}]$$

- n quantity of conductors
- R' resistance load per length [Ω/km]
- d length [km]
- I amperage [A]

Here the losses of a double-bipolar HVDC line with the capacity $P = 10$ GW should be calculated at different voltage levels. It is used a 4-bundle conductor of the type Al/St 805/102. Furthermore, it is sufficient to just take the aluminium cross-section of 805 mm² into account, which electric resistance amounts to 0.0028 $\Omega \cdot \text{mm}^2/\text{m}$.

The rounded value of 0.004 K^{-1} can be used as temperature coefficient α_{20} with usual conductor materials (Flosdorff & Hilgarth, 2003). For a normal operation the temperature $\vartheta = 40 \text{ }^\circ\text{C}$ is determined.

The resistance load per length R' resulting from equation 3 amounts to $0.0094 \text{ } \Omega/\text{km}$. First, the losses of one bipole are calculated by multiplying R' with the number of conductors $n = 2$ and the amperage I . The absolute and relative losses at the conductor length $d = 1000 \text{ km}$ are given in table 4. For a $\pm 600 \text{ kV}$ system the thermal breakeven performance lies at 6500 MW , which corresponds to a current density of 1.7 A/mm^2 (UBA, 2002).

Figure 26 shows the relative losses at different voltage levels on a distance of 4000 km . The losses of a $\pm 800 \text{ kV}$ system come to $14.7 \text{ } \%/4000 \text{ km}$ and thus move in an acceptable scope.

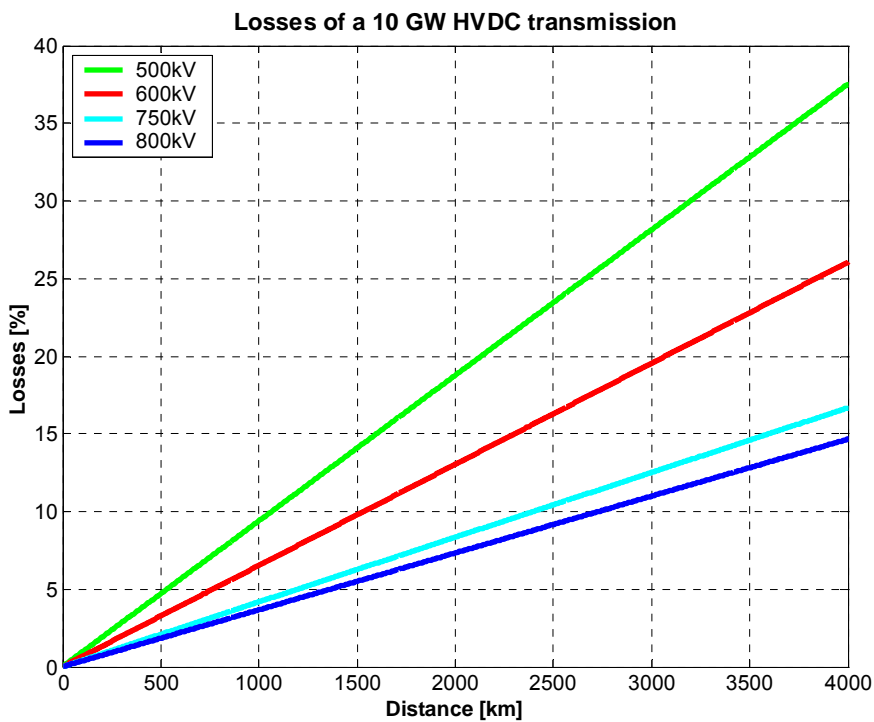


Fig. 26: HVDC losses in dependence on transmission voltage and distance.

Tab. 4: Losses in dependence on transmission voltage (double-bipol)

Voltage U [kV]	Amperage I [A]	Current density [A/mm ²]	Losses P _v [MW/1000km]	Relative Losses [%/1000km]
±500	2 x 5000	1,55	2 x 469	9,4
±600	2 x 4167	1,29	2 x 326	6,5
±750	2 x 3333	1,04	2 x 208	4,2
±800	2x 3125	0,97	2 x 183	3,7

Similar values are mentioned in the literature. Deviations could result from different assumptions about transmission capacity, operating temperature, current density and cross-section area of the conductor.

Tab. 5: Literature information about HVDC losses.

HVDC	Losses [%/1000 km]	Source
±800 kV, 6500 MW	2.5	ESA, 2004
±750 kV	4.2	Eberle, 2000
±600 kV, 2 x 3860 MW, 1 A/mm ² , 4x Al/St 805/102	4.8	DLR/WI, 2002
±500 kV, 3000 MW	6.0	Knoepfel, 1995
Rectifier	Losses [%/Station]	
depending on rated power	0.6 – 1.8	Schneider, 1995
500 kV	0.7	Knoepfel, 1995

Current-independent losses

The current-independent losses consist of losses caused by the corona effect and leakage currents, especially in case of dirty isolators. Both are heavily dependent on the weather and therefore roughly estimated. Knoepfel states losses of 1-10 kW/km for a ±500 kV HVDC system, which can be neglected in this order of magnitude and the voltage-dependent leakage currents as well.

3.3.6 Cable transmission losses

There are no inductive, capacitive and dielectric losses and no current displacements in comparison with an AC cable. Thus compensational measures are not required and the transmission length is not restricted for a DC cable.

According to Eberle (2000) the losses amount to 3.3 %/1000 km at a 500 kV. Based on own calculations the losses of a 800 kV mass-impregnated cable with a 2100 mm² copper conductor come to 1.7 %/1000 km.

4 Comparison of costs

First of all overhead lines predominate over cables in the high voltage section since the cost of an overhead line amount to 15 - 20 % of the cost of a cable (Schlabach, 2003). In Czisch (1999) it is mentioned a ratio of 1:10. But there are distinct differences between electrical transmission technologies and the investment costs mainly depend on transmission length. Figure 27 explains this connection once again.

The so-called 'Break-Even-Distance' terms the shortest distance where the investment costs of a direct current transmission are identical with the costs of an alternating current transmission. It depends on the transmission capacity and topography of the area in detail and lies between 500 and 1000 km for the overhead line (Pehnt, 2002). The 'Break-Even-Distance' for a direct current submarine cable already lies at 30 km (Heuck & Dettmann, 2002).

In the beginning high investment costs of the rectifier make a significant difference compared with the distinct lower costs of transformers. With an increasing transmission length the total costs of HVAC are affected by the higher costs for conduction and network losses so that many advantages result from the use of HVDC from the 'Break-Even-Point'.

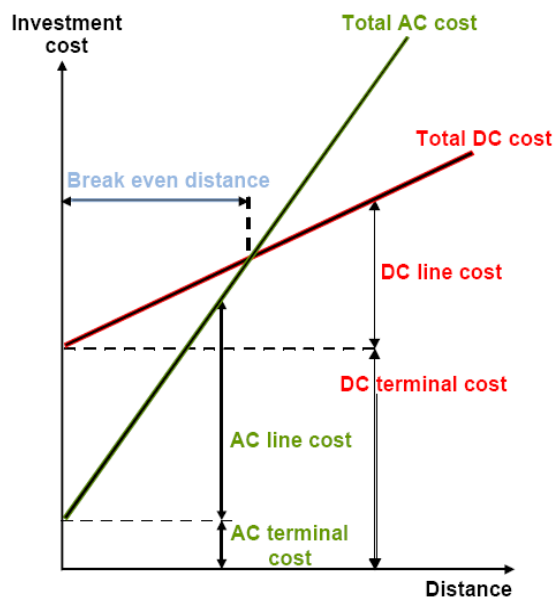


Fig. 27 : Comparison of AC and DC investment costs (Source: Rudervall et al., 2000).

In addition, the maximum transferable loads are not restricted by the thermal limit of the conductors, but by the guaranty of a stable voltage along the line. Thus, in case of HVAC, additional costs must be added for compensational measures realized every 600 km (Rudervall et al., 2000).

Altogether HVDC is predestined to transmit major loads over long distances with regard to efficiency, stability and losses.

Tab. 6: Present costs from the literature.

System	Line costs	Station costs	Source
800 kV DC	300 Mio €/1000 km (5 GW)	350 Mio €/Station (5 GW)	ESA, 2004
1150 kV AC	200 Mio €/1000 km/GW		ESA, 2004
750 kV AC	400-750 Mio €/1000 km		Kießling et al., 2001
2000 MW DC Bipole	250 Mio US\$/1000 km	250 Mio US\$/Station	Rudervall, 2000
2000 MW 2 x AC	500 Mio US\$/1000 km	80 Mio US\$/Station + compensational coil every 600 km	Rudervall, 2000

Case study

In case of a solar electricity import of 2000 MW over 3000 km from MAGHREB to Europe, investment costs amount to 2.5 milliards €. The costs for the transmission especially depend on losses and the utilization of the line. With 4 ct/kWh for the generated electricity and 1.8 ct/kWh for the transmission a cost level for imported electricity of 10 ct/kWh can be achieved on good conditions in 2015. In the long-term 5.5 ct/kWh are also possible (BMU, 2004b).

5 Environmental impacts of overhead lines

High voltage overhead lines have different environmental impacts. For that reason relevant aspects and risks of such a construction project should be clarified in advance. In the following section the decisive impacts of overhead lines are considered, particularly the relevant differences between alternating current and direct current. Where no information to direct current is available, it is related to alternating current. Many considerations refer to conditions in Germany, depending on the data that could be found.

In Germany the interests of nature and landscape are embodied in the 'Federal Nature Conversation Act' (BNatSchG, 2002). Accordingly, the erection of a high voltage overhead line represents an intervention in nature and landscape (section 18 para. 1 BNatSchG):

'Interferences in nature and landscape as defined by this law are changes of the shape or use of land or changes of the ground-water level, which is in conjunction with the living soil layer, and changes which can considerably impair the productive efficiency and function of the natural environment or the characteristic landscape.'

Possible consequences of the intervention already have to be investigated during the strategic planning and, if needed, further alternatives have to be taken into account. The interests of nature protection and landscape conservation can be considered and areas of conflict can be identified in advance using landscaping (section 13 ff. BNatSchG):

'Landscaping has the task to show and to give reasons for the requirements and measures of nature protection and landscape conservation for the prevention, reduction or elimination of impairments... for the respective planned area.'

The bundling of power lines also belongs to the principles of nature protection and landscape conservation (section 2 para. 1 subpara. 12 BNatSchG):

'The planning of ... power lines ... has to take account of natural structures of the landscape. Lines have to be summarized this way that cutting and consumption of the landscape are kept as small as possible.'

Within the scope of consideration it is possible that interests of power generation are of a secondary importance in comparison with interests of nature protection. In this case only an underground cabling is permitted. Unavoidable impairments have to be balanced or compensated reasonably (section 19 para. 1 u. 2 BNatSchG):

‘The responsible party of the intervention has to be obliged to omit avoidable impairments of nature and landscape ... and mainly to balance or in another way to compensate unavoidable impairments by measures of nature protection and landscape conservation (compensatory measures).’

According to section 2 para. 2 (1a) UVPG enclosure 1 para. 19.1.1 there is the general obligation to carry out an environmental impact assessment if a high voltage overhead line from a length of 15 km and a rated voltage of 220 kV upwards is erected or operated.

‘According to enclosure 1 a project is the erection and the operation of a technical system ... which has substantial effects on the environment because of its type, size or location. The environmental impact assessment comprises the investigation, description and evaluation of the direct and indirect effects of a project on human beings, animals and plants, soil, water, air, climate and landscape, cultural assets and other real assets and the interaction between before-mentioned subjects of protection.’

Furthermore, directives on preservation of natural habitats like the ‘Flora-Fauna-Habitat-Directive’ (92/43/EWG) have been issued by the European Union. The FFH-directive regulates the development and protection of the European ecological network ‘Natura 2000’. If a ‘Natura 2000’ area is affected by the power line, the admissibility of the project has to be controlled additionally by a FFH-impact assessment. This underlies stricter criteria than the environmental impact assessment or impact regulation and normally prohibits the permission in case of considerable impairments (§§ 32 ff. BNatSchG).

‘Projects have to be examined before permission ... for their compatibility with the aims of conservation of *Sites of Community Importance (SCI)* or *Special Protected Areas (SPA)* according to the *Bird Sanctuary Directive* ... it is inadmissible in case of considerable impairments.’

5.1 Space requirement

The real space requirement of an overhead line can be subdivided in a permanent use while the line is operated and a temporary use during the construction phase. Areas are occupied permanently by the fundament of pylons, for example approximately 22 m² by the massive concrete fundament of a ton mast medium-sized. A typical Danube mast with four pedestal fundaments can have a local space requirement of nearly 64 m². Knoepfel (1995) states an enclosed area of 50 m²/km for a ±500 kV DC pylon and 100 m²/km for a 750 kV AC pylon. Further space requirement through transformers and rectifiers must be added. A rectifier station with a capacity of 5000 MW requires an area of 800 m x 700 m (560,000 m²) (Normark, 2005), whereas a medium-sized transformer station takes up 10,000-15,000 m².

Moreover, there are time-limited places for barrels and winches every 2-3 km nearby the line and repositories every 20 km with a size of 5000 - 6000 m² where wires, isolators and armatures can be stored. Here a reserve of oil absorber of at least 100 kg is also held (APG, 2004). In addition to this, there is a temporary working stripe with a width of 5 m per month along the line (Knoepfel, 1995).

The actual width of the line depends on the pylon construction, the voltage level and the correlative safety distance, which must be observed between the conductor wires themselves and the surrounding area. For reasons of safety a ±800 kV double-bipole ought to be separated into two lines. Typical pylon constructions for this voltage level and the associated width of the line are shown in figure 29.

Tab. 7: Measurements of a HVAC and HVDC overhead line (Source: Knoepfel, 1995; Arrillaga, 1998).

Capacity 10 GW	800 kV HVAC	±800 kV HVDC
Number of circuits/conductor	5/15	2/4
Pylon height [m]	1-level pylon 30 - 40 Danube pylon 40 - 80	30 - 40
Pylon width [m]	40	15
Fundament [m ² /km]	100	50
Line width [m]	5 x 85	2 x 50

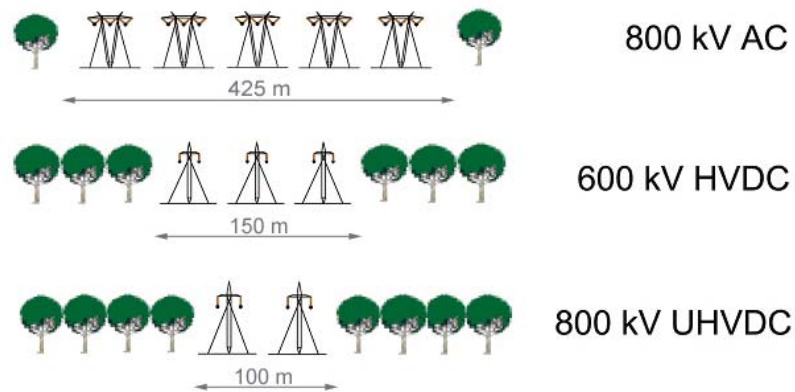


Fig. 28: Required number of parallel standing pylons to transfer 10 GW (Source: Asplund, 2004, changed).

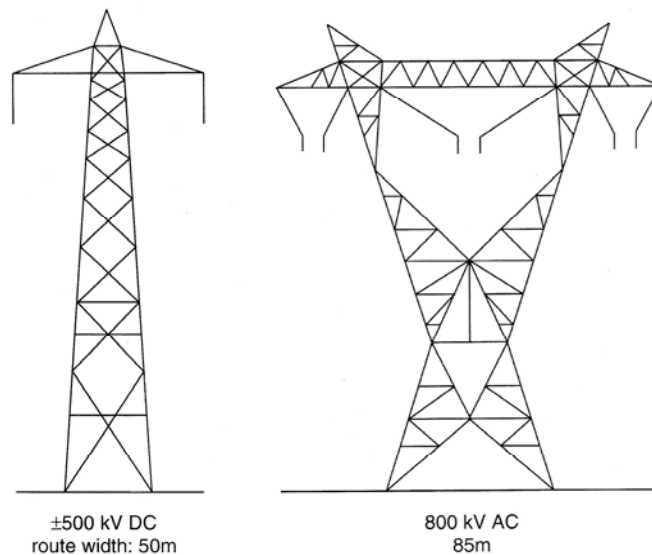


Fig. 29: Typical pylon constructions of a HVAC and HVDC overhead line (Source: Arrillaga, 1998).

5.2 Landscape-image

Impacts on the landscape-image, which are caused by a high voltage overhead line, are unavoidable. Large impacts through overhead lines exist in the open plain. Due to the strong restricted possibility of finding new lines in the Central European region, multiple lines with up to six circuits are used almost exclusively in the high voltage area (Kießling et al., 2001). The very stable-designed, more

conspicuous guyed pylons can considerably reduce the recreation value of the environment. Therefore it is aimed at a bundling of lines. It means that high voltage overhead lines are built preferably along the existing infrastructure like highways, railways and other overhead lines.

Moreover, it is also attempted to achieve an even better integration of steel lattice pylons in the surrounding landscape despite a certain transparency already existing. The easiest way of integration is a coat in 'Camouflage-Green'. However, routing along natural lines and shapes, which is advantageous for the landscape-image, has a higher expenditure of planning. Besides, the visibility of lines can also be reduced considerably within woodlands.

Altogether lower and less pylons have a favourable effect on the landscape-image, but a rise in distance between pylons also causes a rise in the amount of pylons since a threshold of 10 m above the ground is prescribed for the maximum conductor sag.

The normal ratio of guyed pylon to carrying pylon is 1:4 in flat terrain. Here the distance between several pylon sites amounts an average of 400 m. On manufacturing grounds a guyed pylon, which bridges between two line sections, must stand every 2 km. The more difficult the ground is and the more often the direction of the line changes, the higher the number of guyed pylons.

A DC pylon carries only two conductors per circuit in comparison with an AC pylon with three conductors per circuit and therefore is characterized by a lower height and width. The better integration of a DC line into the environment could also have positive influences on the acceptance in the population.

Exactly this acceptance for high voltage transmission projects is particularly low in surroundings of cultural assets, religious places and tourist destinations as the typical landscape-image is affected. Under this point of view a GIS-based analysis of the line visibility can be helpful (see section 8).

5.3 *Electric and magnetic fields*

In the static and low-frequency field of energy transmission systems electric and magnetic fields can be considered separated from each other. From 30 kHz upwards it is spoken of electro-magnetic fields, which have both wave and particle character. The differences in scale regarding the frequency must be taken into account by the evaluation of the physical and biological impacts.

The effects on human organisms primarily depend on the field strength and frequency. In case of static fields it is a pure force action, which becomes noticeable in the form of the movement of hairs, for instance. At low frequency fields up to 30 kHz a stimulus effect chiefly appears and at high frequency fields between 30 kHz and 300 GHz the energy absorbed causes an increase in temperature. Further influence coefficients are the body size, the orientation in the field and the earthing.

The human body is protected by two barriers from the influence of static and low-frequency fields. On one side it is his ability of conductivity so that no electric fields can enter the body. On the other side interfering signals are conducted once the stimulus threshold is exceeded, then they are perceived by the excitation of neurons or muscle cells. Indeed, the human stimulus sensibility is the highest in the very low-frequency range around 50 Hz. Cells are more insensitive at still lower frequencies since the alteration speed of the event decreases. The upper threshold frequency, from which no excitation happens due to the decreasing stimulus length, is individually different (30-100 kHz) (Leitgeb, 2000).

Electric field

Electric fields occur wherever electric charges exist separately. It is spoken of a static field if there is no equalization of charges and consequently no electric current flows. Direction and amount of the field strength of a static field measured in Volt per meter [V/m] are not subject to temporal variations like an alternating electrical field.

In everyday life you rarely meet technically generated, static fields. However, alternating fields exist in the environment of electric energy transmission systems and diverse household appliances. The values of exposure for a 380 kV AC high

voltage line lie between 5-6 kV/m at the place of the largest conductor sag, for a 765 kV AC line between 8-13 kV/m. Sideways the values decrease quickly and come to only 1-2 kV/m in a distance of 30 m (LfU, 2002/Kießling et al, 2001).

In case of a monopolar HVDC transmission a cloud of electric charges is formed in a field with a constant sign by the ionization of air molecules. This space charge cloud can also be transported by the wind (Leitgeb, 2000). The field strength of a 500 kV DC line can amount to 21 kV/m under the positive pole and 16 kV/m under the negative pole respectively. Thus the field strength can be double or threefold higher than the field strength under a comparable AC line, where the fields eliminate one another because of its ever-changing direction.

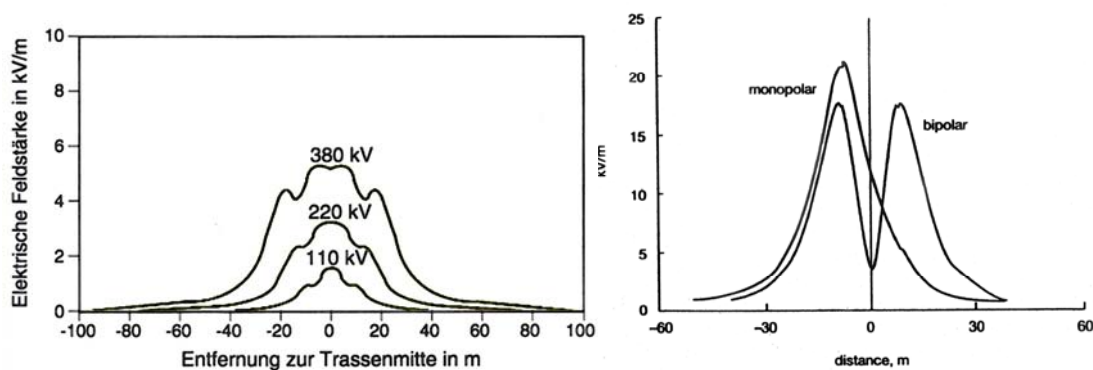


Fig. 30: Left: Electric field under a HVAC overhead line in a height of 1 m over the ground (Source: LfU, 2002); Right: Electric field under a 450kV HVDC overhead line (Source: Arrillaga, 1998).

Furthermore, high voltage overhead lines produce high-frequency interfering fields, which could affect the radio traffic. These fields are audible in form of crackling and droning noises and are caused by spark discharges along the high voltage line. They are also called corona losses and can be reduced by the use of bundle conductors, usually from a rated voltage of 110 kV (Schlabach, 2003).

Direct effects

The stay of a person in a static electrical field distorts it in this way that the electric flux lines are heavily concentrated at the head of the person as the highest point in the environment. At the same time this causes a separation and redistribution of charges (electrostatic induction) on the body surface by the physical conductivity. The electric flux lines end perpendicular to charges accumulated on the body surface. Thus there is no field inside the body as if the body is protected by a

'Faraday Cage', possible leakage currents are negligible. The effect of the electrostatic induction only occurs by entering and escaping the static electrical field, and thus the field is not able to produce permanent body currents. Moreover, the accumulation of similar charges at body hairs causes a mutual repulsion, which can be perceived by 1.5 - 3 % of the population from 1 kV/m (LfU, 2002). Alternating electrical fields change with a frequency of 50 Hz as well as the direction of the electrostatic induction. That is why equalizing currents can flow inside a person standing in a field of 5 kV/m, for instance a current of 0.6 mA/m² in the head zone and of 10 mA/m² in the ankles. A current density value of 10 mA/m² is regarded as lower threshold for a slight influence by stimulus effects, such as ophthalmic fibrillation and the change of the membrane potential. The central nervous system is excitable from 100 mA/m² and an acute health risk by ventricular fibrillation occurs from 1000 mA/m² (Bernhardt, 2002).

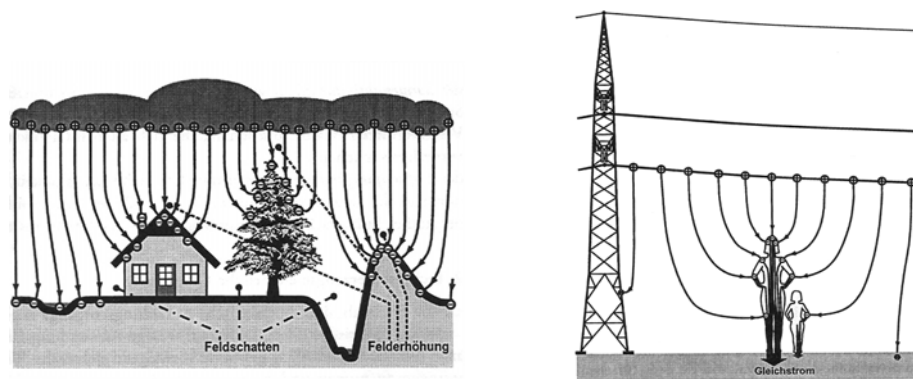


Fig. 31: Left: Natural, static field between ionosphere and earth surface. Electric fields can be shielded well by high and grounded objects, such as trees and houses; Right: 'Lightning Arrester Effect'. The child is protected in the field shadow of the mother (Source: Leitgeb, 2000).

Indirect effects

While touching a car, which stands in an electric field, its leakage current flows additionally through the human being as contact current. The perception threshold lies between 0.2-0.4 mA in case of a finger contact. An amperage value of 0.9-1.8 mA already causes pain, but the sensitivity increases in this order: men < women < children. Between 8-16 mA it comes to a painful shock linked with the incapacity to release the charged object. Serious shock and problems with the respiration appear between 12-23 mA and an acute ventricular fibrillation set in from 100 mA.

Objects which are well-isolated towards the ground can also be charged in an electric field. The amount of stored charges is described as electrical capacity and essentially depends on the height of the object. If it concerns a person, the amount of charge, which can be accumulated by it, is so low that it does not endanger the person in case of a direct discharge at a grounded object, whereas the approach or the touch of a charged car causes dangerous spark discharges in dependency on the potential difference. The average threshold of annoyance through spark discharges lies at a value of 7 kV/m (Bernhardt, 2002).

Magnetic field

A magnetic field results from moving electrical charges and is set up around a current-carrying conductor. The field strength depends on the amperage and the distance to the conductor. It can be described by the magnetic field strength H in ampere per meter [A/m] or the magnetic flux density B in tesla [T] in dependency on the magnetic permeability μ_r .

$$\vec{B} = \vec{H} \times \mu_r \times \mu_o \quad [\text{Eq. 6}]$$

μ_r material constant in vacuum and air approximately ≈ 1

μ_o magnetic permittivity ($= 1.26 \times 10^{-6} \frac{V*s}{A*m}$)

The magnetic field is not disturbed by the human body. It can flow unhindered through the body. But the magnetic field becomes effective if electric charges are moved by bodily functions or the person itself moves through the field. This way an electric voltage is induced at right angles to the direction of movement by charge separation. However, up to now there have not been any indications of a relevant influence of the general human health yet. In table 8 the flux densities of natural and artificial magnetic fields are listed.

Tab. 8: Examples of magnetic flux densities.

	Magnetic flux densities [μT]	Source
Natural magnetic field of the earth	47.0	LfU, 2002
380 kV overhead line	28.0-32.0	Kießling et al., 2001
Bipolare HVDC	23.0	Leitgeb, 2000
Suburban traffic in Germany (600 V DC)	80.0	LfU, 2002
Residential building in a distance of 67 m to the line	0.96	APG, 2004

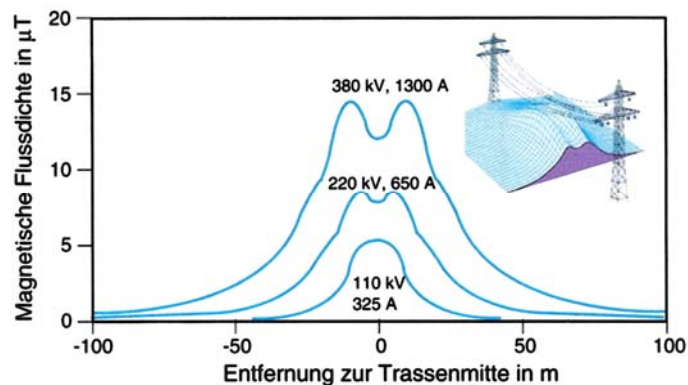


Fig. 32: Magnetic field below a HVAC overhead line in height of 1 m over the ground (Source: LfU, 2002).

Electro-magnetic compatibility

The electro-magnetic compatibility is the capability of electronic facilities and systems to function satisfactory under electro-magnetic influences out of the environment without causing electro-magnetic interferences of their own which would be critical for other facilities and appliances in the immediate surroundings (EU-Rat, 1989). The threshold of malfunctions for very sensitive, unipolar cardiac pacemakers lies at an electrical field strength value of 2 kV/m (50 Hz). Alternating magnetic fields act as interfering source from approximately 20 μT , static magnetic fields from 500 μT (Leitgeb, 2000). Therefore an interfering effect on implanted devices cannot be excluded if this risk group stays directly under a high voltage line (LfU, 2002).

Thresholds

A threshold for electric fields has to be selected so low that an electrical flashover can be prevented, also in case of unfavourable weather conditions. Furthermore, unacceptable high leakage currents must not flow through the body by touching

large objects. Magnetic fields must not induce very dangerous current densities in the body (Leitgeb, 2000).

It has to be distinguished between basic thresholds, which are based on firm thresholds of the physical parameter directly affecting the human tissue, and derived thresholds (reference values), which can be measured more easily. They are measured in air and not in the exposed person (LfU, 2002). In 1999 these thresholds were incorporated in the recommendation of the European Council [1999/519/EG] to create a joint framework in all member states. Already in 1997 thresholds for high-frequency and low-frequency facilities were determined in the 'Directive about Electro-Magnetic Fields' on recommendations of the ICNIRP (26. BImSchV, 1997).

According to sec. 3 para. 1 BImSchV facilities have to be erected and operated in this way that defined thresholds are not exceeded in their effective range. In case of a 380 kV line a safety margin of 20 m to areas which are not only meant for a temporary stay of people is enough.

Reference values for static electrical fields mostly are not determined by the organizations or countries since they cannot be found so often in everyday life. The ICNIRP assumes that no disturbing perception occurs with most of the people at a field strength value of not above 25 kV/m. The association of the electrical engineers in Germany states a value of 20 kV/m for the exposition area 2 (population) in a prestandard [DIN VDE (V) 848-4].

Moreover, the ICNIRP recommends a threshold of 40 mT for fields < 1 Hz regarding the magnetic flux density. According to the '26th Directive of the Federal Immission Control Act' an electrical field strength of 5 kV/m and a magnetic flux density of 100 µT must not be exceeded for low-frequency facilities (50 Hz) transmitting electricity. The ICNIRP states an amperage value of 0.5 mA as reference value for contact currents up to 2.5 kHz.

Tab. 9: Basic threshold for electric and magnetic fields.

		Body current density [mA/m ²]
0 Hz	ICNIRP	8
	European Council	
	26 th BImSchV	
	DIN VDE	
50 Hz	ICNIRP	2
	European Council	2
	26 th BImSchV	not defined
	DIN VDE	2

Tab. 10: Reference values for the permanent stay in electric and magnetic fields (population).

		Electrical field strength E [V/m]	Magnetic field strength H [A/m]	Magnetic flux density B [μ T]
0 Hz	ICNIRP		32,000	40,000
	European Council		32,000	40,000
	26 th BImSchV			
	DIN VDE	20,000	16,880	21,220
50 Hz	ICNIRP	5,000	80	100
	European Council	5,000	80	100
	26 th BImSchV	5,000	80	100
	DIN VDE	6,670	337	424

5.4 Risk potential for fauna and flora

An endangering of the avifauna at high voltage overhead lines hardly exists by a direct electroshock in touching the voltage-carrying conductors or grounded components. Isolators of the hanging type make sure that the distance between conductor and pylon is large enough so that even birds with a large wing range are not able to bridge it. Different to the medium voltage area these hanging isolators cannot be used as raised stand.

Rather it comes to collision accidents with the badly visible earth wire due to a smaller cross-section while birds are trying to approach the conductor or to make way for the same. It particularly concerns inexperienced young birds. The use of bird spirals and flutter bands at the earth wire or the lower one-level masts in principle could contribute to a better visibility at very dangerous line sections. This way the annual death toll could be reduced to almost 90 %.

Migrants and passage migrants are altogether more endangered than sedentary and breeding birds. They rest preferably in the area around waters, wetlands and

open grasslands and sometimes take a lot of space in order to start and alight. Therefore high voltage overhead lines ought not to be erected in such areas. Up to now measures to defuse line sections with a particular risk potential for alighting birds are not legally prescribed and can be carried out voluntarily by the energy supply companies (Schuhmacher, 2002).

Especially what concerns the protected meadow breeders species like European curlew (*Numenius arquata*) and lapwing (*Vanellus vanellus*) it could be proved that breeding areas were depreciated or not so often visited after the erection of a high voltage overhead line. Probably overhead lines impair the environment in a visual way. It happens now and then that the animals keep a distance of 100 m to the line, what in the end amounts to a loss of the breeding area. The sky-lark (*Alauda arvensis*) also showed a significant preference to areas far away the line (Schuhmacher, 2002).

There are often conflicts of interest between nature conservation and energy supply companies concerning the visibility of lines. Finally, it must be found a compromise which connects what is safety-related necessary and what is ecologically reasonable.

Quite another kind of influence on ground breeders is the utilization of the pylon alienated from its purpose as hatchery by diurnal birds of prey and corvids. The raised standing predators cannot be chased away from the nest environment and therefore are a permanent danger for the juvenile waders. Consequently, the shift of the predator-prey-relation for the benefit of the predators could lead to the loss of the population in case of a critical size (Schuhmacher, 2002).

During the examination of grazing and wild animals with regard to a negative influence by electro-magnetic fields no effects turn out as these animals are mobile enough and thereby are not permanently exposed to these fields. Just bees are disturbed in communicating and producing honey at a value of 3-15 kV/m. Therefore a distance from the apiary to the line ought not to be fallen below 50 m (APG, 2004).

The habitats of some plant and animal species are in points affected by the fundamentals of the pylons. Either the impact is negative in case of the loss of the biotope or positive if the pylon location is protected from over-fertilization and pesticide-application and acts as a retreating island.

Interventions into the forest ecosystem are more obvious because the forest aisle can be around 100 m wide. Both the cutting of an intact habitat and the open, unnatural edge of the forest are a serious problem. By the latter the forest climate is disturbed delicately and the forest stand is endangered in dependency on the weather, which causes desiccation and damages due to frost respectively.

Therefore it is important that the safety margin is reforested adapted to the site and transferred into copse in the long-term with the purpose of building a natural edge of the forest (see figure 33).

In 1994 the RWE AG had developed a pilot study about biotope management plans for the maintenance of power lines in collaboration with the University of Freiburg. It has been applied to the whole network of RWE since 2004 according to their own statement. The ecological maintenance measures have also an economical benefit as the costs are 50 % lower than the costs for continual clearings (see figure 34) (RWE, 2005).

Appropriate compensatory measures have to be carried out in case of a complete loss of the biotope. Forests are often spanned on before-mentioned grounds. Accordingly, pylons must be high enough.

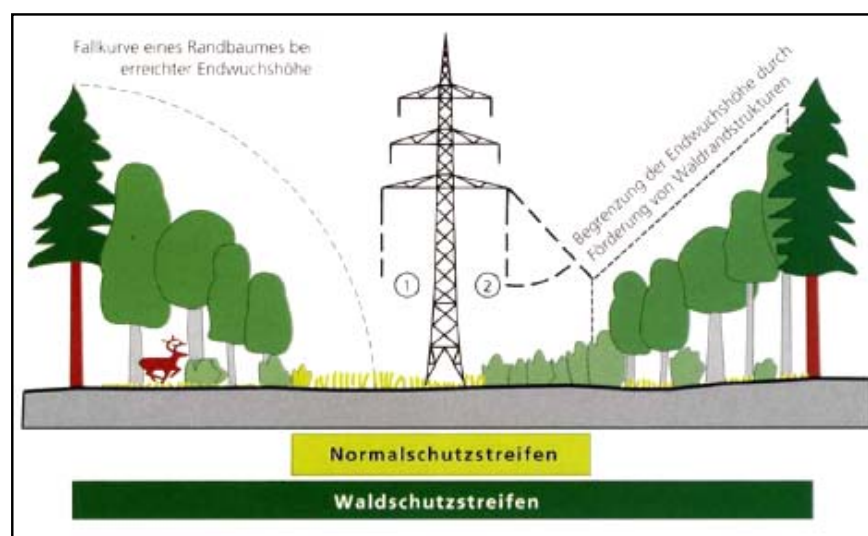


Fig. 33: Management of the safety strip of the line (Source: RWE, 1996).

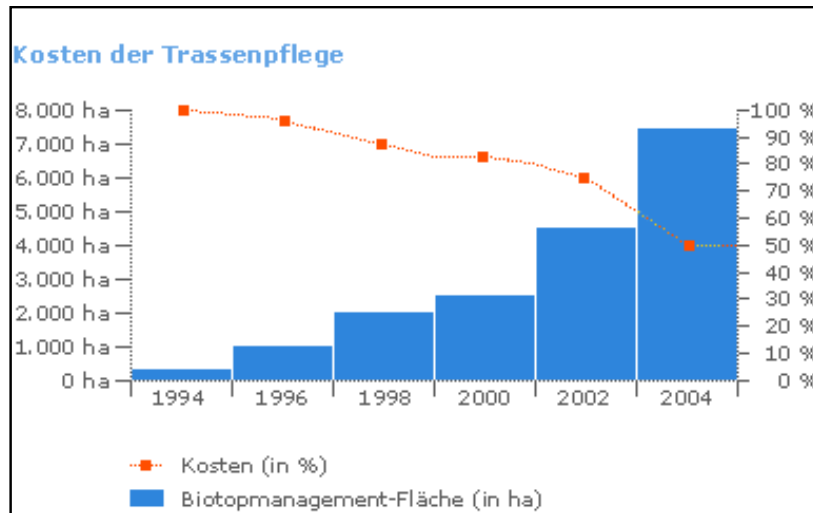


Fig. 34: Costs for the maintenance of the line (Source: RWE, 2005).

5.5 Risk potential for soil and groundwater

Danger of soil compacting by the use of heavy equipment and machinery particularly exists for heavy soils. However, after finishing the building project a depth aerator is carried out to counteract this danger. If necessary, the use of helicopters is recommended in areas which are difficult to access.

A higher endangering is represented by erosion processes at the place where the soil is not covered with vegetation. For that reason there is an urgent need in restoring the initial condition as far as it is possible. This also contains the equalization of a possible subsidence.

Where ever fuel and oil consuming devices are used there is a fundamental risk in contaminating the soil and later the groundwater with hazardous substances. Therefore it calls for special care if the aquifer is affected by constructional measures in the range of waterworks. Heavy metal emissions of the pylon can be neglected since modern pylons, whose hot-dip galvanized steel framework is coated with a protective lacquer, are used (Knoepfel, 1995).

The professional disposal of waste, such as a contaminated excavation, and the curative dismantling and recycling of disused components is presumed and therefore not be further discussed.

Further impacts on the environment

As already mentioned, air molecules are ionized along the conductors by the corona-effect, that in turn causes the formation of ozone (O₃)¹³ and nitrogen oxides (NO_x)¹⁴. Concentrations nearby the high voltage overhead line are often measured. The production rates are heavily dependent on the weather conditions and lie basically higher in case of a HVDC line due to the formation of a space charge cloud. In Knoepfel (1995) $4.0 \cdot 10^{-9}$ kg O₃/MJ_{el}/km are given for the ozone concentration. The laughing-gas concentration (N₂O) amounts to only 10% of the ozone concentration. This is identical to the information in Pehnt (2002), where a laughing-gas concentration of $0.4 \cdot 10^{-9}$ kg N₂O/MJ_{el}/km (4 ppb) is specified. In case of heavy rain or hoarfrost values of 9 ppb can be measured, but altogether it does not lead to a significant increase of the natural, ground-near ozone and nitrogen oxide concentration respectively (APG, 2004).

Other impacts on the human environment are noise emissions of a high voltage overhead line, which come to approximately 55 dB¹⁵ during the construction phase. Generally construction works of this kind ought not to be taken place in sensitive timeframe in the surroundings of populated places. During the operating phase corona-discharges along the conductors cause noise of approximately 20 dB. Such noise is similar to rustling of leaves and is only perceptible in the immediately environment of the line.

¹³ 33th BImSchV (2004): Immission threshold for the population 120 µg/m³ O₃ [60 ppb], highest 8h-mean; Vegetation, in the long-term 18.000 µg/m³h O₃ (AOT40).

¹⁴ 22th BImSchV (2002): Immission threshold for the population 200 µg/m³ NO₂ [105 ppb], averaged over 1 h, full-year 40 µg/m³ NO₂ [21 ppb]; Vegetation, full-year 30 µg/m³ NO_x [16 ppb].

¹⁵ according to the WHO-recommendation for a permanent noise level

6 Environmental impacts of underground cables

The acceptance of the population for overhead lines has heavily decreased because of the unavoidable impairment of the landscape-image. Both in congested areas and also in semi-natural landscapes people are bothered by the high mast constructions, although often on a subjective emotional level. But also lack of space in congested areas and the strict prevention of impairments of special worth protecting areas lead to an intensified use of underground cables in these areas. If a project has effects on the characteristic region, such as high voltage power lines, protracted permit procedures have to be passed through until the construction can be started.

Furthermore, most of the impacts typically caused by overhead lines can be eliminated with cables. First of all this concerns the distinct lower space requirement in comparison with an overhead line. Anyhow, a forest aisle of 5 m width is unavoidable. The placing depth of the cable amounts to nearly 1 m and even after finishing of construction works a radius of 1 m around the cable must not be built over or planted with deep-rooted plants on safety grounds (VDEW, 2001). In Kießling et al. (2001) and in APG (2003) it is given a clearing zone of 10 m if the three phases are grouped in parallel.

The use of AC cables would bring an additional space requirement of 100 m² every 20 km for compensational installations providing reactive power (Laures, 2003). Additionally, there are sockets and clamps respectively in a distance of 2 km caused by the maximum manufacture length of the cable. Because of this space requirement it should be aimed at parallel grouping of cables buried in the public traffic ground.

The cable isolation shields the electric fields almost completely. The measured value of the permeability of matter for electric fields is the relative permittivity ϵ_r . It has not a unit and relatively refers to the permeability in vacuum (=1). Typical values for usual cable isolation materials are 2.2-2.8 for oil and 3.3-4.2 for paper (both at 20 °C) (Schlabach, 2003).

Magnetic fields remain uninfluenced by this and can only be minimized if several cables are buried in closer neighbourhood to each other so that fields eliminate

themselves mutually. Figure 35 shows a double AC cable system with a maximum magnetic flux density of approximately 20 μT directly over the cable ditch. The magnetic field strength rapidly decreases with the increasing distance to the cable and reaches the background value after 5 m.

A further effect of an underground cable is the local dehydration of the surrounding soil. That is because of the reduced quality of heat removal in dependency on the soil texture and humidity.

First of all the soil temperature varies with the season. A soil in Central Europe shows an average temperature of 3 $^{\circ}\text{C}$ in a depth of 1.25 m in February and of 16 $^{\circ}\text{C}$ in August, thereby the specific heat resistance depends on the water content of the soil (Scheffer & Schachtschabel, 2002). For instance, the heat resistance of a sandy soil at a water content of 10 % lies between 0.5 and 1 $\text{K}\cdot\text{m}/\text{W}$ and can increase to 2.5-4 $\text{K}\cdot\text{m}/\text{W}$ in a parched state (see figure 35) (Peschke, 1998).

The resulting, minimized heat emission impairs the operating safety of the cable, but affects the vegetation cover, fruit ripeness and vegetation period only in the closest environment of the cable. The specific influences on the microbiology, flora and fauna are still unknown for the most part.

In case of accident there is an acute risk for the environment by the contamination with hazardous substances, especially for the groundwater. The risk potential by

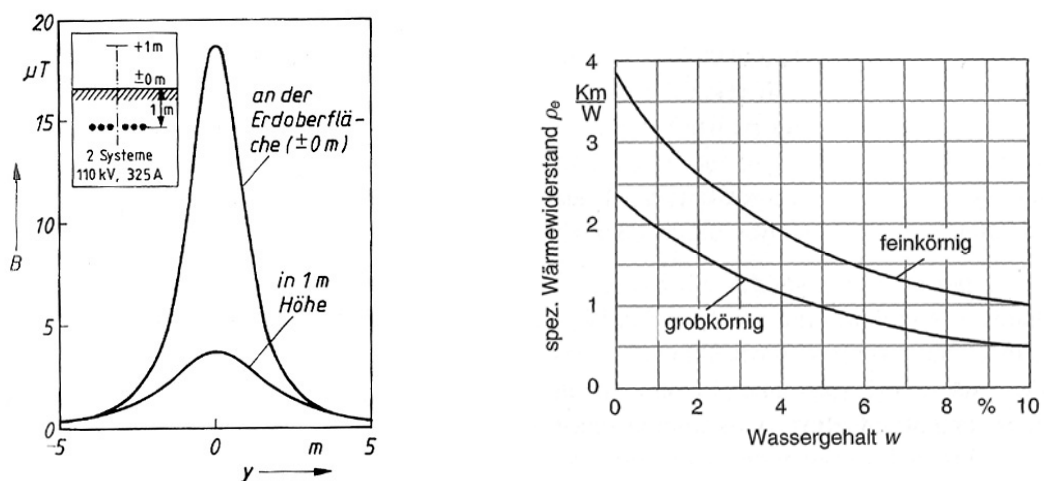


Fig. 35: Left: Magnetic field over a AC underground cable (Source: Flosdorff & Hilgarth, 2003); Right: Specific heat resistance of a sandy soil with a different humidity (Source: Peschke, 1998).

leakages is dependent on the used cable type. In the high voltage area low pressure oil filled cables and mass-impregnated cables are preferably employed. The former must be checked regularly for leakages even after placing out of operation and an alarm and measure plan must be made. For that reason it is better to remove the cable at once, whereas the closure of mass-impregnated cables is not such a danger as the endings are sealed and the high-viscosity paper-oil isolation gets more viscous after the cooling down of the cable. PVC cables, which release heavy metals at a $\text{pH} < 3$ or hazardous hydrogen chlorides such as dioxin in case of fire, are not used any more in the high voltage area (VDEW, 2001).

An underground cable is largely protected from weather effects, but in need of repair the localization and the accessibility to the damage site is time-consuming and therefore more cost-intensive than with an overhead line. Besides, the costs of cable manufacturing and laying together with a shorter operating time (half the overhead line, here 40 years) lead to an overall costs ratio of 1:10 (APG, 2003; Czisch, 1999).

7 Environmental impacts of submarine cables

Most of the direct current submarine cables are laid in the North Sea and Baltic Sea for an electricity import from Scandinavia.



Fig. 36: Direct current submarine cables in the North and Baltic Sea (Source: UCTE, 2004)

Up to now the deepest DC submarine cable in the world has been laid in a depth of maximum 1000 m between Italy and Greece. Figure 37 shows the very rough profile through the ‘Street of Otranto’. The HVDC line starts on the Italian side as a 43 km long underground cable. Then it follows a 160 km long submarine cable section where the cable is rinsed into the seabed on the continental shelf or is simply put down on the sea bottom in deeper areas. On the Greek mainland the transmission line runs as 100 km long overhead line.

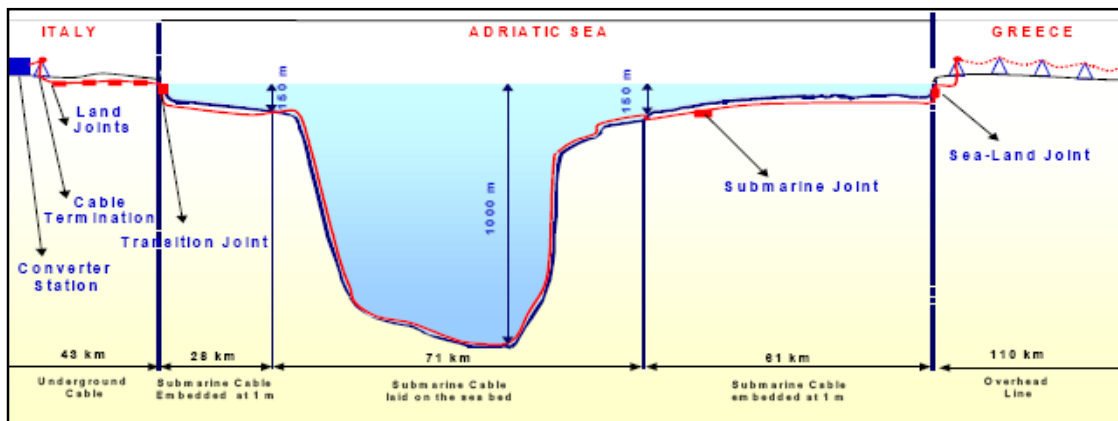


Fig. 37: Profile through the ‘Street of Otranto’ (Source: Cigre, 2002).

Impacts and influences on the environment respectively occur by the laying of the submarine cable during the operating phase.

Laying phase

In the offshore area the cables are directly put down on the sea bottom while they are rinsed in a depth of 1-2 m into the seabed of the shallower coastal zone. In areas with higher morphodynamics, such as in tide-ways and in front of islands, cable-laying is recommended up to a depth of 3 m to avoid possible free-rinsing.

Because of large sediment transfers the loss or influence of the benthic biocoenosis or fish living nearby the ground cannot be avoided (Wirtz & Schuchardt, 2003). The duration of resettlement amounts to at least two years. Furthermore, the fine grain fraction mobilized by sediment transfers also causes a higher turbidity of water, which is separated in time and space. On one hand the activity of the primary producers and the phytoplankton is impaired and on the other hand the simultaneous release of nutrients supports the growth of algae. The latter occurs especially in spring and summer when there is usually a lack of nutrients.

The impairment of the marine mammals and avifauna depends on the extent of disturbances in the form of vibration and noise, but altogether it is considered lowly. Nevertheless, the building measures ought not to be carried out during the breeding time and formation of colonies as a precaution (Wirtz & Schuchardt, 2003).

Operating phase

Electric and magnetic fields arise around the current-carrying conductor during the operating phase. The electric field cannot permeate good cable isolations. First of all the magnetic field of a bipolar DC cable affects the environment, which in turn can induce secondary, electric fields owing to the sea current. In this way also natural, electric fields are generated by moving of water through the earth's magnetic field. For example, the Gulf Stream produces an electric field with a strength of 50 $\mu\text{V}/\text{m}$ (Kullnick & Marhold, 2000).

Up to now most of the submarine cables have been performed as monopolar conductor with back current via seawater so that sea-electrodes are required. The

electric fields in a distance of 10 km to such electrodes move on a level of 10^{-4} V/m, what is comparable to natural electric field strengths in the sea. In table 11 the conditions in the proximity of the sea-electrode called 'Kontek' in front of the 'Coast of Warnemünde' are set against the minimum field strength to start a reaction at the example of the Baltic Sea herring (*Culpea harengus membras*). The electrode is operated as cathode with a surface of 400 m² and amperage of 1500 A DC. The resistance of the seawater amounts to 0.8 Ω*m. Because of the rapid decrease of the field strength with the increasing distance towards the electrode an influence of the fish is hardly expected after 10 cm. Alternatively, the use of land instead of sea-electrodes would be feasible.

Tab. 11: Comparison of the field strength nearby the sea-electrode with the minimum field strength for the release of a reaction in case of the herring (Source: Debus, 1998).

Distance [cm]	Field strength at the sea-electrode [V/m]	Minimum field strength for the herring [V/m]	Realm of reaction at the anode
100	0.03		
40	0.08		
10	0.3		
0	2		
		3	Shy effect
		8	Electro-taxis
		40	Anaesthesia

Although it is known that the biological activity is connected with weak electric field events, the effect of the weak electric fields arising by the transmission of electricity are largely unexplored (Debus, 1998). Fishes are equipped with special electro-receptors and can react more sensitively as they are able to even perceive electric fields around 1 μV/m.

Strong electric fields have field strengths of more than 1 V/m and current densities of at least 5 mA/cm². Such fields produce a galvanic-tactical and anaesthetic effect and have been used as fishing assistance since 1925 (Debus, 1998).

The technical-generated magnetic field of a HVDC line is the strongest at the cable surfaces and decrease with an increasing distance. At a power of 500 MW the field strength in 6 m distance is equivalent to the natural magnetic field (Söderberg & Abrahamsson, 2001). The magnetic field strength can be reduced by overlapping of two reverse-polarised fields.

Therefore it is recommended using closely lying, bipolar conductors ('Touch-Laying'), in future also in a joint cable ('Flat-Type'). Additionally, the transmission capacity can be doubled this way and sea-electrodes can be given up.

An influence on the orientation of far-migrant fishes like eel (*Anguilla anguilla*) and salmon (*Salmo salar*) could be given as they are still able to perceive the field of a 500 MW HVDC cable in a distance of 160 m (Debus, 1998). However, previous examinations outdoor and in the laboratory provided no clear indications of a barrier effect, deflection or influences on communication of fishes (shy and deflection effect). Most likely a multi-factorial orientation during the fish migration is assumed, in which the natural magnetic field represents only one component. The natural magnetic field becomes more and more important for migration if other factors like sunlight, temperature, salinity and velocity of flow appear not so strong. Even the migration of animal groups like molluscs (snails and mussels), crustaceans, marine mammals and zooplankton is controlled by several factors. Altogether there is a considerable need in research with regard to the perception and utilization of the natural magnetic field by marine organisms. Therefore possible influences on migration by technical-generated fields cannot be excluded fully (Kullnick & Marhold, 2000).

Beside the fields an increase in temperature can also be observed in the immediate environment of the cable. In case of a 600 MW bipolar cable buried in a depth of 1 m an increase in soil temperature of 3 °C in within a radius of 50 cm can be measured. The change in temperature at the surface of the sediment amounts to 1 °C at most. This local warming of the soil leads to an intensification of the bacterial metabolic rate and a reduced mortality of invertebrates in winter. Moreover, the settlement of thermophile organisms is possible (Wirtz & Schuchardt, 2003).

Here it is just mentioned that theoretically trawl nets and anchors could get caught by free-rinsed cables. The probability of such an accident lies at 1 event in 200 years at a 12 km long cable section (SEP, 1997). It should therefore be aimed at bundling and multiple-shift usage of submarine lines.

Basically the submarine cable type is determined by the transmission capacity, the length and the conditions on the sea bottom. Since no synthetic-isolated cables¹⁶ are used due to the DC problem with space charge clouds, only mass-impregnated and low-pressure cables are possible (VDEW, 2001). Especially fluid-filled cables have a higher risk of leakage in case of accident, which cannot be limited in the sea by the use of sockets on practical grounds.

Altogether the environmental impacts can be represented like in figure 38. The factors arising during the operating phase decrease with the depth of the cable-laying, whereas the other factors increase.

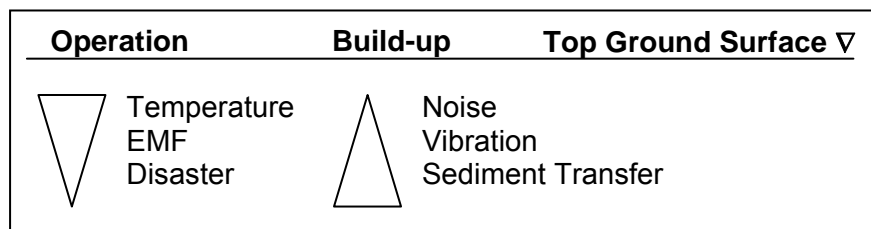


Fig. 38: Environmental impacts of a submarine cable in dependency on the depth under the seabed (here as GOK) during the operating and laying phase.

¹⁶ On environmental grounds it is aimed at the substitution by an extruded synthetic-dielectric or a Polypropylen-Laminated Paper (PPLP) with lower losses in future.

8 Ecologically-optimized line laying (GIS-analysis)

In the sections 2 and 3 the preconditions for a solar electricity transmission from North Africa to Europe have been already sketched. It was shown that large solar irradiation potentials are located in North Africa and that only with the HVDC technology a transmission of electricity over large distances can be realized. In the following it should be clarified, how the connection between supply and demand regions looks like if ecological aspects are taken into account. Altogether three examples for a power line should be considered.

First of all the precise start and target points of the lines have to be determined. The demand centres should have a high population density and therefore a high electricity demand. Actually, the energy is fed into the high voltage network of the UCTE. Because this interconnected network is already operated until its limits of capacity in many places, the solar electricity in this case is carried to the consumer as close as possible. For the selection of the plant locations the DNI map from section 2 (figure 7) is processed with a special exclusion mask adjusted for the operating conditions of solar thermal power plants (Kronshage, 2001; Trieb, 2005). Three sites with a Direct Normal Irradiance > 2800 kWh/m²/y are selected from the remaining areas¹⁷.

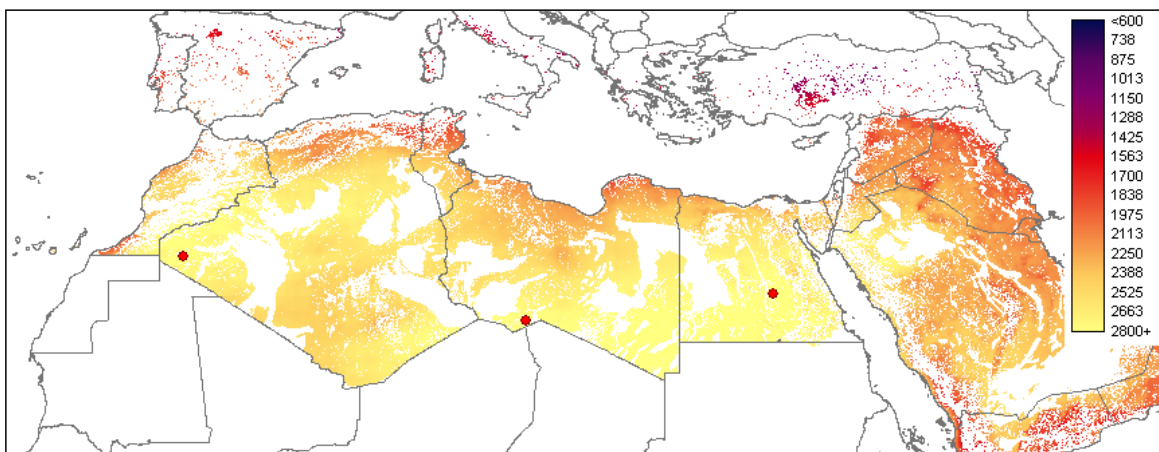


Fig. 39: Map of the Direct Normal Solar Irradiation [kWh/m²/y] with excluded areas (Source: *DLR, 2004).

¹⁷ Simple assumptions were made for the selection of plant sites. A comprehensive site evaluation is possible with the planning tool STEPS developed at the DLR, which also includes the costs and the design of the solar thermal power plant.

Tab. 12: Start and target points of the lines.

	Line 1	Line 2	Line 3
Plant location [x, y]	Algeria [-7°06"; 27°38"]	Libya [15°05"; 23°27"]	Egypt [31°01"; 25°14"]
Elevation [m a. sea-level]	421	686	388
DNI [kWh/m ² *y]	2,835	2,802	2,865
Demand centre	Aachen/Germany [6°01"; 50°47"]	Milano/Italy [9°12"; 45°25"]	Vienna/Austria [16°24"; 48°05"]

In table 12 the exact coordinates of the start and target points of all lines are listed. For the precise course of the lines a suitable model must be developed, which takes into account the interests of nature and landscape and at the same time the interests of the population into account.

On one hand unsuitable and protected areas are excluded due to the impacts of high voltage lines on the environment stated in the sections 5-7 and due to certain technical requirements for the lines. On the other hand the remaining areas should be assessed regarding their diverse feature properties.

First a geographic spatial section is defined which represents the outer boundaries for the modelling. This special section is described as 'Mediterranean Region' and covers an area from 11° to 72° north and from 25° west to 61° east. The required information for the line modelling is included in a variety of different, space-orientated datasets, which must be transferred into a uniform format for calculation. This concerns the spatial section as most of the data is available in a global format, the geographic resolution of 1 km x 1 km¹⁸ and the IDRISI raster format¹⁹ that is used here. All data is converted into the geographic projection system 'WGS84²⁰ – datum'.

The analysis is carried out with the Geographical Information Systems IDRISI 32.11 from Clark Labs, Worcester, Massachusetts (USA) and ARCGIS 8.2 from ESRI, Redlands, California (USA). Figure 86 in the annex shows the scheme of the whole model.

8.1 Generation of an exclusion mask

The areas to be excluded must fulfil at least one of the following criteria and are finally processed to yield an overall exclusion mask.

¹⁸ 0.93 km x 0.93 km at the equator corresponds to 30 arc seconds if an earth radius of 6,371 km and a maximal earth circumference of 40,030 km.

¹⁹ Idrisi image raster (.rst)

²⁰ WGS84: World Geodetic System 1984 if the earth is considered as rotation ellipsoid.

8.1.1 Exclusion criterion: protected area

In the year 1962 the world national parks and reserves were compiled by the United Nations in the 'UN List of Protected Areas'. The latest edition of this list is the '2003 UN List of Protected Areas', which was introduced in September 2003 at the '5th World Parks Congress' in Durban/South Africa.

The compilation has been carried out by the 'United Nations Environment Programme - World Conservation Monitoring Centre' (UNEP-WCMC) and the 'Union for the Conservation of Nature and Natural Resources - World Commission on Protected Areas' (IUCN-WCPA). The underlying information was provided by national authorities and ministries. Furthermore, the UN list was added by the 'World Database on Protected Areas' (WDPA) built up in 2002. Together with further state and non-state organizations the development of the WDPA is pushed. Thus its information and data serves as an improvement and completion of the list (UNEP-WCMC, 2005).

The UN list contains both protected areas based on the IUCN categories and other categorized areas, as the latter with a total area of 3.6 Mio km² should not be neglected.

According to IUCN a protected area is defined as 'an area of land and/or sea especially dedicated to the protection and maintenance of biological diversity, and of natural and associated cultural resources, and managed through legal or other effective means' (IUCN, 1994).

Altogether 6 classes of protected areas are distinguished (IUCN, 1994):

- Ia Strict Nature Reserve/Scientific Reserve
- Ib Wilderness Area
- II National Park
- III Natural Monument
- IV Habitat/Species Management Area
- V Protected Landscape/Seascape
- VI Managed Resource Protected Area

The WDPA 2005 is the newest, digital version of the UN list, optimized for the processing with a Geographic Information System. The database contains both punctual and spatial information about national IUCN protected areas and other categorized, national protected areas. All protected areas from the WDPA which is available as polygon dataset flows into the GIS analysis (*WDPA Consortium, 2005). Punctual information is not considered in this place.

The large number of European protected areas and their different marks leads to a very complex system, which is additionally managed by the 'European Environment Agency' (EEA) according to other methods. Therefore a lot of European protected areas are not included in the WDPA 2005 as vector datasets (WDPA Consortium, 2005). Because of this existing gaps are filled with protected areas from the UN list from the year 1993, which is included in ESRI's ARCATLAS™ as polygon dataset (*ESRI, 1996).

8.1.2 Exclusion criterion: industrial location

Areas that are already occupied with anthropogenic facilities or meant for the winning of raw materials are excluded. The data base for this criterion is formed by vector datasets of the 'Digital Chart of the World' (DCW) (*Ph.D., 1998). The following feature classes are concerned:

- Military base
- Airport/field
- Mine, quarry
- Oil/Gas field
- Desalination plant

Airports and airfields are provided with a safety zone of 3 km to avoid collisions with conductor wires. Further buffer zones of a 3 km width are laid around mineral oil and gas fields as spark discharges often arise along the conductors. The selected safety distances are based on a conservative approach, but this way, possible enlargements of mining fields can be taken into account.

Originally the DCW was developed for the 'Defense Mapping Agency' (DMA) of the Environment Systems Research Institute Inc. (ESRI). The first version from the

year 1992 is founded on aeronautical maps of the DMA with a scale of 1:1 Mio (PSU, 1999). The position accuracy is stated with 500 m. Here it is worked with a commercial cd-rom version of the Canadian software producer Ph.D. Associates Inc. (Kronshage, 2001). Since then, no newer edition of the DCW has been published.

8.1.3 Exclusion criterion: populated places

Generally high voltage lines ought not to be led through dense populated places; therefore such areas have to be excluded from further analysis. Moreover, a minimum distance of 250 m between populated places and the line must be kept for reasons of electric and magnetic fields (see section 5). On one side there is a problem with the resolution of the data that restricts the minimum distance to 30". On the other side a safety distance of 250 m is assured up to the 75th degree of latitude in case of a 30" buffer. Simplistically the most adjacent pixel is additionally excluded with the tool 'Buffer' within IDRISI.

In order to get a dataset to populated places as complete as possible, the features 'Build-Up-Area' and 'Native Settlement' from the DCW are blended with equivalent features from the land cover dataset 'Global Land Cover Characterization' (GLCC) (*USGS, 2000).

Both datasets correspond to only 50.4 % of all pixels. The DCW provides altogether more pixel than the GLCC, which contains just 1.1 % of pixel that are not given by the DCW (see figure 40).

The GLCC was built up in a common project of the US American survey authority (USGS), the university of Nebraska-Lincoln and the European commission for research cooperation (JRC). The original data was recorded with the AVHRR from April 1992 to March 1993. From NDVI compositions of remote sensing data different land cover classes are formed by multi temporal, unsupervised classification methods. The geographic resolution of GLCC amounts to approximately 1 km x 1 km (USGS, 2003).

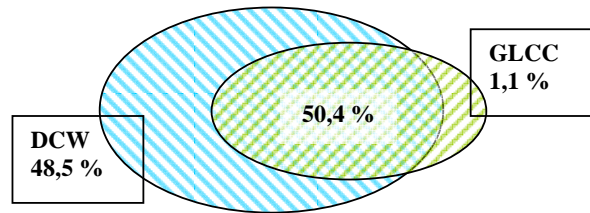


Fig. 40: Joint intersection of DCW und GLCC.

8.1.4 Exclusion criterion: sea depth

Especially for the crossing of the *Mediterranean Sea* a maximum placing depth of 2000 m under sea level is assumed for a submarine cable. The NGDC provides the global, digital elevation model 'ETOPO2 Global 2' Elevations' (*NGDC, 2001). The bathymetrical data was recorded from the 'ERS-1 Altimeter' of the European Space Agency (ESA) and from the 'Geosat Altimeter' of the US Navy (Smith & Sandwell, 2003). In order to cover the whole earth surface the different datasets shown in figure 85 (annex) were combined (Smith & Sandwell, 2003). The spatial resolution of the dataset amounts to nearly 4 km x 4 km²¹ (NGDC, 2005). Statements about the accuracy of the data are not included in the documentation. Areas that lie deeper than -2000 m are excluded and the remaining areas are weighted (s. section 8.2). Up to now the maximum placing depth of a submarine cable amounts to -1000 m, therefore it is a prospective assumption.

8.1.5 Exclusion criterion: hydrological feature

In large areas of the Mediterranean region there are perennial and intermittent inland water bodies. Areas occupied by them are not suitable for the power lines and are therefore excluded. The required spatial information are included in the DCW and there classified according to the following features (*Ph.D., 1998):

- Inland Water: Perennial/Permanent²²
- Inland Water: Non-Perennial/Intermittent/Fluctuating²³

²¹ 3,7 km x 3,7 km at the equator correspond to 2 arc minutes

²² Permanent lakes, currents, estuary, lagoons, not measured currents, reservoirs and navigable canals

²³ Episodically, seasonally fluctuating lakes, currents, wadis, sabkhas and not navigable canals

- Land Subject to Inundation: Perennial/Permanent
- Land Subject to Inundation: Non-Perennial/Intermittent/Fluctuating

In the defined area there is no category 'Land Subject to Inundation: Perennial/Permanent' present. Not permanent areas of inundation are assumed as wetlands and get the same weighting factor (see section 8.2) (Kronshage & Trieb, 2002). Dry valleys in arid areas - the so-called wadis -, which carry water just episodically, but then in large amounts, are included in the category 'Inland Water – Non-Perennial/Intermittent/Fluctuating' and can be taken into account (Diercke, 2001).

As the GLCC land cover dataset also includes inland water, these are intersected with the DCW dataset. This way the DCW is extended by 40.6 % more inland water. The *Black* and *Caspian Sea* are classified as seawater like the *Mediterranean Sea* and the *Atlantic*. In order to assign the criterion 'bridgeable' to extended inland water bodies and a width not more than 1', so e.g. for rivers, a filter²⁴ is used that identifies pixels that have a connection to land at least at one side. All other pixels are excluded.

8.1.6 Exclusion criterion: geomorphologic feature

Certain areas and soils are not suitable to be used as foundation due to their geomorphologic features. Salt areas because of their heavy corrosive features belong to it. But also dynamic structures like glacier form an exclusion area, which additionally is extended by a safety zone for the duration of operating (here 50 years). As the flow velocities can amount to 200 m/y this safety zone has to be at least 10 km width (Kronshage & Trieb, 2002).

Sand dunes are also unsuitable for the erection of pylons as the sand corns do not form a strong compound. Here the exclusion area also contains a safety zone which considers the mobility of certain dune types. Such shifting sands can cover around 30 m/y at a height of 10 m, therefore the safety zone is precautionary

²⁴ 3x3 kernel matrix: $\begin{pmatrix} 1 & 1 & 1 \\ 1 & 1 & 1 \\ 1 & 1 & 1 \end{pmatrix}$

specified with a width of 2 km that eliminates the endangering of the facility for the duration of operating (here 50 years) (Cooke et al., 1993).

Spatial information about sand dunes and salt areas are taken from the 'Digital Soil Map of the World' (DSMW) of the FAO (*FAO, 1995). The DSMW is based on the 'Soil Map of the World' (1:5 Mio.) of the FAO/UNESCO from the year 1978. The spatial resolution of the digital map amounts to approximately 10 km x 10 km²⁵.

Altogether the DSMW identifies in 26 groups of soil types 106 soil types and additional non-soil features, which include the dunes and salt areas of interest. Glaciers are taken from the digital land cover dataset (GLCC) and the DSMW.

According to the exclusion feature before mentioned the exclusion mask for the entire Mediterranean region results (see figure 41).

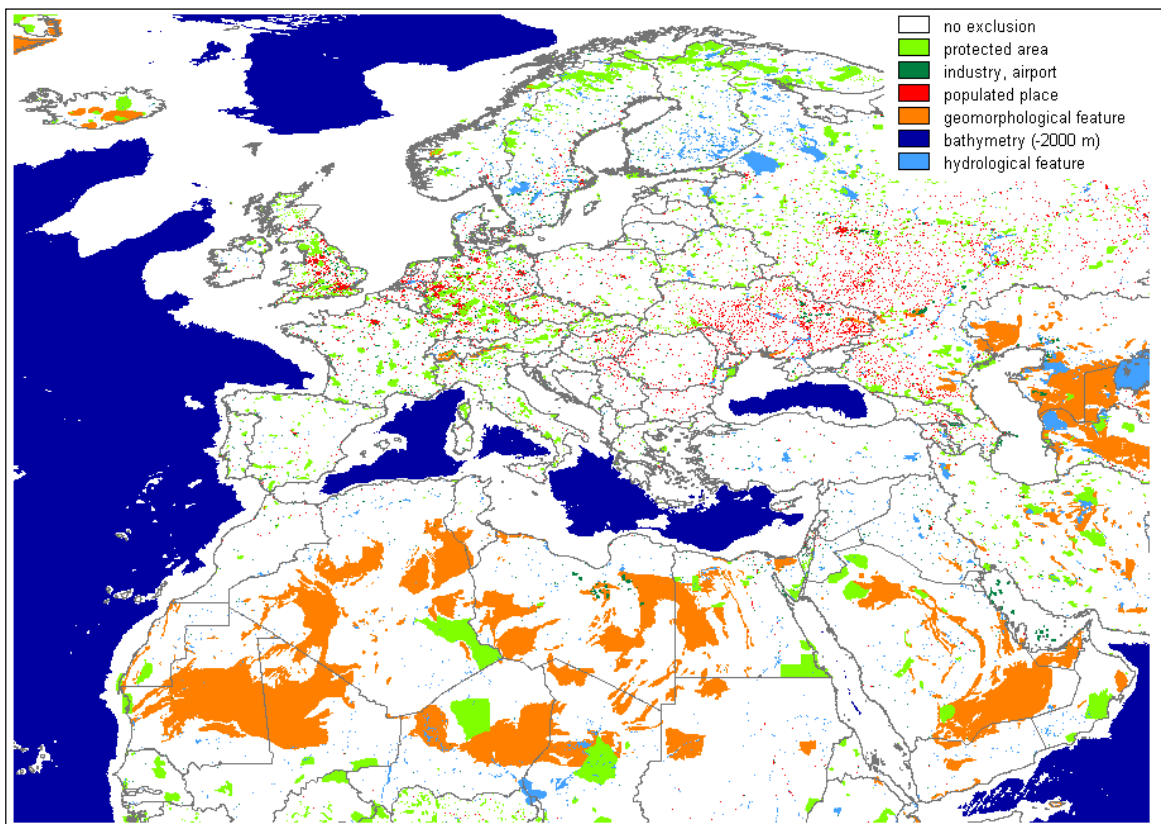


Fig. 41: Exclusion mask for the Mediterranean region.

²⁵ 9,3 km x 9,3 km at the equator corresponds to 5 arc minutes

8.2 Generation of an isotropic friction image

All remaining areas are weighted differently by means of further features to identify the optimum²⁶ way for the connection of the supply and demand sites under ecological aspects. For this, relative costs or friction factors are assigned to the areas and pixels respectively for a weighting in a transferred sense concerning their suitability as line location.

With the Geographic Information System IDRISI friction surface images can be produced based on these factors which are introduced in the calculation of a cost distance image.

8.2.1 Land cover

One weighting criterion is the land cover class of the pixel, which is determined by the GLCC land cover dataset. Here, from seven classification methods provided, the 'Olson Global Ecosystems' classification with 96 designated classes should be used (USGS, 2003). These classes are summarized to 11 main classes for further use.

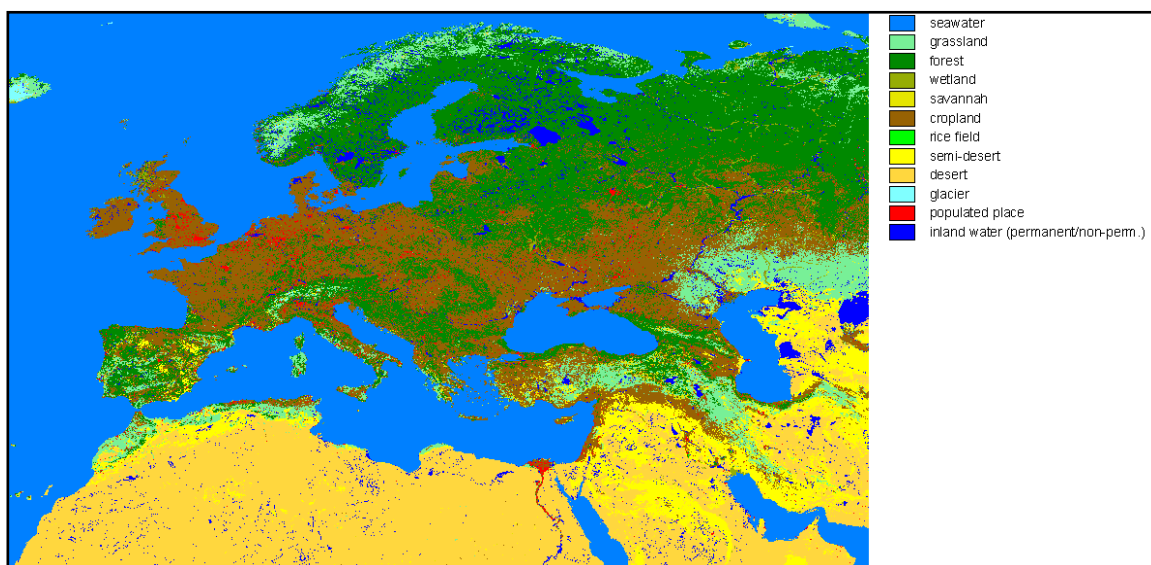


Fig. 42: Land cover in the Mediterranean region (Source: USGS, 2000).

²⁶ In this connection it is also the cheapest way between supply and demand sites.

A value of 1.0 is specified for the base cost value of the friction image. This corresponds to the costs that have to be raised to pass at least one pixel at least (Kronshage & Trieb, 2002). Areas which have been assigned the factor 1.0 are areas with a high priority for the project.

If a factor of 10,000.0 is assigned to certain land cover classes, these classes can be excluded from further calculation steps and can therefore be considered as insurmountable barriers.

As the *Mediterranean Sea*, the *Black Sea* and the *Caspian Sea* do not represent absolute barriers by use of submarine cables, but their use causes considerable higher costs, the factor 10.0 is assigned to large surface water (Czisch, 1999). The residual factors which have been assumed lie in the same order of magnitude as in Kronshage & Trieb (2002), whereas no additional flat value of 5.0 for crossing of seawater regarding the increasing foundation and operating costs with the increasing distance to the coast is charged. The higher costs of forests and wetlands not only refer to their development, but also to ecological aspects, whereby such areas should be used as line location subsequently. A factor of 3.0 means the threefold rate of costs in comparison to the basis value. Rice fields are distinguished from other agricultural areas and are rated like wetlands with regard to their development costs (Kronshage & Trieb, 2002).

The LANDSCAN database 2003 provides global information about the population density in a spatial resolution of 30" x 30" (*ORNL, 2003). The dataset is less based on the precise place of residence of the people, but more on the spatial distribution of the population over a typical 24 hour day in order to carry out a better risk assessment. That means that also the way to work and the place of work of the population is taken into account.

Information about population, mostly on a sub national level, serves as input data, which is distributed among several cells of a 30" raster by means of country-specific likelihood coefficients. The coefficients are derived from remote sensing data about the nearness to roads, slope, land cover, light emissions by night and other datasets (ORNL, 2003).

By means of these databases it is possible to record agglomerations around cities. These areas should not be considered as exclusion feature as otherwise too many areas fall out from a further analysis. The threshold is set on a population density

of 500 inhabitants/km². By assignment of a higher factor this agglomerations can be weighted higher. For this, the areas are blended with the land cover dataset and afterwards classified together with the other features corresponding to the friction factors.

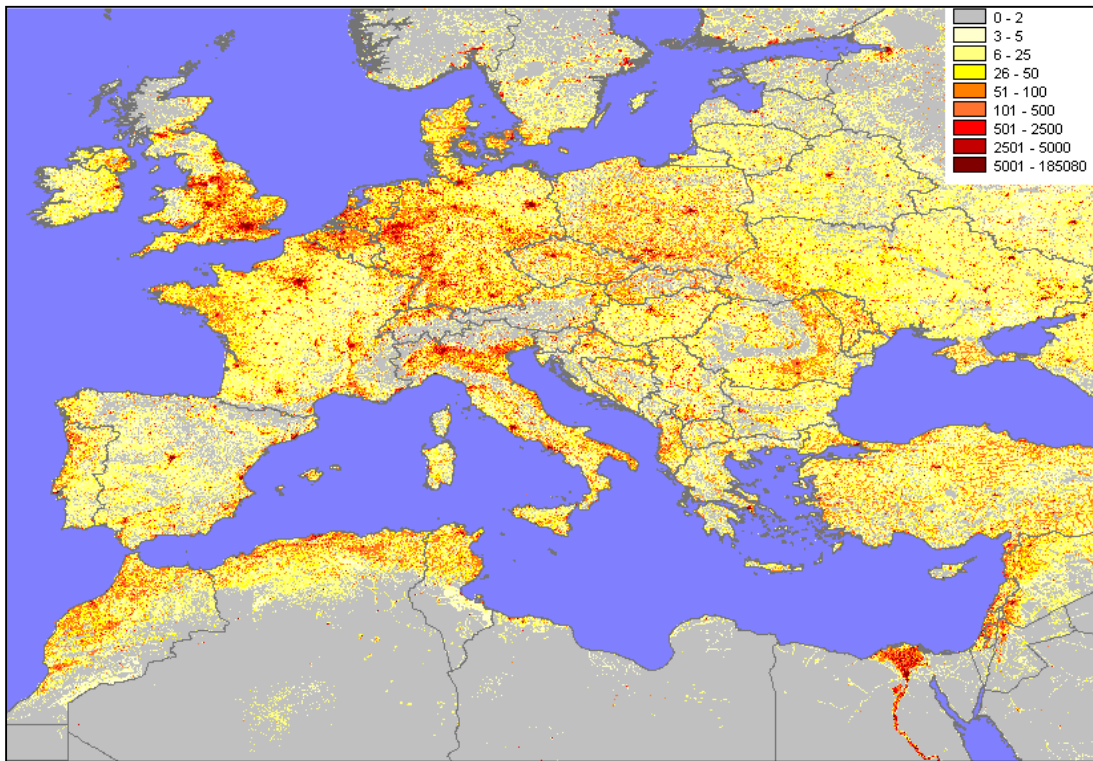


Fig. 43: Population density in the Mediterranean region (Source: *ORNL, 2003).

8.2.2 Cultural and religious sites

An overhead line can lead to a visual impact on the landscape. Therefore the minimization of the visibility should be aspired already within the planning and permission phase. Different methods are used to assess the visibility of an overhead line in the terrain. It is distinguished between two fundamental types (Zewe, 1996):

- Quantitative methods for the assessment of the visual effect by calculation of evaluation parameters for the visibility of a projected overhead line (calculation with the help of simulation processes).
- Qualitative methods for the assessment of the impacts on the landscape by realistic representation of a projected overhead line in the landscape

(photomontages, graphical data processing of air photographs and elevation models, interviews of test persons).

Such models are more and more used, but they are very complex and processing intensive. In case of qualitative methods this models are very realistic, but limited on certain points of views or, with the help of air photographs, with a too low resolution for the vicinity of a line. With a combined model it is aimed at a realistic representation of the line in the terrain and a quantitative visibility assessment (Zewe, 1996).

Due to the immense expenditure in assessing the visual effect of overhead lines and to the size of the section considered here the visibility is examined in the surroundings of cultural and religious sites to simplify matters. This carried out with the IDRISI tool 'Viewshed'. All areas which are visible in a height of 2 m from the viewer's point are charged with a factor of 7.0. The maximum visibility radius is set on 10 km. Areas lying in the sea are excluded from the visibility analysis as submarine cables are used. In wooded areas the visibility of pylons can decrease up to 100 % because of the camouflage effect of trees (Zewe, 1996). Therefore wooded areas which lie in the visual range are not rated higher.

The several site coordinates were taken from the 'GEOnet Names Server' (GNS) of the NGA (*NGA, 2005). This database contains names and coordinates of different cultural and religious sites outside the United States, from which the sites listed in table 29 (annex) were selected for this analysis.

As the accuracy of the coordinates is limited on minutes, spatial deviations of the sites of 1' can result. The error amounts to ± 1.7 km (23°) up to ± 1.2 km (50°).

8.2.3 Infrastructure

On purpose of bundling lines a further weighting criterion must be developed which refers to the distance of existing high voltage lines. The weighting factor is selected in this way that it increases linearly with the increasing distance to the line up to a maximum value of 50.0.

The base data is the DCW, which includes all power lines which have been implemented until the year 1992 with a topographic accuracy of 500 m, however,

without information about the voltage level of the lines. A schematic design (CAD) of existing and projected high voltage lines from 110 kV is available for North Africa and the easterly Mediterranean residential states. After geo-referencing the real course of the lines it is just represented as approximation. Nevertheless, due to a limited access to corresponding information this CAD was included in the analysis. Besides, there was no GIS dataset available for submarine cable transmissions.

The friction image for the distance to line also covers water bodies so that this way also the distance to the coast can be indirectly considered.

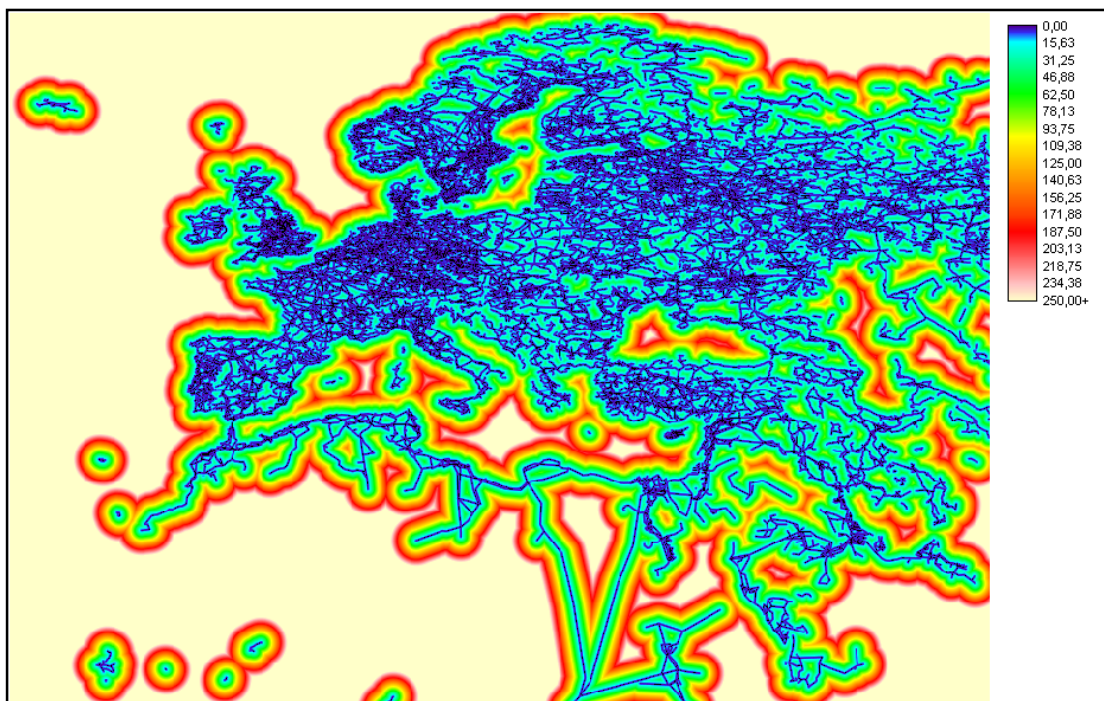


Fig. 44: Distance image of the electricity network in the Mediterranean region in kilometres.

8.2.4 Natural hazards

Up to now only areas of inundation have been taken into account in the model as areas concerned by natural hazards. Furthermore, earthquakes, storms (wind loads), and lightning among others can affect the operating safety of an overhead line. In order to resist such impacts the design of pylons and conductors must be adapted to the site conditions. Heavy wind loads often arising cause a more often use of guyed pylons and a higher demand in repairing within the duration of operation.

The dataset 'World Map of Natural Hazards' of the Munich Re Group contains the spatial distribution of different natural hazards, which are each subdivided in up to six risk classes (see table 13). But not all classes are represented in the Mediterranean region concerned. A risk potential by tropical storm is not present in these latitudes, for instance.

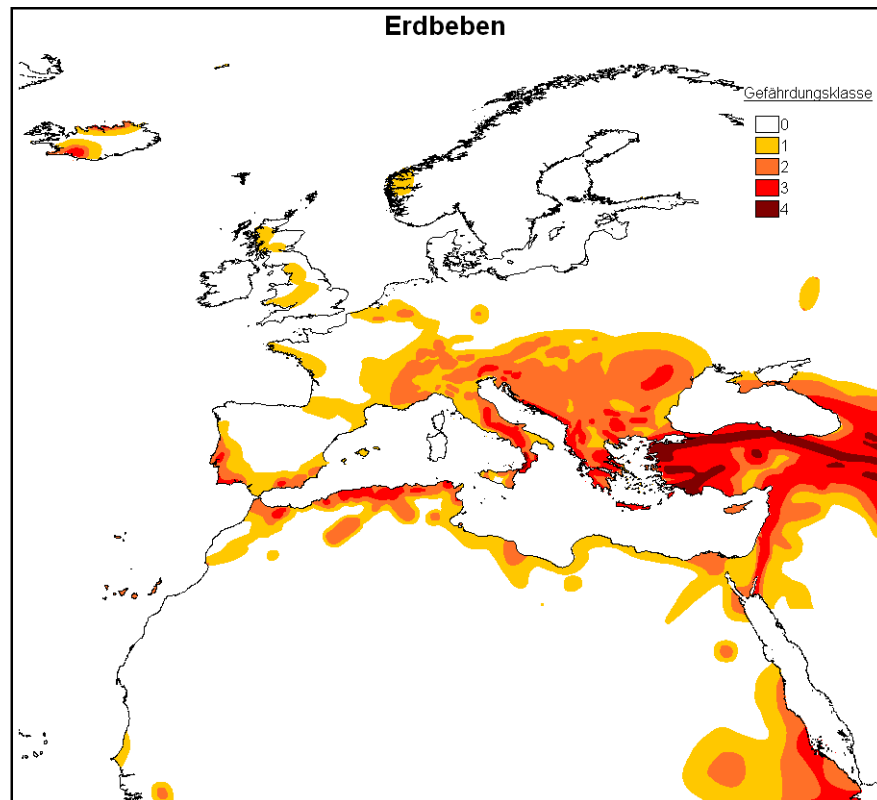


Fig. 45: Danger of earthquakes (Source: OD, Münchener Rück, 2001).

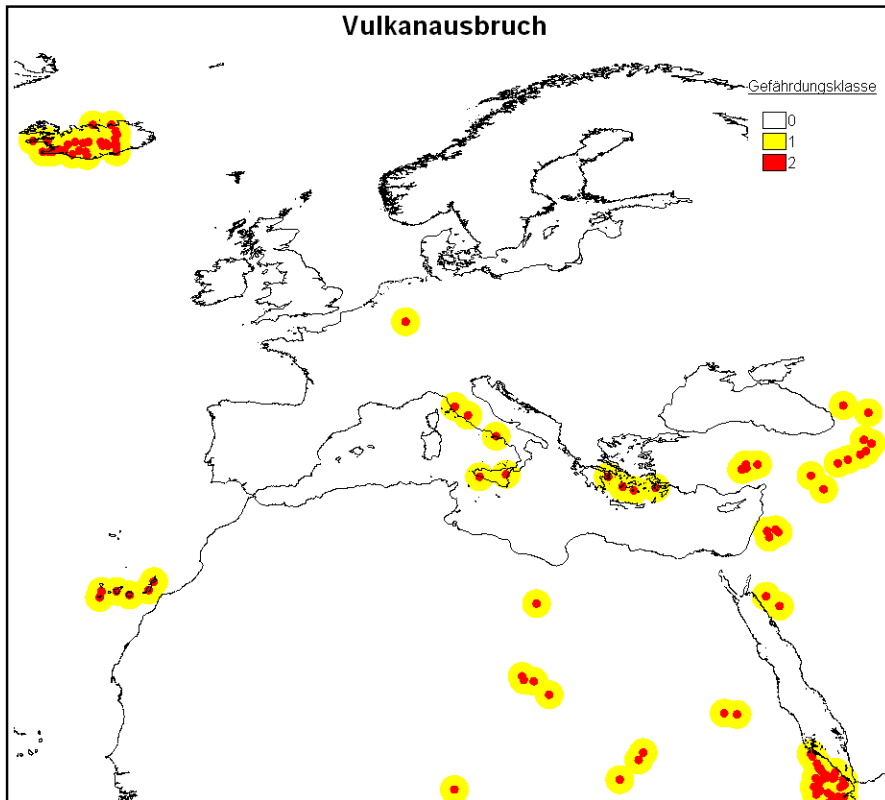


Fig. 46: Danger of volcano eruptions (Source: OD, Münchener Rück, 2001).

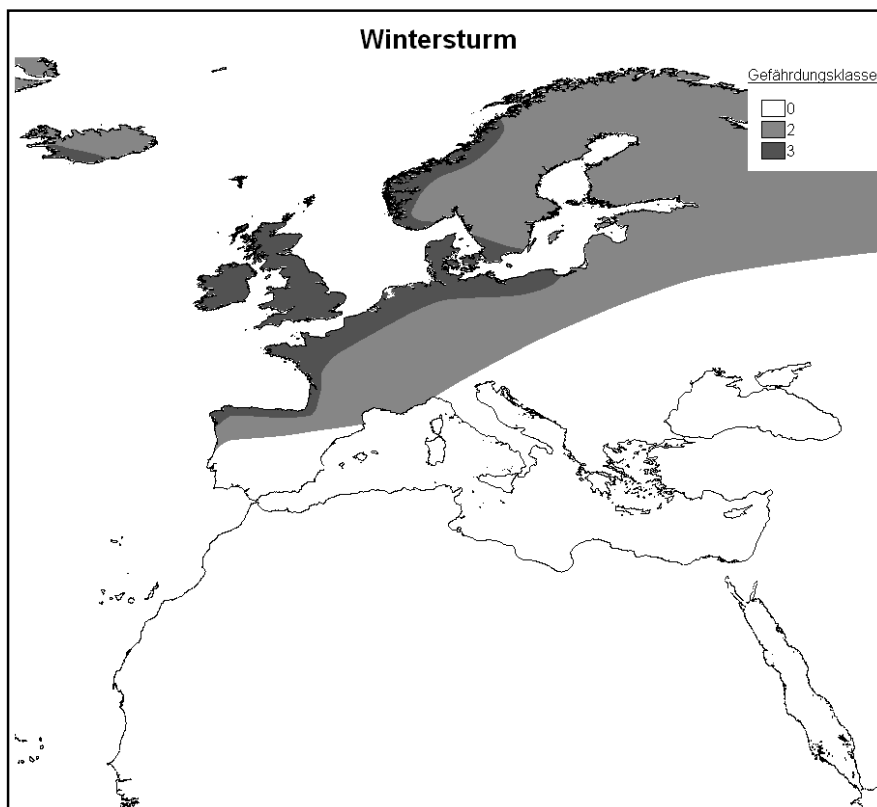


Fig. 47: Danger of winter storms (Source: OD, Münchener Rück, 2001).

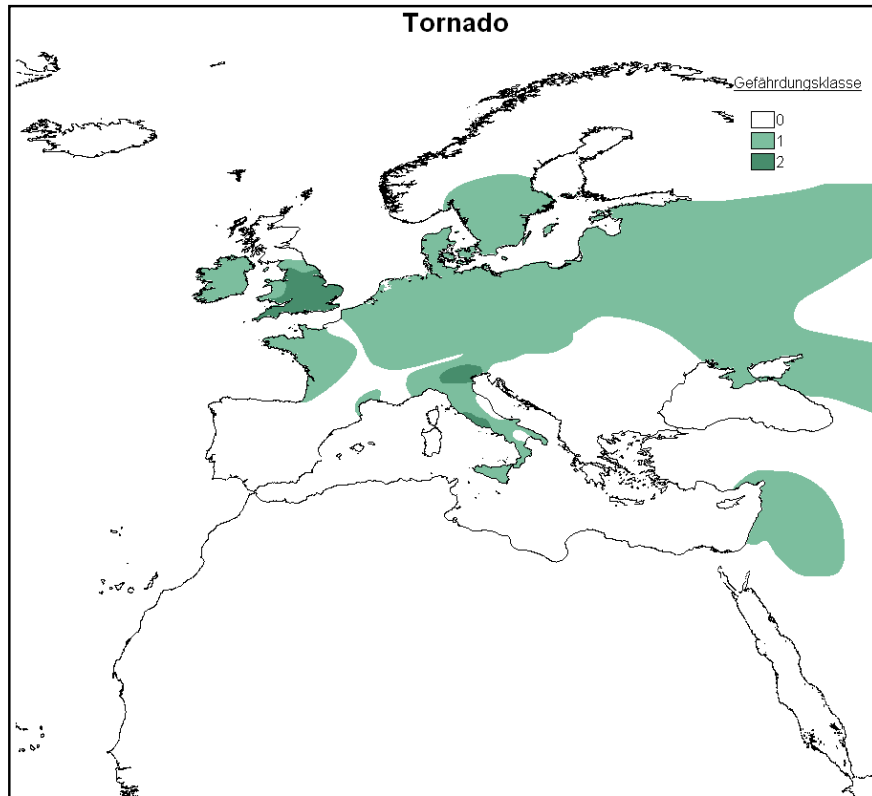


Fig. 48: Danger of tornados (Source: OD, Münchener Rück, 2001).

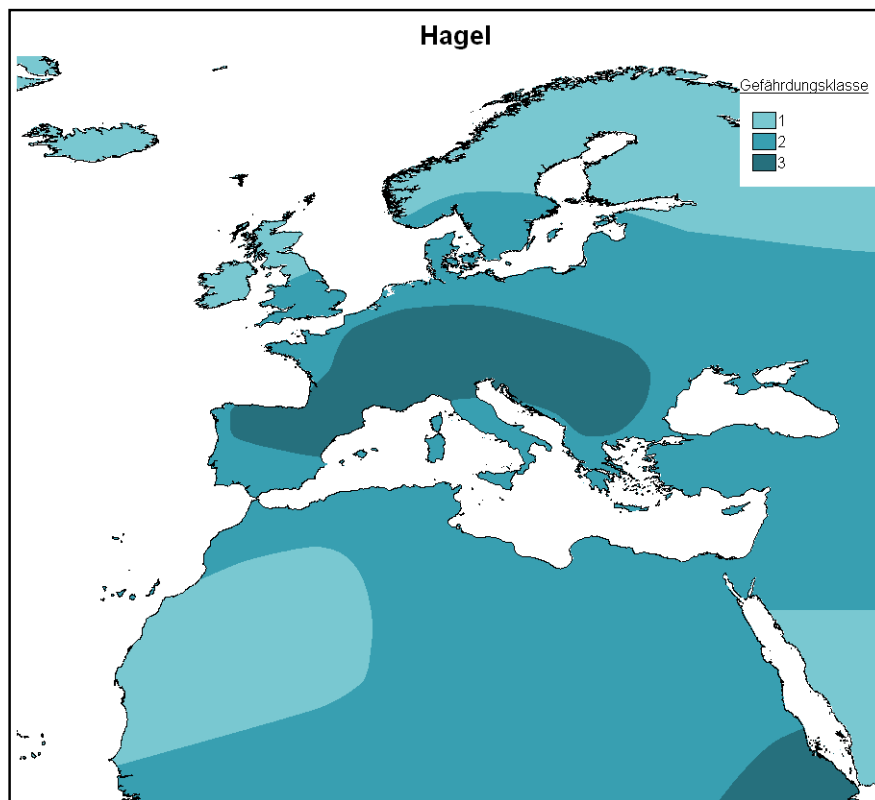


Fig. 49: Danger of hail (Source: OD, Münchener Rück, 2001).

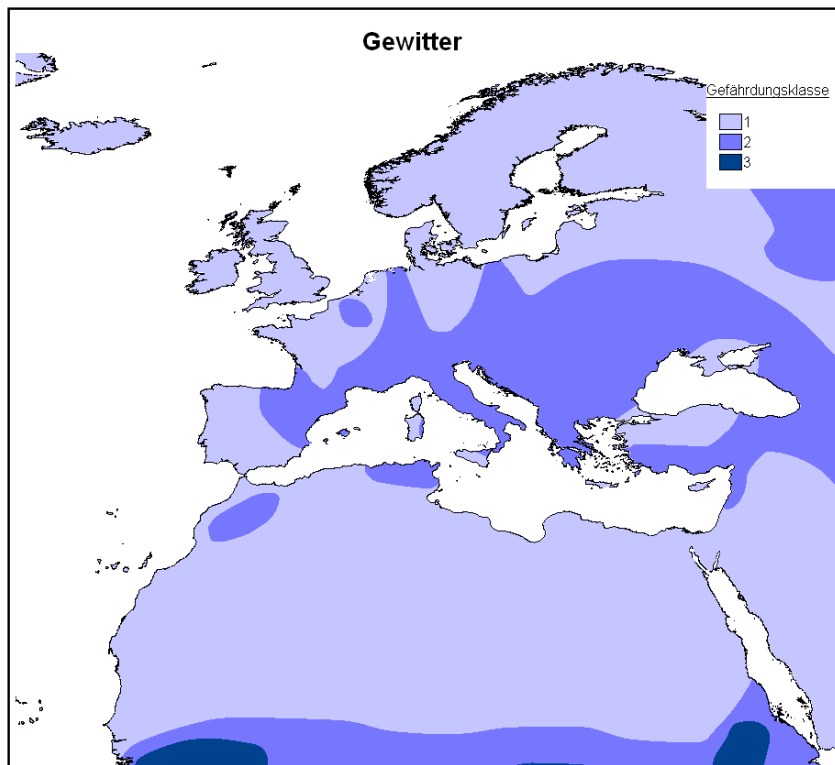


Fig. 50: Danger of lightning (Source: OD, Münchener Rück, 2001).

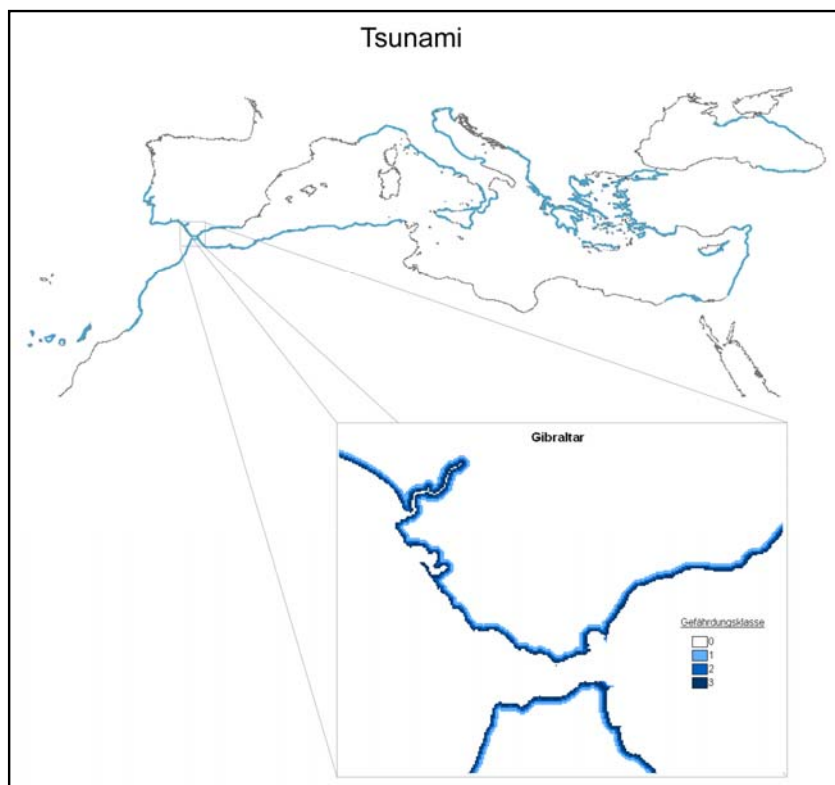


Fig. 51: Danger of tsunami (Source: OD, Münchener Rück, 2001).

Tab. 13: Risk classes of single natural hazards (Source: Münchener Rück, 2001).

Risk	Risk classes						Scale
	0	1	2	3	4	5	
Earthquake	< V	VI	VII	VIII	≥ IX	-	Modified Mercalli, P = 10% (50 years)
Volcano eruption*	no risk	100 km	30 km	-	-	-	geographical position to volcano
Tsunami*	no risk	low < 3 km	medium < 2 km	high < 1 km	-	-	geografische Lage zur Küste
Storm surge	no risk	-	-	high	-	-	geografische Lage zur Küste
Tropical storm	no risk	118 - 153	154 - 177	178 - 209	210 - 249	≥ 250	Saffir-Simpson hurrican scale [km/h]
Winter storm	no risk	-	medium	high	-	-	Wind velocity
Tornado	no risk	< 0.1	0.1 - 2	> 2	-	-	events per 10,000 km ² and year
Hail	-	< 1	1 - 3	> 3	-	-	hail days per year
Lightning	-	< 2	2 - 6	> 6	-	-	amount of strikes per km ² and year

*according to Kronshage, 2001; blue marked classes are not present in the Mediterranean region considered

In this model areas with a higher risk by natural hazards are also assigned higher costs factors (see table 15). These factors are based on an insurance costs model for the site-specific calculation of the insurance premium for natural hazards as described in Kronshage (2001). According to this, the insurance rate $V_{h,F}$ for overhead lines in case of a positive risk is composed of the base insurance rate $V_{h,F \neq zero}$ and an exponential weighting factor $b_h^{r_h} - 1$. The exponential approach describes the spreading of the risk classes. For the exponent r_h it has to be inserted the risk class of the respective natural hazard h . Even if there is no risk, for some natural hazards a risk cannot be fully excluded so that the insurance rate is charged with the positive value $V_{h,zero}$. The values for the base of the insurance rate function b_h of the natural hazards h and the residual insurance charges have been determined on the basis of an expertise of the research group 'Earth Science' of the Munich Re Group (Kronshage, 2001).

$$V_{h,F} = \begin{cases} V_{h,zero} & r_h = 0 \\ (b_h^{r_h} - 1) * V_{h,F \neq zero} & r_h \neq 0 \end{cases} \quad (h = 1, \dots, 9)$$

The damages arising by a storm surge strongly depend on the elevation of the land over the sea and thus are difficult to assess. Only in case of a differentiated

consideration of all coast sections with the associated backland it could be given valid statements about the risk potential. Besides, this kind of risk is not covered by the insurance in general. Therefore this risk as well as tropical storms should not be taken into account. For the danger of lightning the same values as for hail are used.

Tab. 14: Insurance rates and base factors (Source: Kronshage, 2001).

h	Risk	$V_{h,zero}$ [‰]	$V_{h,F\neq zero}$ [‰]	b_h
1	Earthquake	0.2	0.08	4.1*
2	Volcano eruption	0.0	0.03	4.6
3	Tsunami	0.0	0.21	2.5
4	Winter storm	0.1	3.64	1.1
5	Tornado	0.1	0.32	1.6
6	Hail	0.3	4.55	1.1
7	Lightning	0.3	4.55	1.1

*modified (Kronshage, 2005)

Tab. 15: Total insurance rates.

h	Risk	Risk class r				
		0	1	2	3	4
1	Earthquake	0.2	0.3	1.3	5.4	22.5
2	Volcano eruption	0.0	0.1	0.6	-	-
3	Tsunami	0.0	0.3	1.1	3.1	-
4	Winter storm	0.1	-	0.8	1.2	-
5	Tornado	0.1	0.2	0.5	-	-
6	Hail	-	0.5	1.0	1.5	-
7	Lightning	-	0.5	1.0	1.5	-

The insurance costs factors of several risks are added up for every pixel and thus result in the friction feature *natural hazard*. All costs factors of the remaining features (see table 16) are first lowered by the base costs for the purpose of the formation of sums. After summing, the base costs are again added so that just one single isotropic friction image R_{iso} arises:

$$R_{iso} = 1 + \sum F_k \quad [\text{Eq. 7}]$$

- F costs factor lowered by the base costs
- K feature (land cover, infrastructure, natural hazard, visibility)

The greatest possible friction factor of 100.0 is not reached as this would always assume a maximum weighting of all friction images in one place. For example, the areas that are most far away from the network are located in the Atlantic Ocean.

There neither a visibility analysis nor an assessment of natural hazards was carried out.

In the following the exclusion mask is laid over the entire isotropic friction image so that the resulting image additionally includes the maximum value of 10,000.0 for exclusion areas.

Tab. 16: Ratio of raised costs to base costs (= 1.0).

Feature <i>k</i>	Value <i>F</i>	Value according to Kronshage & Trieb (2002)
Land cover		
Grassland	1.0	1.0
Forest	5.0	1.2
Wetland	3.0	2.0
Savannah	1.0	1.0
Cropland	1.0	1.0
Rice field	3.0	2.0
Semi desert	1.0	1.0
Desert	1.0	1.0
Glacier*	10,000.0	10,000.0
Inland water*	10,000.0	15.0
Inland water (bridge)	3.0	2.0
Seawater	10.0	15.0
Populated place*	10,000.0	10,000.0
Agglomeration	10.0	-
Visibility		
Cultural/Religious sites	1.0; 7.0	-
Infrastructure		
Network	1.0 – 50.0	-
Natural hazards		
see table 15	1.0 – 30.9	-
Exclusion mask*	10,000.0	10,000.0
no data	10,000.0	10,000.0

*Sometimes redundant information exist which is included in both in the exclusion mask and other datasets.

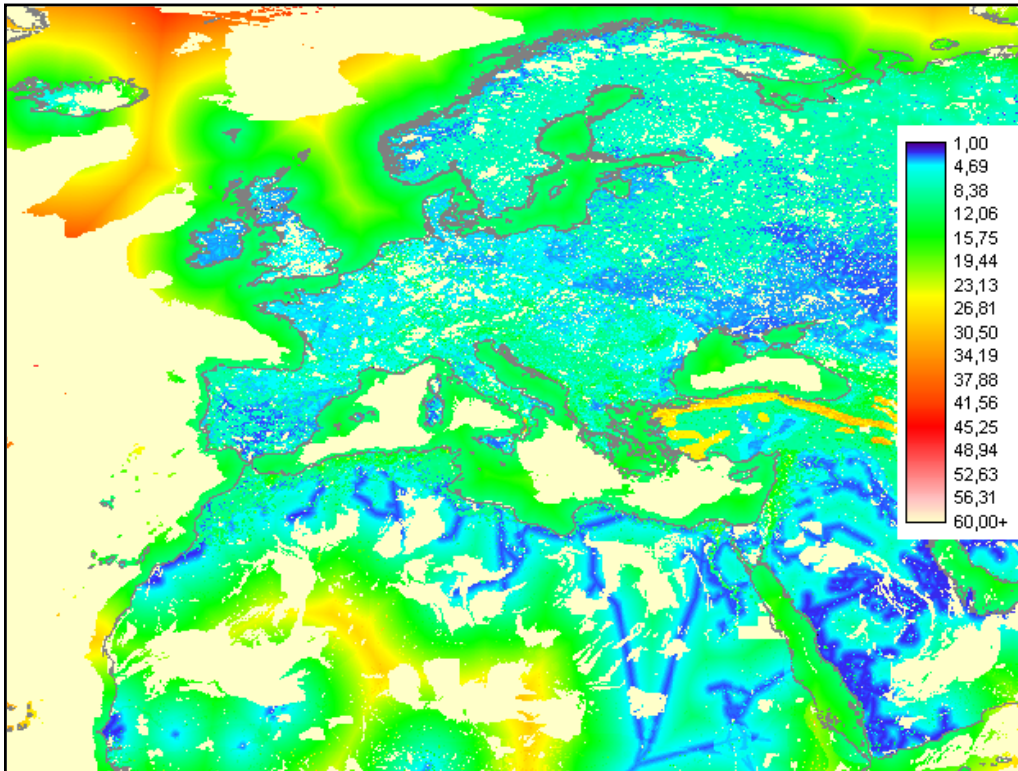


Fig. 52: Isotropic total friction image.

8.3 Generation of an anisotropic friction image

The former friction images contain isotropic features, which have the same value in all directions, whereas the slope is an anisotropic feature.

Slope

Exemplarily, one can imagine a traveller who climbed up a slope, which is inclined to the south (180°), in a northerly direction (0°). In doing this he must overcome the maximum slope on the shortest way. If he would cross the slope from a south-easterly direction (135°), he could overcome the same slope on a longer way. At 90° the traveller would move along the contour line. As explained, the crossing of a non-flat raster cell is direction-dependent. The resulting prolongation of the way finally causes additional costs for the line.

Generally it is assumed that the line costs rise with the increasing slope. In order to spatially determine the continental elevation in the whole Mediterranean region,

it is fallen back on the global digital elevation model 'GLOBE' of the NGDC, one of three national NOAA data centre (*GLOBE Task Team et. al., 1999).

The raster dataset has horizontal resolution of approximately 1 km x 1 km and a vertical resolution of 1 m above sea level. Altogether six raster elevation models and five cartographic vector datasets have been either reprocessed or specially processed for the utilization in GLOBE (30" raster). Data from 18 different sources (see figure 84 in the annex) are included in GLOBE. The main part is provided by the raster dataset 'Digital Terrain Elevation Data' (DTED) of the NIMA and the GTOPO30 raster dataset of the USGS, which was originally produced out of the DCW by raster conversion (Hastings & Dunbar, 1999).

First of all a slope image is calculated with the IDRISI tool 'Slope' out of the digital elevation model and the corresponding aspect image which issues the inclination angle as azimuth²⁷ for each pixel. A slope of 20 % and higher it is assumed as a stronger feature for the laying of the line. Above that, the additional expenditure in costs increases linearly so that classes are formed in steps of 45 %. From 200 % the magnitude of the slope is irrelevant for the additional costs and the maximum value is kept constant (Kronshage & Trieb, 2002). The maximum slope occurring in the Mediterranean region amounts to 151 % at a 1-kilometre digital elevation model.

Slope [%]	Factor
0-20	1.0
20-65	1.2
65-110	1.4
110-155	1.6
155-200	1.8
>200	2.0

With the help of an anisotropic function the effective friction of the pixel is determined out of the aspect image. The full friction is just given for an angle difference of 0° and 180° between walking direction and slope by using a quadratic

²⁷ Azimuth: angle between geographic north (0°) and the inclination.

cosines function. All other angles lead to a decrease in the effective friction until the neutralisation of the slope at 90° and 270° (Eastman, 1999).

effective friction = new rated friction^f

$$f = \cos^2 \alpha \text{ ('Directional Bias Function')}$$

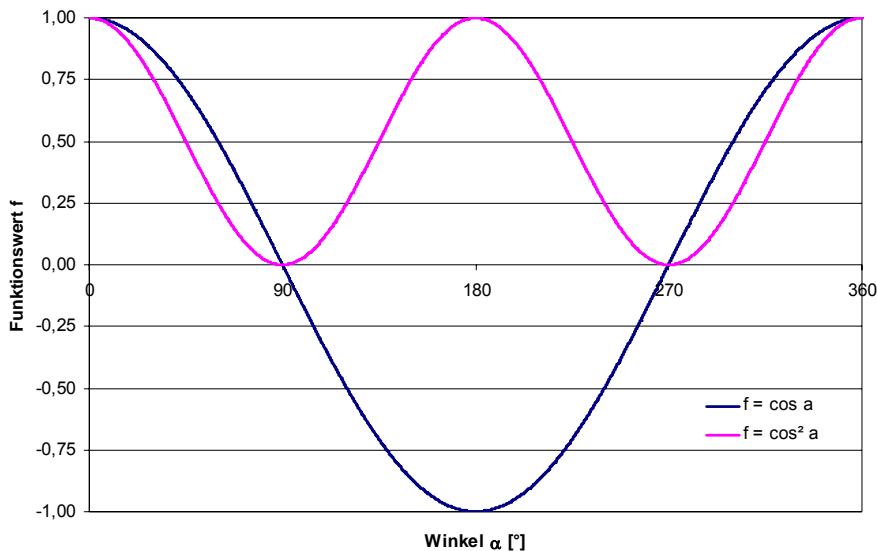


Fig. 53: Directional Bias Function.

8.4 Calculation of the cost-distance image and line laying

With the tool 'Varcost' a cost-distance image is calculated out of the isotropic friction image, the anisotropic friction image and its corresponding aspect image. For this the anisotropic friction image is multiplied by the isotropic friction image which represents the multiplication factor. The starting point is the site of the solar thermal power plant. Then 'Varcost' calculates the costs as distance raster equivalents for each raster image pixel which must be raised at least to get from the adjacent pixel to the plant. Exemplarily, a cell value of 100.00 means that the costs for bridging the distance between this pixel and the target pixel is equivalent to the movement over one-hundred cells with the base costs of 1.0 or over 50 pixel with a costs value of 2.0 or over one pixel with a costs value of 100.0 (Eastman, 1999).

After specifying the target, the tool 'Pathway' gives the favourable course of the line from the plant to the demand centre as line polygon.

Figure 54 shows exemplarily the cost-distance images calculated from the plant location for line 1 and 2 together with the final course of the lines. Due to the weighting of the underlying features, the values represented in figure 54 are no absolute, but relative costs. According to it, the favourable path has been selected.

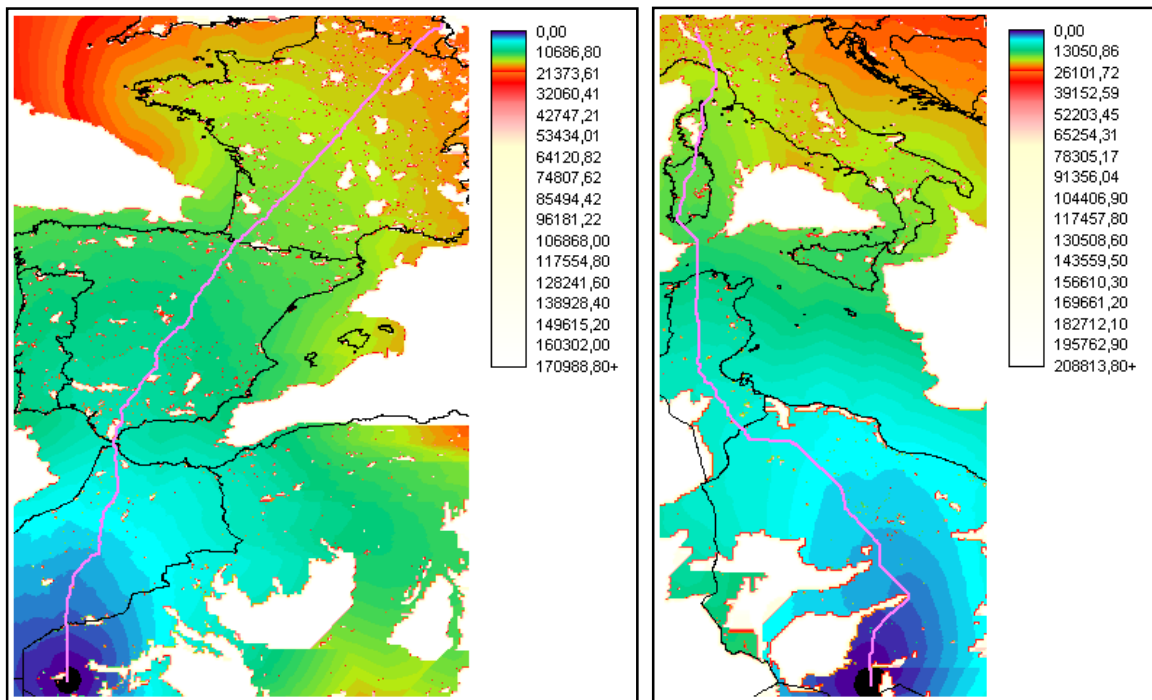


Fig. 54: Cost-distance image for line 1 (left) and line 2 (right).

9 Analysis of the results



Fig. 55: Resulting course of HVDC lines for a solar electricity import.

9.1 Line 1: Algeria-Aachen

The first line starts in the western part of Algeria approximately 100 km to the east of *Tindouf*. From there an overhead line leads exactly in a northerly direction through the desert to Morocco, crosses the *Atlas Mountains* and reaches the *Strait of Gibraltar* after nearly 1090 km. Then the line must be performed as submarine cable on a length of 18 km. At the European coast again it is connected to an overhead line. On the further course the line has to get past the Spain wildlife sanctuaries *Los Alcornocales* and *Sierra de Grazalema* to the east and then to cross the Iberian Peninsula on a length of about 930 km, where the land cover varies heavily between woodlands, grasslands, croplands and semi deserts. On the latitude of the *Pyrenees* the French border is passed. Then the line runs almost straight in a north-easterly direction as only a few areas are excluded in

France. The residual area is mainly used for agriculture. After a total of 3117 km the destination *Aachen* is reached.

Figure 56 shows the ground profile from the centre of demand in the north to the plant site in the south. Along the line a maximum height of 3500 m in the *Atlas Mountains* and a maximum depth of -750 m while the *Mediterranean Sea* must be overcome. The hypsographic summarized curve makes clear that over 50 % of the areas lie between sea level and 500 m above sea level and just 5 % in the high mountain region above 1500 m.

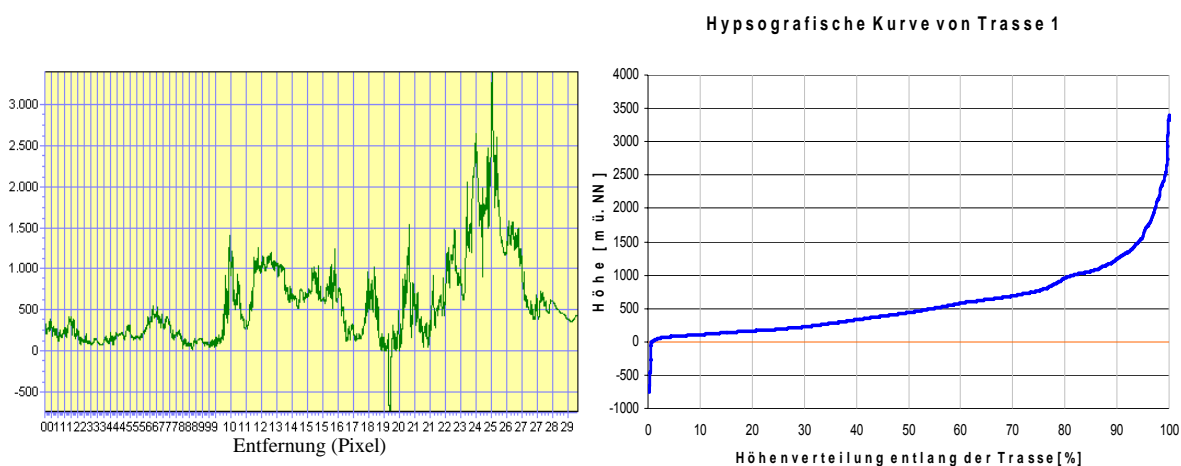


Fig. 56: Ground profile [height above sea level] of line 1 from Aachen to Algeria and the associated hypsographic elevation model.

9.2 Line 2: Libya-Milano

The second line has a total length of 3108 km and begins in the south-western part of Libya around 80 km south-easterly of *Al Wigh*. The first 1330 km leads through the *Libyan Desert* in a north-west direction. There the course of the line is mainly determined by geomorphologic features like dunes and fields of lava around *Al Haruj*. Tunisia is centrally passed on a length of 700 km because of the large sand deserts of the *Sahara (Erg)* in the west. Altogether over 50 % of the line lies in desert areas. In the northern part of Tunisia areas are hardly excluded due to a low population density and a lot of cropland and grassland. Then comes a 220 km long submarine cable to the Italian island *Sardinia*. On the Mediterranean islands the line follows the course of the already existing HVDC line *SACOI*. The large *National-Regional Park of Corsica* forces the line to go past easterly. In order to connect the line with the Italian mainland a submarine cable with a length of

nearly 130 km is used. The national park *Arcipelago Toscano* remains untouched as expected. Afterwards the line has to pass the woodlands of the *Apennines* and croplands in the *Plain of the river Po* until the destination *Milano* is reached after 180 km.

The largest heights about 1200 m can be found on *Sardinia* and in the *Apennines*. The deepest point of the line lies at -1968 m in the *Mediterranean Sea*. Along the whole distance no high mountain regions are crossed and almost 90 % of the areas lie between sea level and 1000 m above sea level.

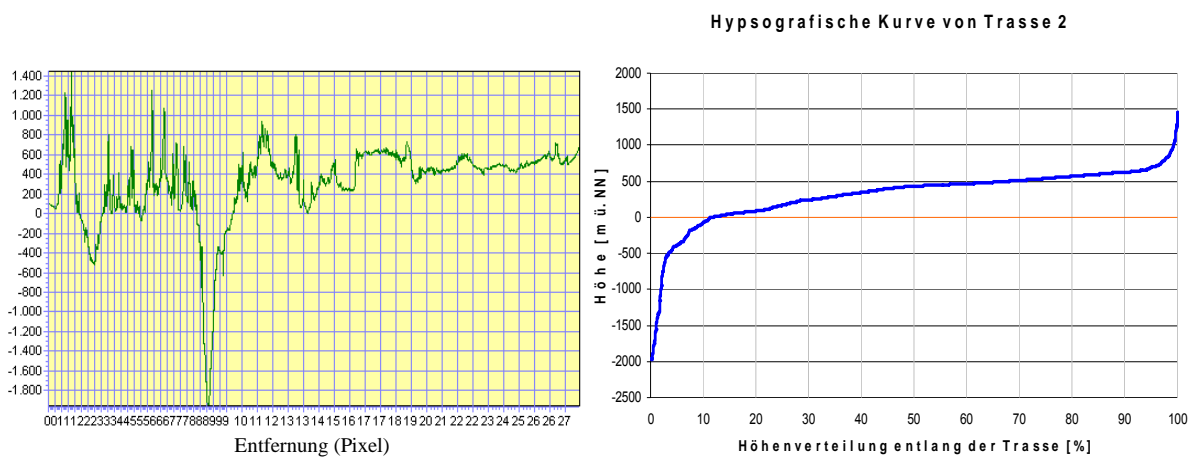


Fig. 57: Ground profile [height above sea level] of line 2 from Milano to Tunisia and the associated hypsographic elevation model.

9.3 Line 3: Egypt-Vienna

The solar thermal power plant, which is the starting point of the third line, is located approximately 50 km in the east of the oasis *Kharga* in Egypt. From there the overhead line runs 860 km through Egypt first in northerly and then in easterly direction. On the way the *Nile* is crossed nearly 35 km in the north-west of *Asyut* and afterwards also the *Gulf of Suez* as the populated places of the city *Suez* and dunes in the northern part of *Sinai Peninsula* are excluded.

On a distance of 60 km the southern part of Israel is passed exactly between the three natural reservations *Har Ha Negev*, *Ashosh* and *Nehalim Gedolim Uqetura* and afterwards the line leads to *Ma'an* in Jordan. After a total of 380 km the national border to Syria is reached. From there the line runs around 500 km through the *Syrian Desert* and then gets past westerly the water reservation *Buhayrat al Asad*. On a distance of 1300 km the line leads further through the

Anatolian part of Turkey, past *Ankara* and *Istanbul* and then runs along the coast of the *Black Sea* over the *Bosporus* and through the European part of Turkey called *Thracia*. Afterwards the countries Bulgaria, Romania and Hungary are passed in a north-westerly direction until the destination *Vienna* is reached after 1370 km. The river *Danube* is first crossed 60 km in the south-west of *Craiova* in Romania and then 60 km in the south of *Budapest*.

The line has a total length of 4511 km and has to overcome large heights of around 2000 m especially on the *Balkan Peninsula*. Altogether 90 % of the areas concerned lie between 0 and 1500 m above sea level.

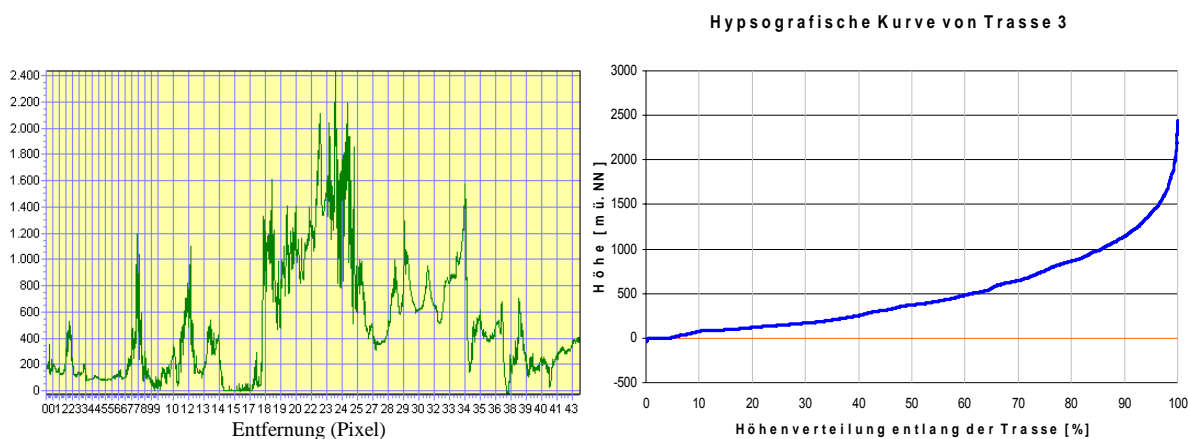


Fig. 58: Ground profile [height above sea level] of line 3 from Vienna to Egypt and the associated hypsographic elevation model.

9.4 Evaluation

In the following the lines are submitted to analysis and the results are evaluated regarding their accuracy among others.

Length of the line

In table 17 the total length, the shared length of all countries and the sea sections are listed. Accordingly, line 2 has the longest submarine section of 373 km, that corresponds to 12 % of the line. Line 1 has to cross the *Strait of Gibraltar* on a length of 18 km and the 30 km long submarine sections of line 3 lie in *Gulf of Suez* and at the *Bosporus*. However, what concerns line 3 the length of the submarine section has been overestimated. As the line leads along the coast, an overlapping with areas of the *Black Sea* is possible.

Altogether line 3 is one and a half times longer than the other lines and has therefore the longest overhead line section with 4481 km.

Tab. 17: Line shares of the concerned countries in kilometres.

Line 1		Line 2		Line 3	
Country	Length [km]	Country	Length [km]	Country	Length [km]
Algeria	256	Libya	1326	Egypt	858
Morocco	835	Tunisia	701	Israel	59
Spain	932	Sardinia/Italy	313	Jordan	378
France	907	Corsica/France	216	Syria	495
Belgium	164	Italy	178	Turkey	1324
Germany	5			Bulgaria	448
				Romania	361
				Hungary	518
				Austria	40
Overhead line	3099	Overhead line	2735	Overhead line	4481
Submarine cable	18 (0.6 %)	Submarine cable	373 (12 %)	Submarine cable	30 (0.7 %)
Sum	3117	Sum	3108	Sum	4511

Land use

The calculation of the respective forms of land use concerned by the lines shows that in all three cases areas are mainly used which have been intended for that. Rice fields and wetlands are not touched by the lines and also agglomerations are almost always omitted (see tables 30-32 in the annex). The share of forest does not exceed 10 %. This is essentially equivalent to a typical land use of an overhead line mentioned in Knoepfel (1995).

Only what concerns line 2 lie about 10 % of the crossed areas in the visual range of certain cultural sites. The shares of the other lines are lower; however, this analysis is based on a database afflicted with a higher uncertainty.

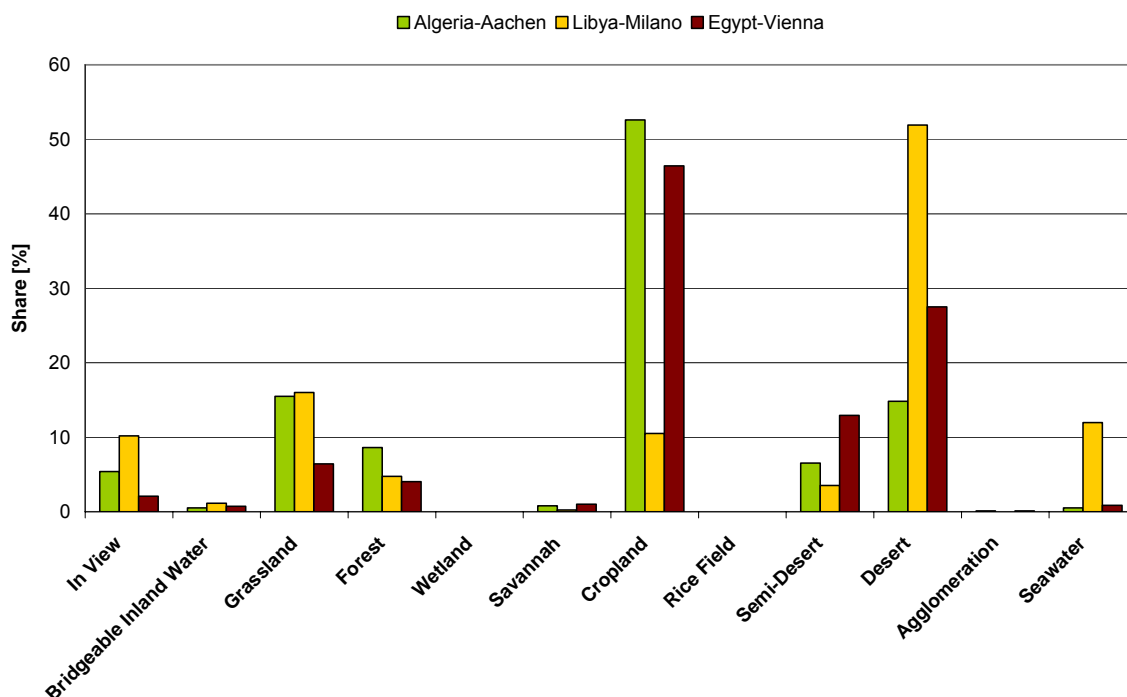


Fig. 59: Degree of land use and visibility of the lines.

If a line width of 100 m is estimated, the space requirement below the line amounts to 100 km² per 1000 km. Further space requirements for several land uses and lines are listed in the tables 30-32 in the annex.

Line bundling

The influence of the criterion 'distance to the line' is just reflected in the results in relative units. Generally the European electricity network is much denser than the North African network. Only 12.9 % of the third line lies in the same raster square of the reference network, what already represents the best result of all lines. A higher accuracy is not possible due to the spatial resolution of data (30').

The dataset for Europe contains topographically exact courses of lines, but does not differentiate voltage levels, whereas the dataset for North Africa identifies all lines from 90 kV, but only in a schematic way. In addition to this the submarine lines of the *Mediterranean Sea* are only partially integrated. Because of these uncertainties of both datasets a heavier weighting to the benefit of line bundling is not made.

Tab. 18: Statistical parameters of the line distance to the reference network in km.

Line	Mean	Standard deviation	Maximum	Minimum (share in total line)
1	33.9	68.9	314	0 (5.4 %)
2	50.5	62.6	299	0 (7.4 %)
3	11.3	13.9	88	0 (12.9 %)

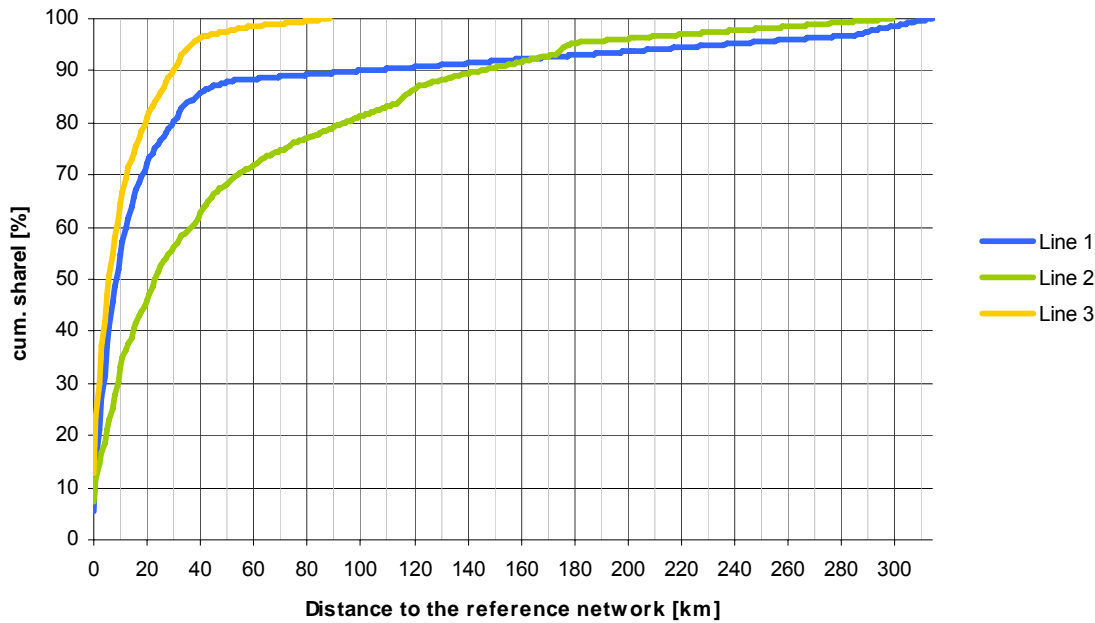


Fig. 60: Line distances to the reference network.

Distance to congested areas

In case that it is intended to branch power at another place in future, what means that the line should be operated as multi-terminal, the direct distances to important cities along the lines are listed in table 19. At that place the branch line can only be realized by a further rectifier terminal. If larger loads are taken out, the line should be extended so that following demand centres can be supplied with electricity.

Tab. 19: Line distances to selective cities in km.

Line 1 City	Distance	Line 2 City	Distance	Line 3 City	Distance
Marrakech	96	Tripoli	141	Aswan	233
Casablanca	152	Sfax	128	Cairo	83
Rabat	92	Tunis	79	Suez	12
Fes	39	Cagliari	40	Amman	82
Sevilla	70	Florence	104	Damascus	108
Madrid	57	Genoa	62	Aleppo	72
Zaragoza	96			Ankara	12
Toulouse	132			Istanbul	19
Bordeaux	78			Sofija	99
Paris	105			Budapest	55

Altogether the accuracy of the course of the three lines depends on the underlying datasets, especially on their completeness.

Especially what concerns the protected areas within the European Union, better datasets could be provided by the cataloguing of the 'Natura 2000' areas after their finalization in the near future.

Regarding the infrastructure there has not been provided an updated and topographically correct dataset together with attributes up to now. The difficulty lies chiefly in the spatial reproduction of these structures.

Furthermore, the dataset used for the visibility analysis is rated uncertain. Anyhow, it concerns a subjective criterion so that the impacts on the landscape-image should be clarified at another scale and with another method. Here just an approximate estimation for this criterion can be done.

For the residual datasets it is assumed a sufficient accuracy with regard to the formulation of the question and the size of the considered section. It has been attempted to take a scientific method as a base for the determination of the friction factors in principal, otherwise the estimation happened in all conscience.

Altogether it seems that the results, especially with regard to the land use, are plausible and fulfil the requirement of a general representation.

The multitude of possibilities to visualize the results within a GIS can contribute to give a clear imagination of the topographic course of the lines. If it is considered on country level, the results could also be interesting for political decision maker. Nevertheless, this analysis does not substitute a detailed planning.

10 Product Eco-balance - Life Cycle Assessment

'...compilation and evaluation of the inputs and outputs and potential environmental impacts of a product system throughout its life cycle' (ISO, 2005).'

By means of a life cycle assessment (LCA) it is possible to record the environmental pollutions of a product through its whole life cycle. In the sense of an integral view not only the actual process of the manufacture is examined, but also those processes which guarantee the provision of energy and materials in the preceding production chain. Furthermore, environmental pollutions, which arise during the utilization and the final use of the product, are important parts of LCA. For this, emissions, waste, land and resource consumption is assessed in a quantitative form and evaluated regarding environmental impacts.

As a rule eco-balances are prepared as comparative assessment, in which products, processes or services with the same purpose are compared concerning their environmental effects (Guinée, 2002). An eco-balance does not provide additional data, but aggregates available data in a way that new findings are gained (Schmidt & Häuslein, 1996).

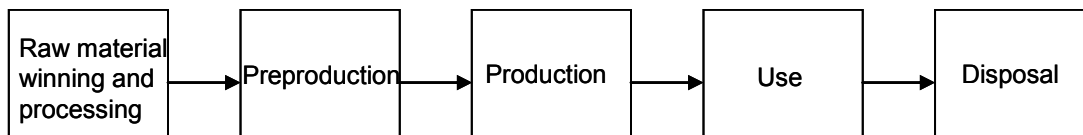


Fig. 61: Product chain 'from cradle to grave'.

The higher aims of an eco-balance are the preservation of energetic and material resources and the conservation of the ecological and human health and recovery respectively (Knoepfel, 1995).

In a narrow sense it is possible to take an inventory of the product-related environmental impacts by means of an eco-balance as well as to identify specific problem areas within a product chain. With this realization environment-friendly products can be developed. For a company additional, economic benefits result through the saving of resources, the increase in productivity and the possibility of a direct connection with the costs side. Besides, the chance of success of a product on the market is higher if it is advertised with the results of the eco-balance. The

environment-friendliness of a product becomes particularly clear by using special environmental labels. In addition to this, product eco-balances complete reasonably the environment management system of the company (ISO, 2005).

An eco-balance can also be used for the long-term, strategic planning of the government. There it serves as an environmental decision help for the awarding of environmental labels, the levy of eco-taxes and the development of aims, for the minimization of the pollutants and emissions, for instance (ISO, 2005).

10.1 ISO Standardization

The international organization for standardization (ISO) is a private organization, which includes national institutions of both industrialized countries and developing countries and whose object to standardize a wide range of products and activities. The 14040-series 'Environmental Management - Life Cycle Assessment' produced by the ISO contains general standards and technical reports for a LCA. These international valid standards provide guidelines for a preparation, analysis and evaluation of an eco-balance.

Procedure according to ISO 14040²⁸ (ISO, 2005)

- Definition of goal and scope (ISO 14041²⁹)

First the actual goal of the study is defined. At the same time the client and other interested parties can be determined. Furthermore, the products to be balanced are described and the study background is explained. Appropriate temporal and spatial system boundaries have to be chosen for a sufficient containment of the scope of examination according to the object. How far a substance flow can be neglected depends on its share in total substance flow and energy flow and its environmental effect relevance.

Generally, different product systems should only be compared if they have the same function, which is constituted in a material form, energetic form or as service. A reference value, the so-called 'Functional Unit', is defined in order to quantify this function. Products must be comparable, also with respect to the

²⁸ ISO 14040: Environmental management – Life cycle assessment. A standard on principles and framework. 1st Edition (1997).

²⁹ ISO 14041: A standard on goal and scope definition and inventory analysis. 1st Edition (1998).

coverage and depth of the study, i.e., which partial processes are recorded at which level of sophistication (simplified, detailed).

Selected impact categories may already be listed at this place with reference to the object.

▪ Inventory analyses (ISO 14041)

This contains the registration of all relevant substance and energy flows of the product system and the preparation of a data inventory. A subdivision into partial processes might be helpful to answer the question for essential input and output flows:

- Production and processing of raw materials
- Production of important auxiliary and operating materials
- Transports
- Production and use of primary energy carriers, electricity and heat
- Use of the product
- Disposal of waste and products.

After this, all necessary raw, auxiliary and operating materials have to be registered on the input side and emissions of air, soil, water and waste flows on the output side. For the entire system an inventory of the material flows, which pass the system boundaries, is obtained by the interconnection of single processes.

▪ Impact assessment (ISO 14042³⁰)

In order to estimate potential impacts of the product on the environment, the inventory analysis values are summarized with respect to their impact. The assignment of the material flows to the before determined impact categories is denoted as *classification*, whereas a material flow may also be assigned to several categories. In the scope of a *characterisation* the material flows are converted into equivalent characterisation factors of the respective reference substance in accordance with their contribution to impact categories and afterwards they are summarized. Experiences from the ecological impact

³⁰ ISO 14042: A standard on life cycle impact assessment. 1st Edition (2000)

research are included, e.g., impact thresholds, danger potential and the established priorities of the society to environmental thresholds and goals (Schmidt & Häuslein, 1996). *Classification* and *characterisation* form obligatory elements in the scope of an impact assessment. Optional elements are *normalisation* (ratio indicator to reference value), *ranking* and *weighting* of the impact categories (UBA, 2000).

One method for the evaluation of eco-balances was developed by the Federal Environmental Agency (UBA, 1995). At the same time it proposes the impact categories listed in table 20. Which impact category is considered as important, cannot always be judged objectively, especially since the impact categories can differ in their reference area.

Tab. 20: Fields of examination of the Federal Environmental Agency (Source: UBA, 1995/1999/2000).

Impact category	Reference area	Characterisation factor
Consumption of fossil energy carriers and material resources	local	upper heat value[MJ], [kg]
Global warming	global	CO ₂ -equivalent [kg], <i>Global Warming Potential (GWP)</i> , time horizon: 100 years
Stratospheric ozone depletion	global	FCKW R11 <i>Ozone Depletion Potential (ODP)</i>
Photo-oxidant formation	local/regional	C ₂ H ₄ -equivalent [kg], <i>Photochemical Ozone Creation Potential (POCP)</i>
Acidification	local	SO ₂ -equivalent [kg], <i>Acidification Potential (AP)</i>
Eutrophication (terrestrial/aquatic)	local	PO ₄ ³⁻ -equivalent [kg], <i>Nutrification Potential (NP)</i>
Human toxicity (direct damages of the human health)	local/regional	critical contaminated body mass [kg]
Ecotoxicity (direct impairment of ecosystems)	local	critical contaminated water amount [m ³] soil amount [kg]
Land consumption	local	area [km ²]

- Interpretation (ISO 14043³¹)

Here, the results from the inventory analysis and impact assessment with reference to the object are summarized and interpreted. The easiest way to carry out the ecological interpretation of the products to be compared is by means of graphical representations. Within the result interpretation the quality of the LCA is also examined. This means that statements are made about completeness, consistency, sensitivity and limitations of the LCA. By means of

³¹ ISO 14043: A standard on life cycle interpretation 1st Edition (2000)

the results conclusions and recommendations can be derived for policy, producers and other participants.

Possible limitations of a product balance are often generic process databases with a low quality of data for the modelling of initial products. It concerns the age of data, the geographic reference area and the underlying technology (Guinée, 2002). Additionally, is must be paid attention to the formation of joint products. This means that appropriate allocation rules, which add the environmental impacts of the process proportionately to the joint product, have to be applied if several products originate from one process.

10.2 Material flow networks

The software UMBERTO[®] of the ifeu institute Heidelberg and the ifu institute Hamburg (*IFEU/IFU, 2005) use the method of material flow networks, which models the material and energy flows in a system as a grid as well as their conversion in production and reduction processes. Thus UMBERTO[®] is able to reproduce the whole course of life of one or more products, finally, to determine the target-related, quantitative expenditure for the generation, utilization and disposal of one product unit.

The software is based on a large database. The method of material flow networks is suited for both site-related operational eco-balances and product-related eco-balances (Schmidt & Keil, 2002).

The basis is a Petri net with three essential net elements:

- Place (= repository)
- Transition (= material or energy conversion process)
- Edge (= connection of nodes).

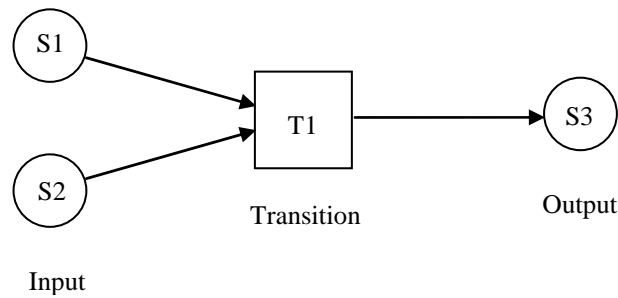


Fig. 62: Petri-Grid with the essential grid elements.

The materials and energies respectively (so-called *marks*) are provided by the *places* and lead along the *edges* to the *transition*, where they are transformed. On the output side the product is again picked up and stored by a *place*. Special forms of *places* can be *input* and *output places*, which define the system boundary, and *connection places*, which refuse the storage of materials.

In order to clarify which materials in the material flow network are useful at all, eco-account-frames are employed, which show the raw materials and energy on the input side and products and waste on the output side. A material is a yield in the product system (*reference flow*) if two requirements are fulfilled (IFEU/IFU, 2005):

- a) It must be a flow which either leads to an output or comes from an input, running over the boundaries of the system.
- b) The flow must have the material type *good* if it leads to an output and the material type *bad* if it comes from an input.

Tab. 21: Extended eco-account-frame with yields/reference flows (green) and expenditures (red) (Source: IFEU/IFEU, 2005).

Type	Input	Output
Good	resource consumption	product manufacture
Bad	waste disposal	waste production

The assignation of additional information about material type is particularly useful if there are joint productions in the networked system and if it is not obvious whether a material represents a product or an initial material for the following process. Altogether three cases can be distinguished (IFEU/IFU, 2005):

- Good → welcome (products, raw materials)
- Bad → unwelcome (emissions, waste)
- Neutral → not relevant (O₂, H₂O)

Raw materials are welcome regarding the fact that they are fundamentally required for the product manufacture and should be available in an adequate amount, whereas waste is unwelcome and whose disposal is sometimes expensive. However, waste can be reduced by recycling and added again to the process on the input side.

Due to the modular structure of a material flow network the representation of the energy and material flows and their transformation in the system can be realized up to the level of individual production processes, but information about the respective input and output flows is required for the calculation of single partial processes. Nevertheless, not all flows in the entire network have to be known as missing values and can be derived from well-known values in the course of a sequential calculation. The direction of the calculation does not depend on the actual direction of the material flow.

Calculation of the network is started by manual insertion of a material flow at a certain place in the network. The calculation rules for the determination of unknown material flows are specified in the transitions. Generally, the calculation is always executed locally, i.e., related to the respective transition. If missing input or output values are detected during the first calculation step, the calculation of the transition fails. In a second iteration conditions could have been changed so that the second calculation succeeds (Schmidt & Häuslein, 1996).

Linearity is often supposed for the modelling of single processes. This simplifies the scaling of the product amount on the functional unit of the product concerned as well as the consideration of cyclic material flows in the product system. Unlike current software applications in the field of LCA there are other possibilities within Umberto[®] to describe production processes (Schmidt & Keil, 2002):

- Production coefficients (linear approach)
- Production functions (non-linear approach)
- Hierarchical network (erection of a sub network)

- Empirically determined data inventory via flows ('Library')
- External model (different software)
- Definition via script-languages (Java, VBA, Python).

The tabular compilation of all calculated material and energy flows can be realized via the *inventory inspector* in the form of an input-output-comparison. In the so-called *balance sheet* the LCA data can be subdivided according to concerned processes or materials for the entire network, single sub networks or transitions and form together the product balance. Furthermore, there is the possibility of a graphic representation using a *sankey* or circle diagram. Within Umberto[®] the ecological evaluation of the LCA results is put into action by applying assessment systems and reference number systems to the LCA data. Besides, evaluation procedures can be imported or new defined with the *valuation system editor* (Schmidt & Häuslein, 1996).

Umberto[®] supports exporting of all results for the purpose of a further processing or extended representation and importing in current calculation tools.

11 Life Cycle Assessment of a solar electricity production and transmission scheme

11.1 Goal and scope definition

The goal is the preparation of a balance of the environmental impacts caused by a solar electricity transmission from North Africa to Europe. A balance is made up for all three lines composed of the solar thermal power plant and the associated HVDC line derived from the Geographic Information System analysis so that they are comparable among each other regarding their ecological weak points. On one hand, the environmental impacts arising at different life phases of the solar power plant and the transmission line shall be investigated in detail; on the other hand the impacts associated with individual components of the system shall be examined.

Generally accepted guidelines for the preparation of a Life Cycle Assessment (LCA) can be found in ISO 14040ff. Modelling of material and energy flows is carried out within the database and modelling tool Umberto[®] by means of material flow networks. The procedure of the Federal Environmental Agency (UBA) is used for the preparation of the impact assessment. Afterwards the results are normalized to 1 kWh_{el} and compared with a reference electricity mix among other things. In a broad sense the question should be answered if environmental impacts associated with the provision of electricity from fossil primary energy carriers can be reduced by an electricity import from renewable energy resources. Furthermore, it is also interesting to what extent a changed electricity mix for the production of the facilities could have an effect on the balance. Therefore two balance cases with different reference periods of time are set against each other.

11.1.1 Specification of system boundaries

The system operating time is defined uniformly as 30 years according to the plant. Thus, just 60 % of the HVDC line, which has an operating time of 50 years, is considered for the balance. The functional unit amounts to 1 kWh_{el} free network supply.

Within the balancing of the plant exploration, mining, processing and transportation of the fuels, especially for the electricity mix as well as the required infrastructure, are covered. Furthermore, the production of single components is

considered. This comprises the solar field, the steam generator, the mechanical and electrical engineering, the constructional engineering, the storage and the steam turbine. Certain recycling quotas are given for steel, aluminium and copper. Modelling of the facility operation includes maintenance, i.e., cleaning and material exchange. The disposal of the facility is composed of the demolition (except the buildings) and the depository.

Modelling of the HVDC line comprises the winning of the raw materials, the production and transportation of the materials and components with respect to their destination. Besides, emissions arising during the operating time of the facility are incorporated. There is no reliable data available about maintenance, cleaning measures and the final disposal.

11.1.2 Subject of modelling

A solar thermal power plant (type Parabolic Trough Solar Electricity Generating System 'SEGS') with thermal storage and dry cooling tower is used for the generation of electricity. The transmission line is a ± 800 kV HVDC system performed as double-bipole. Plant location and course of the line correspond to the respective line from the GIS analysis. Both systems are designed for a capacity of 10 GW. The year 2030³² is defined as temporal reference for the facility construction. Accordingly, the electricity mix, the manufacture of steel, aluminium, copper, rock wool, ceramics and flat glass are extrapolated to this year.

11.1.3 Databases and processes

An existing model for an 80 MW SEGS power plant with reference to the year 2010 from the SOKRATES project was adjusted to a 10 GW SEGS power plant (Viebahn, 2004). The quality of the original data from the year 1996 is rated high because it concerns information of the producer. Besides, it was updated and added. Input data for the modelling of overhead lines and cables is primary data from the producer ABB (Normark, 2005). In some places it is supplemented with

³² The year 2030 was chosen as reference period of time for the facility construction since the realization of the project before this period of time is unlikely. This prognostic balance assumes the best available technology and extrapolates it with scenarios, which are especially suited for a long-term prognosis.

own calculations and bibliographical references (Knoepfel, 1995; ESA, 2004). In addition, the process database of Umberto® (*IFEU/IFU, 2005) and partially the Switzer database ecoinvent 2000 is used (*ecoinvent Zentrum, 2003)

11.1.4 Used Modules

- Electricity mix 2010/2030

This module includes all plant processes for the electricity generation, the fuel production chain and the power distribution system together with the involved losses. The composition of the mix 2010 represents the ‘Business-as-Usual-Development’ in Germany and is derived from the reference scenario ‘Sustainable Energy Supply’ of the Enquete commission (Enquete, 2002). The mix 2030 is calculated following the sustainability scenario of the Federal Environmental Agency (UBA, 2002) and assumes a forced expansion of renewable energies, an increasing rational energy use and the integration of fuel cells (DLR et al., 2003).

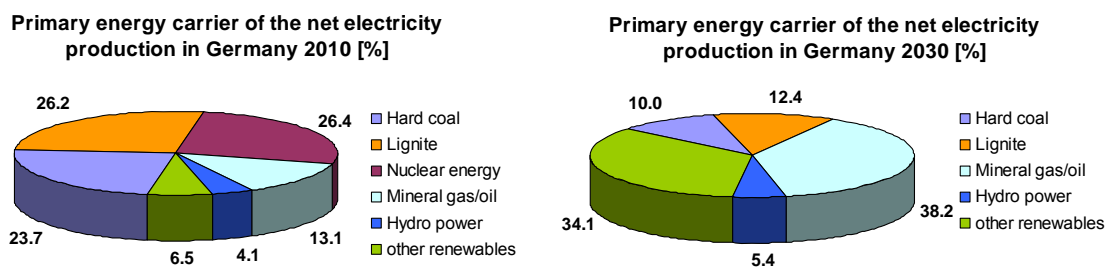


Fig. 63: Electricity mix 2010 und 2030 (Source: DLR et al., 2003).

- Steel 2010/2030

The production of different sorts of steel is developed further from an Umberto® module by taking the new defined electricity mix 2010 and 2030 respectively as a base. The recycling quota in 2010 amounts to 46 %, independent of the sort of steel (Viebahn, 2004). For 2030 a quota of 75 % is assumed (BMU, 2004b).

- Aluminium 2010/2030

The reference balance represents an eco-balance of the primary and secondary production of aluminium of the European aluminium industry (Boustead, 2000). The used electricity mixes are the same as mentioned above. The recycling quota in 2010 is set on 85 % and in 2030 on 90 % (Viebahn, 2004; BMU, 2004b).

- Copper 2010/2030

In 2010 the recycling quota lies at 80 % because of worldwide increasing demand. The same quota is used for 2030. The reference balance for primary copper comes from a module of the LCA software GaBi (PE & IKP, 1998) and for secondary copper from the Umberto[®] process database (Viebahn, 2004).

- Rock wool, Fine ceramics, Flat glass 2010/2030

These materials are exclusively needed for the erection of the solar thermal power plant. The electricity mixes in 2010 und 2030 applied on the reference balance from the Umberto[®] process database are taken as a base for the production of these materials.

11.1.5 Services

The building materials are produced in Germany, Sweden and North Africa and transported to the destination partly over water and partly over land. In table 33 ff. model specifications for the truck transport in Germany and North Africa and the ship transport are listed. Within the plant modelling installation, dismantling and cleaning of mirrors are included via the Umberto[®] module 'Construction Machinery' (Viebahn, 2004).

11.1.6 Limitations and geographic consistency

Simplistically German conditions are assumed for the production of all components of the facility as, for this, appropriate databases and process modules are available. The reference solar thermal power plant is designed for a location in the north-eastern part of Morocco and shows therefore building materials which are manufactured there. It concerns steel and concrete for buildings and the carrying structure of the solar field and to 50 % steel, ceramics and PVC for parts

of the mechanical engineering and the steam generator (Viebahn, 2004). Also for the HVDC line an on-site production of concrete is assumed. However, this circumstance is just taken into account for the transportation of the materials. Other components use data corresponding to a manufacture in Germany and Sweden respectively.

11.1.7 Selection of Impact Categories

For the evaluation of the results from the life cycle inventory analysis selected impact categories of the Federal Environmental Agency are used (Viebahn, 2004). On the level of the life cycle inventory analysis the cumulated energy expenditure, however just final primary energy carrier, and the material expenditures of iron, bauxite and copper on the input side are considered. On the output side PM10 and CO₂ emissions are extra shown. The latter is also included in the global impact category *global warming*.

Tab. 22: Used impact categories and expenditures (Source: Viebahn, 2004; BMU, 2004b).

Expenditure	Balance flow	Unit	
Cumulated energy expenditure	exhaustive	[MJ]	
material resource expenditure	Iron Bauxite Copper	[g]	
Emissions	CO ₂ Particle < 10 µm	[kg] [mg]	
Impact category	Balance flow	Category factor	kg/kg _{Reference}
Global warming	CO ₂	CO ₂ -Equivalent [g]	1
	CH ₄		21
	N ₂ O		310
Photo-oxidant formation (summer smog)	NO _x	Ethylene-Equivalent [mg]	0.83
	NM VOC		0.416
	CH ₄		0.007
Acidification	...		
	SO ₂	SO ₂ -Equivalent [mg]	1
	NO ₂		0.7
	NH ₃		1.88
Terrestrial eutrophication	NO ₂	PO ₄ ³⁻ -Equivalent [mg]	0.13
	NH ₃		0.33

11.2 *Inventory Analysis*

In the following the required process data is compiled and the material flow network for the modelling of the plant and HVDC line is set up. In this respect it is tried to record all relevant material and energy flows in the energy transfer system. The complete data inventory and the parameter specifications are listed in table 33 ff. in the annex. Particularly for the metal expenditures only the elementary portions, the so-called reference flows, are represented. Recycled materials are not considered. In this context we must mention that for lead a recycling quota of 50 % is assumed.

11.2.1 **Modelling of the solar thermal power plant**

A present material flow network from the SOKRATES project is used for the modelling of the solar thermal power plant. In that a Parabolic Through System of the type 'SEGS' with a pure solar capacity of 80 MW, without fossil co-firing and with a storage time of one hour is represented. It is designed for a location in the north-east of Morocco with a Direct Normal Irradiation (DNI) of 2337 kWh/m²/y and annual full-load operating time of 1816 hours per year. The life cycle amounts to 30 years and the reference period of time for the eco-balance is 2010 (Viebahn, 2004).

Different plant parameters must be adapted to the respective locations for the balancing of 10 GW power plants. In the study ESA (2004) the performance of diverse plant designs for different periods of time, loads and locations in North Africa has been simulated. As all plant locations that are considered here lie in zones with a DNI of more than 2800 kWh/m²/y and a plant construction cannot be assumed before 2030, the case 'STP - 100 GW base load in 2020/2030'³³ described in the study ESA (2004) is used as reference. Based on that, the size of the solar field and the capacity of the thermal storage are scaled down. The current storage time amounts to 23 hours so that the plant can provide base load. Further assumptions can be found in table 33 ff.

³³ The simulation of a 10 GW power plant was executed for a location in Zone A1, but here the DNI lies just between 2150-2643 kWh/m²/y.

Tab. 23: Technical assumption for a 10 GW base load production of a solar thermal power plant in 2030 (Source: derived from ESA, 2004).

	Unit	ESA (2004) Zone A3	Site Algeria	Site Libya	Site Egypt
DNI at the site	kWh/m ² /y	$\bar{x} = 2,961$	2,835	2,802	2,865
Capacity	GW _{el}	138	10	10	10
Solar field size	Mio m ²	3,107.8	227.0	227.0	227.0
Thermal storage	GWh _{th}	8,089	590.5	590.5	590.5
Electricity production	TWh/y	1,102.5	77.1	76.2	77.9
Full load hours	h/y	7,989	7,710	7,620	7,790

Balancing comprises the following areas:

Construction of the components: solar field, steam generator, mechanical engineering, electrical and control engineering, constructional engineering, thermal storage, steam turbine;

Maintenance: replacement of mirrors, water and heat carrier medium;

Services: ship and truck transport, mirror cleaning, installation and dismantling works, disposal.

Simple distance specifications have been defined for the transport of the building materials. First the truck transport in Germany to the *Hamburg Harbour* is specified with 400 km. Afterwards follows the ship transport to the respective harbours in North Africa (see figure 69). From there the materials are carried again with a truck to the projected plant location. A more detailed description of single services, which concerns the reference power plant, can be found in Viebahn (2004). In figure 64 the entire material flow network is shown. Because the plant is prepared for 100 % solar operation, the network section for the fossil operation remains inactive.

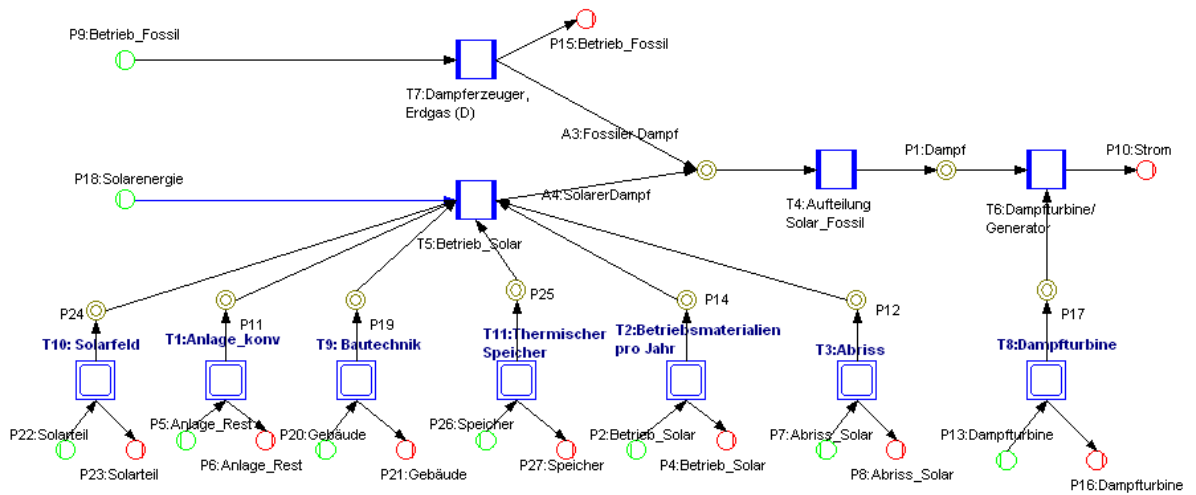


Fig. 64: Material flow network of a parabolic through.

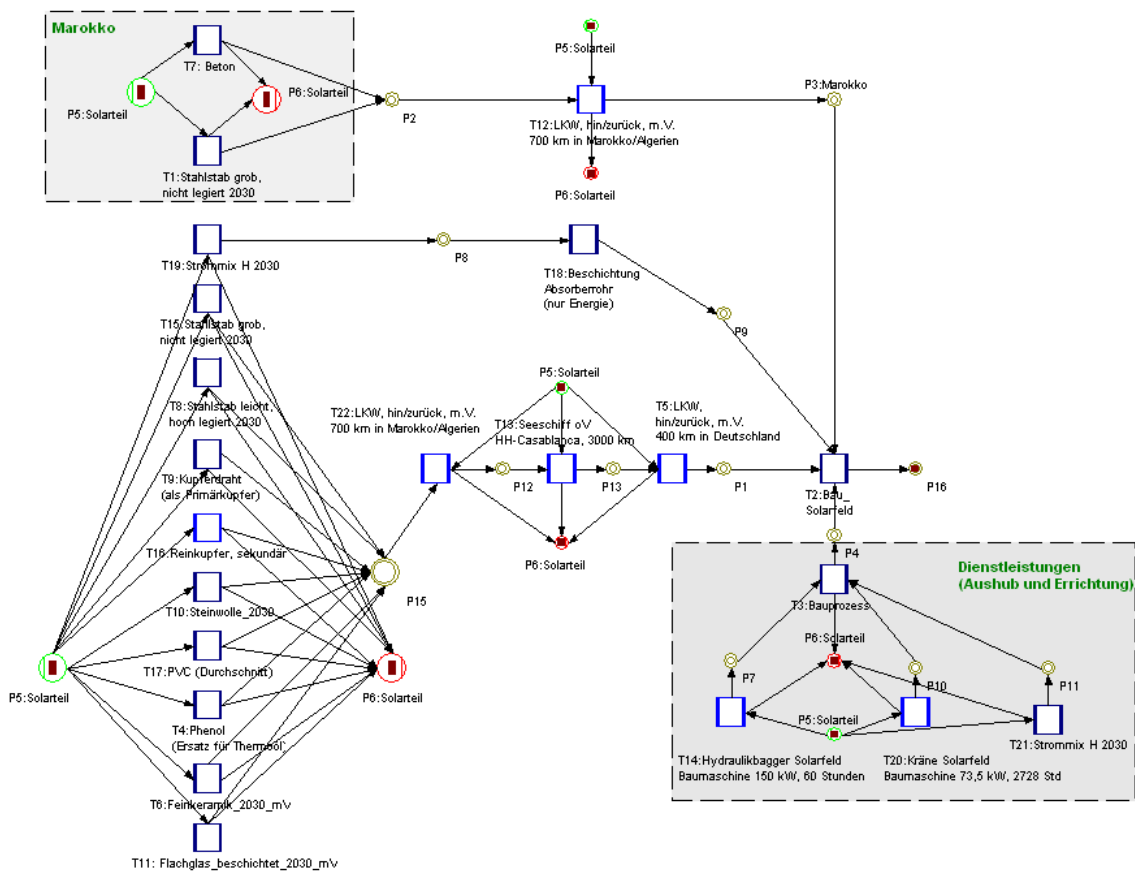


Fig. 65: Sub network for the production of the solar field.

11.2.2 Modelling of the HVDC line

For the long-distance transport of 10 GW a ± 800 kV double-bipole system on two separate lines with a capacity of 5 GW each is used. The conductor deployed is an aluminium-steel compound wire (Al/St 805 mm²/102 mm²). In a 4-string-bundle 2500 MW per Pole can be transmitted with it. The pylons are steel lattice pylons with a concrete fundament and long-rod ceramic isolators.

In order to cross the sea a ± 800 kV mass-impregnated cable with a central copper conductor (2100 mm²) is used. Altogether 8 cables are required to transmit 10 GW.

The rectifier stations and transformers are compounded from many different materials, for which no data was available, but they are of no consequence for the balance due to the large length of the HVDC line. The operating time of the HVDC line exceeds the operating time of the plant, therefore only 60 % of the material and energetic expenditures go into the entire balance.

Tab. 24: Parameters for the long-distance transport of 10 GW of electric load.

HVDC	± 800 kV Overhead line (2 lines)	± 800 kV Submarine cable (8 cables)	Source
Technical Data			
Length	3099 km	18 km	berechnet
Conductor	4	8	Normark (2005)
Line losses	3.7 %/1000 km	1.7 %/1000 km	berechnet
Station losses (2x)	1.4 %	1.4 %	ESA (2004)
Durability	50 a	50 a	Pehnt (2002)
O ₃ -emissions	$4.0 \cdot 10^{-9}$ kg/MJ _{el} · km		Knoepfel (1995)
N ₂ O-emissions	$0.4 \cdot 10^{-9}$ kg/MJ _{el} · km		Knoepfel (1995)
Materials*			
Aluminium	2 x 17.4 t/km		Normark (2005)
Steel, hoch legiert	2 x 6.4 t/km	8 x 24 t/km	"
Steel, niedrig legiert	2 x 75 t/km		"
Concrete	2x 200 t/km		"
Ceramics	2 x 2 t/km		"
Copper		8 x 19 t/km	"
Lead		8 x 17 t/km	"
Polypropylen		8 x 2.3 t/km	"
Paper		8 x 6 t/km	"
Impregnation		8 x 1 t/km	"

*Conductor wires, cables, pylons, without rectifier stations

Over 30 years of operation the total energy transmitted less the losses is listed in table 25.

Tab. 25: Transported energy amounts in 30 years operating time.

	Line 1	Line 2	Line 3
TWh	2,019	2,013	1,921
kJ	$7.27 \cdot 10^{15}$	$7.25 \cdot 10^{15}$	$6.92 \cdot 10^{15}$

Figure 66 shows the network for the balancing of the HVDC line on the uppermost level. Within transition 1 losses arising by the conversion of alternating current into direct current and losses and emissions appearing along the line during the operating phase are modelled. In transitions T2 and T3 the production and transportation processes of the overhead line and submarine cable respectively are described in a sub network (see figure 67 and 68). Production chains for construction materials from different databases were imported into these sub networks. For the materials steel, copper and aluminium it is about the same modules as already mentioned in section 11.1.4, the rest is taken from the Umberto[®] database.

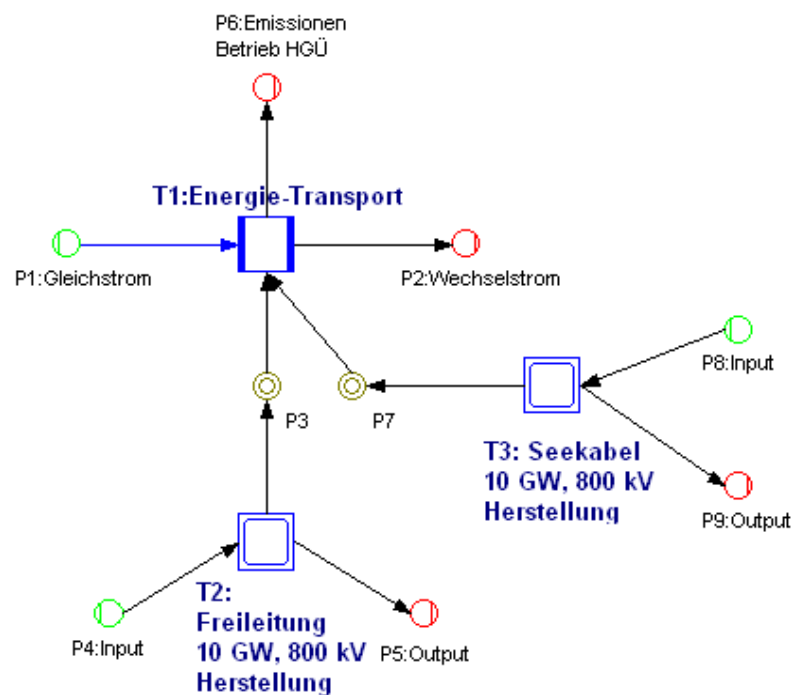


Fig. 66: Material flow network of a HVDC transmission line.

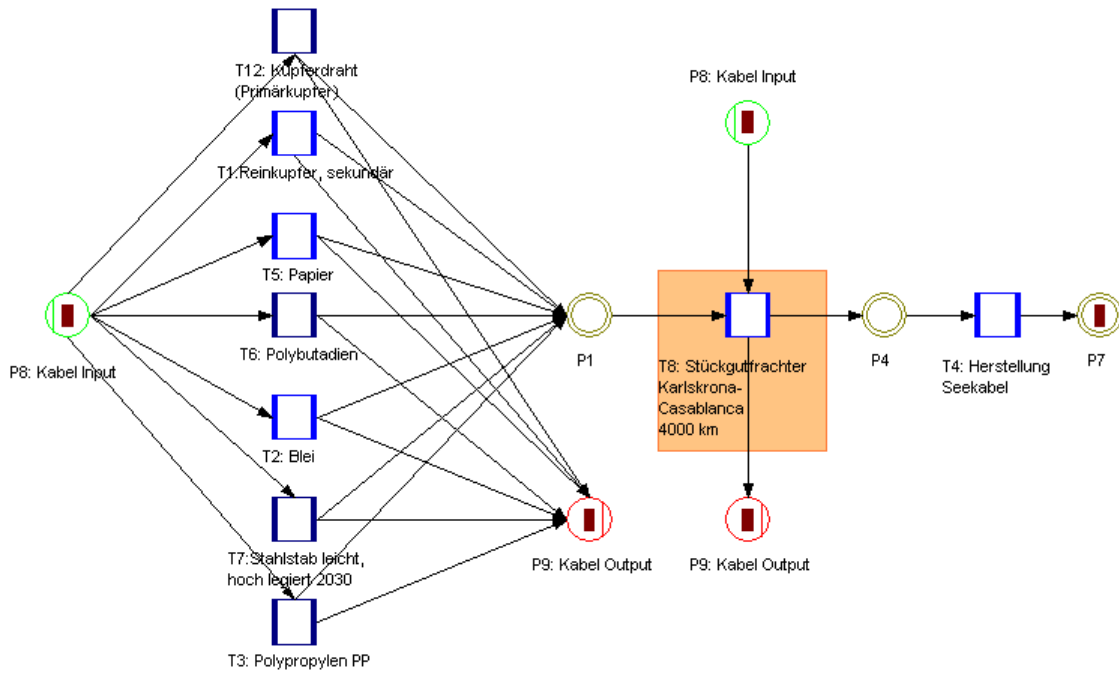


Fig. 67: Sub network for the cable manufacture.

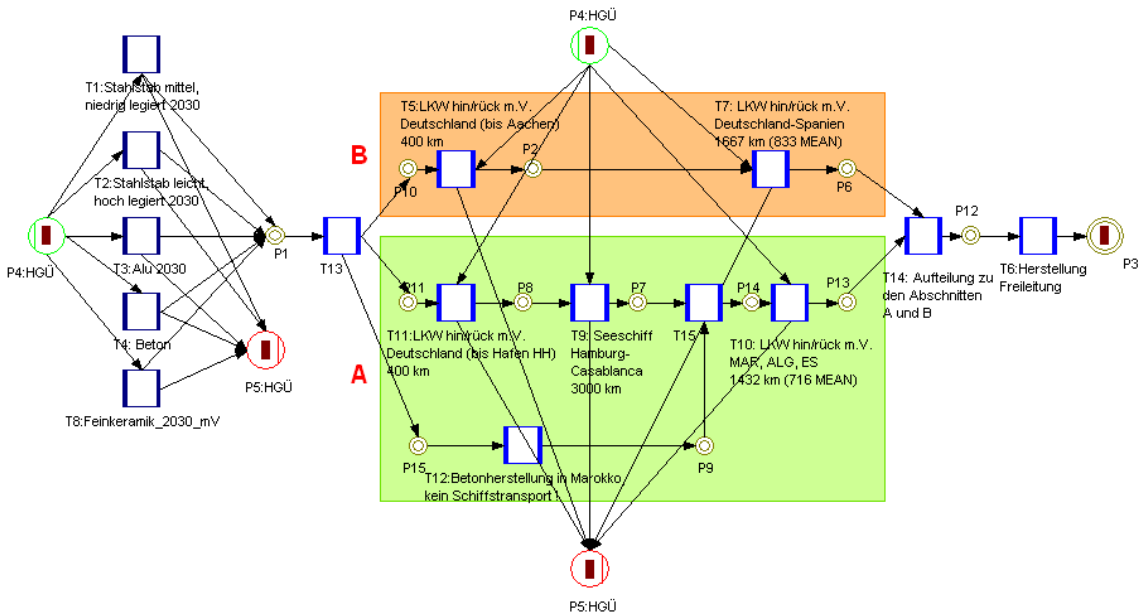


Fig. 68: Sub network for the overhead line manufacture.

It is do justice to the large length of the HVDC line through an adapted balancing of the transport. Therefore a case differentiation is carried out for the transport of materials and the line is divided in two sections (see figure 69).

- Section A begins at the solar plant and ends at a defined point approximately in the middle of the line. The materials of the overhead line of this section are transported via ship from *Hamburg Harbour* to a harbour located in North Africa. From there the materials are brought to the respective projected locations by trucks. For this the mean distance is defined for all truck transports. Because Germany is laid down as location for the production of all components, except concrete, 400 km are additionally included for the truck transport to *Hamburg Harbour*. Hence the ship transport for concrete is cancelled since a production in North Africa is assumed. The submarine sections are directly supplied by ship from the cable factory in *Karlskrona* (Sweden).



Fig. 69: Subdivision of the lines in two sections for the modelling of the transport.

- Section B starts at the end of section A und finishes at the respective demand centre. The overhead line section is supplied with building materials by trucks from Germany. For this a distance of 400 km (line 1) and 600 km (line 2, 3) respectively must be bridged up to the line start. From there the mean distance is defined again for the supply of the entire section. Possible submarine cable transports to the respective locations in the *Mediterranean Sea* takes place again by ship.

11.3 Impact Assessment and Interpretation

In the following the environmental impacts and material and energetic resource expenditures of the plant and HVDC transmission line with the reference year 2030 are represented in the form of environmental impact profiles. The entire facility providing solar electricity is simplistically called ‘line’ from now.

How the environmental impacts distribute to single phases of the course of life and single functional components is described for line 1 for instance. The profiles of the other lines can be found in the annex.

The proportional shares of plant and line in the environmental impacts of the entire facility is given in figure 70. Here it becomes evident that the impacts are mainly caused by the solar thermal power plant. Only the aluminium demand is significantly higher for the HVDC line. If the submarine cable link is just long enough, approximately 300 km, the need of copper also increases (see figure 91).

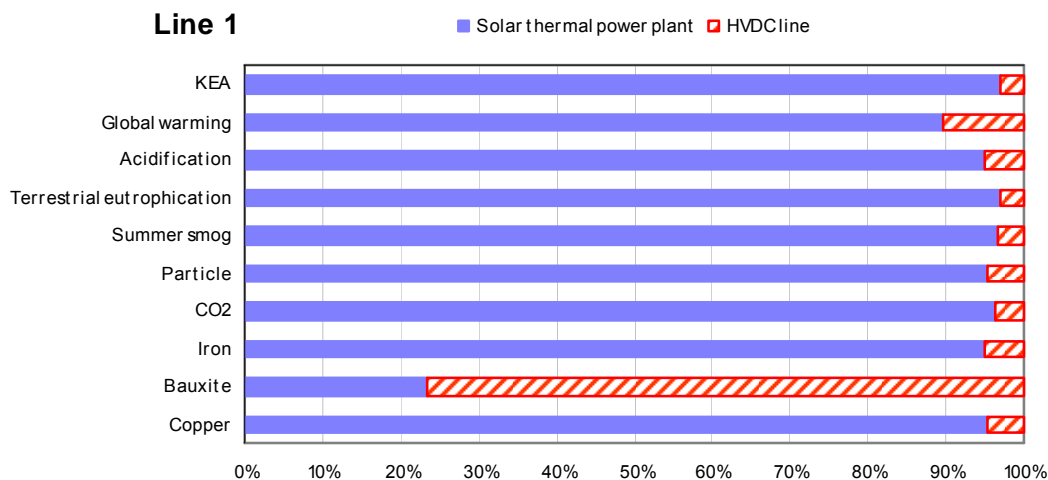


Fig. 70: Proportional shares of the plant and the line in environmental impacts (line 1, reference year 2030).

11.3.1 Solar thermal power plant

Negative impacts and resource consumptions are mainly caused by the production process of the solar field, which requires a considerable material expenditure because of a size of 15 km x 15 km. Altogether 91 % of the *iron* flows into the production of the steel girder for the solar field and 97 % of the *copper* is used for the production of pumps and control lines. About 93 % of the *bauxite* is meant for the alloy of high-grade steel, which is mostly needed for the absorber tube of the solar heat collecting element. The material expenditure of the residual components of the facility is low in comparison to the solar field.

The *cumulated energy expenditure* mainly accounts for 47 % of the construction of the solar field, of that nearly 41 % are used for steel, 30 % for the heat carrier oil phenol and just 15 % for flat glass (see figure 71).

In a high degree also the construction of the thermal storage, the material transport and the plant operation beside the solar field participate in emissions. Thus *global warming potential* of the solar field comes to 46 % and of the large designed storage to 27 %.

However, the material transport dominates the *terrestrial eutrophication potential* with 48 % and the *summer smog* with 37 %, explained in more detail, the transport by trucks due to a large transport capacity.

The *acidification potential* of the solar field amounts to 43 %. The share of the ship transport is 10 % and is caused by using heavy oil as fuel.

Particle of the size < 10 µm are especially released during the steel production, accordingly high is the share of the solar field (69 %).

During the plant operation impacts arise chiefly in the form of *summer smog*. Furthermore, a certain need in energy must be met, which follows for the most part from the substitution of phenol. Every year 4 % of it is lost (Viebahn, 2004).

Besides, the entire facility engineering, the constructional engineering and the steam turbine are not so important in the considered spectrum of impacts and material expenditures.

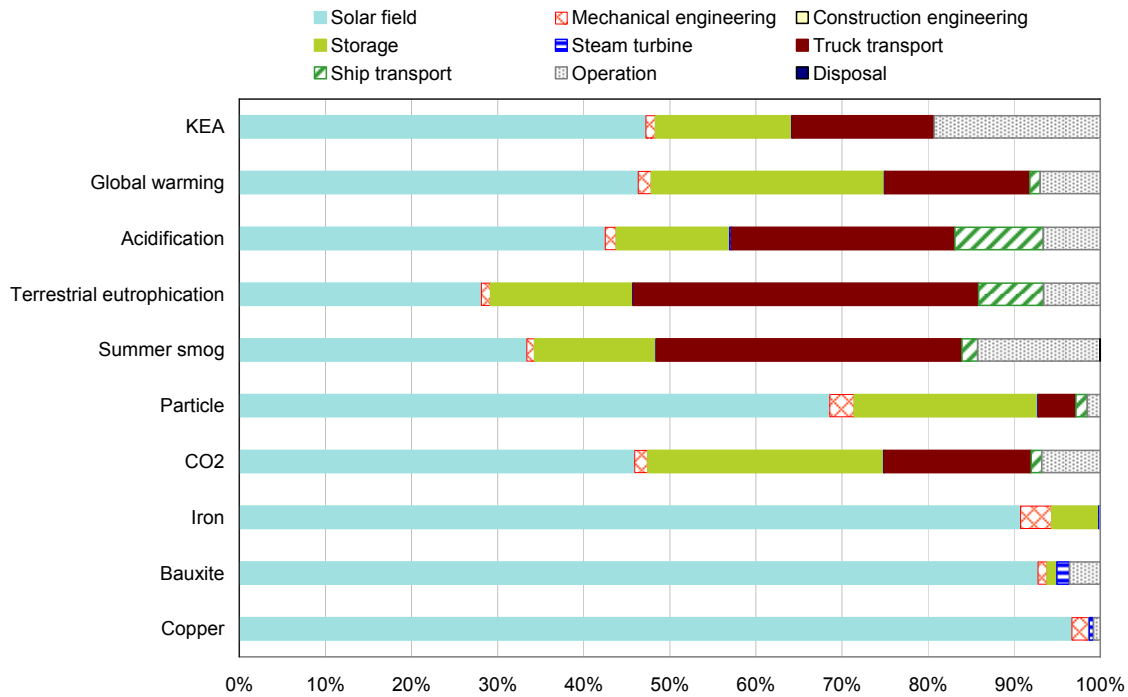


Fig. 72: Impacts and resource consumptions of single plant components and life cycle phases of the plant respectively (line 1, reference year 2030).

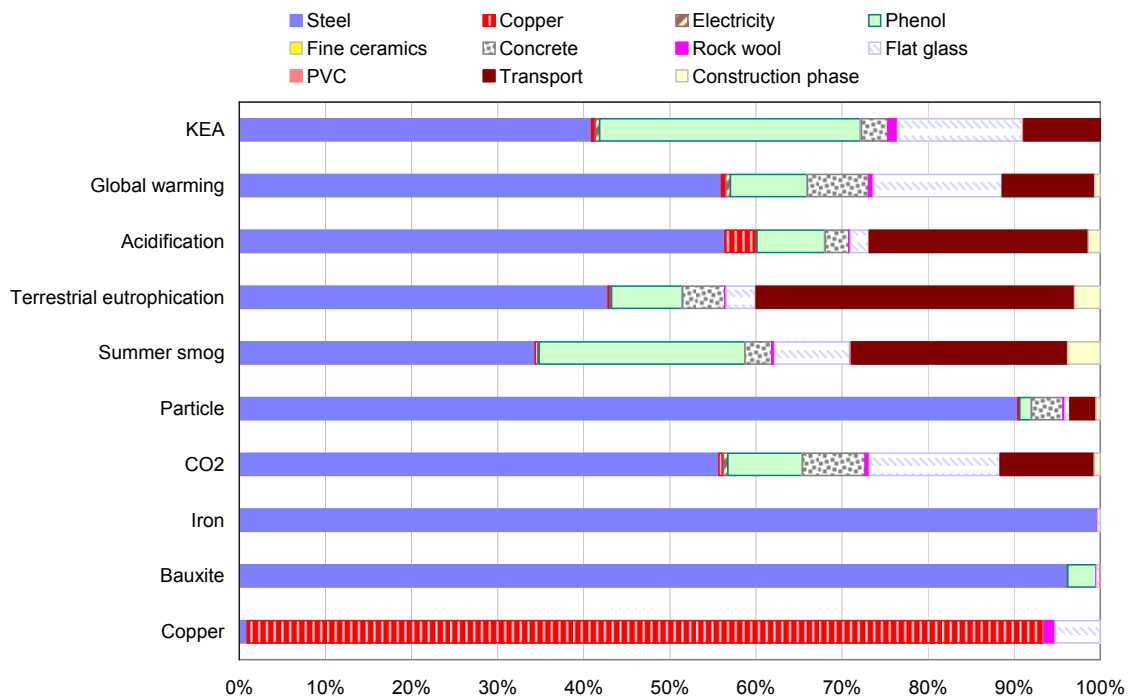


Fig. 71: Impacts and resource consumptions of the solar field components and life cycle phases of the solar field (line 1, reference year 2030).

11.3.2 HVDC transmission line

According to the low submarine cable share of 0.6 % in the total line the environmental impacts of the overhead line predominate.

About 67 % of the *global warming potential* is solely caused by the operation of the overhead line. The importance of the ionization of air molecules along the high voltage overhead line for the climate is normally rated as low. Because of the large length of the overhead line a distinct higher influence emerges. First of all it is because of the formation of the laughing gas (N₂O), which is a 310 times more effective climate gas than CO₂.

About 75 % of the *acidification potential* is caused by the manufacture of the overhead line and only 6 % by the submarine cable manufacture. Altogether the transport amounts to 19 %.

The *terrestrial eutrophication potential* is still predominated from the overhead line with 55 %, but the share of transport (43 %) becomes important as well, especially the truck transport with 36 %.

In the category *summer smog* the influence of the overhead line predominates; it adds 34 % to the steel production and 32 % to the aluminium production. The direct formation of ground near ozone because of ionization processes could not be represented with the underlying evaluation procedure yet.

Associated with the steel production it turns out that the overhead line again predominates the *particle formation*. Just 16 % go into the production of aluminium and concrete. *Iron and bauxite resources* are almost exclusively used for the manufacture of conductor wires and pylons, whereas the main portion of the *copper consumption* is caused by the submarine cable link in spite of its shortness.

About 84 % of the *cumulated energy expenditure* lies at the overhead line manufacture, of which 59 % go into the steel production and 21 % into the aluminium production.

Within the submarine cable manufacture the considered impacts have to be added to the *copper and lead production* beside the steel production. The share of lead in the *eutrophication potential* amounts to 43 %, followed by steel (20 %) and the ship transport (19 %). The other components of the submarine cable such as paper, impregnation and synthetic envelopments have a smaller share in impacts.

Their share in the *cumulated energy expenditure* comes to just 12 %, in *summer smog* due to a higher share of impregnation to 23 %. This picture looks different for the other lines because of a longer transport distance (see figure 93-98).

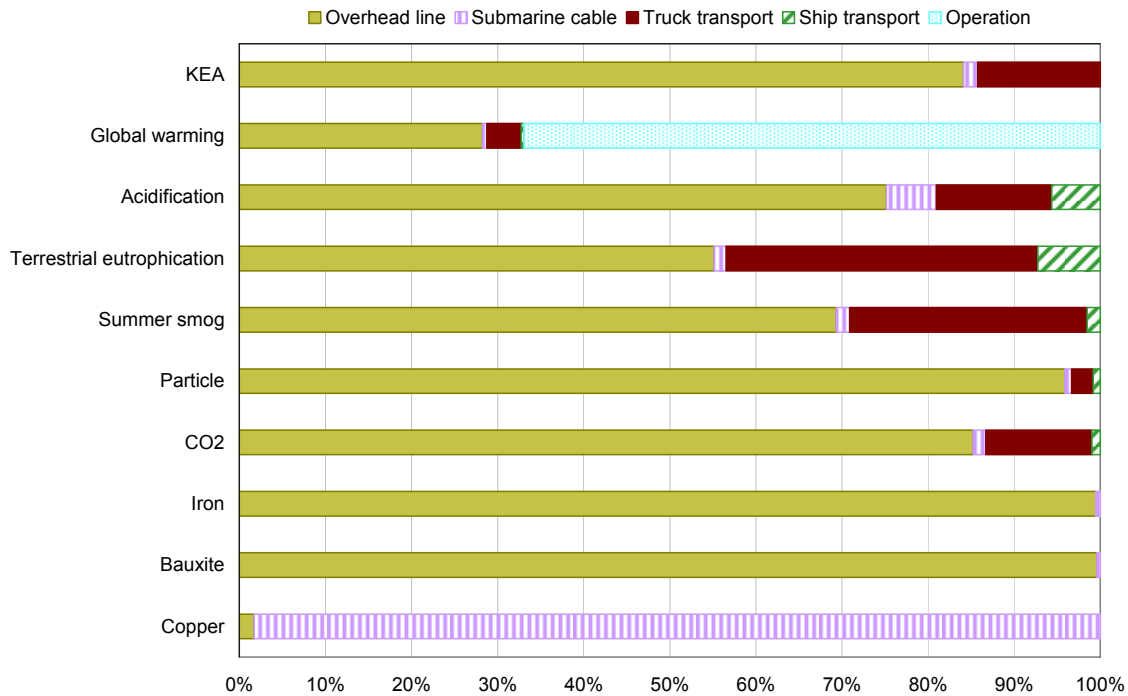


Fig. 73: Impacts and resource consumptions in the phases of life of the HVDC transmission line (line 1, reference year 2030).

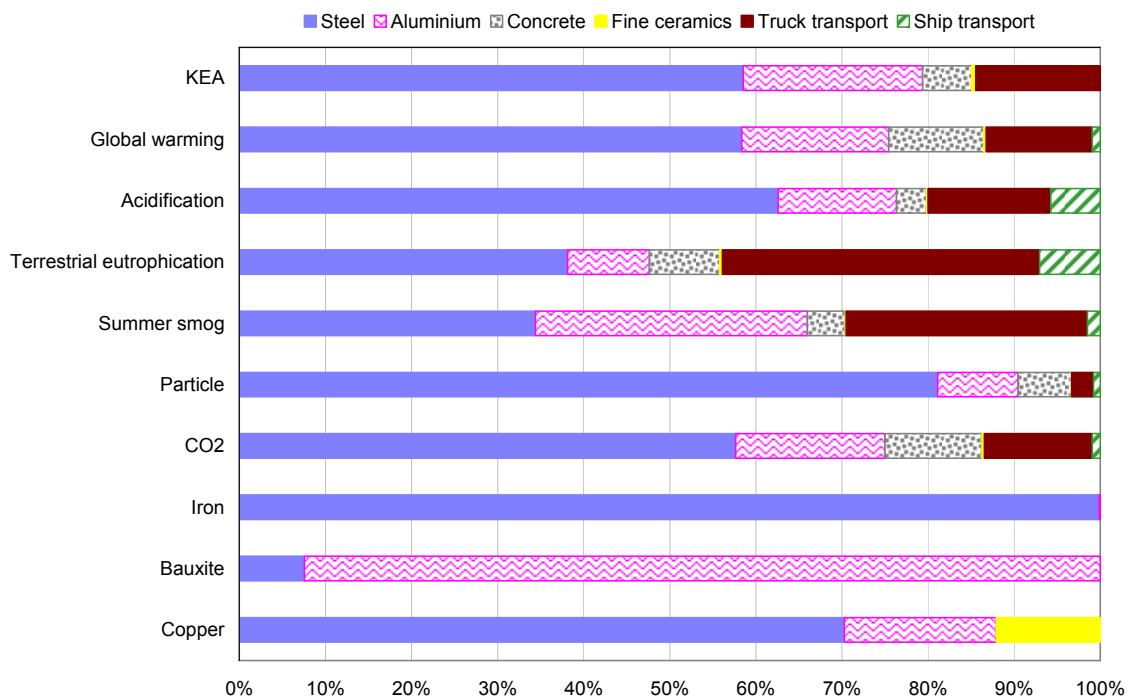


Fig. 74: Impacts and resource consumptions of the overhead line components and the transport (line 1, reference year 2030).

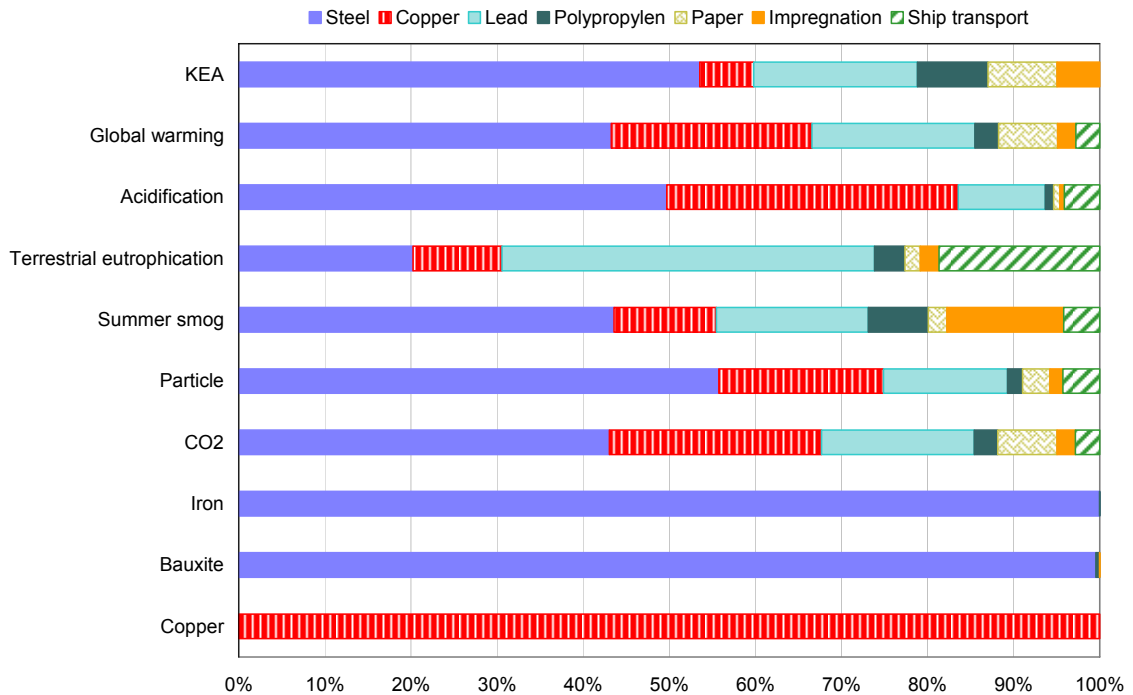


Fig. 75: Impacts and resource consumptions of the submarine cable components and the transport (line 1, reference year 2030).

11.3.3 Comparison of the balances of all three lines

The environmental impacts of all three lines are normalized to 1 kWh free network supply and depicted in the following diagrams for a comparative representation of the impacts categories and the energetic and material resource consumptions respectively.

Line 2 has the highest *cumulated energy expenditure* with 0.21 MJ/kWh because more energy must be raised for the truck transport.

It looks similar for *the global warming potential*, which is also the highest by line 2. If the emissions arising during the operation of the HVDC transmission lines are considered, the differences in the length of single overhead line sections become clear.

The transport participate considerably in the *acidification potential*, *eutrophication potential* and *summer smog*, in case of line 2 even to more than 50 %. The impacts of the ship transport increase according to the distance to North African harbours from line 1 to line 3.

In the *acidification potential* of line 2 the long submarine cable section turns out. The *particle load* is the highest in case of line 3. As all values have been normalized to 1 kWh_{el}, the higher losses of line 3 affect the results.

Altogether the impacts of the plant predominate in comparison with the line. This concerns also the *iron consumption*, only the *bauxite consumption* is mainly defined by the length of the overhead line section. The share of the line of the *copper consumption* increases if the submarine cable section is just long enough.

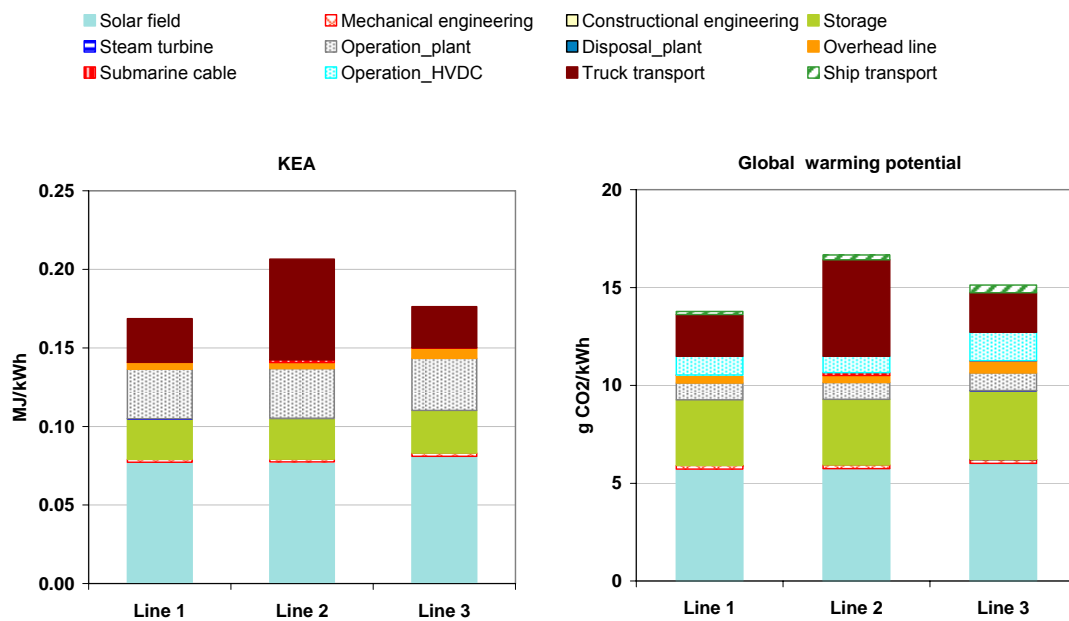


Fig. 76: Line comparison for cumulated energy expenditure and global warming potential.

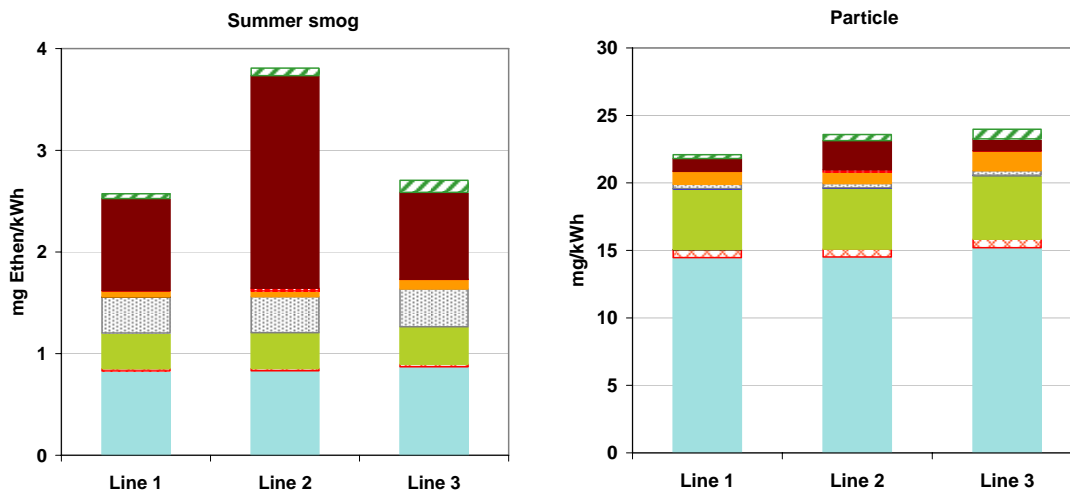


Fig. 77: Line comparison for summer smog and particle load.

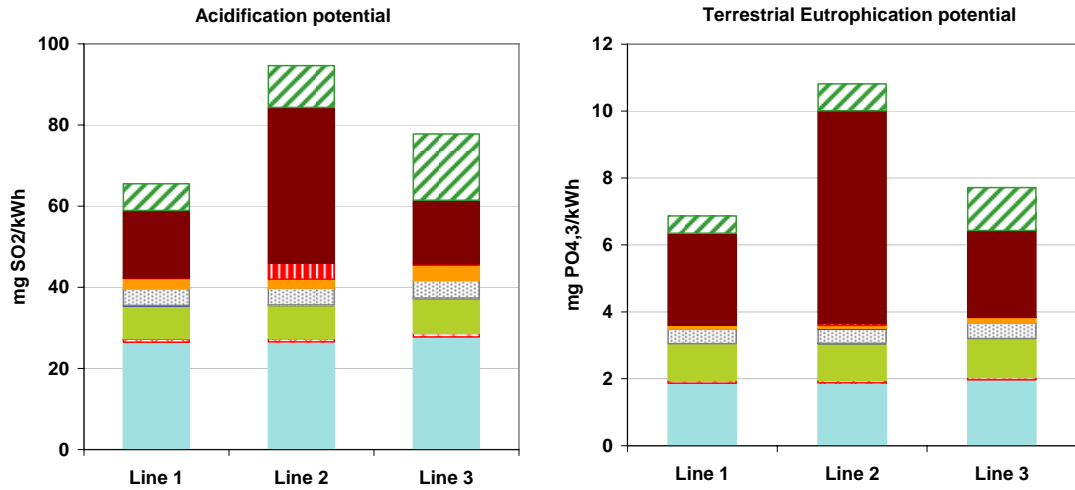


Fig. 78: Line comparison for acidification and eutrophication potential.

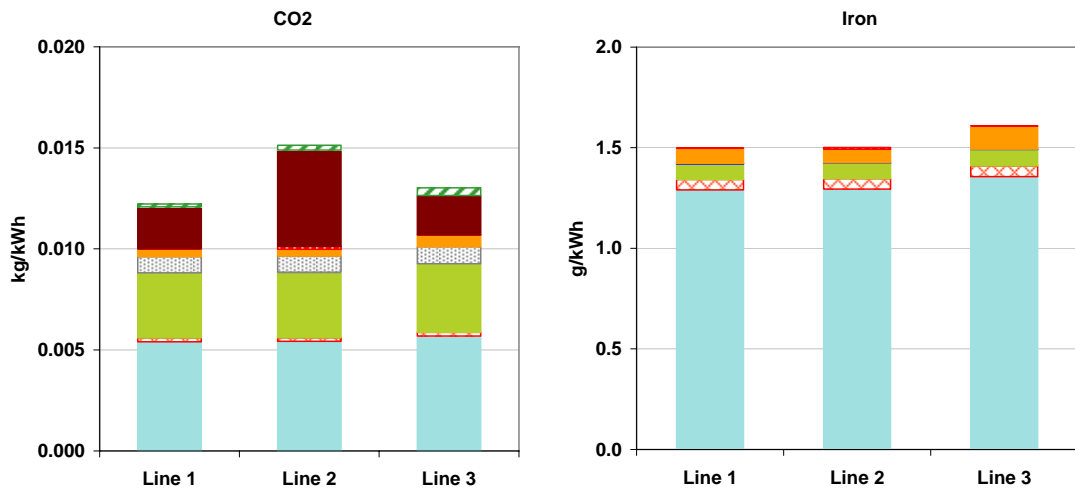


Fig. 79: Line comparison for CO₂ and iron.

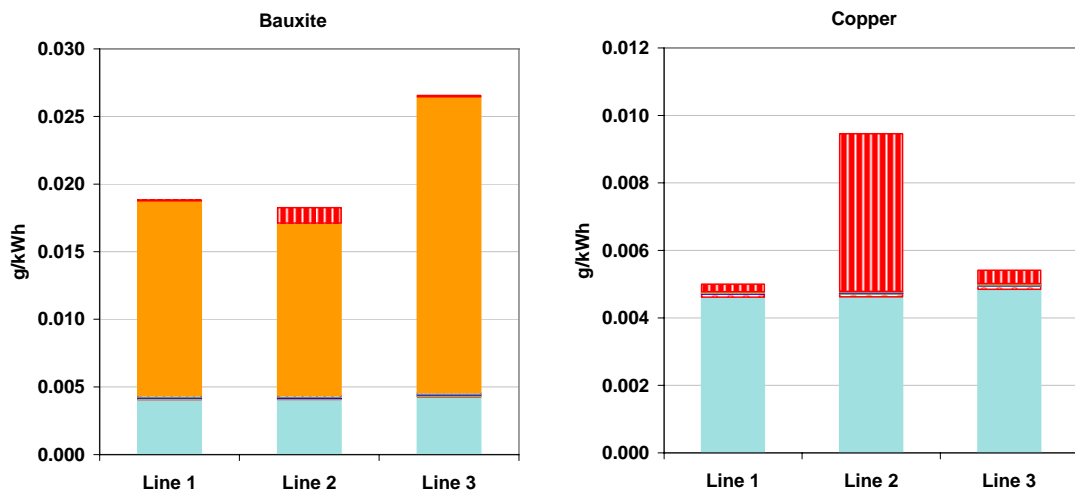


Fig. 80: Line comparison for bauxite and copper.

11.3.4 Energetic amortization time

The energetic amortization time states how long it takes until all energetic expenditures for the construction of the facility are compensated by the own electricity production. The mathematical equation reads:

$$EAT[a] = \frac{KEA_H}{\left(\frac{E_{net}}{g} - KEA_B\right)} \quad [\text{Eq. 8}]$$

KEA_H Cumulated energetic expenditure for the facility construction [MJ]

E_{net} Annual generated net energy amount [MJ/y]

g mean degree of utilization of the German power plant mix [%]

KEA_B Cumulated energetic expenditure for the facility operation [MJ/y]

For g a value from literature of 31.4 % is used (Viebahn, 2004). In table 26 the amortisation times for all three solar thermal power plants including the HVDC transmission lines are listed (reference year 2030).

Tab. 26: Energetic amortization time for all lines.

	Unit	Line 1	Line 2	Line 3
KEA_H	[MJ]	2.76E+11	3.50E+11	2.74E+11
KEA_B	[MJ/y]	2.16E+09	2.20E+09	2.16E+09
E_{net}	[MJ/y]	2.42E+11	2.42E+11	2.31E+11
g	[%]	31.4	31.4	31.4
EAT	[year]	0.36	0.46	0.37
EAT	[month]	4.3	5.5	4.5

The *cumulated energetic expenditure* for the single HVDC transmission lines depends on the length of the line and the transport capacity. Line 2 requires the highest *cumulated energetic expenditure* regarding plant construction due to a high transportation capacity, particularly in North Africa. The differences in the solar electricity generation depend on the DNI on-site. Altogether the energetic expenditure amortizes after 4-6 months.

11.3.5 Additional load with changed modules (reference year 2010)

The Sensitivity of the results is examined here with regard to another reference year for the construction of the facility. In the year 2010 the electricity mix is composed of almost 90 % fossil primary energy carrier. This also affects the production chains for the provision of steel, copper, aluminium, fine ceramics, flat glass and rock wool. Besides, there are lower recycling quotas for the metals.

Under these conditions a proportional additional load results in all categories as figure 81 shows. Especially, the changed recycling quota leads to an increase of the primary *iron consumption* by more than 50 % in comparison to the year 2030. At the same time the *particle load* increases because of the same. The rise in *copper consumption*, however minimal, is associated with the steel production, which also has a certain copper demand. The impacts in the other categories increase by 10-20 %. Finally, also the rise in CO₂ emissions by 20 % causes an increase in the *global warming potential*.

The differences between single lines are founded in the different shares of overhead line and submarine cable. Altogether the highest additional load is caused by the longest line (line 3).

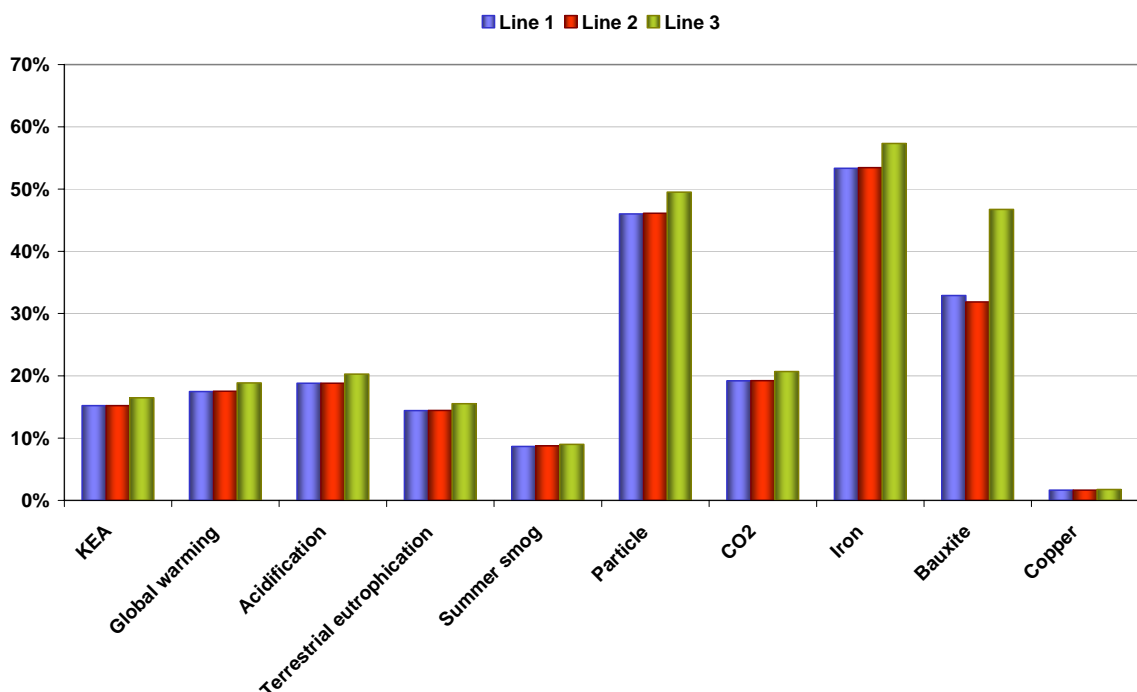


Fig. 81: Proportional additional load of the respective line from the year 2030 if a changed electricity mix and changed production chains with the reference year 2010 are taken as a base.

11.3.6 Normalization with respect to a reference electricity mix in 2010/2030

The result from the impact assessment for line 1, which leads from Algeria to Germany, are normalized to 1 kWh_{el} and afterward compared with a reference electricity mix of Germany in 2030 and 2010 (see table 27). In figure 82 the proportional deviations to the references are shown, which have been fixed on 100 % for it.

Tab. 27: Comparative values of 1 kWh_{el} solar electricity with the German high voltage electricity mix in 2010 und 2030.

Impact category	Unit per kWh _{el}	Electricity mix 2030, Trasse 1	Electricity mix, 2030	Electricity mix, 2010
KEA	MJ	0.17	5.17	8.52
Global warming	g CO ₂ -Equi.	13.78	403.54	539.42
Acidification	mg SO ₂ -Equi.	65.5	463.11	718.51
Eutrophication	mg SO ₂ -Equi.	6.87	51.32	55.99
Summer smog	mg Ethylene-Equi.	2.57	23.26	16.99
Particle	mg	22.09	46.8	41.86
CO ₂	kg	0.012	0.38	0.51
Iron	g	1.5	2.22	1.05
Bauxite	g	0.019	0.033	0.033
Copper	g	0.005	0.019	0.016

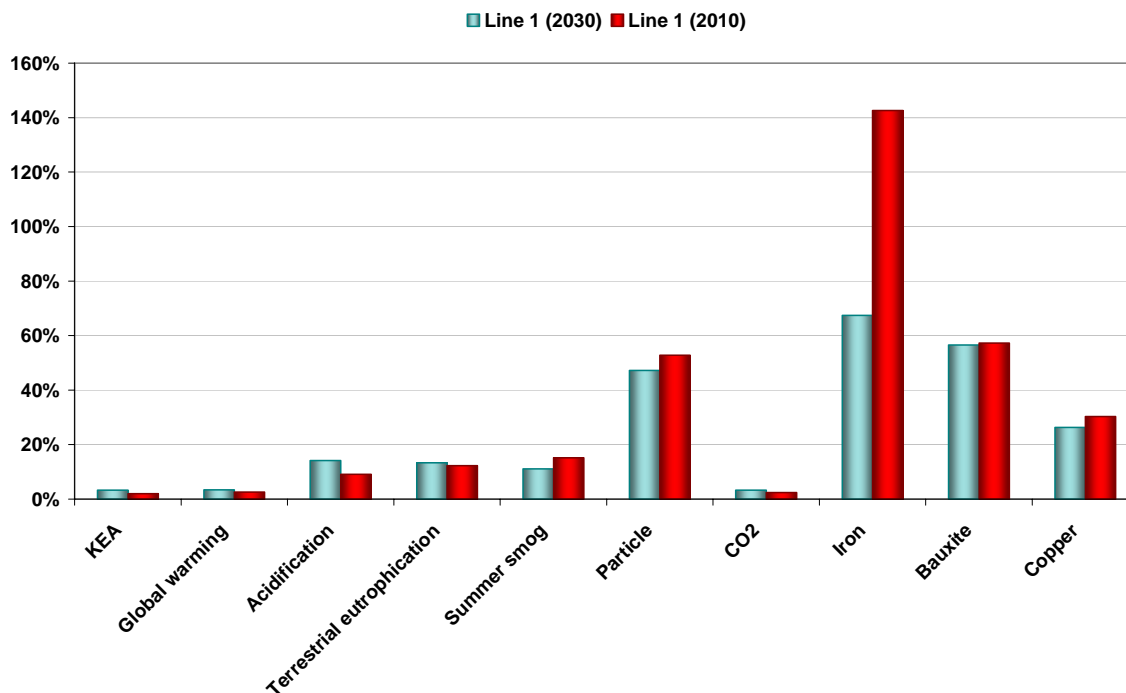


Fig. 82: Normalization of the LCA results for line 1 (plant+HVDC line in 2030) on 1 kWh, solar electricity, reference: electricity mix in 2030 and 2010 respectively has been set on 100%.

If the results are compared with the reference electricity mix 2030, lower loads in all impacts categories turn out by importing solar electricity. The *global warming potential* of the solar electricity import constitutes only 3.4 % of that of the reference electricity mix, the *acidification potential* 14.1 %, *eutrophication potential* 13.4 % and *summer smog* just 11.1 %. The *cumulated energetic expenditure* for the construction and operation of plant and line makes up only 3.3 %. Furthermore, 52.8 % less *particle* and 96.8 % less *carbon dioxide* arise.

The share of *iron consumption* amounts to 67.4 % of the reference electricity mix in 2030, *bauxite consumption* comes to 56.5 % and *copper consumption* to 26.3 %. However, the *iron consumption* increases by 42.6 % as compared with the electricity mix in 2010. This is connected with a different composition of the electricity mix in 2010, which has a lower share of renewable energy carriers in comparison with the mix in 2030. Therefore the iron consumption in 2030 is higher than in 2010 as for the most renewable energies appropriate infrastructures has to be erected at first. On the other hand a smaller share of renewable energies in the reference electricity mix also causes a solar electricity import with relatively lower impacts. Besides, environmental impacts arise typically more by tapping renewable energy resources than during the actual facility operation.

In the strict sense it is difficult to make this comparison with the other lines as no suitable electricity mix of Italy and Austria is available. Just in order to represent the influence of a longer submarine cable and overhead line section respectively on the normalized LCA results the German electricity mix is used. Altogether differences of 20 % averaged over all categories exist between single lines. The statements, which have been made concerning the comparison of the first line with the reference electricity mix, are valid for the other lines in principle. Only what concerns the material resource expenditures an increased demand arise in accordance with the increase of the HVDC transmission length.

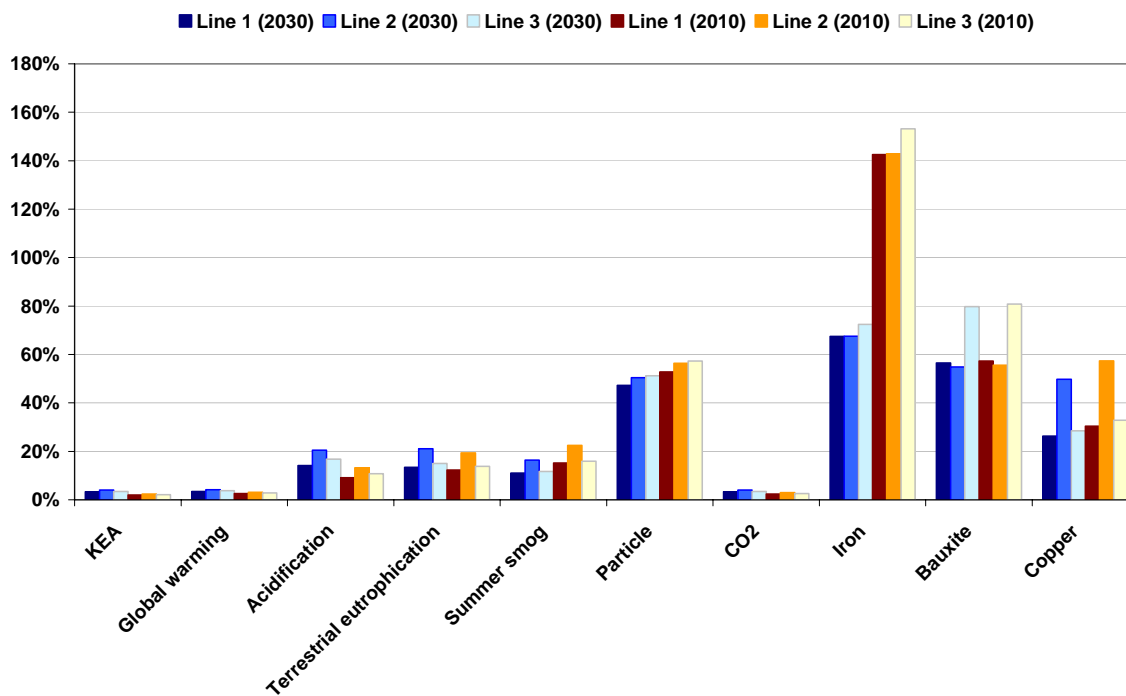


Fig. 83: Normalization of all lines with the reference year 2030 on 1 kWh_{el} and comparison with the reference electricity mix in 2030 and 2010 respectively (both have been set on 100 %).

12 Results and conclusions

Because not all environmental impacts were taken into account, the performed eco-balance can only be considered as general view of an eco-balance. A certain simplification of some aspects was also needed to restrict the balance expenditure on a size which is easy to survey. At some places not all information required was provided so that, especially what concerns the model of the HVDC lines, certain services could not be represented such as the actual construction of the overhead line, cleaning of isolators and the possible use of helicopters for transports and control flights. The share of the HVDC system in environmental impacts in comparison with the entire installation amounts to an average of 5 %, whereas a share of 80 % can be achieved material expenditures.

It already turned out that the share of waste disposal in the total balance is small. The non-consideration of this process for the HVDC line should not increase the actual end result significantly.

In order to clarify technology-specific aspects several parts of the system must be investigated in more detail. This is managed well within the model of the solar thermal power plant as former eco-balances show (SOKRATES). Nevertheless, a description of thermal oil leakages endangering water and soil is missing. Such danger can be eliminated by using another heat carrier. Relating to this, systems are already developed which directly produce steam by evaporating water.

The quantitative registration of land consumption by the entire installation, especially by preceding production chains, represents an extensive additional analysis and is not considered in this paper. Weighting and ranking of impact categories were not carried out because all selected categories have an equal weight.

One important statement of the result of the eco-balance is that each installation composed of solar thermal power plant and associated HVDC line causes distinct lower environmental pollution than the reference electricity mix. The energetic expenditure makes up a very small fraction of the reference electricity mix related to one kilowatt-hour. Merely the demand in iron is increased at 40 % due to the

erection of the new infrastructure, but this does not represent any limitation regarding the feasibility of such a project.

Differences in performance of the three HVDC lines concerning the share of overhead line and submarine cable hardly influence the result. Only in case of a distinct longer submarine cable section (line 2) or overhead line section (line 3) appears a higher demand in material resources like copper, iron and bauxite.

By means of these results it turns out that, even in an integrated consideration from the provision of original materials over the production and operation of the installation to its disposal, the cumulated environmental impacts are many times lower than the impacts through the conventional energy supply system. Besides, no highly risky waste products are produced, which survive in the long-term such as nuclear waste, whose consequence for the future, anyway, can be hardly estimated.

Besides, it is also a cheap kind of energy supply possible if solar thermal power plants are used in a large scale and all cost reduction potentials are exhausted. Nevertheless, its expansion decisively depends on political framework conditions. At the end of this paper the general statement can be formulated that, from an ecological point of view, nothing is opposed to the expansion of solar thermal energy in North Africa and a transmission of the generated solar electricity to Europe.

Finally it is remarked that the different renewable energies in their great variety show together a major capacity, what does justice to a secured, independent, socially and environmentally compatible and affordable, global energy supply in the long-term.

13 Bibliography

26. BImSchV (1997): *26. Verordnung zur Durchführung des Bundes-Immissionsschutzgesetzes*. Verordnung vom 1.1.1997 über elektromagnetische Felder. URL: http://bundesrecht.juris.de/bundesrecht/bimschv_26/index.html, 06.01.2005.
- 400 kV-FG (1966): *Energieübertragung mit hochgespanntem Gleichstrom (HGÜ) - Wiederaufnahme der Forschung in der Bundesrepublik Deutschland*. Bericht Nr. 20a, 400 kV-Forschungsgemeinschaft e.V., Heidelberg.
- ABB (2005): *HVDC References - ABB HVDC Classic and Light Projects*. Asea Brown Boveri Ltd, Zurich. URL: <http://www.abb.com>, 17.07.2005.
- APG (2004): *Umweltverträglichkeitsgutachten zur Errichtung der 380 kV-Freileitung in der Steiermark*. Verbund Austria Power Grid AG, Wien. URL: <http://www.energie.steiermark.at>, 6.3.2005.
- APG (2003): *Untersuchung der APG zur Frage der Verkabelung der Steiermark-Leitung*. Verbund Austrian Power Grid. URL: <http://www.verbund.at/at/apg/>, 09.03.2005.
- Arrillaga, J. (1998): *High Voltage Direct Current Transmission*. 2nd Edition, IEE Power and Energie Series 29, the Institution of Electrical Engineers, London.
- Asplund, G. (2005): *Techno-economic feasibility of HVDC systems up to 800 kV*. Workshop on 25th February 2005 in Delhi, ABB Power Technologies, Sweden. URL: <http://www.abb.com>, 20.07.2005.
- Asplund, G. (2004): *HVDC Outlook*. ABB Power Technologies, Sweden. URL: <http://www.abb.com>, 14.03.2005.
- Asplund, G. (o. J.): *Sustainable energy systems with HVDC transmission*. ABB Power Technologies, Sweden. URL: <http://www.abb.com>, 11.03.2005.
- Beck, H.-P. (2000): *Energiesysteme Teil: Elektrische Energieversorgungssysteme*. Manuskript zur Vorlesung (W 8804), Institut für Elektrische Energietechnik, Technische Universität Clausthal, Clausthal-Zellerfeld. URL: <http://www.iee.tu-clausthal.de>, 12.03.2005.
- Bernhardt, J.-H. (2002): *Gesundheitliche Aspekte niederfrequenter Felder der Stromversorgung*. Deutsches Ärzteblatt 99, Ausgabe 27 vom 5.7.2002.
- BMU (2004a): *Erneuerbare Energien - Innovationen für die Zukunft*. Fachliche Bearbeitung von DLR, WI, IFEU im Auftrag des Bundesministerium für Umwelt, Naturschutz und Reaktorsicherheit, Referat Öffentlichkeitsarbeit, Berlin.

- BMU (2004b): *Ökologisch optimierter Ausbau der Nutzung erneuerbarer Energien in Deutschland*. Arbeitsgemeinschaft Deutsches Zentrum für Luft- und Raumfahrt, Institut für Energie- und Umweltforschung Heidelberg GmbH, Wuppertaler Institut, Forschungsvorhaben im Auftrag des BMU (FKZ 901 41 803), Berlin.
- BNatSchG (2002): *Gesetz über Naturschutz und Landschaftspflege*. Ausfertigung von 25. März 2002, Bundesministerium für Umwelt, Naturschutz und Reaktorsicherheit. URL: http://bundesrecht.juris.de/bundesrecht/bnatschg_2002, 08.05.2005.
- Boustead, I. (2000): *Environmental Profile Report for the European Aluminium Industry*. European Aluminium Association (EAA), Brüssel.
- Cooke, R. U., Warren, A., Goudie, A. S. (1993): *Desert Geomorphology*. UCL Press Limited, University College, London.
- Czisch, G. (1999): *Potentiale der regenerativen Stromerzeugung in Nordafrika - Perspektiven ihrer Nutzung zur lokalen und großräumigen Stromversorgung*. Vortrag zur Tagung der Deutschen Physikalischen Gesellschaft am 18.03.1999, Tagungsband, Heidelberg. URL: <http://www.dpg-physik.de/fachgremien/ake/tagungsband9900pdf>, 27.04.2005.
- Debus, L. (1998): *Elektrosmog im Meer durch gleichstromerzeugte elektrische und magnetische Felder - eine Literaturstudie*. Deutsche Hydrographische Zeitschrift, Supplement 8, S. 167-180, Bundesamt Hamburg.
- DLR (2005): *Concentrating Solar Power for the Mediterranean Region (MED-CSP)*. Study Project prepared for the German Federal Ministry for the Environment, Nature Conservation and Nuclear Safety (BMU) by German Aerospace Centre (DLR), Stuttgart.
- DLR et al. (2003): *Umweltauswirkungen, Rahmenbedingungen und Marktpotenziale des dezentralen Einsatzes von Brennstoffzellen*. Untersuchung im Rahmen des Zukunftsinvestitionsprogramms der Bundesregierung, 2. Zwischenbericht, DLR Stuttgart, IFEU Heidelberg, Wuppertaler Institut Wuppertal, LEE Bochum, ZSW Stuttgart, FHG ISE Freiberg.
- Eastman, R. J. (1999): *Guide to GIS and Image Processing, Volume 2*. IDRISI32, Clark Labs, Worcester, Massachusetts.
- Eberle, R. (2000): *Methodik zur ganzheitlichen Bilanzierung im Automobilbau*. Schriftenreihe B - Fahrzeugtechnik, Institut für Straßen- und Schienenverkehr, Technische Universität Berlin.
- Enquete (2002): *Nachhaltige Energieversorgung unter den Bedingungen der Globalisierung und der Liberalisierung*. Endbericht der Enquete-Kommission des Deutschen Bundestages, Bundestags-Drucksache 14/9400 vom 7.7.2002, Berlin.

- ESA (2004): *Solar Power from Space: European Strategy in the Light of Sustainable Development. Phase 1: Earth and Space based power generation systems*. C. Hendriks, N. Geuder, P. Viebahn, F. Steinsiek, J. Spies, by order of the European Space Agency (ESA), Collaboration of Ecofys Netherlands, DLR Germany and EADS Germany.
- EU-Rat (1989): *Richtlinie des Rates zur Angleichung der Rechtsvorschriften der Mitgliedstaaten über die elektromagnetische Verträglichkeit*. [89/336/EWG] vom 3.5.1989. URL: http://www.vdi-nachrichten.com/admin/cerichtlinien.de/library/Richtlinienpdf/16_89_336_EWG.pdf, 04.03.2005.
- Eurelectric (2003): *Mediterranean Interconnection - State of the Art 2003*. 1stSYSTMED Report, WG SYSTMED, Updated Version, Union of the Electricity Industry, Brüssel.
- Flosdorff, R., Hilgarth, G. (2003): *Elektrische Energieverteilung*. 8. Auflage, B.G. Teubner, Stuttgart.
- Guinée, J. B. (2002): *Handbook on Life Cycle Assessment - Operational Guide to the ISO Standards*. Ministry of Housing, Spatial Planning and the Environment (VROM) and Centre of Environmental Science, Leiden University (CML), Kluwer Academic Publishers, Dordrecht.
- Hafner, M. (2005): *Mediterranean Energy Markets and the Mediterranean Electricity Ring: Status and Perspectives for a Clean Power Market*. Observatoire Méditerranéen de l'Énergie (OME), Presentation on the Menarec 2 Conference in Amman, 9.5.2005.
- Hastings, D. A., Dunbar, P. K. (1999). *Global Land One-kilometer Base Elevation (GLOBE) Digital Elevation Model*. Documentation, Volume 1.0, Key to Geophysical Records Documentation (KGRD) 34. National Oceanic and Atmospheric Administration, National Geophysical Data Center, 325 Broadway, Boulder, Colorado.
URL: <http://www.ngdc.noaa.gov/mgg/topo/report/index.html>, 25.04.2005.
- Heuck, K., Dettmann, K. D. (2002): *Elektrische Energieversorgung - Erzeugung, Transport und Verteilung elektrischer Energie für Studium und Praxis*. 5. Auflage, Vieweg Verlag, Braunschweig.
- ICNIRP (1998): *Guidelines for limiting exposure to time-varying electric, magnetic, and electromagnetic fields (up to 300 GHz)*. Health Physics 74 (4): 494-522, International Commission on Non-Ionizing Radiation Protection (ICNIRP), Oberschleissheim. Deutsche Übersetzung in: Berichte der Strahlenschutzkommission (SSK), Heft 23. URL: <http://www.icnirp.de/documents/emfgdlger.pdf>, 14.01.2005.
- IFEU/IFU (2005): *Umberto - Software für das innerbetriebliche Stoffstrommanagement*. Benutzerhandbuch, Umberto Version 5, Institut für Energie- und Umweltforschung Heidelberg GmbH (ifeu), Institut für Umweltinformatik Hamburg GmbH (ifu).

- ISO (2005): *DIN EN ISO 14040: Umweltmanagement - Produkt-Ökobilanz - Prinzipien und allgemeine Anforderungen*. Deutsches Kompetenzzentrum für Nachhaltiges Wirtschaften (DKNW) der privaten Universität Witten/Herdecke, Lehrstuhl für Umweltmanagement der Universität Hohenheim. URL: <http://www.oekoradar.de/de/gesetzte/norm/01993/index.html>, 07.06.2005.
- IUCN (1994): *Guidelines for Protected Areas Management Categories*. IUCN, Cambridge, UK and Gland, Switzerland. <http://www.iucn.org/themes/wcpa/pubs/guidelines.htm#categories>, 17.05.2005.
- Kießling, F., Nefzger, P., Kaintzyk, U. (2001): *Freileitungen: Planung, Berechnung, Ausführung*. 5. Auflage, Springer-Verlag, Berlin.
- Knies, G., Bennouna, A. (1999): *Vereinigter Klimaschutz Afrika-Europa*. Hamburger Klimaschutzfonds e.V. (HKF), Centre National de la Recherche (CNR).
- Knoepfel, I. (1995): *Indikatorensystem für die ökologische Bewertung des Transports von Energie*. Forschungsbericht Nr. 20, Laboratorium für Energiesysteme, ETH Zürich, Juris Druck + Verlag Dietikon.
- Kronshage, S. (2005): Persönliches Gespräch am 01.07.2005, DLR, Stuttgart.
- Kronshage, S., Trieb, F. (2002): *Berechnung von Weltpotenzialkarten*. Erstellung einer Expertise für den Wissenschaftlichen Beirat der Bundesregierung Globale Umweltveränderung (WBGU). Dokumentation, DLR, Stuttgart.
- Kronshage, S. (2001): *Standortanalyse für solarthermische Kraftwerke am Beispiel des Königreiches Marokko. Eine Weiterentwicklung des Planungsinstruments STEPS zur Durchführung detaillierter Länderstudien*. Diplomarbeit am DLR, Stuttgart.
- Kullnick, U., Marhold, S. (2000): *Elektrokabel im Meer*. In: Technische Eingriffe in marine Lebensräume, BfN-Skripten 29, Seite 4-30. Workshop des Bundesamtes für Naturschutz, Internationale Naturschutzakademie Insel Vilm, 27.-29.10.1999. Bundesamt für Naturschutz, Bonn-Bad Godesberg.
- Laures, W. (2003): *Untersuchungen zum Einsatz von Höchstspannungskabeln großer Längen in der 400-kV-Ebene*. Dissertation an der Universität Duisburg-Essen.
- Lebrecht, L. (1966): *HGÜ – Hochspannungs-Gleichstromübertragung*. Forschungs-Berichte 9, Deutsche Forschungsgemeinschaft, Franz Steiner Verlag GmbH, Wiesbaden.
- Leitgeb, N. (2000): *Machen elektromagnetische Felder krank? Strahlen, Wellen, Felder und ihre Auswirkungen auf unsere Gesundheit*. Springer-Verlag, Wien.
- Leuschner, U. (2005): *Energie - Wissen*. Heidelberg. URL: <http://www.udo-leuschner.de/basiswissen/index.htm>, 1.3.2005.

- LfU (2002): *Elektromagnetische Felder im Alltag*. Landesanstalt für Umweltschutz Baden-Württemberg, Karlsruhe.
- Münchener Rück (2001): *Weltkarte der Naturgefahren*. Dokumentation, Münchener Rückversicherungs-Gesellschaft AG, München.
- NGA (2005): *GEOnet Names Server (GNS)*. National Geospatial Intelligence Agency (NGA). URL: <http://www.nga.mil>, 20.05.2005.
- NGDC (2005): *2-Minute Gridded Global Relief Data (ETOPO2)*. Online-Documentation, National Geophysical Data Center, Boulder, Colorado. URL: <http://www.ngdc.noaa.gov/mgg/fliers/01mgg04.html>, 27.04.2005.
- Nitsch, J. (2003): *Faktensammlung - Nationale und globale Szenarien für: Solar Generation – Fahrplan für eine saubere Energieversorgung*. Greenpeace e.V., Stuttgart. In: BMU (2004b): *Ökologisch optimierter Ausbau der Nutzung erneuerbarer Energien in Deutschland*.
- Normark, B. (2005): Persönliche Mitteilung am 23.07.2005, ABB, Schweden.
- OME (2003): *Electricity Interconnections in the Mediterranean Countries*. Observatoire Méditerranéen de l'Énergie, Paper for the Conference in Tripoli, 17.-18.03.2003.
- ORNL (2003): *LandScan Global Population 200x Database Release*. Documentation, Oak Ridge National Laboratory, Oak Ridge, Tennessee. URL: <http://www.ornl.gov/sci/gist/>, 01.05.2005.
- Pehnt, M. (2002): *Ganzheitliche Bilanzierung von Brennstoffzellen in der Energie- und Verkehrstechnik*. Fortschritt-Berichte VDI, Reihe 6 Energietechnik, Nr. 476, Dissertation am DLR Stuttgart, VDI-Verlag GmbH, Düsseldorf.
- PE, IKP (1998): *GaBi3 - Das Softwaresystem zur ganzheitlichen Bilanzierung*. Product Engineering (PE), Institut für Kunststoffkunde und Kunststoffprüfung (IKP), Universität Stuttgart.
- Peschke E., v. Olshausen, R. (1998): *Kabelanlagen für Hoch- und Höchstspannung. Entwicklung, Herstellung, Prüfung, Montage und Betrieb von Kabeln und deren Garnituren*. Siemens AG, Berlin und München. Publicis MCD Verlag, Erlangen und München.
- Poweron (2005): URL: <http://www.poweron.ch>, 26.07.2005.
- PSU (1999): *About the Digital Chart of the World Data Server*. Pennsylvania State University Libraries, Pennsylvania. URL: http://www.maproom.psu.edu/dcw/dcw_about.shtml, 21.04.2005.
- Rio Agenda 21 (1992): *Conference on Environment and Development, Agenda 21: Programme of Action for Sustainable Development*. United Nations Department of Public Information, New York.

- Rudervall, R., Charpentier, J. P., Sharma, R. (2000): *High Voltage Direct Current (HVDC) Transmission Systems*. Paper presented at Energy Week 2000 in Washington D.C. on March 7-8, 2000. ABB Power Systems Sweden, World Bank United States, ABB Financial Services Sweden.
URL: <http://www.abb.com>, 17.03.2005.
- RWE (2005): *Projekt Trassenpflege*. Rheinisch-Westfälisches Elektrizitätswerk AG, Essen. URL: <http://www.rwe.com/generator.aspx/konzern/verantwortung/nachhaltigkeit/projekte/language=de/id=43364/projekttrassenpflege-page.html>, 08.05.2005.
- RWE (1996): *Biotopmanagement in walddurchquerenden Trassen*. In: Raumordnungsverfahren - Planung einer Freileitung für Offshore-Strom im Raum Weser-Ems. Unterlagen für die Antragskonferenz der Bezirksregierung Weser-Ems. Windland Energieerzeugung GmbH Berlin und Planungsgruppe Ökologie + Umwelt GmbH Hannover.
URL: http://www.meerwind.de/Unterlagen/ROV_Skoping.pdf, 22.05.2005.
- Scheffer F., Schachtschabel, P. (2002): *Lehrbuch der Bodenkunde*. Spektrum Lehrbuch, 15. Auflage, Spektrum Akademischer Verlag, Heidelberg.
- Schillings, C., Mannstein, H., Meyer, R. (2003): *Operational method for deriving high resolution direct normal irradiation from satellite data*. German Aerospace Center Stuttgart/Oberpfaffenhofen. In: Solar Energy 76 (2004) 475-484, Elsevier.
- Schlabbach, J. (2003): *Elektroenergieversorgung*. VDE Verlag GmbH, Berlin und Offenbach.
- Schmidt, M., Keil, R. (2002): *Stoffstromnetze und ihre Nutzung für mehr Kostentransparenz sowie die Analyse der Umweltwirkung betrieblicher Stoffströme*. Beiträge der Hochschule Pforzheim Nr. 103, Hrsg.: A. Häfner, N. Jost, K.-H. Rau, R. Scherr, C. Wehner, H. Wienert.
- Schmidt, M., Häuslein, A. (1996): *Ökobilanzierung mit Computerunterstützung*. Springer-Verlag, Berlin.
- Schneider, J. (1995): *Bewertung von Drehstrom- und Gleichstromvarianten für Hochleistungsfernübertragungen im Großverbund*. Dissertation am Institut für Elektrische Anlagen und Energiewirtschaft Forschungsgesellschaft Energie an der RWTH Aachen. Aachener Beiträge zur Energieversorgung, Band 26, Verlag der Augustinus Buchhandlung, Aachen.
- Schumacher, A. (2002): *Die Berücksichtigung des Vogelschutzes an Energiefreileitungen im novellierten Bundesnaturschutzgesetz*. In: Naturschutz in Recht und Praxis - Online, Heft 1. URL: http://www.naturschutzrecht.net/online-zeitschrift/NRPO_Heft1.pdf, 22.02.05.
- Schymroch, H. D. (1985): *Hochspannungs-Gleichstrom-Übertragung*. Teubner Studienskripten Elektrotechnik 109, B. G. Teubner, Stuttgart.

- SEP (1997): *Umweltverträglichkeitsstudie der Hochspannungsverbindung Norwegen-Niederlande*. NV Sammwerkende Elektriciteitc-Productiebedrijven, Arnheim.
- Smith, W. H. F., Sandwell, D. T. (2003): *Exploring the Ocean Basins with Satellite Altimeter Data*. Scripps Institution of Oceanography San Diego, California & Geosciences Laboratory, NOAA, Washington, District of Columbia. URL: <http://www.ngdc.noaa.gov/mgg/bathymetry/predicted/explore.html>, 28.04.2005.
- Söderberg, L., Abrahamsson, B. (2001): *SwePol Link sets new environmental standard for HVDC transmission*. ABB Review 4/2001. URL: <http://www.abb.com>, 18.07.2005.
- Statistisches Bundesamt (2004): *Statistisches Jahrbuch für das Ausland*. Wiesbaden.
- Trieb, F. (2005a): Persönliche Mitteilung am 14.07.2005, DLR, Stuttgart.
- Trieb, F., Milow, B. (2000): *State of the Art 2000 - Solar Thermal Power Plants*. German Aerospace Centre (DLR) Stuttgart/Cologne. URL: <http://www.dlr.de/tt/institut/abteilungen/system/publications>, 17.07.2005.
- Trieb et al. (1998): *Markteinführung solarthermischer Kraftwerke - Chance für die Arbeitsmarkt- und Klimapolitik*. Energiewirtschaftliche Tagesfragen, 48. Jg., Heft 6.
- UBA (2002): *Langfristszenarien für eine nachhaltige Energienutzung in Deutschland*. Arbeitsgemeinschaft Deutsches Zentrum für Luft und Raumfahrt, Wuppertaler Institut, Forschungsbericht (FKZ 200 97 104) im Auftrag des Umweltbundesamtes, Berlin.
- UBA (2000): *Hintergrundpapier - Handreichung Bewertung in Ökobilanzen*. Umweltbundesamt, Dessau. URL: http://www.probas.umweltbundesamt.de/download/uba_bewertungsmethode.pdf, 17.07.2005.
- UBA (1999): *Bewertung in Ökobilanzen*. UBA-Texte 92/99, Berlin.
- UBA (1995): *Ökobilanz für Getränkeverpackungen*. UBA-Texte 52/95, Berlin.
- UCTE (2005a): URL: http://www.ucte.org/publications/library/e_default_2005.asp, 16.08.2005.
- UCTE (2005b): URL: http://www.ucte.org/statistics/production/e_default.asp, 16.08.2005.
- UNEP-WCMC (2005): *United Nations List of Protected Areas*. United Nations Environment Programme - World Conservation Monitoring Centre, Cambridge, UK. URL: <http://sea.unep-wcmc.org>, 20.04.2005.

- USGS (2003): *Global Land Cover Characteristics Data Base*. U.S. Geological Survey, Earth Resources Observation System (EROS) Data Center, Sioux Falls, South Dakota. URL: http://edcdaac.usgs.gov/glcc/globdoc2_0.asp, 21.04.2005.
- VDEW (2001): *Kabelhandbuch*. 6. Auflage, Verband der Elektrizitätswirtschaft e.V., VDEW-Verlag, Frankfurt am Main.
- Viebahn, P. (2004): *Solarthermische Kraftwerkstechnologie für den Schutz des Erdklimas - SOKRATES-Projekt*. Projektbericht, Deutsches Zentrum für Luft- und Raumfahrt Stuttgart.
- WDPA Consortium (2005): *World Database on Protected Areas 2005*. CD-ROM-Documentation, World Conservation Union (IUCN) and UNEP-World Conservation Monitoring Centre (UNEP-WCMC).
- Wirtz, K. W., Schuchardt, B. (2003): *Auswirkungen von Rohrleitungen und Stromkabeln*. In: Warnsignale aus Nordsee und Wattenmeer – Ein aktuelle Umweltbilanz. J. L. Lozán, Seite 154-156. Wissenschaftliche Auswertungen, Hamburg.
- Zewe, R. (1996): *Einfluß von Freileitungen auf das Landschaftsbild. Neue und verbesserte Verfahren zur Beurteilung der Sichtbarkeit*. Dissertation, Technische Fakultät, Universität des Saarlandes, Saarbrücken.

14 Used datasets

- *DLR (2004): ***Direktnormalstrahlung für das Jahr 2002***. Deutsches Zentrum für Luft- und Raumfahrt, Institut für Technische Thermodynamik, Abteilung Technikbewertung und Systemanalyse, Stuttgart.
- *ecoinvent Zentrum (2003): ***ecoinvent Daten v1.01***. CD-ROM des Schweizer Zentrums für Ökoinventare, Dübendorf.
- *ESRI (1996): ***ArcAtlas™: Our Earth***. CD-ROM, Environmental Systems Research Institute Inc., California, USA.
- *FAO (1995): ***Digital Soil Map of the World and Derived Soil Properties (DSMW)***. CD-ROM, Version 3.5, Land and Water Digital Media Series 1, Food and Agriculture Organization of the United Nations, Rome, Italy.
- *IFEU/IFU (2005): ***Umberto - Software für das innerbetriebliche Stoffstrommanagement***. Version Umberto 5, Institut für Umweltinformatik Hamburg GmbH (ifu), Institut für Energie- und Umweltforschung Heidelberg GmbH (ifeu).
- *Meteonorm (2005): ***Global Meteorological Database for Solar Energy and Applied Meteorology***. Version 5.0, Meteotest, GmbH, Nördlingen.
URL: <http://www.meteotest.de/>, 16.08.2005.
- *Münchener Rück (2001): ***Weltkarte der Naturgefahren***. Münchener Rückversicherungs-Gesellschaft AG, München.
- *NGA (2005): ***GEOnet Names Server (GNS)***. National Geospatial-Intelligence Agency, Bethesda, Maryland. URL: <http://www.nga.mil>, 20.04.2005.
- *NGDC (2001): ***2-minute Gridded Global Relief (ETOPO2)***. National Geophysical Data Center (NGDC), National Oceanic Atmospheric Administration (NOAA), Boulder, Colorado, USA.
URL: http://www.ngdc.noaa.gov/mgg/gdas/gd_designagrid.html, 24.05.2005.
- *GLOBE Task Team and others (Hastings, David A., Paula K. Dunbar, Gerald M. Elphinstone, Mark Bootz, Hiroshi Murakami, Hiroshi Maruyama, Hiroshi Masaharu, Peter Holland, John Payne, Nevin A. Bryant, Thomas L. Logan, J.-P. Muller, Gunter Schreier, and John S. MacDonald), eds. (1999): ***The Global Land One-kilometer Base Elevation (GLOBE) Digital Elevation Model***, Version 1.0. National Oceanic and Atmospheric Administration, National Geophysical Data Center, 325 Broadway, Boulder, Colorado. (empfohlene Zitierweise) URL: <http://www.ngdc.noaa.gov/mgg/topo/globe.html>, 25.04.2005.
- *ORNL (2003): ***LandScan Worldwide Population Database 2003***. Oak Ridge National Laboratory, Oak Ridge, Tennessee. URL: <http://www.ornl.gov/gist>, 25.03.2005.
- *Ph.D. (1998): ***Digital Chart of the World in ASCII (DCW)***. CD-ROM, Version 3.0, Ph.D. Associates Inc., Toronto, Ontario, Canada.

*USGS (2000): **Global Land Cover Characterization (GLCC) Data Base**. Version 2.0, U.S. Geological Survey, Earth Resources Observation System (EROS) Data Center, Sioux Falls, South Dakota.
URL: <http://edcdaac.usgs.gov/glcc/glcc.asp>, 21.04.2005.

*WDPA Consortium (2005): **World Database on Protected Areas 2005**. CD-ROM, World Conservation Union (IUCN) and UNEP-World Conservation Monitoring Centre (UNEP-WCMC). URL: <http://sea.unep-wcmc.org/wdbpa>, 20.04.2005.

With this I declare that I have prepared this diploma thesis independently and only with the stated sources and aids.

Braunschweig, 17th August 2005

Nadine May

Annex

Tab. 28: Decrease of the alongside meridian distance to the poles.

Latitude x [°]	Resolution [bg]		
	30"	2'	5'
		Meridian distance y [km]	
0	0.93*	3.71*	9.27*
10	0.92	3.65	9.13
20	0.87	3.49	8.71
30	0.81	3.21	8.03
40	0.71	2.84	7.1
50	0.6	2.39	5.96
60	0.47	1.86	4.64
70	0.32	1.27	3.17
80	0.16	0.64	1.61
90	0	0	0

*corresponds to the latitude degree distance [km], otherwise $y = [y(0^\circ)] * \cos x$

Tab. 29: Features for the visibility analysis (Source: NGA, 2005).

Abbreviation	Feature	German name
AMTH	amphitheater	Amphitheater
ANS	ancient site	antike Stätte
CARN	cairn	Grenzmal, Hügelgrab
CH	church	Kirche
CMTY	cemetery	Friedhof
CRRL	corral	Tiergehege, Wagenburg
CSTL	castle	Burg
CTRR	religious center	religiöses Zentrum
CVNT	convent	Nonnenkloster
GDN	garden	Gärten
GRVE	grave	Grabstätte
HSTS	historical site	historische Stätte
LOCK	lock	Schloss, Schleuse
MNMT	monument	Monument, Denkmal
MSQE	mosque	Moschee
MSTY	monastery	Mönchskloster
MUS	museum	Museum
OBPT	observation point	Aussichtspunkt
OBS	observatory	Observatorium
PAL	palace	Palast
PYR	pyramid	Pyramide
PYRS	pyramids	Pyramiden
RGL	religious site	religiöse Stätte
RGLR	retreat	spiritueller Ort
RSRT	resort	Erholungsort
RUIN	ruin	Ruine
SHRN	shrine	Schrein
TMB	tomb	Grabmal
TMPL	temple	Tempel
TOWR	tower	Turm, Warte
ZOO	zoo	Tierpark

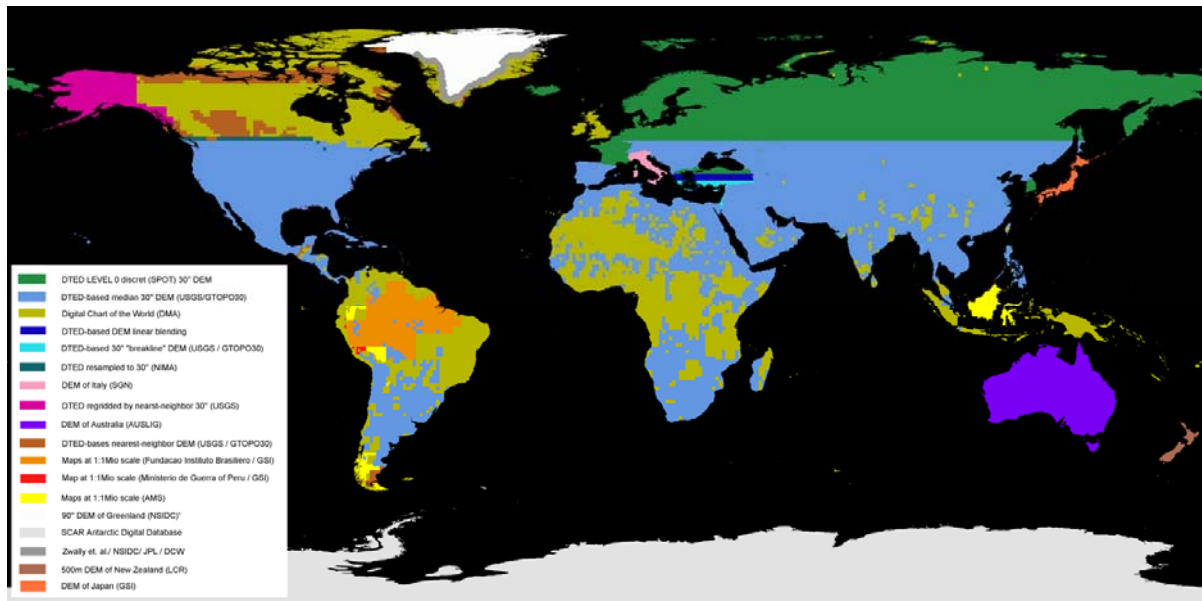


Fig. 84: GLOBE-Dataset (Source: Hastings et al., 1999, changed).

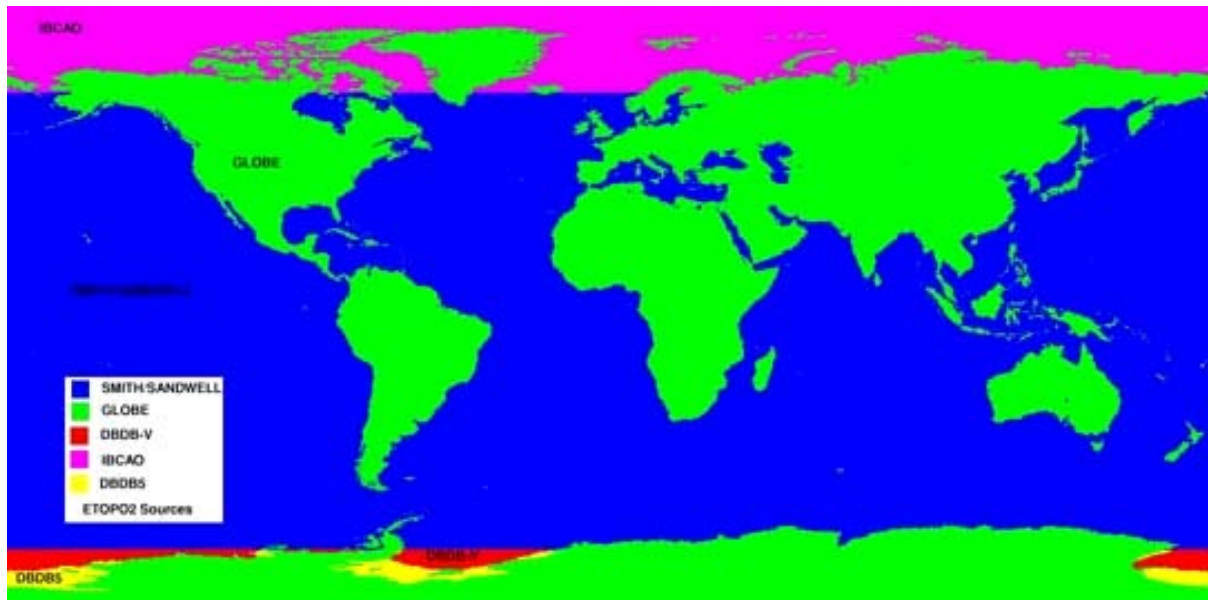


Fig. 85: ETOPO2-Dataset (Source: NGDC, 2005).

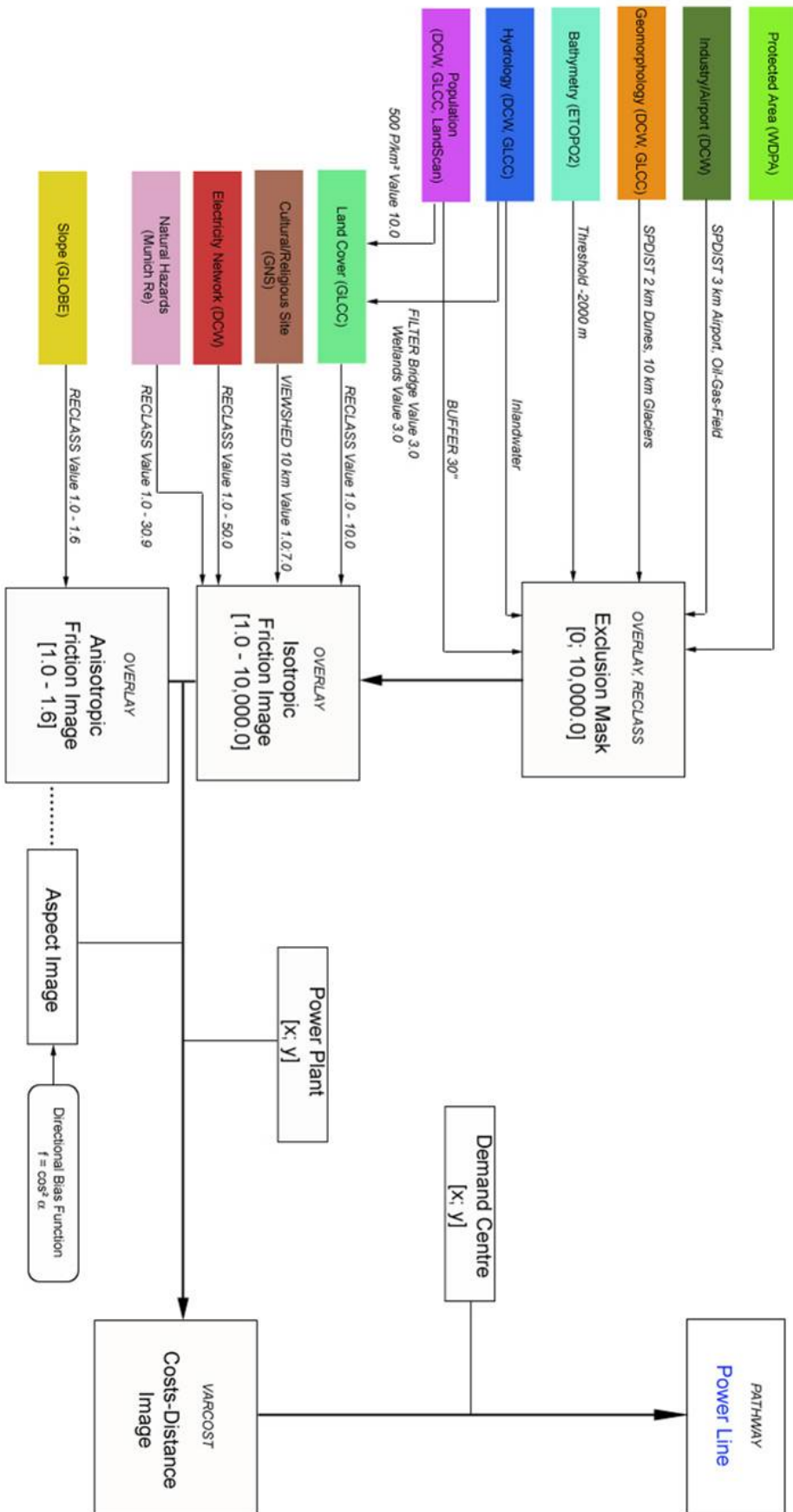


Fig. 86: Line laying model.

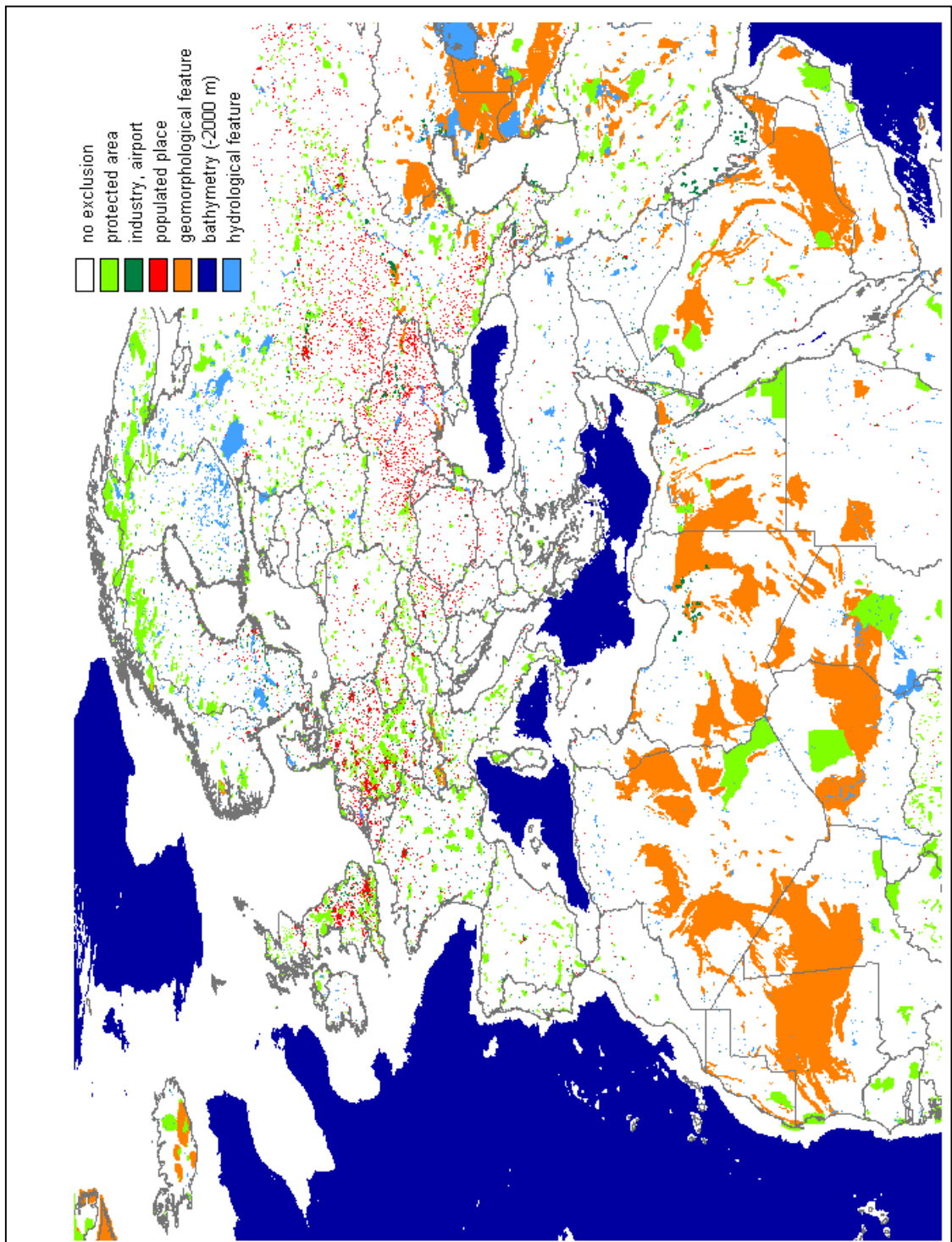


Fig. 87: Exclusion mask for the line.

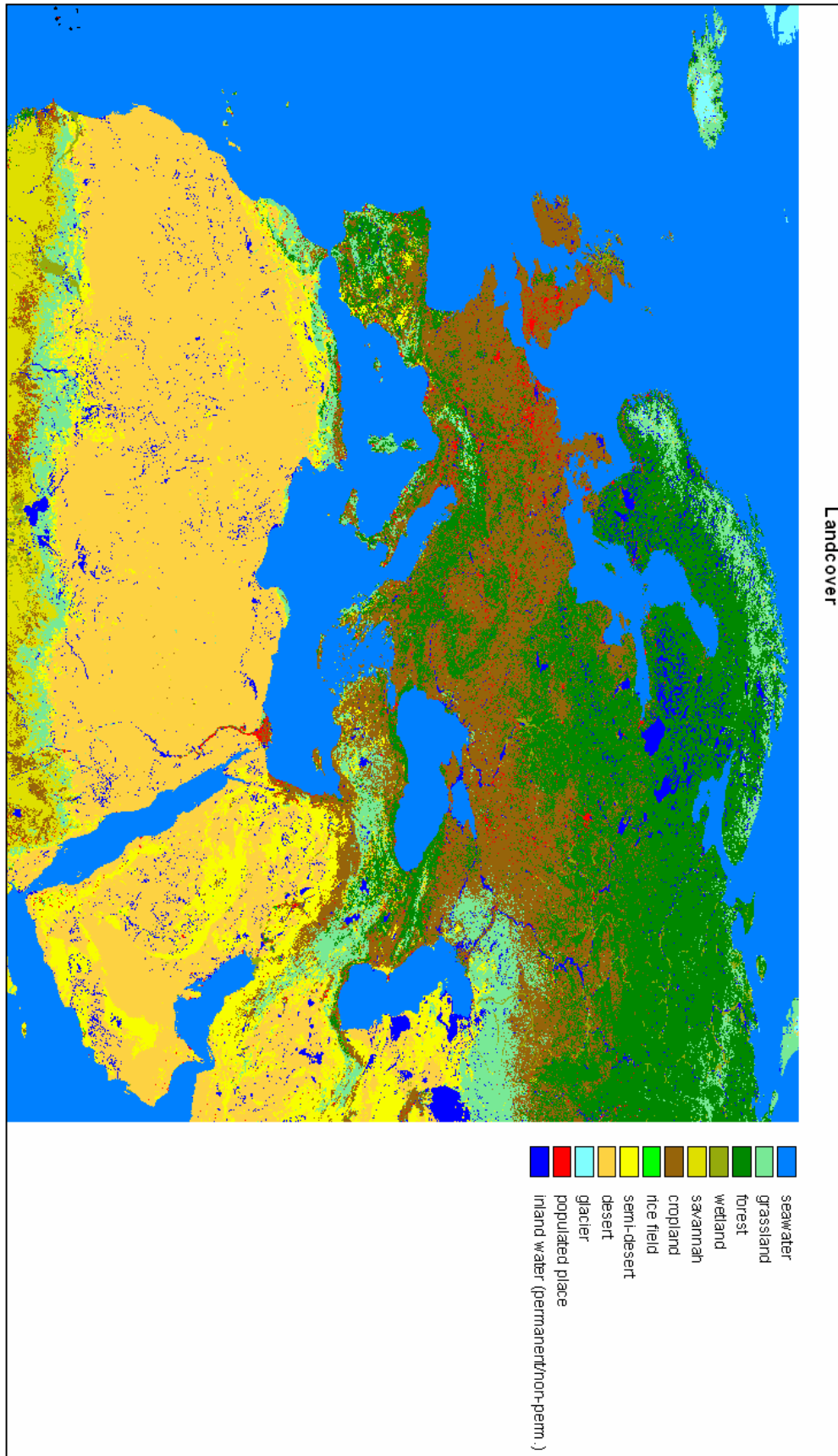


Fig. 88: Land cover in the Mediterranean region (Source: *USGS, 2000).

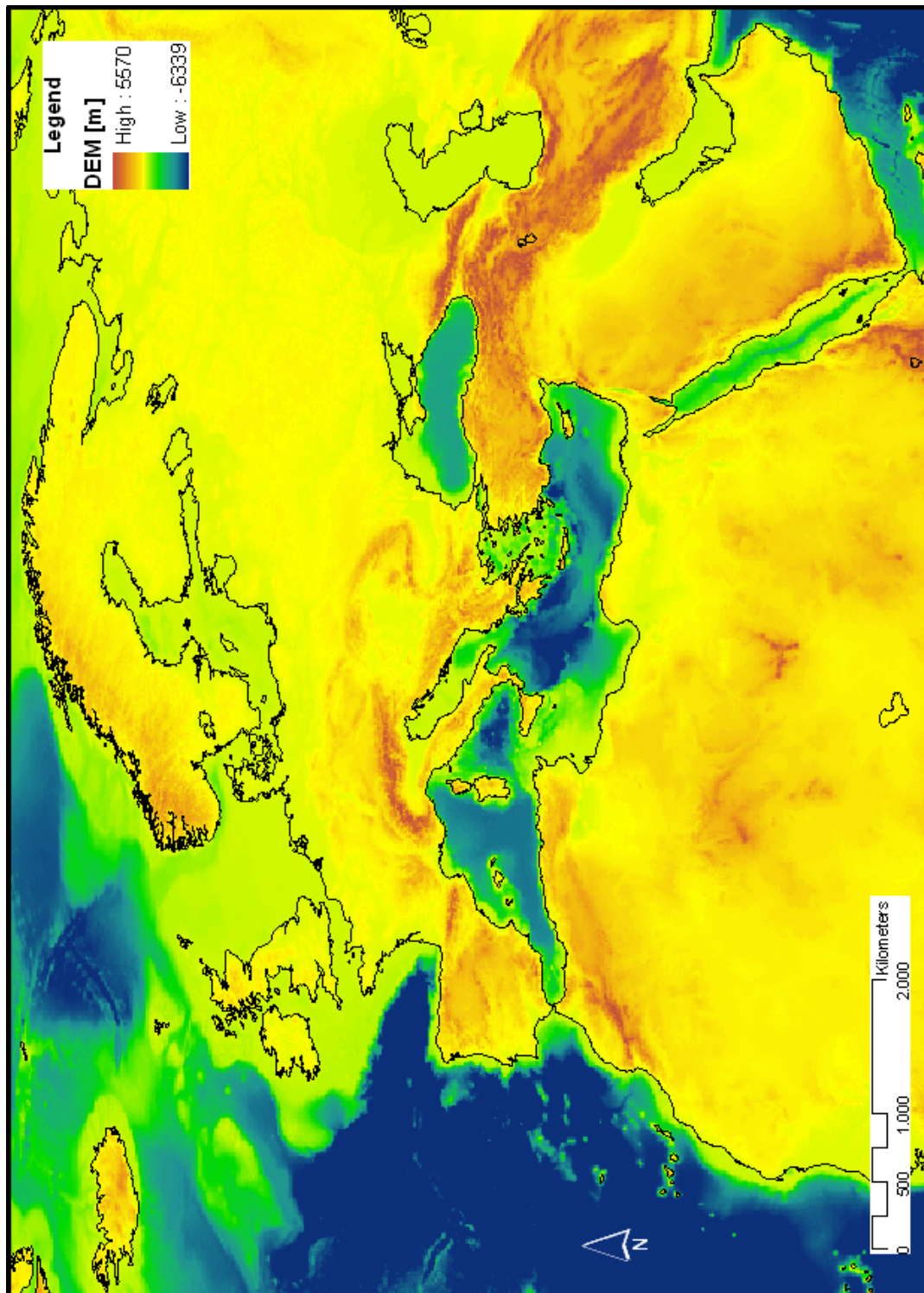


Fig. 89: Digital elevation model (Source: *Globe Task Team et al., 1999; NGDC, 2001).

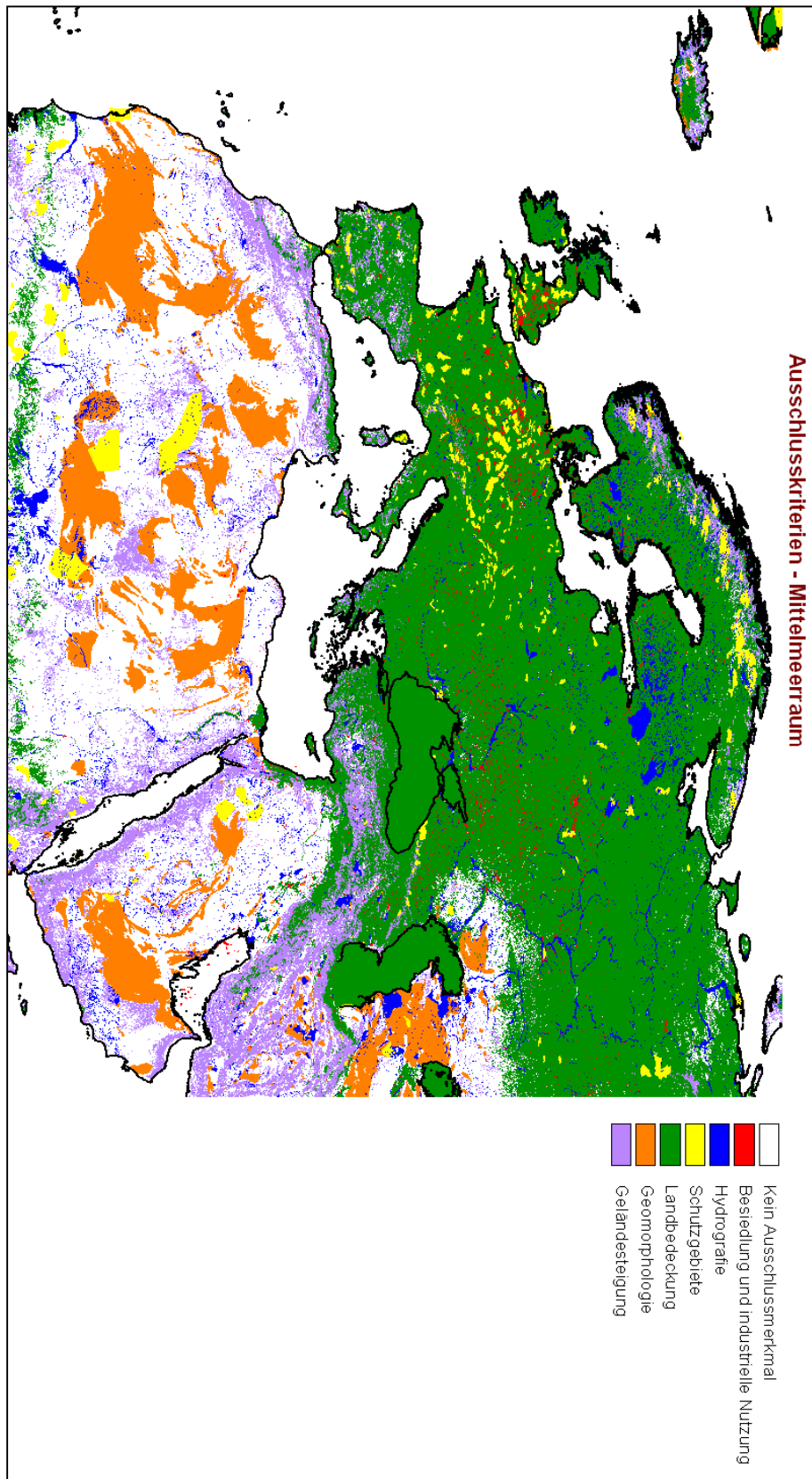


Fig. 90: Exclusion mask for the solar thermal power plant.

Tab. 30: Space requirement of line 1 structured by land cover classes.

Algeria-Aachen	Pixel-Frequency	Share [%]	Area [km²]
Bridgeable water	15	0.52	1.61
Grassland	451	15.49	48.30
Forest	251	8.62	26.88
Wetland	0	0.00	0.00
Savannah	23	0.79	2.46
Cropland	1531	52.59	163.95
Rice field	0	0.00	0.00
Semi-desert	190	6.53	20.35
Desert	432	14.84	46.26
Agglomeration	3	0.10	0.32
Seawater	15	0.52	1.61
Sum	2911	100.00	311.73
In the visual range	157	5.39	16.81

Tab. 31: Space requirement of line 2 structured by land cover classes.

Libya-Milano	Pixel-Frequency	Share [%]	Area [km²]
Bridgeable water	33	1.16	3.59
Grassland	457	16.00	49.72
Forest	135	4.73	14.69
Wetland	0	0.00	0.00
Savannah	7	0.25	0.76
Cropland	300	10.50	32.64
Rice field	0	0.00	0.00
Semi-desert	100	3.50	10.88
Desert	1483	51.91	161.34
Agglomeration	0	0.00	0.00
Seawater	342	11.97	37.21
Sum	2857	100.00	310.83
In the visual range	291	10.19	31.66

Tab. 32: Space requirement of line 3 structured by land cover classes.

Egypt-Vienna	Pixel-Frequency	Share [%]	Area [km²]
Bridgeable water	33	0.74	3.33
Grassland	287	6.43	28.99
Forest	180	4.03	18.18
Wetland	0	0.00	0.00
Savannah	45	1.01	4.54
Cropland	2072	46.41	209.27
Rice field	0	0.00	0.00
Semi-desert	577	12.92	58.28
Desert	1228	27.50	124.03
Agglomeration	5	0.11	0.50
Seawater	38	0.85	3.84
Sum	4465	100.00	450.96
In the visual range	93	2.08	9.39

Parameter specifications

Tab. 33: Parameter determination for the modelling of the HVDC line 1.

Parameter	Variable ⁺	Quantity	Unit
Share of primary copper	CU_P	20	%
Share of secondary copper	CU_S	80	%
Length of the overhead line	KM_HG	3099	km
Length of the submarine cable	KM_CA	18	km
Life time of the HVDC line	LEB_H	50	a
Capacity	P_AKT	10	GW
Utilization degree_HVDC_all	EELHG	100	%
Utilization degree_HVDC_Cable	EELCA	98.3	%/1000 km
Utilization degree_HVDC_converter	EELKS	98.6	%
Utilization degree_HVDC_Line	EELLE	96.3	%/1000 km
System operating time	T_SYS	30	a
Full-load operating time	VOLL	7710	h
Truck: Germany-Hamburg - Section A	LD_A	400	km
Truck: Germany-Line - Section B	LD_B	400	km
Truck: Line - Section A (1432 km overhead line)	LT_A	716.2	km
Truck: Line - Section B (1667 km submarine cable)	LT_B	833.8	km
Truck type		5 = trucks > 32 t	
Truck utilization on the way there		100	%
Truck utilization on the way back		0	%
Share of highway (Germany/Africa)		51/20	%
Share of country road (Germany/Africa)		30/70	%
Share of city streets (Germany/Africa)		19/10	%
Ship-overhead line - section A	SF_A	3000	km
Ship type		1 = general cargo vessel	
Ship-submarine cable - section A (18 km submarine cable)	SSK_A	4000	km
Ship type		1 = general cargo vessel	

⁺customized parameter within the Input-Monitor of Umberto[®]

Tab. 34: Parameter determination for the modelling of the HVDC line 2.

Parameter	Variable ⁺	Quantity	Unit
Share of primary copper	CU_P	20	%
Share of secondary copper	CU_S	80	%
Length of the overhead line	KM_HG	2735	km
Length of the submarine cable	KM_CA	373	km
Life time of the HVDC line	LEB_H	50	a
Capacity	P_AKT	10	GW
Utilization degree_HVDC_all	EELHG	100	%
Utilization degree_HVDC_Cable	EELCA	98.3	%/1000 km
Utilization degree_HVDC_converter	EELKS	98.6	%
Utilization degree_HVDC_Line	EELLE	96.3	%/1000 km
System operating time	T_SYS	30	a
Full-load operating time	VOLL	7710	h

Truck: Germany-Hamburg - Section A	LD_A	400	km
Truck: Germany-Line - Section B	LD_B	600	km
Truck: Line - Section A (2027 km overhead line)	LT_A	1013.7	km
Truck: Line - Section B (708 km submarine cable)	LT_B	354.2	km
Truck type		5 = trucks > 32 t	
Truck utilization on the way there		100	%
Truck utilization on the way back		0	%
Share of highway (Germany/Africa)		51/20	%
Share of country road (Germany/Africa)		30/70	%
Share of city streets (Germany/Africa)		19/10	%
Ship-overhead line - section A	SF_A	4500	km
Ship type		1 = general cargo vessel	
Ship-submarine cable - section A (373 km submarine cable)	SSK_A	6000	km
Ship type		1 = general cargo vessel	

⁺ customized parameter within the Input-Monitor of Umberto®

Tab. 35: Parameter determination for the modelling of the HVDC line 3.

Parameter	Variable ⁺	Quantity	Unit
Share of primary copper	CU_P	20	%
Share of secondary copper	CU_S	80	%
Length of the overhead line	KM_HG	4481	km
Length of the submarine cable	KM_CA	30	km
Life time of the HVDC line	LEB_H	50	a
Capacity	P_AKT	10	GW
Utilization degree_HVDC_all	EELHG	100	%
Utilization degree_HVDC_Cable	EELCA	98.3	%/1000 km
Utilization degree_HVDC_converter	EELKS	98.6	%
Utilization degree_HVDC_Line	EELLE	96.3	%/1000 km
System operating time	T_SYS	30	a
Full-load operating time	VOLL	7710	h
Truck: Germany-Hamburg - Section A	LD_A	400	km
Truck: Germany-Line - Section B	LD_B	600	km
Truck: Line - Section A (1790 km overhead line)	LT_A	895.2	km
Truck: Line - Section B (2691 km submarine cable)	LT_B	1345.8	km
Truck type		5 = trucks > 32 t	
Truck utilization on the way there		100	%
Truck utilization on the way back		0	%
Share of highway (Germany/Africa)		51/20	%
Share of country road (Germany/Africa)		30/70	%
Share of city streets (Germany/Africa)		19/10	%
Ship-overhead line - section A	SF_A	7000	km
Ship type		1 = general cargo vessel	
Ship-submarine cable - section A (30 km submarine cable)	SSK_A	8000	km
Ship type		1 = general cargo vessel	

⁺ customized parameter within the Input-Monitor of Umberto®

Tab. 36: Parameter determination for the modelling of the solar thermal power plant (line 1).

Parameter	Variable ⁺	Quantity	Unit
Solar share in the electricity yield	SOLAR	100	%
DNI	DNI	2835	kWh/m ² /a
Life time of the steam turbine	LEB_D	30	a
Life time of the buildings	LEB_B	60	a
Life time of the solar part	LEB_S	30	a
Capacity_current	P_AKT	10,000	MW
Capacity_reference	P_REF	80	MW
Capacity_storage_current	PSAKT	25,600*	MW _{th}
Capacity_storage_reference	PSREF	200	MW _{th}
Utilization degree_steam turbine	EELDT	39*	%
Utilization degree_solar part	ETHSO	45*	%
Storage time_current	TSAKT	23*	h
Storage time_reference	TSREF	1	h
Mirror size_current	SFAKT	227,000,000	m ²
Mirror size_reference	SFREF	495,770	m ²
System operating time	T_SYS	30	a
Ship transport (Hamburg-Casablanca), simple distance	S_AFR	3000	km
Ship type		Type 1 = general cargo vessel	
Truck transport (Germany), simple distance	LKW_D	400	km
Truck transport (Africa), simple distance	LKW_A	700	km
Truck type		Type 5 = trucks > 32 t	
Truck utilization on the way there		100	%
Truck utilization on the way back		0	%
Share of highway (Germany/Africa)		51/20	%
Share of country road (Germany/Africa)		30/70	%
Share of city streets (Germany/Africa)		19/10	%

⁺ customized parameter within the Input-Monitor of Umberto[®]; *agreement with Trieb (2005a)

Tab. 37: Parameter determination for the modelling of the solar thermal power plant (line 2).

Parameter	Variable ⁺	Quantity	Unit
Solar share in the electricity yield	SOLAR	100	%
DNI	DNI	2802	kWh/m ² /a
Life time of the steam turbine	LEB_D	30	a
Life time of the buildings	LEB_B	60	a
Life time of the solar part	LEB_S	30	a
Capacity_current	P_AKT	10,000	MW
Capacity_reference	P_REF	80	MW
Capacity_storage_current	PSAKT	25,600*	MW _{th}
Capacity_storage_reference	PSREF	200	MW _{th}
Utilization degree_steam turbine	EELDT	39*	%
Utilization degree_solar part	ETHSO	45*	%
Storage time_current	TSAKT	23*	h
Storage time_reference	TSREF	1	h
Mirror size_current	SFAKT	227,000,000	m ²
Mirror size_reference	SFREF	495,770	m ²

System operating time	T_SYS	30	a
Ship transport (Hamburg-Casablanca), simple distance	S_AFR	4600	km
Ship type		Type 1 = general cargo vessel	
Truck transport (Germany), simple distance	LKW_D	400	km
Truck transport (Africa), simple distance	LKW_A	1700	km
Truck type		Type 5 = trucks > 32 t	
Truck utilization on the way there		100	%
Truck utilization on the way back		0	%
Share of highway (Germany/Africa)		51/20	%
Share of country road (Germany/Africa)		30/70	%
Share of city streets (Germany/Africa)		19/10	%

⁺ customized parameter within the Input-Monitor of Umberto[®]; *agreement with Trieb (2005a)

Tab. 38: Parameter determination for the modelling of the solar thermal power plant (line 3).

Parameter	Variable ⁺	Quantity	Unit
Solar share in the electricity yield	SOLAR	100	%
DNI	DNI	2865	kWh/m ² /a
Life time of the steam turbine	LEB_D	30	a
Life time of the buildings	LEB_B	60	a
Life time of the solar part	LEB_S	30	a
Capacity_current	P_AKT	10,000	MW
Capacity_reference	P_REF	80	MW
Capacity_storage_current	PSAKT	25,600*	MW _{th}
Capacity_storage_reference	PSREF	200	MW _{th}
Utilization degree_steam turbine	EELDT	39*	%
Utilization degree_solar part	ETHSO	45*	%
Storage time_current	TSAKT	23*	h
Storage time_reference	TSREF	1	h
Mirror size_current	SFAKT	227,000,000	m ²
Mirror size_reference	SFREF	495,770	m ²
System operating time	T_SYS	30	a
Ship transport (Hamburg-Casablanca), simple distance	S_AFR	7000	km
Ship type		Type 1 = general cargo vessel	
Truck transport (Germany), simple distance	LKW_D	400	km
Truck transport (Africa), simple distance	LKW_A	600	km
Truck type		Type 5 = trucks > 32 t	
Truck utilization on the way there		100	%
Truck utilization on the way back		0	%
Share of highway (Germany/Africa)		51/20	%
Share of country road (Germany/Africa)		30/70	%
Share of city streets (Germany/Africa)		19/10	%

⁺ customized parameter within the Input-Monitor of Umberto[®]; *agreement with Trieb (2005a)

Tab. 39: Inventory data of the HVDC line 1 (2030).

Overhead line (100 % of concrete for section A is produced in North Africa)		
Production	Steel, high alloyed (75% recycled)	23,800 t
	Stahl, low alloyed (75% recycled)	278,910 t
	Aluminium (90% recycled)	64,707 t
	Concrete	743,760 t
	Fine ceramics	7,438 t
Transport (Section A) 46.2% of the materials	Truck>32t, 400 km Germany	69,273,211 tkm
	Truck>32t, 716.2 km Line Section A	370,132,266 tkm
	Sea ship, 4000 km	692,732,114 tkm
Transport (Section B) 53.8% of the materials	Truck>32t, 400 km Germany	240,725,957 tkm
	Truck>32t, 833.8 km Line Section B	501,793,257 tkm
Submarine cable (100 % produced in Sweden)		
Production	Steel, high alloyed (75% recycled)	2,074 t
	Lead	1,469 t
	Copper (80% recycled)	1,642 t
	Paper (Nature, non bleached)	518 t
	Polybutadien	86 t
	Polypropylen (PP)	199 t
Transport	Sea ship, 4000 km	23,950,080 tkm

Tab. 40: Inventory data of the HVDC line 2 (2030).

Overhead line (100 % of concrete for section A is produced in North Africa)		
Production	Steel, high alloyed (75% recycled)	21,005 t
	Stahl, low alloyed (75% recycled)	246,150 t
	Aluminium (90% recycled)	57,107 t
	Concrete	656,400 t
	Fine ceramics	6,564 t
Transport (Section A) 74.1% of the materials	Truck>32t, 400 km Germany	98,056,708 tkm
	Truck>32t, 1013.7 km Line Section A	741,556,188 tkm
	Sea ship, 4500 km	1,103,137,963 tkm
Transport (Section B) 25.9% of the materials	Truck>32t, 600 km Germany	153,414,858 tkm
	Truck>32t, 354.2 km Line Section B	90,565,905 tkm
Submarine cable (100 % produced in Sweden)		
Production	Steel, high alloyed (75% recycled)	42,970 t
	Lead	30,437 t
	Copper (80% recycled)	34,018 t
	Paper (Nature, non bleached)	10,742 t
	Polybutadien	1,790 t
	Polypropylen (PP)	4,118 t
Transport	Sea ship, 6000 km	744,448,320 tkm

Tab. 41: Inventory data of the HVDC line 3 (2030).

Overhead line (100 % of concrete for section A is produced in North Africa)		
Production	Steel, high alloyed (75% recycled)	34,414 t
	Stahl, low alloyed (75% recycled)	403,290 t
	Aluminium (90% recycled)	93,563 t
	Concrete	1,075,440 t
	Fine ceramics	10,754 t
Transport (Section A) 39.9% of the materials	Truck>32t, 400 km Germany	86,506,673 tkm
	Truck>32t, 895.2 km Line Section A	577,732,755 tkm
	Sea ship, 7000 km	1,513,866,776 tkm
Transport (Section B) 60.1% of the materials	Truck>32t, 600 km Germany	583,256,711 tkm
	Truck>32t, 1345.8 km Line Section B	1,308,244,802 tkm
Submarine cable (100 % produced in Sweden)		
Production	Steel, high alloyed (75% recycled)	3,456 t
	Lead	2,448 t
	Copper (80% recycled)	2,736 t
	Paper (Nature, non bleached)	864 t
	Polybutadien	144 t
	Polypropylen (PP)	331 t
Transport	Sea ship, 8000 km	79,833,600 tkm

Tab. 42: Inventory data of the solar thermal power plant of line 1 (2030).

Solar field (100 % produced in Germany)		
	Steel, unalloyed (75% rec.)	5,064,769 t
	Steel, high alloyed (75% rec.)	145,283 t
	Copper (80% rec.)	31,181 t
	Flat glass, laminated	2,579,019 t
	Concrete	6,612,748 t
	Fine ceramics	33,562 t
	Rock wool	114,409 t
	Phenol	496,335 t
	Polyvinylchlorid	4,441 t
Absorber lamination	Energy, electric	5,672,596 kWh
Construction	Energy, electrical	165,144,480 kWh
	Energy, mechanical	95,928,184 kWh
Transport	Truck>32t, 700 km North Africa	10,557,223,436 tkm
	Truck>32t, 400 km Germany	6,032,699,106 tkm
	Sea ship, 3000 km	45,245,243,298 tkm
Steam generator (50 % of steel and ceramics are produced in North Africa)		
	Steel rough, unalloyed	34,813 t
	Fine ceramics	2,261 t

Transport	Truck>32t, 700 km North Africa	25,951,562 tkm
	Truck>32t, 400 km Germany	7,414,732 tkm
	Sea ship, 3000 km	55,610,491 tkm

Mechanical engineering (19.4 % of steel and 48.9 % of PVC are produced in North Africa)

Steel, unalloyed (75% rec.)	167,324 t
Copper (80% rec.)	104 t
Aluminium (90% rec.)	46 t
Zinc	9 t
Concrete	540,599 t
Polyvinylchlorid	11,824 t

Transport	Truck>32t, 700 km North Africa	503,934,564 tkm
	Truck>32t, 400 km Germany	231,588,052 tkm
	Sea ship, 3000 km	1,739,169,265 tkm

Electrical engineering (100 % produced in Germany)

Steel, unalloyed (75% rec.)	2,496 t
Steel, high alloyed (75% rec.)	1,145 t
Polyvinylchlorid	294 t
Copper (80% rec.)	558 t

Transport	Truck>32t, 700 km North Africa	3,145,042 tkm
	Truck>32t, 400 km Germany	1,797,167 tkm
	Sea ship, 3000 km	13,478,752 tkm

Constructional engineering (100% produced in North Africa)

Steel, unalloyed (75% rec.)	300 t
Flat glass, laminated	3 t
Concrete	5,558 t
Polyvinylchlorid	12 t
Construction machinery	169,764 t

Transport	Truck>32t, 700 km North Africa	122,945,756 tkm
-----------	--------------------------------	-----------------

Storage (100 % of steel and concrete are produced in North Africa)

Phenol	122,216 t
PU foam, rigid	28,031 t
Steel, unalloyed (75% rec.)	313,950 t
Concrete	42,740,564 t

Transport	Truck>32t, 700 km North Africa	30,243,332,762 tkm
	Truck>32t, 400 km Germany	60,098,926 tkm
	Sea ship, 3000 km	450,741,944 tkm

Steam turbine (100 % produced in Germany)

Steel, unalloyed (75% rec.)	3,818 t
Steel, high alloyed (75% rec.)	2,070 t
Aluminium (90% rec.)	44 t
Copper (80% rec.)	176 t

	Fine ceramics	88 t	
Transport	Truck>32t, 700 km North Africa	4,337,280 tkm	
	Truck>32t, 400 km Germany	2,478,446 tkm	
	Sea ship, 3000 km	18,588,345 tkm	
Operating materials (100% produced in Germany)			
Mirror replacement	Copper (80% rec.)	20 t	
	Flat glass, laminated	360,961 t	
	Fine ceramics	4,853 t	
Cleaning	Energy, mechanical	152,375,759 kWh	
	Water, unspecific	127,142 t	
Losses	Phenol	575,688 t	
	Process water	195,079,287 t	
Transport	Truck>32t, 700 km North Africa	659,065,511 tkm	
	Truck>32t, 400 km Germany	376,608,864 tkm	
	Sea ship, 3000 km	2,824,566,477 tkm	
Disposal			
	Construction machinery, mechanical energy	204,000 kWh	
	Aluminium scrap	9,006 t	
Transport	Truck>32t, 100 km North Africa	900,600 tkm	

Tab. 43: Inventory data of the solar thermal power plant of line 2 (2030).

Solar field (100 % produced in Germany)			
	Steel, unalloyed (75% rec.)	5,064,769 t	
	Steel, high alloyed (75% rec.)	145,283 t	
	Copper (80% rec.)	31,181 t	
	Flat glass, laminated	2,579,019 t	
	Concrete	6,612,748 t	
	Fine ceramics	33,562 t	
	Rock wool	114,409 t	
	Phenol	496,335 t	
	Polyvinylchlorid	4,441 t	
Absorber lamination	Energy, electric	5,672,596 kWh	
Construction	Energy, electrical	165,144,480 kWh	
	Energy, mechanical	95,928,184 kWh	
Transport	Truck>32t, 1700 km North Africa	25,638,971,202 tkm	
	Truck>32t, 400 km Germany	6,032,699,106 tkm	
	Sea ship, 4600 km	69,376,039,724 tkm	

Steam generator (50 % of steel and ceramics are produced in North Africa)

	Stahl grob, nicht legiert	34,813 t
	Keramik, fein	2,261 t
Transport	Truck>32t, 1700 km North Africa	63,025,223 tkm
	Truck>32t, 400 km Germany	7,414,732 tkm
	Sea ship, 4600 km	85,269,419 tkm

Mechanical engineering (19.4 % of steel and 48.9 % of PVC are produced in North Africa)

	Steel, unalloyed (75% rec.)	167,324 t
	Copper (80% rec.)	104 t
	Aluminium (90% rec.)	46 t
	Zinc	9 t
	Concrete	540,599 t
	Polyvinylchlorid	11,824 t
Transport	Truck>32t, 1700 km North Africa	1,223,841,083 tkm
	Truck>32t, 400 km Germany	231,588,052 tkm
	Sea ship, 4600 km	2,666,726,207 tkm

Electrical engineering (100 % produced in Germany)

	Steel, unalloyed (75% rec.)	2,496 t
	Steel, high alloyed (75% rec.)	1,145 t
	Polyvinylchlorid	294 t
	Copper (80% rec.)	558 t
Transport	Truck>32t, 1700 km North Africa	7,637,960 tkm
	Truck>32t, 400 km Germany	1,797,167 tkm
	Sea ship, 4600 km	20,667,420 tkm

Constructional engineering (100% produced in North Africa)

	Steel, unalloyed (75% rec.)	300 t
	Flat glass, laminated	3 t
	Concrete	5,558 t
	Polyvinylchlorid	12 t
	Construction machinery	169,764 t
Transport	Truck>32t, 1700 km North Africa	298,582,551 tkm

Storage (100 % of steel and concrete are produced in North Africa)

	Phenol	122,216 t
	PU foam, rigid	28,031 t
	Steel, unalloyed (75% rec.)	313,950 t
	Concrete	42,740,564 t
Transport	Truck>32t, 1700 km North Africa	73,448,093,850 tkm
	Truck>32t, 400 km Germany	60,098,926 tkm
	Sea ship, 4600 km	691,137,647 tkm

Steam turbine (100 % produced in Germany)			
	Steel, unalloyed (75% rec.)	3,818	t
	Steel, high alloyed (75% rec.)	2,070	t
	Aluminium (90% rec.)	44	t
	Copper (80% rec.)	176	t
	Fine ceramics	88	t
Transport	Truck>32t, 1700 km North Africa	10,533,395	tkm
	Truck>32t, 400 km Germany	2,478,446	tkm
	Sea ship, 4600 km	28,502,129	tkm
Operating materials (100% produced in Germany)			
Mirror replacement	Copper (80% rec.)	20	t
	Flat glass, laminated	360,961	t
	Fine ceramics	4,853	t
Cleaning	Energy, mechanical	152,375,759	kWh
	Water, unspecific	127,142	t
Losses	Phenol	575,688	t
	Process water	195,079,287	t
Transport	Truck>32t, 1700 km North Africa	1,600,587,670	tkm
	Truck>32t, 400 km Germany	376,608,864	tkm
	Sea ship, 4600 km	4,331,001,931	tkm
Disposal			
	Construction machinery, mechanical energy	204,000	kWh
	Aluminium scrap	9,006	t
Transport	Truck>32t, 100 km North Africa	900,600	tkm

Tab. 44: Inventory data of the solar thermal power plant of line 3 (2030).

Solar field (100 % produced in Germany)			
	Steel, unalloyed (75% rec.)	5,064,769	t
	Steel, high alloyed (75% rec.)	145,283	t
	Copper (80% rec.)	31,181	t
	Flat glass, laminated	2,579,019	t
	Concrete	6,612,748	t
	Fine ceramics	33,562	t
	Rock wool	114,409	t
	Phenol	496,335	t
	Polyvinylchlorid	4,441	t
Absorber lamination	Energy, electric	5,672,596	kWh
Construction	Energy, electrical	165,144,480	kWh
	Energy, mechanical	95,928,184	kWh

Transport	Truck>32t, 600 km North Africa	9,049,048,660 tkm
	Truck>32t, 400 km Germany	6,032,699,106 tkm
	Sea ship, 7000 km	105,572,234,363 tkm

Steam generator (50 % of steel and ceramics are produced in North Africa)

	Steel rough, unalloyed	34,813 t
	Fine ceramics	2,261 t
Transport	Truck>32t, 600 km North Africa	22,244,196 tkm
	Truck>32t, 400 km Germany	7,414,732 tkm
	Sea ship, 7000 km	129,757,812 tkm

Mechanical engineering (19.4 % of steel and 48.9 % of PVC are produced in North Africa)

	Steel, unalloyed (75% rec.)	167,324 t
	Copper (80% rec.)	104 t
	Aluminium (90% rec.)	46 t
	Zinc	9 t
	Concrete	540,599 t
	Polyvinylchlorid	11,824 t
Transport	Truck>32t, 600 km North Africa	431,943,912 tkm
	Truck>32t, 400 km Germany	231,588,052 tkm
	Sea ship, 7000 km	4,058,061,619 tkm

Electrical engineering (100 % produced in Germany)

	Steel, unalloyed (75% rec.)	2,496 t
	Steel, high alloyed (75% rec.)	1,145 t
	Polyvinylchlorid	294 t
	Copper (80% rec.)	558 t
Transport	Truck>32t, 600 km North Africa	2,695,750 tkm
	Truck>32t, 400 km Germany	1,797,167 tkm
	Sea ship, 7000 km	31,450,422 tkm

Constructional engineering (100% produced in North Africa)

	Steel, unalloyed (75% rec.)	300 t
	Flat glass, laminated	3 t
	Concrete	5,558 t
	Polyvinylchlorid	12 t
	Construction machinery	169,764 t
Transport	Truck>32t, 600 km North Africa	105,382,077 tkm

Storage (100 % of steel and concrete are produced in North Africa)

	Phenol	122,216 t
	PU foam, rigid	28,031 t
	Steel, unalloyed (75% rec.)	313,950 t
	Concrete	42,740,564 t
Transport	Truck>32t, 600 km North Africa	25,922,856,653 tkm
	Truck>32t, 400 km Germany	60,098,926 tkm

	Sea ship, 7000 km	1,051,731,202	tkm
Steam turbine (100 % produced in Germany)			
	Steel, unalloyed (75% rec.)	3,818	t
	Steel, high alloyed (75% rec.)	2,070	t
	Aluminium (90% rec.)	44	t
	Copper (80% rec.)	176	t
	Fine ceramics	88	t
Transport	Truck>32t, 600 km North Africa	3,717,669	tkm
	Truck>32t, 400 km Germany	2,478,446	tkm
	Sea ship, 7000 km	43,372,804	tkm
Operating materials (100% produced in Germany)			
Mirror replacement	Copper (80% rec.)	20	t
	Flat glass, laminated	360,961	t
	Fine ceramics	4,853	t
Cleaning	Energy, mechanical	152,375,759	kWh
	Water, unspecific	127,142	t
Losses	Phenol	575,688	t
	Process water	195,079,287	t
Transport	Truck>32t, 600 km North Africa	564,913,295	tkm
	Truck>32t, 400 km Germany	376,608,864	tkm
	Sea ship, 7000 km	6,590,655,112	tkm
Disposal			
	Construction machinery, mechanical energy	204,000	kWh
	Aluminium scrap	9,006	t
Transport	Truck>32t, 100 km North Africa	900,600	tkm

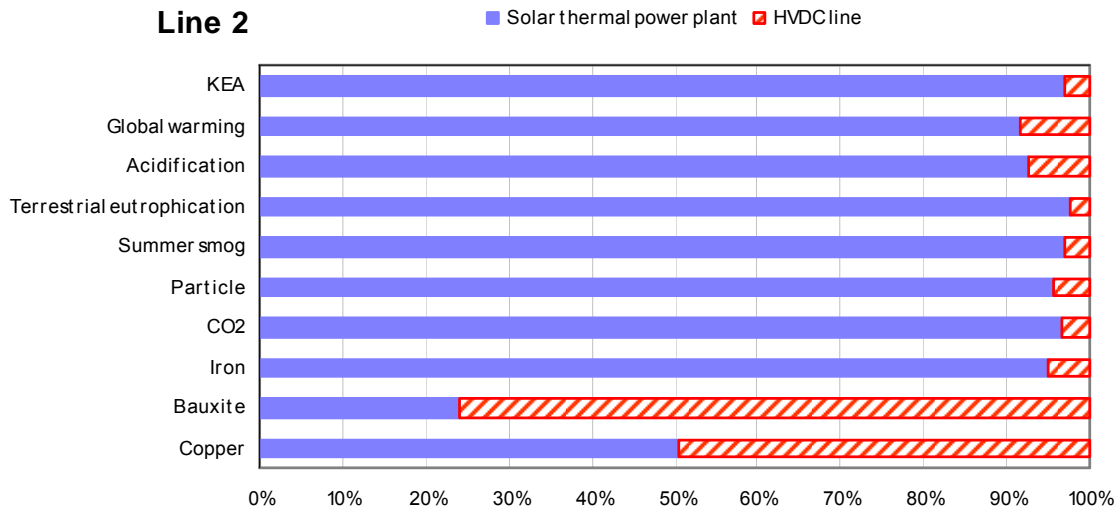


Fig. 91: Proportional shares of the plant and the line in environmental impacts (line 2, reference year 2030).

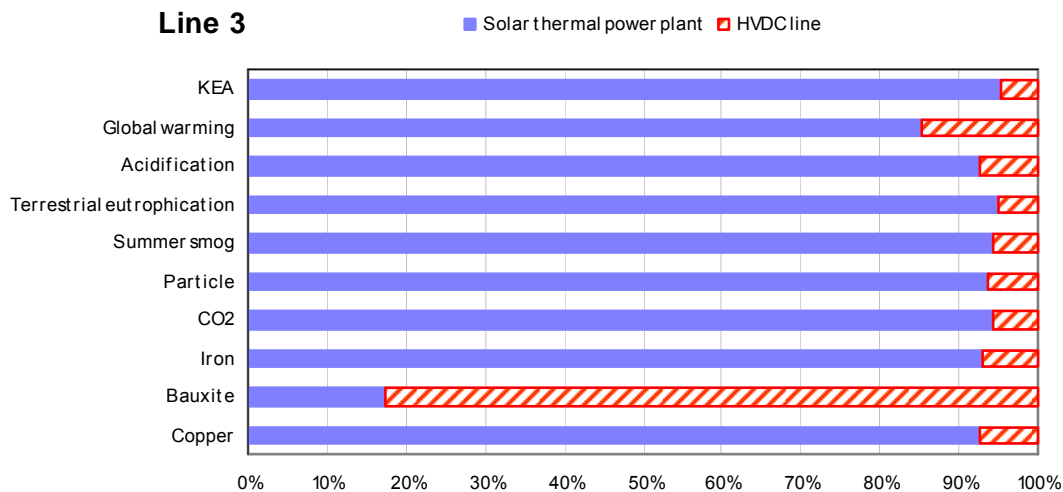


Fig. 92: Proportional shares of the plant and the line in environmental impacts (line 3, reference year 2030).

Tab. 45: Results of the impact assessment of the HVDC line 1 (2030) normalized to 1 kWh.

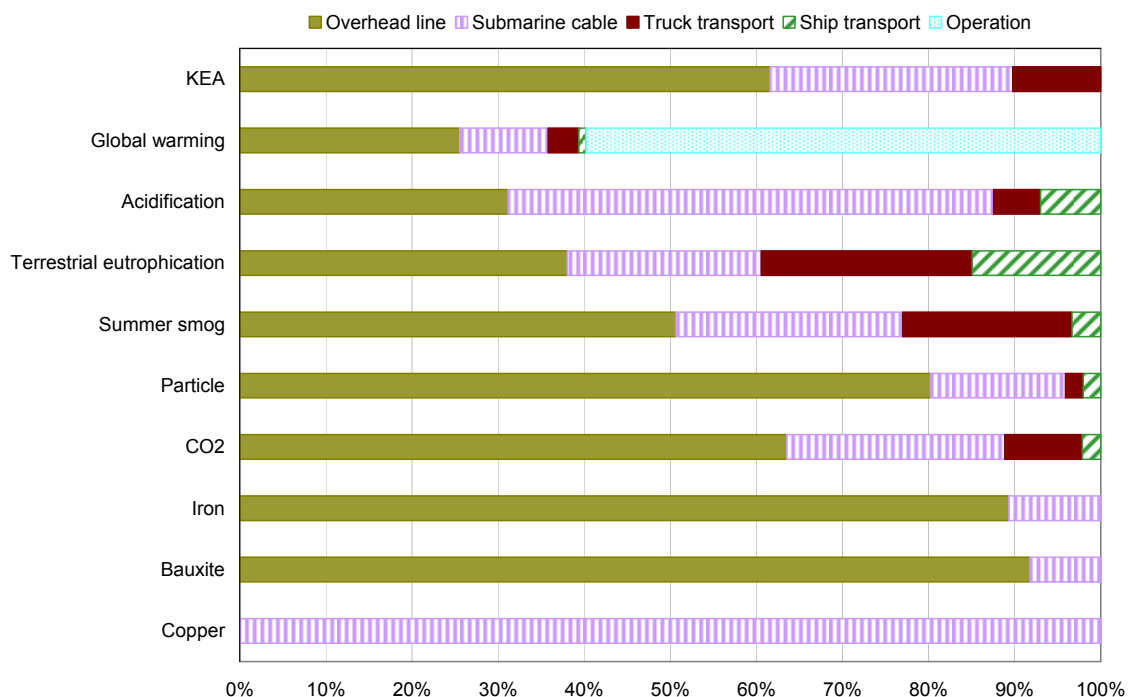
HVDC line 1	Overhead line	Submarine cable	Truck transport	Ship transport	Operation	Sum
KEA	0.0044	0.000085	0.00074	0	0	0.0052
Global warming	0.40	0.0069	0.057	0.0044	0.95	1.42
Acidification	2.49	0.19	0.44	0.19	0	3.31
Eutrophication	0.112	0.0028	0.074	0.0147	0	0.20
Summer smog	0.062	0.00138	0.025	0.00137	0	0.090
Particle	0.96	0.0080	0.025	0.0081	0	1.00
CO2	0.00038	0.0000065	0.000055	0.0000043	0	0.00045
Iron	0.076	0.00038	0	0	0	0.076
Bauxite	0.0144	0.000055	0	0	0	0.014
Copper	0.0000039	0.00022	0	0	0	0.00023

Tab. 46: Results of the impact assessment of the HVDC line 2 (2030) normalized to 1 kWh.

HVDC line 2	Overhead line	Submarine cable	Truck transport	Ship transport	Operation	Sum
KEA	0.0039	0.0018	0.00064	0	0	0.0063
Global warming	0.36	0.143	0.050	0.0117	0.83	1.39
Acidification	2.20	3.98	0.39	0.49	0	7.07
Eutrophication	0.099	0.059	0.064	0.039	0	0.26
Summer smog	0.055	0.029	0.021	0.0036	0	0.109
Particle	0.85	0.17	0.022	0.0213	0	1.06
CO2	0.00034	0.000134	0.000048	0.0000113	0	0.00053
Iron	0.067	0.0080	0	0	0	0.075
Bauxite	0.0127	0.00114	0	0	0	0.014
Copper	0.0000035	0.0047	0	0	0	0.0047

Tab. 47: Results of the impact assessment of the HVDC line 3 (2030) normalized to 1 kWh.

HVDC line 3	Overhead line	Submarine cable	Truck transport	Ship transport	Operation	Sum
KEA	0.0066	0.000149	0.00162	0	0	0.0084
Global warming	0.61	0.0121	0.125	0.0157	1.46	2.22
Acidification	3.78	0.34	0.97	0.66	0	5.75
Eutrophication	0.170	0.0050	0.161	0.052	0	0.39
Summer smog	0.095	0.0024	0.055	0.0048	0	0.16
Particle	1.46	0.0140	0.055	0.029	0	1.56
CO2	0.00058	0.0000113	0.000121	0.0000152	0	0.00073
Iron	0.115	0.00067	0	0	0	0.12
Bauxite	0.022	0.000096	0	0	0	0.022
Copper	0.0000060	0.00039	0	0	0	0.00040

**Fig. 93: Impacts in the life cycle phases of the HVDC line 2 (2030).**

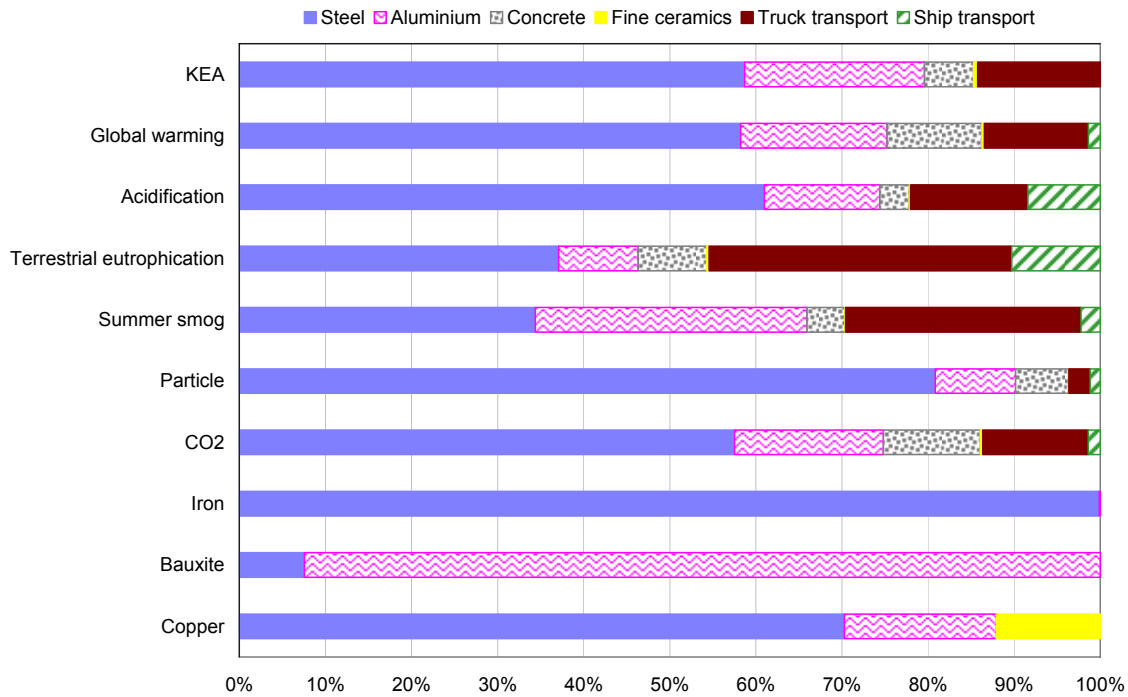


Fig. 94: Impacts of the overhead line section of line 2 (2030).

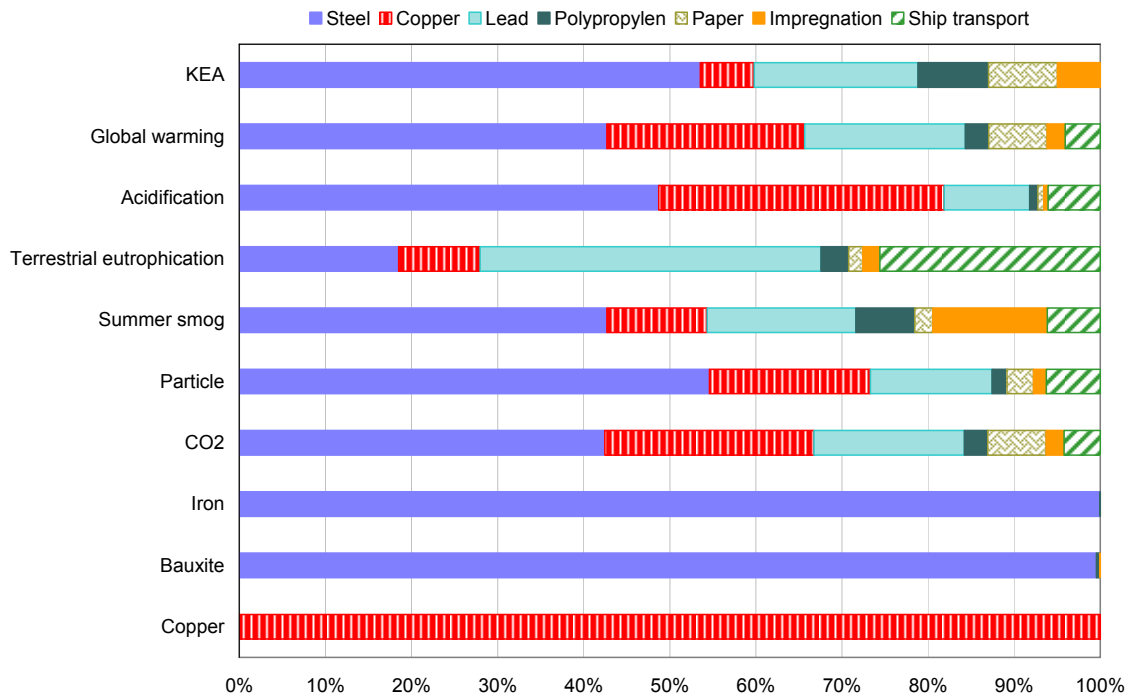


Fig. 95: Impacts of the submarine cable section of line 2 (2030).

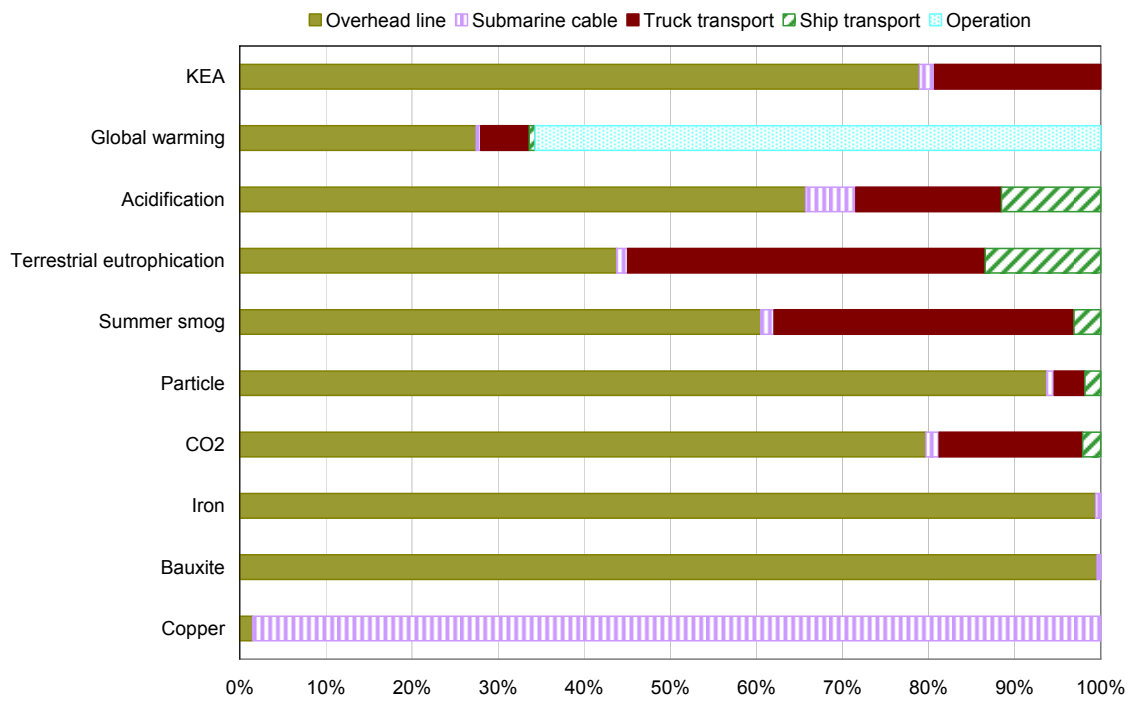


Fig. 96: Impacts in the life cycle phases of the HVDC line 3 (2030).

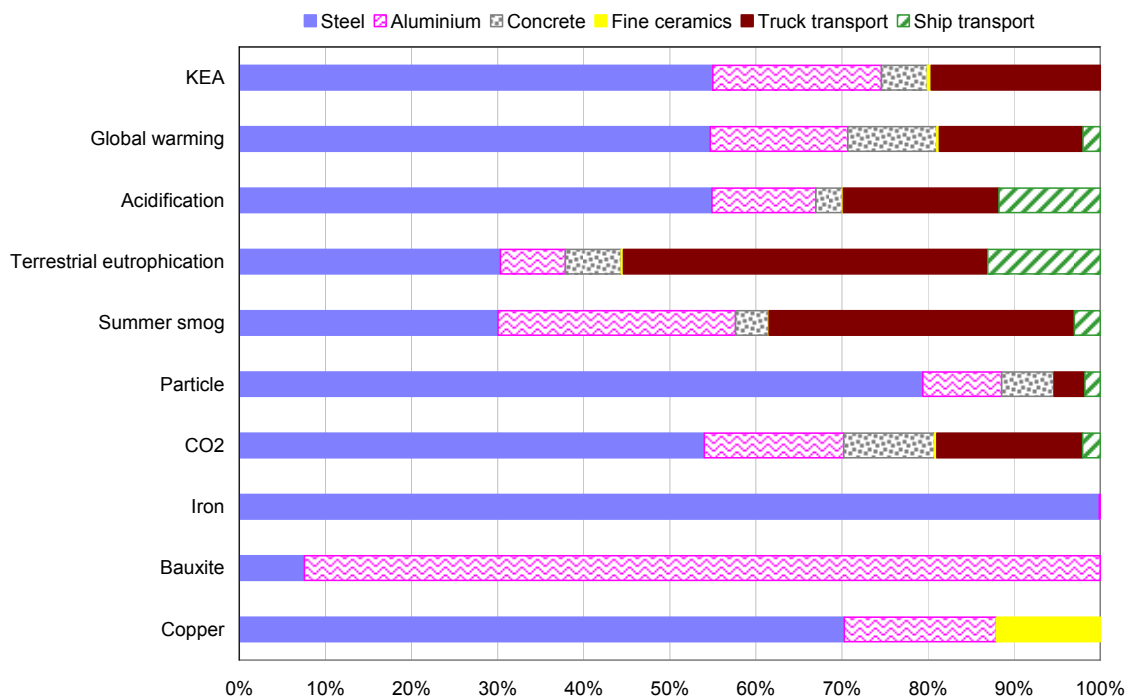


Fig. 97: Impacts of the overhead line section of line 3 (2030).

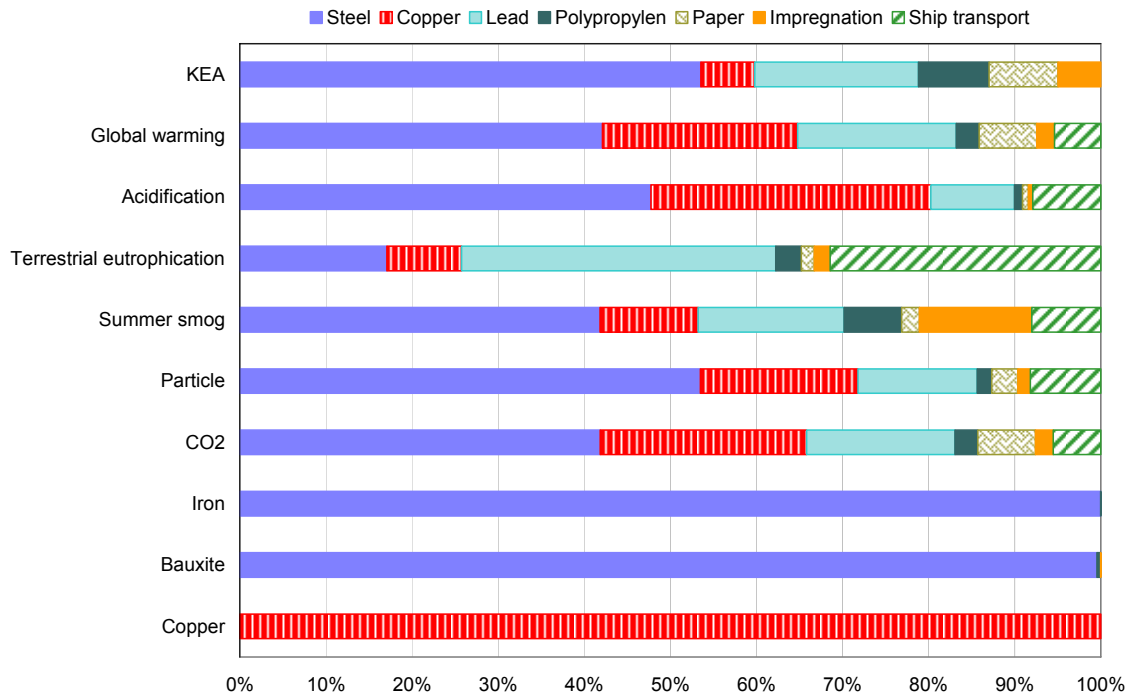


Fig. 98: Impacts of the submarine cable section of line 3 (2030).

Tab. 48: Results of the impact assessment for the HVDC line 1 (2010) normalized to 1 kWh.

HVDC line 1	Overhead line	Submarine cable	Truck transport	Ship transport	Operation	Sum
KEA	0.0064	0.000094	0.00074	0	0	0.0072
Global warming	0.57	0.0078	0.057	0.0044	0.95	1.60
Acidification	3.40	0.20	0.44	0.19	0	4.23
Eutrophication	0.176	0.0031	0.074	0.0147	0	0.27
Summer smog	0.057	0.00145	0.025	0.00137	0	0.085
Particle	1.96	0.0130	0.025	0.0081	0	2.00
CO2	0.00055	0.000073	0.000055	0.0000043	0	0.00061
Iron	0.162	0.00082	0	0	0	0.163
Bauxite	0.0216	0.000082	0	0	0	0.022
Copper	0.0000032	0.00022	0	0	0	0.00023

Tab. 49: Results of the impact assessment for the HVDC line 2 (2010) normalized to 1 kWh.

HVDC line 2	Overhead line	Submarine cable	Truck transport	Ship transport	Operation	Sum
KEA	0.0057	0.0020	0.00064	0	0	0.0082
Global warming	0.51	0.161	0.050	0.0117	0.83	1.56
Acidification	3.01	4.08	0.39	0.49	0	7.97
Eutrophication	0.156	0.065	0.064	0.039	0	0.32
Summer smog	0.050	0.030	0.021	0.0036	0	0.106
Particle	1.73	0.27	0.022	0.0213	0	2.05
CO2	0.00048	0.000152	0.000048	0.0000113	0	0.00069
Iron	0.143	0.0171	0	0	0	0.161
Bauxite	0.0191	0.00170	0	0	0	0.021
Copper	0.0000029	0.004668	0	0	0	0.0047

Tab. 50: Results of the impact assessment for the HVDC line 3 (2010) normalized to 1 kWh.

HVDC line 3	Overhead line	Submarine cable	Truck transport	Ship transport	Operation	Sum
KEA	0.0097	0.000165	0.00162	0	0	0.0115
Global warming	0.87	0.0136	0.125	0.0157	1.46	2.49
Acidification	5.17	0.34	0.97	0.66	0	7.14
Eutrophication	0.268	0.0055	0.161	0.052	0	0.49
Summer smog	0.087	0.0025	0.055	0.0048	0	0.15
Particle	2.97	0.0228	0.055	0.029	0	3.08
CO2	0.00083	0.0000128	0.000121	0.0000152	0	0.00098
Iron	0.246	0.00144	0	0	0	0.25
Bauxite	0.033	0.000144	0	0	0	0.033
Copper	0.0000049	0.00039	0	0	0	0.00040

Tab. 51: Results of the impact assessment for the plant (line 1, 2030) normalized to 1 kWh.

Plant (Algeria)	Unit/kWh	Solar field	Mechanical engineering	Constructional engineering
KEA	MJ	0.077	0.0018	0.0000044
Global warming	g CO2	5.72	0.19	0.00067
Acidification	mg SO2	26.45	0.79	0.0025
Eutrophication	mg PO4,3	1.87	0.070	0.00036
Summer smog	mg Ethylene	0.83	0.022	0.000090
Particle	mg	14.46	0.60	0.0013
CO2	kg	0.0054	0.00018	0.00000064
Iron	g	1.29	0.051	0.000075
Bauxite	g	0.0041	0.000045	0.000000007
Copper	g	0.0046	0.000092	0.000000003

Plant (Algeria)	Unit/kWh	Storage	Steam turbine	Truck transport
KEA	MJ	0.026	0.000072	0.027
Global warming	g CO2	3.35	0.0059	2.08
Acidification	mg SO2	8.20	0.12	16.14
Eutrophication	mg PO4,3	1.10	0.0017	2.67
Summer smog	mg Ethylene	0.35	0.00092	0.88
Particle	mg	4.50	0.015	0.92
CO2	kg	0.0032	0.0000055	0.0020
Iron	g	0.078	0.0013	0
Bauxite	g	0.000051	0.000064	0
Copper	g	0.000025	0.000024	0

Plant (Algeria)	Unit/kWh	Ship transport	Operation	Disposal	Sum
KEA	MJ	0	0.031	0.0000056	0.16
Global warming	g CO2	0.15	0.86	0.00047	12.36
Acidification	mg SO2	6.38	4.11	0.0029	62.19
Eutrophication	mg PO4,3	0.50	0.44	0.00026	6.67
Summer smog	mg Ethylene	0.046	0.35	0.00056	2.48
Particle	mg	0.28	0.32	0.00037	21.09
CO2	kg	0.00015	0.00080	0.00000047	0.012
Iron	g	0	0.00078	0	1.42
Bauxite	g	0	0.00016	0	0.0044
Copper	g	0	0.000037	0	0.0048

Tab. 52: Results of the impact assessment for the plant (line 2, 2030) normalized to 1 kWh.

Plant (Libya)	Unit/kWh	Solar field	Mechanical engineering	Constructional engineering
KEA	MJ	0.077	0.0018	0.0000044
KEA	g CO2	5.74	0.19	0.00067
Global warming	mg SO2	26.52	0.79	0.0026
Acidification	mg PO4,3	1.88	0.070	0.00036
Eutrophication	mg Ethylene	0.83	0.022	0.000090
Summer smog	mg	14.50	0.60	0.0013
Particle	kg	0.0054	0.00018	0.0000064
CO2	g	1.29	0.051	0.000075
Iron	g	0.0041	0.000046	0.00000007
Bauxite	g	0.0046	0.000093	0.00000003

Plant (Libya)	Unit/kWh	Storage	Steam turbine	Truck transport
KEA	MJ	0.026	0.000073	0.063
Global warming	g CO2	3.36	0.0059	4.89
Acidification	mg SO2	8.22	0.12	37.96
Eutrophication	mg PO4,3	1.11	0.0017	6.29
Summer smog	mg Ethylene	0.35	0.00092	2.07
Particle	mg	4.51	0.015	2.15
CO2	kg	0.0032	0.0000055	0.0047
Iron	g	0.078	0.0013	0
Bauxite	g	0.000051	0.000064	0
Copper	g	0.0000026	0.000024	0

Plant (Libya)	Unit/kWh	Ship transport	Operation	Disposal	Sum
KEA	MJ	0	0.032	0.0000056	0.20
Global warming	g CO2	0.23	0.86	0.00047	15.28
Acidification	mg SO2	9.81	4.12	0.0029	87.54
Eutrophication	mg PO4,3	0.77	0.44	0.00026	10.56
Summer smog	mg Ethylene	0.070	0.35	0.00056	3.70
Particle	mg	0.42	0.32	0.00037	22.53
CO2	kg	0.00023	0.00080	0.0000047	0.015
Iron	g	0	0.00078	0	1.43
Bauxite	g	0	0.00016	0	0.0044
Copper	g	0	0.000037	0	0.0048

Tab. 53: Results of the impact assessment for the plant (line 3, 2030) normalized to 1 kWh.

Plant (Egypt)	Unit/kWh	Solar field	Mechanical engineering	Constructional engineering
KEA	MJ	0.081	0.0019	0.0000046
Global warming	g CO2	6.01	0.20	0.00070
Acidification	mg SO2	27.78	0.83	0.0027
Eutrophication	mg PO4,3	1.97	0.073	0.00038
Summer smog	mg Ethylene	0.87	0.023	0.000095
Particle	mg	15.20	0.63	0.0014
CO2	kg	0.0057	0.00019	0.0000068
Iron	g	1.36	0.054	0.000078
Bauxite	g	0.0043	0.000048	0.00000008
Copper	g	0.0048	0.000097	0.00000003

Plant (Egypt)	Unit/kWh	Storage	Steam turbine	Truck transport
KEA	MJ	0.027	0.000076	0.025
Global warming	g CO2	3.52	0.0062	1.89
Acidification	mg SO2	8.61	0.12	14.68
Eutrophication	mg PO4,3	1.16	0.0018	2.43
Summer smog	mg Ethylene	0.37	0.00097	0.80
Particle	mg	4.73	0.016	0.83
CO2	kg	0.0034	0.000058	0.0018
Iron	g	0.082	0.0014	0
Bauxite	g	0.000053	0.000067	0
Copper	g	0.000027	0.000025	0

Plant (Egypt)	Unit/kWh	Ship transport	Operation	Disposal	Sum
KEA	MJ	0	0.033	0.000059	0.17
Global warming	g CO2	0.37	0.90	0.00050	12.90
Acidification	mg SO2	15.64	4.32	0.0030	72.00
Eutrophication	mg PO4,3	1.23	0.46	0.00028	7.33
Summer smog	mg Ethylene	0.112	0.37	0.00058	2.55
Particle	mg	0.68	0.34	0.00039	22.41
CO2	kg	0.00036	0.00084	0.0000050	0.012
Iron	g	0	0.00082	0	1.49
Bauxite	g	0	0.00016	0	0.0046
Copper	g	0	0.000039	0	0.0050

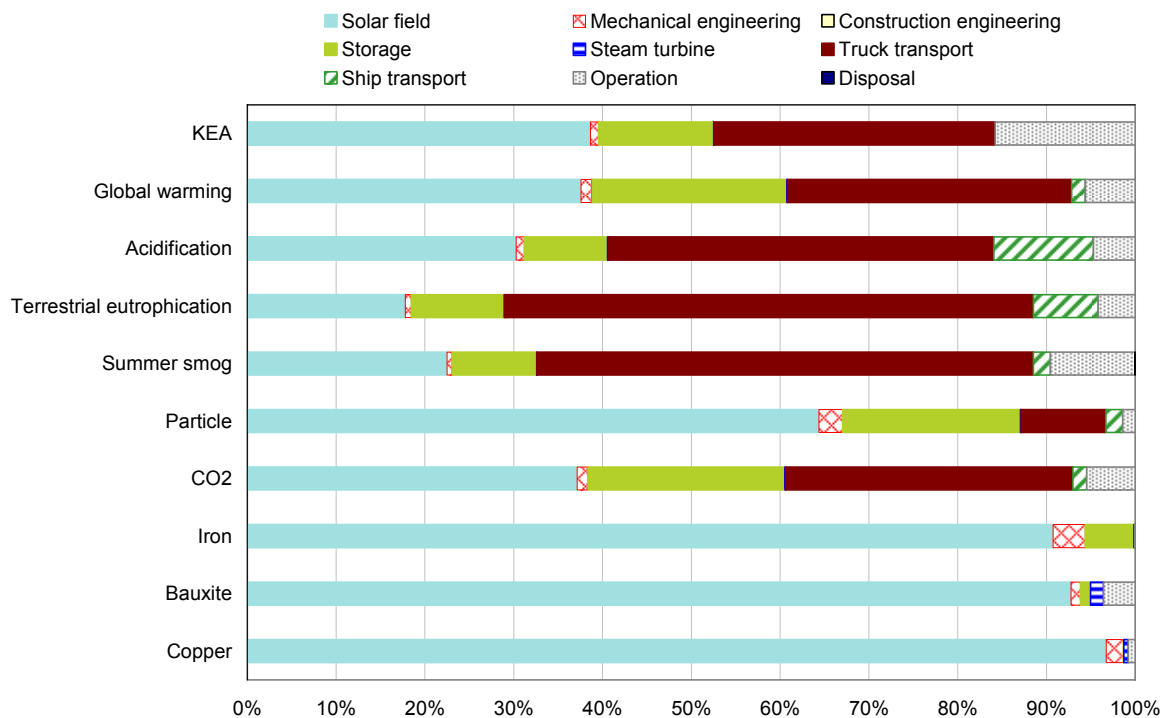


Fig. 99: Life cycle phases of the solar thermal power plant 2 (2030).

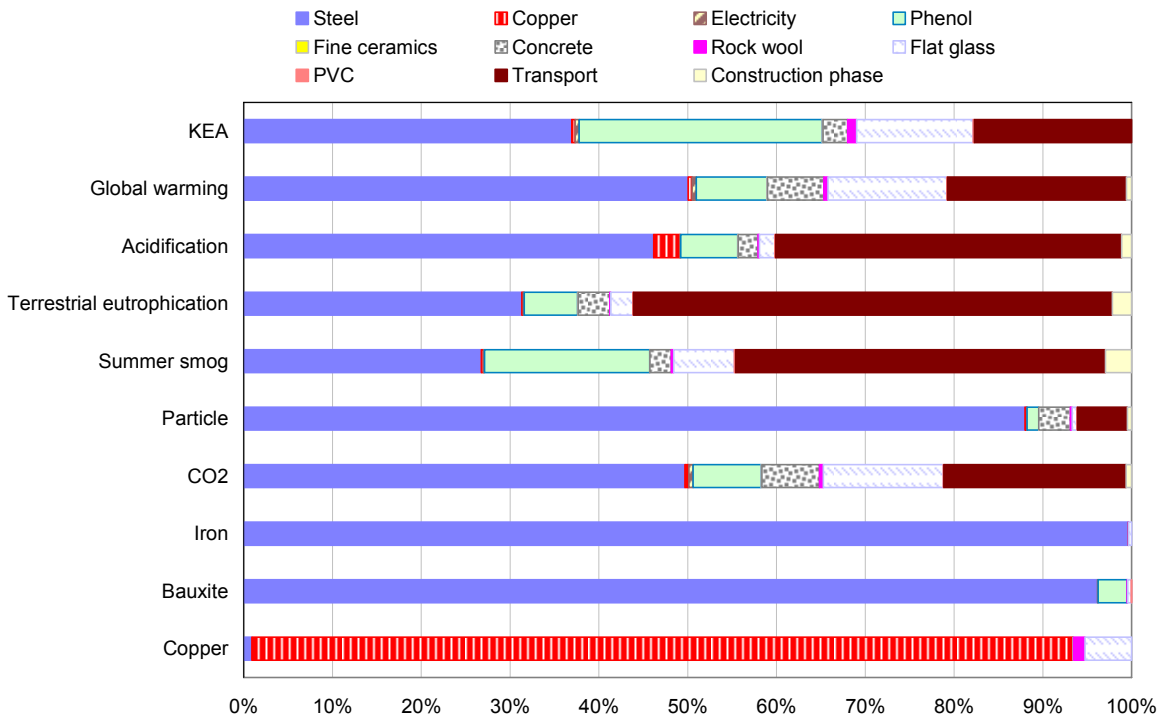


Fig. 100: Components and life cycle phases of the solar field of plant 2 (2030).

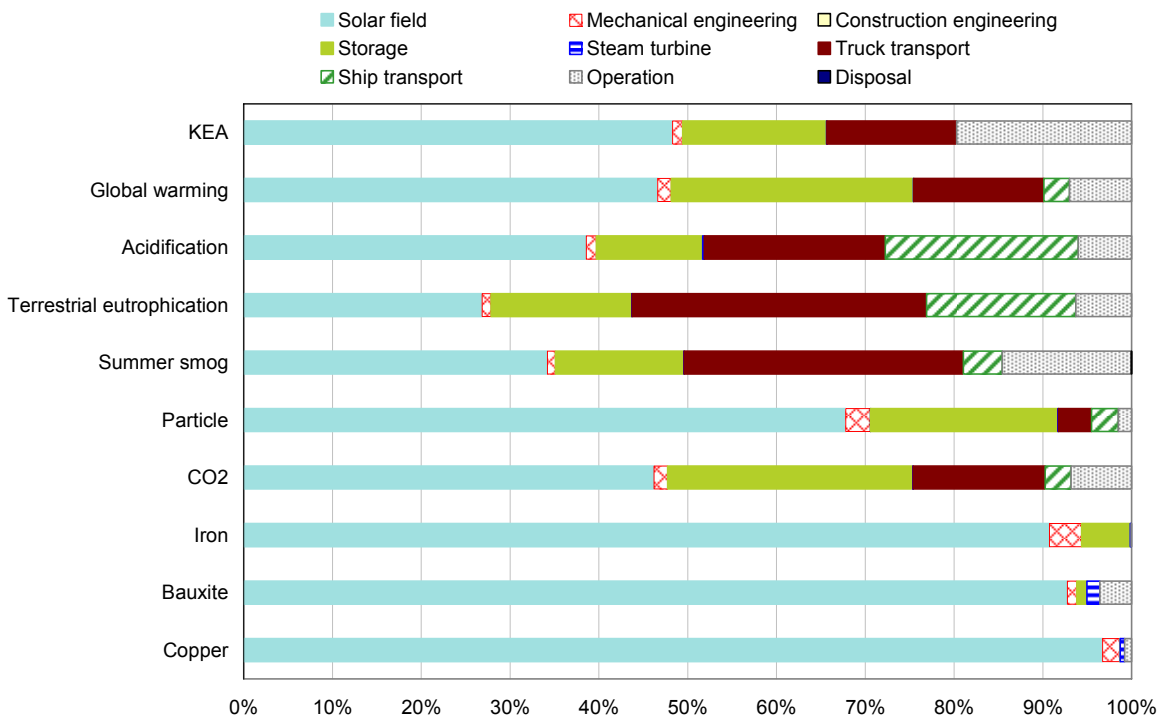


Fig. 101: Life cycle phases of the solar thermal power plant 3 (2030).

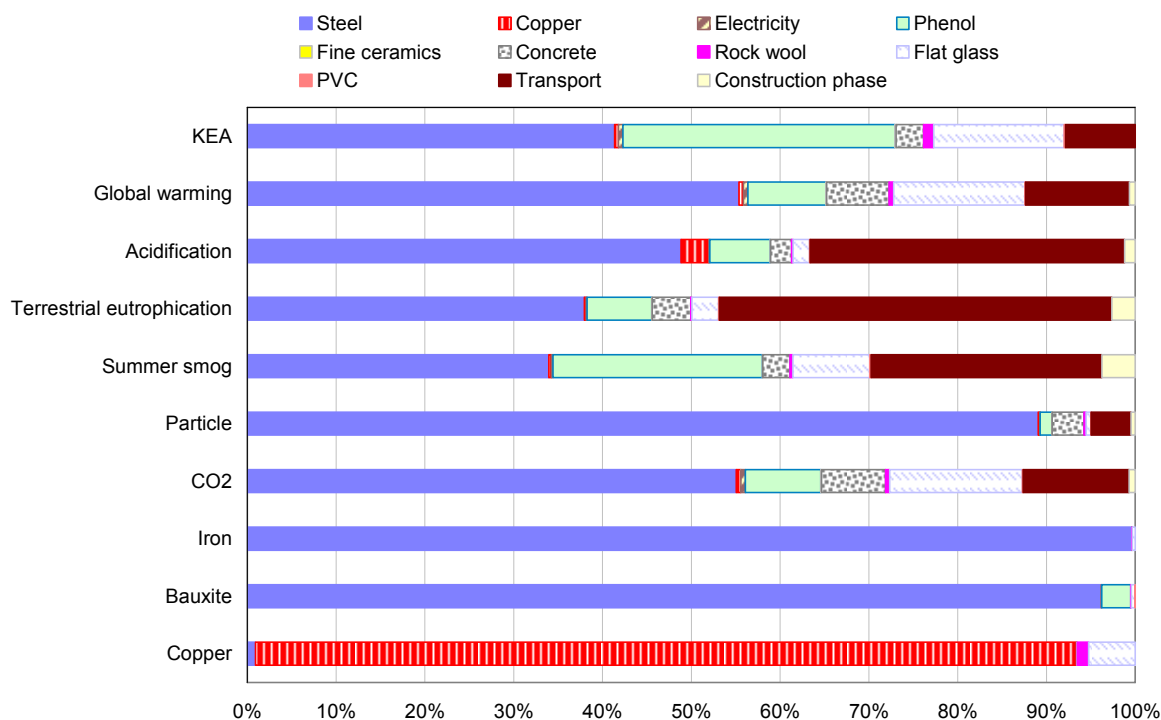


Fig. 102: Components and life cycle phases of the solar field of plant 3 (2030).

Tab. 54: Results of the impact assessment for the plant (line 1, 2010) normalized to 1 kWh.

Plant (Egypt)	Unit/kWh	Solar field	Mechanical engineering	Constructional engineering
KEA	MJ	0.103	0.0028	0.0000058
Global warming	g CO2	8.34	0.29	0.00082
Acidification	mg SO2	39.40	1.29	0.0033
Eutrophication	mg PO4,3	2.87	0.109	0.00042
Summer smog	mg Ethylene	1.06	0.031	0.000103
Particle	mg	30.66	1.24	0.0023
CO2	kg	0.0079	0.00028	0.00000078
Iron	g	2.77	0.110	0.000160
Bauxite	g	0.0060	0.000065	0.000000007
Copper	g	0.0047	0.000092	0.000000002

Plant (Egypt)	Unit/kWh	Storage	Steam turbine	Truck transport
KEA	MJ	0.027	0.000099	0.027
Global warming	g CO2	3.50	0.0086	2.08
Acidification	mg SO2	8.97	0.13	16.14
Eutrophication	mg PO4,3	1.16	0.0027	2.67
Summer smog	mg Ethylene	0.36	0.00114	0.88
Particle	mg	5.48	0.032	0.92
CO2	kg	0.0034	0.0000081	0.0020
Iron	g	0.168	0.0029	0
Bauxite	g	0.000050	0.000095	0
Copper	g	0.000019	0.000024	0

Plant (Algeria)	Unit/kWh	Ship transport	Operation	Disposal	Sum
KEA	MJ	0	0.032	0.0000056	0.19
Global warming	g CO2	0.15	0.86	0.00047	15.24
Acidification	mg SO2	6.38	4.12	0.0029	76.46
Eutrophication	mg PO4,3	0.50	0.44	0.00026	7.76
Summer smog	mg Ethylene	0.046	0.35	0.00056	2.73
Particle	mg	0.28	0.32	0.00037	38.92
CO2	kg	0.00015	0.00080	0.00000047	0.015

Iron	g	0	0.00074	0	3.05
Bauxite	g	0	0.00016	0	0.0063
Copper	g	0	0.000037	0	0.0049

Tab. 55: Results of the impact assessment for the plant (line 1, 2010) normalized to 1 kWh.

Plant (Libya)	Unit/kWh	Solar field	Mechanical engineering	Constructional engineering
KEA	MJ	0.103	0.0028	0.0000058
Global warming	g CO2	8.37	0.29	0.00082
Acidification	mg SO2	39.51	1.30	0.0033
Eutrophication	mg PO4,3	2.87	0.109	0.00042
Summer smog	mg Ethylene	1.06	0.031	0.000104
Particle	mg	30.74	1.24	0.0023
CO2	kg	0.0079	0.00028	0.00000079
Iron	g	2.77	0.110	0.000161
Bauxite	g	0.0060	0.000065	0.00000007
Copper	g	0.0047	0.000092	0.00000002

Plant (Libya)	Unit/kWh	Storage	Steam turbine	Truck transport
KEA	MJ	0.027	0.000100	0.063
Global warming	g CO2	3.51	0.0086	4.89
Acidification	mg SO2	9.00	0.13	37.96
Eutrophication	mg PO4,3	1.17	0.0027	6.29
Summer smog	mg Ethylene	0.37	0.00115	2.07
Particle	mg	5.50	0.032	2.15
CO2	kg	0.0034	0.0000082	0.0047
Iron	g	0.168	0.0029	0
Bauxite	g	0.000050	0.000096	0
Copper	g	0.000020	0.000024	0

Plant (Libya)	Unit/kWh	Ship transport	Operation	Disposal	Sum
KEA	MJ	0	0.032	0.0000056	0.23
Global warming	g CO2	0.23	0.86	0.00047	18.17
Acidification	mg SO2	9.81	4.13	0.0029	101.85
Eutrophication	mg PO4,3	0.77	0.44	0.00026	11.65
Summer smog	mg Ethylene	0.070	0.35	0.00056	3.95
Particle	mg	0.42	0.32	0.00037	40.41
CO2	kg	0.00023	0.00080	0.00000047	0.017
Iron	g	0	0.00074	0	3.06
Bauxite	g	0	0.00016	0	0.0063
Copper	g	0	0.000037	0	0.0049

Tab. 56: Results of the impact assessment for the plant (line 3, 2010) normalized to 1 kWh.

Plant (Egypt)	Unit/kWh	Solar field	Mechanical engineering	Constructional engineering
KEA	MJ	0.108	0.0030	0.0000061
Global warming	g CO2	8.77	0.31	0.00086
Acidification	mg SO2	41.40	1.36	0.0035
Eutrophication	mg PO4,3	3.01	0.115	0.00044
Summer smog	mg Ethylene	1.11	0.033	0.000109
Particle	mg	32.21	1.30	0.0024
CO2	kg	0.0083	0.00029	0.00000082
Iron	g	2.91	0.115	0.000168
Bauxite	g	0.0063	0.000068	0.00000007
Copper	g	0.0049	0.000097	0.00000002

Plant (Egypt)	Unit/kWh	Storage	Steam turbine	Truck transport
KEA	MJ	0.029	0.000104	0.025
Global warming	g CO2	3.68	0.0091	1.89
Acidification	mg SO2	9.43	0.14	14.68
Eutrophication	mg PO4,3	1.22	0.0029	2.43

Summer smog	mg Ethylene	0.38	0.00120	0.80
Particle	mg	5.76	0.033	0.83
CO2	kg	0.0035	0.0000085	0.0018
Iron	g	0.176	0.0030	0
Bauxite	g	0.000052	0.000100	0
Copper	g	0.0000020	0.000025	0

Plant (Egypt)	Unit/kWh	Ship transport	Operation	Disposal	Sum
KEA	MJ	0	0.033	0.0000059	0.20
Global warming	g CO2	0.37	0.91	0.00050	15.93
Acidification	mg SO2	15.64	4.33	0.0030	86.98
Eutrophication	mg PO4,3	1.23	0.46	0.00028	8.48
Summer smog	mg Ethylene	0.112	0.37	0.00058	2.81
Particle	mg	0.68	0.34	0.00039	41.15
CO2	kg	0.00036	0.00084	0.00000050	0.015
Iron	g	0	0.00078	0	3.20
Bauxite	g	0	0.00016	0	0.0066
Copper	g	0	0.000039	0	0.0051

Tab. 57: Additional load of line 1 (reference year 2010).

2010		Line 1				
	Unit	Plant 1	HVDC line 1	Sum	Difference to 2030	Additional load %
KEA	MJ	0.19	0.01	0.20	0.030	0.15
Global warming	g CO2	15.24	1.60	17.47	3.057	0.18
Acidification	mg SO2	76.46	4.23	80.68	15.180	0.19
Eutrophication	mg PO4,3	7.76	0.27	8.03	1.157	0.14
Summer smog	mg Ethylene	2.73	0.08	2.82	0.244	0.09
Particle	mg	38.92	2.00	40.93	18.837	0.46
CO2	kg	0.015	0.0006	0.02	0.003	0.19
Iron	g	3.05	0.16	3.21	1.713	0.53
Bauxite	g	0.01	0.022	0.028	0.009	0.33
Copper	g	0.0049	0.00023	0.00508	0.000	0.02

Tab. 58: Additional load of line 2 (reference year 2010).

		Line 2				
	Unit	Plant 2	HVDC line 2	Sum	Difference to 2030	Additional load %
KEA	MJ	0.23	0.01	0.24	0.030	0.15
Global warming	g CO2	18.17	1.56	20.28	3.062	0.18
Acidification	mg SO2	101.85	7.97	109.81	15.203	0.19
Eutrophication	mg PO4,3	11.65	0.32	11.98	1.159	0.14
Summer smog	mg Ethylene	3.95	0.11	4.06	0.247	0.09
Particle	mg	40.41	2.05	42.46	18.870	0.46
CO2	kg	0.02	0.00	0.02	0.003	0.19
Iron	g	3.06	0.16	3.22	1.716	0.53
Bauxite	g	0.01	0.02	0.03	0.009	0.32
Copper	g	0.00	0.004671	0.01	0.000	0.02

Tab. 59: Additional load of line 3 (reference year 2010).

		Line 3				
	Unit	Plant 3	HVDC line 3	Sum	Difference to 2030	Additional load %
KEA	MJ	0.20	0.01	0.21	0.033	0.16
Global warming	g CO2	15.93	2.49	19.39	3.294	0.19
Acidification	mg SO2	86.98	7.14	94.13	16.377	0.20
Eutrophication	mg PO4,3	8.48	0.49	8.96	1.246	0.16
Summer smog	mg Ethylene	2.81	0.15	2.96	0.254	0.09
Particle	mg	41.15	3.08	44.23	20.261	0.50

CO2	kg	0.02	0.00	0.02	0.003	0.21
Iron	g	3.20	0.25	3.45	1.840	0.57
Bauxite	g	0.01	0.03	0.04	0.013	0.47
Copper	g	0.01	0.00	0.01	0.000	0.02

Tab. 60: End result of line 1 normalized to 1 kWh.

2030		Line 1					
		Plant 1	HVDC line 1	Sum	norm_2030	norm_2010	
KEA	MJ	0.163	0.005	0.169	0.033	0.020	
Global warming	g CO2	12.356	1.421	13.777	0.034	0.026	
Acidification	mg SO2	62.190	3.312	65.503	0.141	0.091	
Eutrophication	mg PO4,3	6.665	0.203	6.868	0.134	0.123	
Summer smog	mg Ethylene	2.483	0.090	2.573	0.111	0.151	
Particle	mg	21.088	1.002	22.090	0.472	0.528	
CO2	kg	0.012	0.000	0.012	0.032	0.024	
Iron	g	1.422	0.076	1.498	0.674	1.426	
Bauxite	g	0.004	0.014	0.019	0.565	0.573	
Copper	g	0.005	0.000	0.005	0.263	0.303	

Tab. 61: End result of line 2 normalized to 1 kWh.

2030		Line 2					
		Plant 2	HVDC line 2	Sum	norm_2030	norm_2010	
KEA	MJ	0.200	0.006	0.207	0.040	0.024	
Global warming	g CO2	15.276	1.392	16.668	0.041	0.031	
Acidification	mg SO2	87.543	7.067	94.610	0.204	0.132	
Eutrophication	mg PO4,3	10.558	0.261	10.818	0.211	0.193	
Summer smog	mg Ethylene	3.700	0.109	3.809	0.164	0.224	
Particle	mg	22.528	1.060	23.588	0.504	0.564	
CO2	kg	0.015	0.001	0.015	0.040	0.029	
Iron	g	1.426	0.075	1.501	0.675	1.428	
Bauxite	g	0.004	0.014	0.018	0.548	0.556	
Copper	g	0.005	0.005	0.009	0.497	0.574	

Tab. 62: End result of line 3 normalized to 1 kWh.

2030		Line 3					
		Plant 3	HVDC line 3	Sum	norm_2030	norm_2010	
KEA	MJ	0.168	0.008	0.176	0.034	0.021	
Global warming	g CO2	12.899	2.223	15.122	0.037	0.028	
Acidification	mg SO2	71.995	5.754	77.749	0.168	0.108	
Eutrophication	mg PO4,3	7.328	0.389	7.717	0.150	0.138	
Summer smog	mg Ethylene	2.548	0.156	2.705	0.116	0.159	
Particle	mg	22.412	1.557	23.970	0.512	0.573	
CO2	kg	0.012	0.001	0.013	0.035	0.025	
Iron	g	1.494	0.115	1.609	0.724	1.532	
Bauxite	g	0.005	0.022	0.027	0.797	0.808	
Copper	g	0.005	0.000	0.005	0.285	0.328	